Campus Universitário Darcy Ribeiro
Departamento de Biologia Celular

Estudos do potencial do fungo *Aspergillus tamarii* na degradação da biomassa lignocelulósica.

ANTONIELLE VIEIRA MONCLARO

Brasília/DF

Março/2018

Campus Universitário Darcy Ribeiro
Departamento de Biologia Celular

Estudos do potencial do fungo *Aspergillus tamarii* na degradação da biomassa lignocelulósica.

ANTONIELLE VIEIRA MONCLARO

Orientador: Prof. Dr. Edivaldo Ximenes Ferreira Filho

Tese apresentada ao programa de Pós-graduação em Biologia Molecular da Universidade de Brasília, como parte dos requisitos para obtenção do título de Doutora.

Brasília/DF

Março/2018

Universidade de Brasília
Departamento de Biologia Celular
Programa de Pós-Graduação em Biologia Molecular

Estudos do potencial do fungo *Aspergillus tamarii* na degradação da biomassa lignocelulósica.

Antonielle Vieira Monclaro

Banca Examinadora:

Prof. Dr. Robert Neil Gerard Muller

Examinador interno vinculado ao programa (Universidade de Brasília)

Prof. Dra. Fabrícia Paula de Faria

Examinador externo não vinculado ao programa (Universidade Federal do Goiás)

Prof. Dra. Leonora Rios de Souza Moreira

Examinador interno não vinculado ao programa (Universidade de Brasília)

Prof. Dr. Gabriel Sérgio Costa Alves

Examinador suplente (Universidade de Brasília)

Prof.Dr. Edivaldo Ximenes Ferreira Filho

Orientador (Universidade de Brasília)

Brasília/DF

Março/2018

"Se muito vale o já feito

Mais vale o que será

E o que foi feito é preciso

Conhecer para melhor prosseguir"

(Milton Nascimento & Elis Regina – O que foi feito devera)

AGRADECIMENTOS

Ao meu orientador, Prof. Dr. Edivaldo, incentivador da minha vida acadêmica, exemplo de pesquisador, professor e pessoa que levarei para a vida. Eternamente grata pela confiança depositada em mim para seguir meus projetos pessoais. E agradecimento especial por não ter perdido a paciência comigo quando eu quis abraçar o mundo pesquisando mas atrasei todos os deadlines possíveis.

Ao meu supervisor no exterior, Dr. Vincent Eijsink, por me mostrar que uma mente realmente brilhante não apaga o brilho das outras, mas coopera com elas. Outro exemplo de pesquisador que levarei para a vida.

À minha co-supervisora no exterior, Dra. Aniko Várnai, por toda ajuda, resolução de dúvidas, prestatividade e confiança. Sou eternamente grata pela recepção que tive na Noruega.

Ao Dr. Dejan Petrović, por ser meu guia na bancada e ter me treinado em técnicas novas, enquanto fiz meu doutorado-sanduíche. Sou grata pela gentileza de ter disponibilizado tanto tempo para me ensinar.

Aos membros da banca, muito obrigada por terem aceitado participar da minha defesa. Espero que vocês sejam bonzinhos comigo.

Aos professores do Laboratório de Enzimologia e demais professores do Instituto de Biologia, agradeço muito pelo conhecimento compartilhado ao longo dos anos.

Ao Dr. Fábio Squina, por ter me recebido em seu laboratório em Campinas.

Aos amigos do CTBE e de Campinas, João, Lívia, Eduardo, Ivan, Djalma, Bruno e Guglielmo. Eternamente grata ao Thiago, por ter me treinado em técnicas de biologia molecular, o que me fez decidir trabalhar com as AA9 (e mudou minha vida). E em especial ao Robson, Carla e Diogo, foi um dos melhores anos da minha vida, graça a vocês. Talvez graças ao Club88, Echos e Armazém Bar também. Mas vocês estavam lá!

Aos amigos da Enzimologia e da UnB, Leonora, Caio, Helder, Raissa, Andreza, Carol, Babi, Guilherme Sperandio, Guilherme Recalde, Diandra, Pedro Fontes, Alisson,

Elenilde, Brenda e Leo, Fran, Sadia, Jéssica, Alonso, Ju Peixoto, Renata, Samuel, Paula, Thiago, Marisia e Margarete, Joanna, João Heitor, João Paulo, Michelle e Gabriel, Gláucia, Amandas, Karol e André. Como sempre, vocês tornaram o trabalho mais leve. Vou sentir muita falta de trabalhar com vocês. E sou eternamente grata a toda ajuda que vocês me deram. Não sou grata das ressacas que tive após os happy hours e festas juninas, mas faz parte da vida.

Aos meus amigos de vários cantos do Brasil, obrigada por serem meus companheiros de caminhada de vida. Em especial para as incríveis mulheres da minha vida: Ananda, Bela, Ju Muller, Sissy, Aninha, Lidia, Ellen, Rapha, Ju Infante, Karen, Pri Kartz, Paty, Cla, Duda, Luiza, Carol, Camila, Mila, Wal e Lorena. " *Mulheres, nós juntas podemos botar o mundo abaixo, balançar todas as estruturas. Vocês me lembram que somos incríveis e livres. Eu lembro vocês que somos cura. Somos mulheres que lutam.*" (adaptado de Ryana Leão – Tudo nela brilha e queima).

Aos meus amigos de idas e vindas da Noruega, Monise, Rodrigo, Arthur, Marco, Sérgio, Rafael, Federica, Brittany, Radziah, Sara, Ricardo, Ana Cristina, Yen, Giusi, Paulo, Tati e Mellanie. A experiência aqui foi incrível, e devo muito a vocês, especialmente por me manterem sã (brincadeira, com fundo de verdade). Agradeço também a Sussi, a gata que tornou minhas noites mais emocionantes. E bem especial para o Thales e a Danuza, pois eu realmente não sei o que teria sido de mim sem vocês dois. *Now, sashay away.*

Ao meu companheiro Rodolpho, obrigada por me mostrar que a vida é uma grande aventura e melhor vivida quando compartilhada. Estamos apenas começando. Obrigada pelo amor, carinho, compreensão e cumplicidade. E correções de português e inglês. E discussões filosóficas e existenciais quando meus experimentos não davam certo. E aceitar que há um *tamarii* na minha vida.

Por fim, minha família, o que tenho mais de especial: Monclaro e Cris, Tho, Marina e Nina. Vocês formam o alicerce da minha vida e são os verdadeiros responsáveis pelas minhas conquistas. Amo vocês, de uma forma inexplicável. Dedico esse trabalho, que foi meu projeto de vida, a vocês.

APOIO FINANCEIRO

Esta pesquisa foi desenvolvida com o apoio financeiro da CAPES por meio de concessão de bolsa de estudos e pelos projetos de pesquisa: Rede Centro Oeste/CNPq/FAPDF, Universal/CNPq, Pronex/FAPDF, INCT do Bioetanol/CNPq, National Institute for Science and Technology of Bioethanol e o projeto Biomim financiando pelo Norwegian Research Council (n° 243663).

SUMÁRIO

LISTA DE FIGURAS

LISTA DE TABELAS

ABREVIAÇÕES

AA Atividade auxiliar

BeX Beech wood xylan

BrX Birch wood xylan

CBM Módulo de ligação ao carboidrato

CC Clean cotton residue

CCD Central Composite Design

CCRD Central Composite Rotatable Design

DC Dirty cotton

DP Dark cellulosic pulp

FA Ferulic acid

FP Filter powder

LPMO Monooxigenase lítica de polissacarídeo

OSX Oat spelt xylan

PASC Celulose Avicel inchada com ácido fosfórico

SB Sugarcane bagasse

WP White cellulosic pulp

RESUMO

Nesta tese foram feitos estudos mais aprofundados de enzimas produzidas pelo fungo *Aspergillus tamarii* em diferentes contextos de degradação de biomassa lignocelulósica. O primeiro trabalho avaliou a influência de condições de cultivo na ação de celulases e xilanases e demonstrou que ferramentas estatísticas (CCD e CCRD) são necessárias para avaliar o comportamento da enzima em diferentes condições. Os resultados demonstraram que utilização de triptona como fonte de nitrogênio inibiu fortemente a atividade das celulases, enquanto aumentou das xilanases. Além disso, a suplementação com $CuSO_4$ aumentou a atividade de todas as enzimas. Sugere-se que influência dos componentens do meio de culturam devem ser considerados ao fazer um planjamento de coquetel enzimático de fungo. O segundo trabalho avaliou os parâmetros termodinâmicos de uma xilanase pura de baixa massa molecular (22 kDa) de *A. tamarii* ativa em ácido ferúlico. Após análise de *molecular docking* de uma xilanase de *A. niger* com ácido ferúlico, identificou-se que o possível sítio de ligação do ácido ferúlico é no sítio catalítico da enzima. Baseado nisso, foi feita uma avaliação dos parâmetros termodinâmicos de ligação do ácido ferúlico na xilanase de *A. tamarii* e demonstrou-se que há uma mudança conformacional da enzima na presença do ácido ferúlico, que influencia no encaixe do substrato no sítio catalítico, e dessa forma a enzima se torna ativa ou tolerante. Por fim, dois genes de LPMOs da família AA9 foram clonadas e expressas em *Pichia pastoris* da linhagem PichiaPink™. As enzimas foram expressas apenas com seus domínios catalíticos. As duas AA9, nomeadas *AtAA9.1_SD* e *AtAA9.2_SD*, foram caracterizadas em função da regioseletividade e especificidade ao substrato. *AtAA9.1_SD* é uma AA9 com oxidação na posição C4 que possui atividade em celulose (PASC), celopentose, xiloglucana e possivelmente xilana e liquenana. *AtAA9.2_SD* é uma AA9 com oxidação na posição C1/C4 e que possui atividade em celulose (PASC), xiloglucana e possivelmente xilana. Utilizando o fungo *A. tamarii* como objeto de estudo, mostrou-se que ele possui potencial na aplicação da degradação da biomassa por possuir enzimas com características únicas.

ABSTRACT

This thesis discusses in-deep studies from enzymes produced by *Aspergillus tamari* in different contexts of lignocellulose biomass degradation. The first part of this work evaluated the influence of different conditions in cellulase and xylanase activity. Statistic tools (CCD and CCRD) demonstrated their importance to evaluate the behavior of these enzymes in different conditions. The results showed that the use of tryptone as a nitrogen source inhibited cellulase activity while activated xylanase activity. Supplementation with $CuSO_4$ increased activity of both enzymes. The influence of culture medium composition in the enzymatic activity might be considered when designing enzymatic cocktail from fungi. The second part of this work evaluated thermodynamic parameters of a pure low molecular-weight xylanase (22 kDa) from *A. tamarii* that was active in the presence of ferulic acid. Molecular docking of a xylanase from *A. niger* with ferulic acid displayed that most probably the ligand interacts with the catalytic site of the enzyme. Based on this, thermodynamic parameters of the xylanase from *A. tamarii* with ferulic acid were assessed. The results indicated that there was a conformational change of the enzyme in the presence of ferulic acid, and this influenced the fitting of the substrate in the catalytic site, making the enzyme active in or tolerante to the presence of ferulic acid. The last part of this work studied two AA9 LPMOs from *A. tamarii*. They were cloned and expressed in PichiaPink™. These two enzymes were expressed in a truncated version, with only the catalytic domain, because the vector could not express the proteins's full length. They were named *AtAA9.1_SD* and *AtAA9.2_SD* and were characterized based on their regioselectivity and specificity to substrate. *AtAA9.1_SD* is a C4-oxidizer with activity in cellulose (PASC), cellopentaose, xyloglucan and probably xylan and lichenan. *AtAA9.2_SD* is a C1/C4-oxidizer with activity in cellulose (PASC), xyloglucan and probably xylan. This thesis showed that *A. tamarii* has potential in biomass degradation mainly due to its enzymes with exclusive features.

INTRODUÇÃO GERAL

O etanol de segunda geração, proveniente de biomassa lignocelulósica, representa uma fonte de energia renovável promissora e alternativa ao uso de fontes fósseis (JEGANNATHAN; NIELSEN, 2013). A parede celular da biomassa é uma estrutura complexa formada por três componentes principais: celulose, hemicelulose e lignina. Esses componentes são arranjados em uma configuração organizada, formando estruturas recalcitrantes para a degradação enzimática. Essa recalcitrância é um dos fatores limitantes para a conversão da biomassa em produtos finais de valor agregado por enzimas lignocelulolíticas (DE SIQUEIRA et al., 2010; ZHANG; DONALDSON; MA, 2012). Fungos filamentosos são reconhecidos pelo seu grande potencial na decomposição da biomassa na natureza. Essa característica é utilizada em várias áreas da indústria biotecnológica como, por exemplo, na produção de enzimas, degradação de resíduos agroindustriais e vários tipos de processos fermentativos, visando agregar valor a utilização desses resíduos (CONESA et al., 2001; NEVALAINEN; TE'O; BERGQUIST, 2005; SARROUH et al., 2012). Os fungos do gênero *Aspergillus*, utilizados amplamente na indústria, são eficientes decompositores de biomassa lignocelulósica e produtores de enzimas glicosil hidrolases (GH), com extensa literatura descrevendo suas ações (DUARTE et al., 2012; DUQUE JARAMILLO et al., 2013; MALVESSI; DA SILVEIRA, 2004; MCKELVEY; MURPHY, 2010; PIROTA; DELABONA; FARINAS, 2014; SZENDEFY; SZAKACS; CHRISTOPHER, 2006; TE BIESEBEKE et al., 2006).

Durante anos, a visão clássica da conversão enzimática dos polissacarídeos da parede celular envolvia apenas enzimas hidrolíticas, como endo e exo-celulases. No entanto, em 2010 foi descoberto um sistema enzimático oxidativo que atuava juntamente com as hidrolases na degradação da biomassa (VAAJE-KOLSTAD et al., 2010). As monooxigenases líticas de polissacarídeos (LPMOs) são uma nova classe de enzimas com ação oxidativa em polissacarídeos. Elas são classificadas como "AA" (atividade auxiliar). Existem 14 classes de AA, onde cinco são LPMOs – AA9, AA10, AA11, AA13 e AA14. As enzimas da família AA9 são exclusivas de fungo (LEVASSEUR et al., 2013). Sua ação diminui a recalcitrância da parede celular, aumentando a ação hidrolítica das GHs e permitindo uma hidrólise eficiente da biomassa (HEMSWORTH et al., 2013; HORN et al., 2012). Até o presente momento já foram detectadas as atividades das AA9 em: celulose (QUINLAN et al., 2011), xiloglucana (AGGER et al., 2014), amido (LO

LEGGIO et al., 2015; VU et al., 2014a) e xilana (FROMMHAGEN et al., 2015). Foi demonstrado que várias espécies de fungos contém uma grande variedade de LPMOs em seus genomas. A análise dessas sequências, algumas contendo a presença de módulos de ligações a carboidratos (CBMs), indicam uma vasta diversidade funcional dessas enzimas, que não foram ainda exploradas (HORN et al., 2012).

O presente trabalho foi desenvolvido com intuito de contribuir para o desenvolvimento de formas mais eficientes de sacarificação enzimática da biomassa lignocelulósica com foco na produção do etanol de segunda geração. A tese se encontra dividida em capítulos, visando dar ênfase aos objetivos propostos e resultados obtidos:

- Capítulo 1 – Revisão bibliográfica, que contextualiza a importância do projeto de tese;
- Capítulo 2 – Objetivos gerais e específicos que nortearam o trabalho;
- Capítulo 3 – Manuscrito entitulado “Response Surface Methodology as a Tool to Evaluate cellulase and xylanase activities under different conditions of culture media and lignocellulosic biomass sources”;
- Capítulo 4 – Manuscrito entitulado “Xylanase from *Aspergillus tamarii* Shows Different Kinetic Parameters and Substrate Specificity in the Presence of Ferulic Acid”;
- Capítulo 5 – Review publicado na revista *International Journal of Biological Macromolecules* entitulado “Fungal lytic polysaccharide monooxygenases from family AA9: Recent developments and application in lignocelullose breakdown”;
- Capítulo 6 – Estudos do mecanismo de degradação oxidativa de biomassa lignocelulósica por monooxigenases líticas de polissacarídeos (LPMO) de *Aspergillus tamarii*.

CAPÍTULO 1 – REVISÃO BIBLIOGRÁFICA

1.1 A biomassa lignocelulósica como fonte renovável de energia

A matriz energética de um país corresponde a todas as fontes de energia que o país utiliza, desde o consumo diário de residências, até em indústrias. No Brasil, a matriz energética é composta de fontes renováveis e não renováveis. O Brasil é líder mundial na utilização de fontes renováveis para geração de energia - a média mundial é de apenas 14,2% de utilização. Dentre as fontes renováveis, a biomassa corresponde à 40,1% da oferta interna de produção de energia (MME (MINISTÉRIO DE MINAS E ENERGIA), 2017). Dessa forma, a bioenergia, conceitualmente entendida como energia produzida de biomassa, demonstra que possui um potencial de geração de energia muito alto, podendo se equiparar ao potencial de energia de fontes fósseis. Estudos com foco nas otimizações dos processos de geração de energia se fazem necessários, principalmente para potencializar a produção de seus biocombustíveis derivados: etanol, etanol de segunda geração, biodiesel e biogás.

A biomassa pode ser definida como material orgânico de origem vegetal e que armazena energia na forma de ligações químicas (CLAASSEN et al., 1999; MCKENDRY; MCKENDRY, 2002). A biomassa mais utilizada na geração de energia no Brasil é a cana-de-açúcar. A cana-de-açúcar é a segunda principal produção agrícola brasileira, ficando atrás apenas da soja. Ela gera dois produtos principais, o açúcar e o álcool (anidro e hidratado). A safra estimada de 2016/207 correspondeu a 694,54 milhões de tonelada de cana, o que gerou 39,8 milhões de tonelada de açúcar e 16,5 bilhões de litro de etanol (CONAB, 2016). Atualmente, além das pesquisas buscarem a produção do etanol a partir do bagaço de cana-de-açúcar, há um grande interesse também na utilização das biomassas em biorefinarias. A conversão enzimática da biomassa para geração de produtos de valor agregado surge como uma tecnologia promissora, pois o Brasil é um dos países que mais produz material lignocelulósico através da agricultura, e o volume de geração dos resíduos é significativo. Considerando o potencial que outras biomassas lignocelulósicas além da cana-de-açúcar apresentam, estudos em sua conversão requerem inovação e pesquisa extensiva (LIMA et al., 2014; SILVA; VAZ; FILHO, 2017).

As indústrias de papel, celulose e de artefatos de papel compõe o setor de celulose e papel; em 2007 o setor contribuiu com 43,5 bilhões de reais para a economia brasileira

(MONTEBELLO; BACHA, 2013). A principal origem da matéria-prima do papel, a celulose, é obtida pelo beneficiamento da madeira, principalmente de eucalipto, em que o Brasil não é somente o maior produtor mundial como também é líder mundial de produtividade de madeira (IBÁ, 2017; MONTEBELLO; BACHA, 2013). Em 2016, a produção de celulose foi de 18,8 mt (IBÁ, 2017). Dependendo da utilização do papel, este precisará sofrer algum tipo de tratamento especial, como por exemplo, para a escrita. Nesse caso, é necessário que o papel tenha uma característica absorvente e áspera, e por estética, preferencialmente branco. A lignina é a responsável pela cor escura da polpa, então uma das etapas de processamento é o branqueamento do papel. Atualmente, há uma modalidade de branqueamento utilizando hemicelulases, ou branqueamento enzimático, que reduz a necessidade dos reagentes químicos tóxicos e traz vantagem econômica e ambiental (VIIKARI et al., 1994; WEERACHAVANGKUL et al., 2012).

O Brasil é o quinto maior produtor de algodão no mundo. De acordo com a ABRAPA, Associação Brasileira dos Produtores de Algodão, a safra de algodão do Brasil de 2016/2017 foi de 1,529 mt. Na indústria têxtil, o fardo de algodão é limpo e uniformizado, e então ocorre a separação e estiramento das fibras de algodão. Todas as impurezas obtidas nestas quatro etapas de processamento são recolhidas por tubulações e acumuladas em filtros, gerando o resíduo chamado pó de filtro. Já o piolho de algodão é obtido pela etapa de descaroçamento do algodão (DE SIQUEIRA et al., 2010; DUARTE et al., 2012; RAFAELA; EURICH; FRANCO, 2002). Como o volume de produção de resíduos gerados pelo cultivo de algodão chega a ser cinco vezes maior que o volume de fibra produzida (AGBLEVOR et al., 2006), a conversão desses resíduos para produtos com valor agregado foi e ainda é extensivamente estudada, pois além de encaminhar um fim para o seu acúmulo no meio ambiente, apresenta um grande potencial para várias aplicações.

1.1.1 Composição da parede celular da biomassa vegetal

A parede celular da biomassa vegetal é composta por uma rede de microfibrilas, constituída de polissacarídeos (celulose, hemicelulose e pectina) e complexos fenólicos (lignina), além da presença de algumas proteínas estruturais. Sua composição varia entre espécies de plantas e entre os tecidos da própria planta (DE SIQUEIRA et al., 2010; MINIC; JOUANIN, 2006). Durante a vida da planta, a parede possui importantes papeis

em suas funções fisiológicas, como a comunicação intercelular, defesa contra patógenos, resistência mecânica e interação com o meio ambiente, além de ser a maior reserva de carbono na natureza (DE VRIES et al., 2001; MINIC; JOUANIN, 2006). As células das plantas possuem dois tipos de deposição em suas paredes, a primária e a secundária. A parede primária é sintetizada durante a expansão celular nos primeiros estágios de desenvolvimento, é uma estrutura altamente hidratada e possui redes de microfibrilas de celulose incorporadas em compostos pécticos, hemicelulose e glicoproteínas; a parede secundária é formada dentro da parede primária, sendo mais densa e menos hidratada que a primária. Além disso, há uma camada exterior denominada lamela média e formada basicamente de compostos pécticos e proteínas (Jouanin and Minic, 2006; Siqueira *et al*, 2010; Wong *et al*, 1988).Os polissacarídeos que constituem a parede celular de planta são compostos orgânicos que correspondem a quase 90% do conteúdo da parede, além de representar cerca de 70% da biomassa do planeta. O termo holocelulose define, de forma mais específica, esses grupos de polissacarídeos presentes na parede celular e que ocorrem em estreita associação com a lignina; esta associação forma uma estrutura insolúvel e altamente recalcitrante, conforme pode ser visto na figura 1 (HU et al., 2011; ZHANG; DONALDSON; MA, 2012).

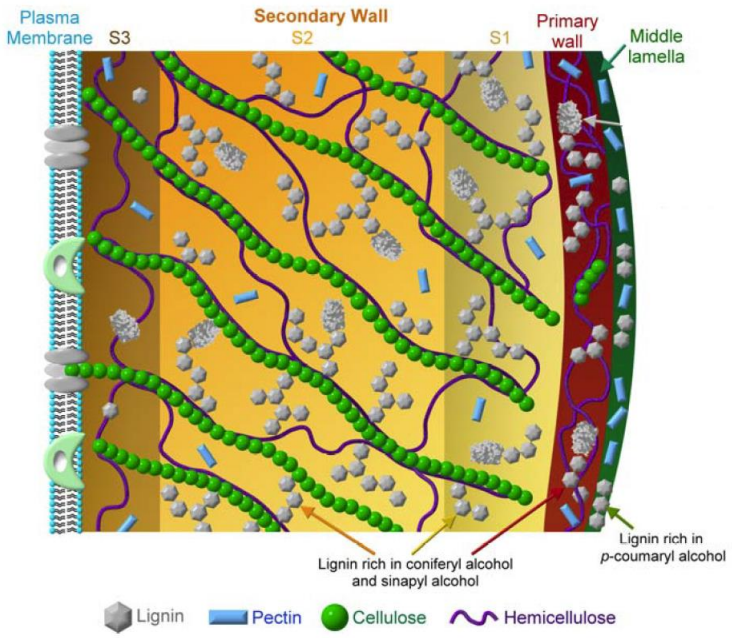

Figura 1. Ilustração da parede celular da planta. Retirado de (ACHYUTHAN et al., 2010).

A recalcitrância à decomposição biológica é uma das etapas mais limitantes da conversão da biomassa lignocelulósica para produtos finais de valor agregado. A holocelulose, proteínas e lignina fazem da estrutura da parede celular um desafio para sistemas enzimáticos. As celulases, hemicelulases e pectinases, que pertencem ao grupo de enzimas chamadas holocelulases, são glicosídeo hidrolases que realizam a quebra da holocelulose por hidrólise das ligações glicosídicas, formando oligo e monossacarídeos. As exo-holocelulases agem nas extremidades redutoras e não-redutoras, liberando unidades de monossacarídeos; as endo-holocelulases hidrolisam ligações glicosídicas internas, em posições específicas ou variadas, dependendo da presença de ramificação ou não. As enzimas que clivam essas regiões ramificadas são essenciais para uma hidrólise mais completa. Várias dessas enzimas contêm módulos de ligação ao carboidrato (CBM), domínios não catalíticos ou com fraca ação catalítica, que ancoram e orientam a ação da enzima. A especificidade cruzada de substratos é uma das características das holocelulases. Neste caso, algumas enzimas possuem especificidade relaxada e conseguem hidrolisar a ligação independente do tipo de açúcar presente. A hidrólise eficiente da parede celular, realizada pelas holocelulases, está relacionada com características estruturais da planta (como a natureza e extensão das ligações cruzadas entre diferentes polissacarídeos); a interação da lignina com alguns carboidratos através de ligações-cruzadas; a estrutura cristalina da celulose e o tamanho das microfibrilas desses polissacarídeos (DE SIQUEIRA et al., 2010; DE VRIES et al., 2001; ZHANG; DONALDSON; MA, 2012).

A celulose, principal polissacarídeo presente na biomassa, consiste de um polímero linear não ramificado de resíduos de glicose. Esses polímeros estão estruturados ordenadamente em fibrilas com a função principal de garantir a rigidez da parede celular. Estruturalmente, a celulose consiste de uma cadeia de D-glicopiranose com ligações do tipo β-1,4 e condensada por ligações de hidrogênio em estruturas cristalinas, chamadas de microfibrilas. Estas microfibrilas são formadas por mais de 250 cadeias de glicose e estão inseridas dentro da estrutura da hemicelulose. O arranjo cristalino fornece às microfibrilas uma impermeabilidade relativa, não apenas para macromoléculas como as enzimas, mas também para micromoléculas como a água. A estrutura da celulose apresenta duas regiões distintas, a cristalina e amorfa, e a proporção dessas regiões dependerá de sua origem (LEE R. LYND, PAUL J. WEIMER, WILLEM H. VAN ZYL,

2002; PERCIVAL ZHANG; HIMMEL; MIELENZ, 2006; SUKUMARAN; SINGHANIA; PANDEY, 2005).

A hemicelulose é um heteropolissacarídeo que pode apresentar na sua estrutura uma variedade de resíduos de açúcares, incluindo D-xilose, D-manose, D-glicose, D-galactose e L-arabinose. A xilana é o segundo principal componente da holocelulose e mais abundante dentre as hemiceluloses. É um heteropolissacarídeo que possui uma estrutura muito variada, mas basicamente consiste de uma cadeia principal de β-1,4-xilose, e grupos laterais como resíduos de L-arabinofuranosil com ligações do tipo α-1,2 ou α-1,3 e resíduos de ácido 4-O-metil-glicurônico. As cadeias laterais podem ser estendidas, onde os resíduos de arabinofuranosil podem possuir substituintes adicionais, como o ácido-ρ-cumárico e o ácido ferúlico. Além disso, os resíduos de xilose na cadeia principal podem ser acetilados. As xilanas podem ser classificadas em arabinoxilana, glicuronoxilana e glicuronoarabinoxilana. As arabinoxilanas possuem grandes quantidades de resíduos de L-arabinofuranosil. As glicuronoxilanas possuem o ácido-4-O-metil-glicurônico como cadeia lateral e podem ser acetiladas. As glicuronoarabinoxilanas possuem na sua cadeia lateral o ácido-4-O-metil-glicurônico e de L-arabinofuranosil, e não são acetiladas (DODD; CANN, 2009; MINIC; JOUANIN, 2006; POLIZELI et al., 2005).

O segundo polímero mais encontrado no grupo das hemiceluloses é a manana. Ela pode ser dividida em quatro grupos: manana linear, glicomanana, galactomanana e galactoglicomana. Todas elas possuem uma cadeia principal de resíduos de D-manose, podendo se intercalar com resíduos de D-glicose e D-galactose. As mananas lineares são homopolissacarídeos compostos de cadeias lineares de β-D-manopiranosil e contêm menos de 5% de galactose. As galactomananas são constituídas de uma cadeia de resíduos de β-D-manopiranosil com ligações do tipo β-1,4, e possuem cadeias laterais de resíduos de α-D-galactopiranosil com ligações do tipo α-1,6. As glicomananas possuem uma cadeia principal de β-D-manopiranosil e β-D-glicose, intercaladas numa taxa de três de manose para um de glicose, e um grau de polimerização maior que 200. As galactoglucomananas possuem a cadeia composta de β-D-manopiranosil, β-D-glicose α-D-galactopiranosil intercaladas numa proporção de 3:1:1, respectivamente (MOREIRA; FILHO, 2008).

Outra importante hemicelulose é a xiloglucana. Como a celulose, a xiloglucana possui uma cadeia principal de D-glicopiranose com ligações do tipo β-1,4 e possui ramificações de α-D-xilosil na posição C6. Os resíduos xilosil podem ser também substituídos por galactosil, fucosil, e/ou arabinosil, para formar cadeias oligoméricas laterais. Uma das principais características da xiloglucana é sua capacidade de formar associações fortes não-covalentes com a celulose (PAULY et al., 1999).

As pectinas formam outro grupo de heteropolissacarídeos e consistem de uma cadeia principal de resíduos de ácido galacturônico com ligações do tipo α-1,4. Elas possuem duas regiões distintas, as regiões "não densas" onde a cadeia pode ser acetilada em O-2 e O-3 e metilada em O-6; e regiões específicas "densas", que possuem duas estruturas diferentes, uma onde o ácido galacturônico da cadeia principal é interrompido por resíduos de L-ramnose com ligações do tipo α-1,2 formando a ramnogalacturônica e outra onde há resíduos de D-xilose, formando a xilogalacturônica. As longas cadeias laterais consistem principalmente de resíduos de L-arabinose e alguns resíduos de D-galactose podem estar ligados aos resíduos de ramnose. Em algumas determinadas pectinas, o ácido ferúlico pode estar presente como um resíduo terminal ligado ao O-5 do resíduo de arabinose ou ao O-2 do resíduo de galactose (DE VRIES et al., 2001; JAYANI; SAXENA; GUPTA, 2005).

A lignina é um complexo polifenólico que confere rigidez a planta, além de ser essencial para a integridade da parede celular, impermeabilizando-a, e protegendo contra ação de patógenos e enzimas hidrolíticas. É formada por três monômeros de álcool hidroxicinamil, que diferem apenas no nível de metoxilação, os ácidos p-cumaril (dando origem a lignina H), coniferil (dando origem a lignina G) e sinapil (dando origem a lignina S). Estes monômeros formam respectivamente os p-hidroxifenil, guaiacil e siringil fenilpropanóides, quando incorporados à lignina (BOERJAN; RALPH; BAUCHER, 2003; DE SIQUEIRA et al., 2010). A xilose pode formar ligação cruzada com a lignina através dos resíduos de L-arabinofuranosil, que podem também ser esterificados com ácidos ferúlicos ou p-cumáricos (MINIC; JOUANIN, 2006).

1.1.2 Degradação da parede celular

As enzimas que degradam a parece celular são agrupadas e classificadas pelo banco de dados CAZy (Carbohydrate-Active enZYmes Database – http://www.cazy.org).

A maior parte dessas enzimas, ativas em carboidratos, são glicosídeo hidrolases (EC 3.2.1.-) e sua nomenclatura é baseada tanto em sua especificidade ao substrato quanto ao mecanismo molecular. Sua classificação por famílias se baseia na sequência de aminoácidos. As enzimas que compõem as famílias normalmente possuem estruturas terciárias únicas e muito similares, principalmente no sítio ativo (HENRISSAT et al., 1995). A quebra da ligação glicosídica pelas glicosídeo hidrolases (GH) se dá por dois mecanismos ácido/base: retenção dupla ou inversão da configuração anomérica no ponto de clivagem, com envolvimento de um intermediário glicosil oxicarbônico (MCCARTER; STEPHEN WITHERS, 1994).

Existem três classes de enzimas envolvidas na degradação hidrolítica da celulose: endoglicanases (EG) (EC 3.2.1.4), que hidrolisam regiões internas amorfas da cadeia principal, gerando oligossacarídeos de vários tamanhos; celobiohidrolases (CBH) (EC 3.2.1.91), que atuam nas extremidades não-redutoras e redutoras da cadeia de celulose, liberando celobiose; e β-glicosidades (EC 3.2.1.21), que hidrolisam celobiose em glicose (DE VRIES et al., 2001; LEE R. LYND, PAUL J. WEIMER, WILLEM H. VAN ZYL, 2002; PERCIVAL ZHANG; HIMMEL; MIELENZ, 2006; SUKUMARAN; SINGHANIA; PANDEY, 2005).

As enzimas que hidrolisam a xilana podem ser divididas em duas categorias: as que degradam a cadeia polissacarídea principal, endo-β-1,4-xilanase (EC 3.2.1.8) e β-xilosidases (EC 3.2.1.37); e enzimas que liberam grupos laterais, as enzimas acessórias, que incluem α-glucuronidase (EC 3.2.1.139), arabinofuranosidase (EC 3.2.1.55), acetilxilana esterase (EC 3.1.1.6), feruloil esterase (EC 3.1.1.73) e ácido ρ-cumárico esterase (EC 3.1.1.-). As endo-β-1,4-xilanase clivam as ligações glicosídicas da estrutura principal da xilana. Esta clivagem não é aleatória, depende da natureza do substrato, do tamanho da cadeia, do grau de ramificação e presença de substituintes. As β-xilosidases podem ser classificadas de acordo com suas afinidades relativas para xilobiose e xilooligossacarídeos, quanto maior o xilooligômero, menor sua afinidade. As acetilxilana esterases removem os grupos O-acetil das posições 2 e 3 do resíduo de β-D-xilopiranosil. As L-arabinases atuam retirando os resíduos de L-arabinose de duas maneiras, clivando arabinanas ramificadas (exo-α-L-arabinofuranosidase – EC 3.2.1.55) ou arabinanas lineares (endo-1,5- α-L-arabinase EC 3.2.1.99). As α-glucuronidases clivam a ligação α-1,2 entre o resíduo do ácido glicurônico e de β-D-xilopiranosil. As duas esterases, feruloil

e ácido ρ-cumárico, clivam as ligações éster; a primeira cliva entre a arabinose e o ácido ferúlico, a segunda entre a arabinose e o ácido ρ-cumárico (DODD; CANN, 2009; POLIZELI et al., 2005).

As xiloglucanases (EC 3.2.1.151) são enzimas ativas em xiloglucana e capazes de hidrolisar a ligação β-1,4 dos resíduos de glicopiranosil, mesmo quando eles possuem ramificações. Apesar da estrutura da xiloglucana ser semelhante à celulose, os grupos laterais formam uma barreira para a ação das EG. Porém, há algumas EG que são ativas em xiloglucana, especificamente no resíduo onde não há ramificação (BENKO et al., 2008; VLASENKO et al., 2010).

A degradação da cadeia principal de galacto(glico)manana depende da ação da β-endomananases (EC 3.2.178) e β-manosidades (EC 3.2.1.25). As β-endomananases hidrolisam a cadeia principal, liberando manooligosacarídeos. Sua habilidade em hidrolisar galactomananas e galactoglicomananas depende de vários fatores, como número e distribuição dos substituintes da cadeia e a conteúdo de glicose. Elas são mais ativas em galactomananas com poucos substituintes em sua cadeia principal e liberam basicamente manobiose e manotriose. As β-manosidades são enzimas exo-ativas, liberando manoses da região terminal não redutora dos manooligosacarídeos. A degradação completa da cadeia de galacto(glico)manana depende também da ação de β-glicosidades, acetilmanana esterase (EC 3.1.1.6) e a α-galactosidase (EC 3.2.1.22) (DE VRIES et al., 2001; MOREIRA; FILHO, 2008).

As enzimas que degradam a pectina podem ser divididas em três grupos, as despolimerases, esterases e protopectinases. As despolimerases degradam a substância péctica através de dois mecanismos, pela hidrólise ou por lise trans-eliminatória, e podem ser divididas em quatro grupos: poligalacturonase e polimetilgalacturonase que atuam através da hidrólise, podendo ser exo- (EC 3.2.1.67) ou endo- (EC 3.2.1.15); e poligalacturonato liase e polimetilgalacturonato liase, podendo ser exo- (EC 4.2.2.9) ou endo- (EC 4.2.2.2). As pectinaesterases (EC 3.1.1.11) desesterificam as ligações metil-éster da cadeia de galacturonana, liberando pectinas ácidas e metanol. As protopectinases clivam a pectina insolúvel, tornando-a solúvel (JAYANI; SAXENA; GUPTA, 2005).

1.2 Novo paradigma da conversão de celulose

A visão clássica da degradação da celulose envolve a ação sinérgica de três enzimas: i) Endo-1,4-β-glicanase; ii) Exo-1,4-β-glicanase; iii) β –glicosidase. Essas enzimas atuam de maneira sinérgica através da ação de enzimas do tipo endo, que geram novos finais redutores e não redutores para a ação das exos; estas liberam celobiose, que são convertidas em glicose pelas β-glicosidases. Sistemas celulolíticos contêm vários tipos de exo e endo, com preferências variadas para as diferentes formas de celulose. Todas essas enzimas são hidrolases, ou seja, atuam na quebra da ligação glicosídica através da adição de uma molécula de água. Apesar dessas enzimas serem essenciais para a degradação efetiva da celulose, a processividade das hidrolases é muito lenta, comparada a outros tipos de enzimas (HORN et al., 2012).

Em 2010, a descoberta da quebra oxidativa da quitina mudou o paradigma da conversão de celulose, por demonstrar a presença de enzimas não hidrolíticas presentes nessa conversão, introduzindo regiões oxidadas nas extremidades redutoras e não-redutoras na cadeia de quitina (VAAJE-KOLSTAD et al., 2010). O modelo atual considera que o consórcio celulolítico apresenta, além das três enzimas clássicas da conversão, duas enzimas oxidativas: as monooxigenases líticas de polissacarídeos (LPMO), que oxidam porções C-1 e C-4 da celulose na cadeia principal e geram celo-oligossacarídeos (possibilitando a ação das celobiohidrolases); e as celobiose desidrogenases (CBDH), que atuam oxidando as porções terminais das celobiose, captando esses elétrons e doando para as monooxigenases. Dessa forma, as cinco enzimas do consórcio celulolítico apresentam uma ação orquestrada e coordenada, com uma ação sinergética para alcançar uma alta eficiência na degradação da celulose (HORN et al., 2012).

1.2.1 Monooxigenases líticas de polissacarídeos (LPMO)

As LPMOs são agrupadas de acordo com o CAZy (Carbohydrate-Active enZYmes Database – www.cazy.org) como “AA” (atividade auxiliar). Existem 14 classes de AA, onde cinco são LPMOs – AA9, AA10, AA11, AA13 e AA14. A família AA9, antigamente classificada como GH61, é encontrada em fungos, enquanto a família

correlata para as bactérias é a AA10 (antigamente classificada como CBM33). As famílias AA11, AA13 e AA14 apresentam atividade oxidativa em quitina, amido e xilana, respectivamente (COUTURIER et al., 2018; HEMSWORTH et al., 2015). A família AA9 é amplamente distribuída entre os fungos, principalmente basidiomicetos e ascomicetos. Estudos recentes (HARRIS et al., 2010; KRACHER et al., 2016) mostraram que há, além da prevalência de genes de LPMOs em mais de 90% dos genomas fúngicos analisados, a presença de vários genes de LPMOs no mesmo organismo, indicando que a presença dessas enzimas é crucial para a degradação da biomassa (DIMAROGONA; TOPAKAS; CHRISTAKOPOULOS, 2012; JAGADEESWARAN et al., 2016; MONCLARO; FILHO, 2017)

O modelo de mecanismo de ação sugerido para as LPMOs mais aceito atualmente foi proposto por Kjaergaard (KJAERGAARD et al., 2014) e Kim (KIM et al., 2014). Resumidamente, na presença de O_2 e com a doação de dois elétrons livres, há a formação de um intermediário cobre-oxil responsável por hidroxilar o substrato e desestabilizar e quebrar a ligação glicosídica por uma reação de eliminação. Porém estudos recentes demonstraram que o H_2O_2, ao invés do O_2, é o co-substrato preferido pela enzima (BISSARO et al., 2017), indicando que o modelo do mecanismo de ação deve ser reconsiderado.

A estrutura tridimensional das LPMOs é muito similar entre as diferentes famílias. Elas compartilham uma estrutura terciária semelhante ao domínio da imunoglobulina (Ig) e da fibronectina tipo III (FnIII): módulo β-sanduíche, formado por sete a nove folhas β antiparalelas em estrutura "Greek Key", às vezes acompanhada por alfa-hélices (HEMSWORTH et al., 2013; SPAN; MARLETTA, 2015). Os domínios apresentam 3 "loops": o L2, próximo ao N-terminal, que faz uma ligação dissulfídica com a folha β8; o LC, na região C-terminal, é uma região flexível sem presença de estruturas secundárias; e LS, que forma interações hidrofóbicas com o "loop" LC e é muito flexível (figura 2-A) (WU et al., 2013). O sítio ativo é formado por uma região plana chamada "braço de histidina" que possui a presença de dois resíduos de histidina conservados: uma como primeiro aminoácido na porção N-terminal (que pode ser metilada ou não) e outra localizada posteriormente. Ambos aminoácidos estão envolvidos na coordenação do íon de cobre. Além disso, há a presença de um resíduo de tirosina, que ocupa uma posição

axial mais afastada, e seu grupo fenol também ajuda a estabilizar o sítio (figura 2-B e 2-C) (BORISOVA et al., 2015; WU et al., 2013).

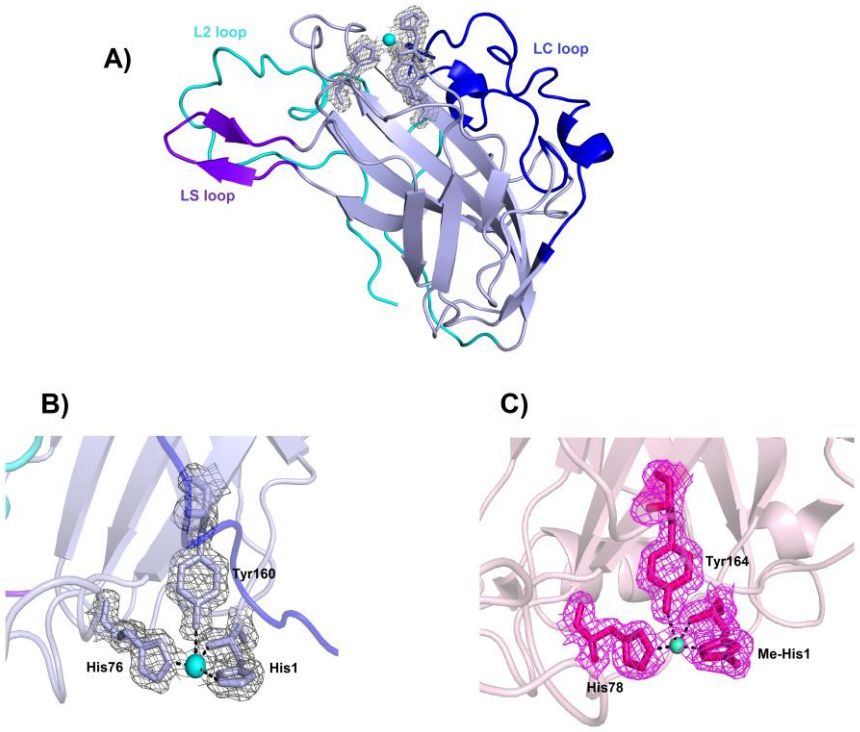

Figura 2. Estruturas tridimensionas das LPMOs da família AA9. **A)** Estrutura da enzima PchGH61D de *Phanerochaete chrysosporium*, com o cobre representado como uma esfera azul; **B)** Mapa eletrodenso do sítio catalítico de PchGH61D; **C)** Mapa eletrodenso do sítio catalítico da enzima LsAA9 de *Lentinus similis*, com a histidina N-termina metilada. Retirado de (MONCLARO; FILHO, 2017).

As AA9 podem ser divididas em três grupos de regioseletividades para a hidroxilação: tipo 1 (LPMO1), que hidroxila o carbono C1; tipo 2 (LPMO2), que hidroxila o carbono C4; e tipo 3 (LPMO3), que hidroxila os carbonos C1 e C4 (VU et al., 2014b). Apesar das implicações funcionais dessas variações não terem sido completamente elucidadas, sabe-se que para as LPMO1, há uma tirosina na superfície da enzima que se liga ao substrato, dificultando o acesso a essa região; as LPMO2 possuem ou alanina ou aspartato, que permitem maior permissividade da enzima ao substrato; e as LPMO3 possuem uma prolina no lugar da tirosina, sendo um intermediário entre as LPMO1 e LPMO2 (BORISOVA et al., 2015).

Os CBMs são domínios independentes que normalmente apresentam superfícies planas contendo aminoácidos hidrofóbicos que interagem com o substrato; eles estão ligados ao domínio catalítico através de *linkers*, que podem apresentar uma composição variável. Sabe-se que os CBMs possuem diferentes papéis na degradação da biomassa, incluindo o reconhecimento dos polissacarídeos, determinando a especificidade ao substrato, aumentando a eficiência enzimática e, de certa forma, podendo causar algum tipo de clivagem no substrato (ABBOTT; VAN BUEREN, 2014; GILBERT; KNOX; BORASTON, 2013). Os fungos costumam apresentar múltiplos genes de AA9, sendo que alguns deles possuem CBM. Porém, existem muitas questões sobre CBMs que precisam ser elucidadas, como o que está guiando e determinando a especificidade de ligação e como exatamente os módulos afetam a eficiência enzimática. Vários estudos indicam que os CBMs também aumentam a atividade das LPMOs, dessa forma auxiliando também na maior degradação da celulose (BENNATI-GRANIER et al., 2015; BORISOVA et al., 2015; HU; ARANTES; PRIBOWO, 2014).

1.3 O fungo filamentoso *Aspergillus tamarii*

Os fungos são componentes de um grupo de eucariotos morfologicamente complexos e amplamente distribuídos na natureza, onde possuem um papel importante como decompositores biológicos. Dentre os fungos, os Ascomicetos e Basidiomicetos saprófitos são os mais eficientes na decomposição da biomassa lignocelulósica e conseguem se adaptar a diferentes fontes de carbono e nitrogênio (BOUWS; WATTENBERG; ZORN, 2008). O filo Ascomiceto se diferencia dos outros por sua reprodução, onde há produção de esporos em ascos (esporângios). A maior parte dos Ascomicetos são filamentosos, ou seja, exibem formas estruturais distintas durante seu ciclo de vida. A estrutura vegetativa básica é a hifa, um filamento tubular originado da germinação do esporo reprodutivo. O crescimento da hifa produz micélios. Quando o micélio se encontra em culturas líquidas, ele apresenta diferentes formas, entre filamentos de micélios dispersos a massas miceliais densas (PAPAGIANNI, 2004).

A habilidade dos fungos filamentosos em decompor o substrato é explorada em várias áreas das indústrias biotecnológicas. A escolha da linhagem é baseada nas taxas de produções e em questões de biossegurança, como o conceito *GRAS (Generally Regarded as Safe)*. As vantagens das utilizações dos fungos filamentosos são o seu potente sistema

de secreção protéica, que é superior ao de bactérias e leveduras; não formação de corpúsculos de inclusão; realização de modificações pós-traducionais; facilidade de cultivo; boa capacidade de fermentação e um nível alto de produção proteica (DE VRIES et al., 2001; GRIMM et al., 2005; GUIMARÃES et al., 2006; KULKARNI; SHENDYE; RAO, 1999). Industrialmente, os fungos filamentosos são utilizados para produzir peptídeos recombinantes e metabólitos secundários usados na indústria alimentícia e farmacêutica (ADRIO; DEMAIN, 2003; GHORAI et al., 2011), se destacando os fungos *Aspergillus niger*, *Aspergillus oryzae*, *Aspergillus phoenicis*, *Trichoderma reesei*, *Trichoderma viride*, *Trichoderma konignii*, *Trametes versicolor*, *Rhizopus delemar*, *Aureobasidium pullulans*, *Schizophyllum commune*, *Acremonium chrysogenum*, *Tolypocladium nivenum*, *Claviceps purpurea*, *Monascus rubber*, dentre outros (MEYER, 2008). Na conversão de resíduos agrícolas, o uso de fungos filamentosos pode ser aplicado para obtenção de proteínas de uso industrial, óleos, quitina; além disso, a biomassa fúngica pode ser utilizada no tratamento da água (CHAN et al., 2018), sendo os fungos *T. reesei*, *A. niger*, *Agariscus bisporus*, *Fusarium venenatum* e o gênero *Penicillium* mais comumente utilizados (ARO; PAKULA; PENTTILÄ, 2005; MEYER, 2008).

Dentre o filo Ascomiceto, o gênero *Aspergillus* é um anamórfico que possui 344 espécies oficialmente reconhecidas e existe há mais de 200 milhões de anos. (FRISVAD, 2014). A seção Flavi inclui os fungos relacionados morfologicamente e filogeneticamente, e possui 6 espécies de grande importância econômica, que são subdivididos em dois grupos, dependendo do impacto na indústria alimentíca e saúde humana. O primeiro grupo inclui *Aspergillus flavus*, *A. parasiticus* e *A. nomius*, que contaminam e danificam grãos, castanhas e cereais estocados, além de poderem produzir aflatoxinas. Além disso, *A. flavus* pode causar aspergilose. O segundo grupo é formado por fungos não produtores de aflatoxinas e incluem *A. tamarii*, *A. oryzae* e *A. sojae* (GODET; MUNAUT, 2010). As linhagens de *A. tamarii* são comumente encontradas em plantações de algodão (COTTY, 1997), e apesar de possuir genes de aflatoxina em seu genoma, não é tido como espécie produtora de aflatoxina – a espécie identificada como produtora foi renomeada como *A. pseudotamarii* (ITO et al., 2001). Porém o *A. tamarii* pode produz o ácido ciclopiazínico, micotoxina com menor toxicididade que a aflatoxina (T GOTO, 1996) e que há relatos de ser alergênico (VERMANI et al., 2011). É

reconhecido como um excelente fungo para produção de proteases (ANANDAN; MARMER; DUDLEY, 2007; BOER; PERALTA, 2000), xilanases (EL-GINDY; SAAD; FAWZI, 2015; FARANI DE SOUZA; GIATTI MARQUES DE SOUZA; PERALTA, 2001; GOUDA; ABDEL-NABY, 2002; MONCLARO et al., 2016) e para degradação da cafeína, composto que normalmente é tóxico para microrganismos (GUTIÉRREZ-SÁNCHEZ; ROUSSOS; AUGUR, 2004).

CAPÍTULO 2 – OBJETIVOS

2. Objetivo Geral

O objetivo geral dessa tese de doutorado foi um estudo mais aprofundado do potencial do fungo *A. tamarii* na degradação de biomassa lignocelulósica com foco na caracterização de enzimas com importância industrial, em especial as monooxigenases líticas de polissacarídeos.

2.1 Objetivos específicos

- Estudo da ação das enzimas xilanases e celulases produzidas pelo fungo *A. tamarii* em função de diferentes substratos e diferentes condições de cultivos, visando futura aplicação industrial das enzimas e otimização do meio para o fungo;
- Estudo da interação de uma xilanase de baixa massa molecular em função de diferentes substratos e na presença de um inibidor fenólico, focando em seus parâmetros termodinâmicos;
- Caracterização de duas AA9 de *A. tamarii*, visando futura aplicação em consórcios enzimáticos para processos de conversão da biomassa vegetal:

CAPÍTULO 3 - RESPONSE SURFACE METHODOLOGY AS A TOOL TO EVALUATE CELLULASE AND XYLANASE ACTIVITIES UNDER DIFFERENT CONDITIONS OF CULTURE MEDIA AND LIGNOCELLULOSIC BIOMASS SOURCES

3. Introdução

A utilização de resíduos agroindustriais para o crescimento de fungos filamentosos é de grande interesse, pois os resíduos possuem alto teor de polissacarídeos em sua parede celular, são encontrados de forma abundante na natureza, são fontes renováveis e apresentam potencial aplicação na indústria biotecnológica (DE SIQUEIRA et al., 2010; WONG; TAN; SADDLER, 1988). Um dos fatores que mais influencia a produção das enzimas hidrolíticas pelos microrganismos é seu crescimento. E o crescimento do microrganismo é determinado pela disponibilidade de macronutrientes no meio, principalmente nitrogênio e carbono, mas outros micronutrientes influenciam também, como íons e vitaminas, dente outros (BROWN; RIES; GOLDMAN, 2014). Atualmente há um grande investimento em pesquisas que busquem otimizações que aumentem atividade, estabilidade e especificidade das enzimas, em comparação aos coquetéis comerciais, melhorando o custo-benefício de sua produção e tornando-as mais competitivas comercialmente em relação às catálises químicas (SARROUH et al., 2012). Um entedimento mais profundo do comportamento das enzimas em diferentes condições se faz necessário para uma melhor racionalização delas no uso industrial. Dessa forma, utilização de ferramentas estatísticas são de grande atrativo para estudos envolvendo a produção de enzimas com potencial biotecnológico com foco na hidrólise eficiente de biomassa. O manuscrito foi submetido para a revista *Biocatalysis and Biotransformation* (Online ISSN: 1029-2446).

Response surface methodology as a tool to evaluate cellulase and xylanase activities under different conditions of culture media and lignocellulosic biomass sources

Antonielle Viera Monclaro[a,*], Pedro Ribeiro Fontes[a], Guilherme Lima Recalde[a], Francides Gomes da Silva Jr[b], Edivaldo Ximenes Ferreira Filho[a]

[a] *Enzymology Laboratory, University of Brasília, Campus Universitário Darcy Ribeiro, Brasília - DF, 70910-900, Brazil*

[b] *Laboratory of Chemistry, Cellulose and Energy, Department of Forest Sciences, ESALQ, University of São Paulo, Piracicaba, SP, 13418-220, Brazil*

*Corresponding author at: Enzymology Laboratory, University of Brasília, Campus Universitário Darcy Ribeiro, Brasília - DF, 70910-900, Brazil

E-mail address: antonielle@gmail.com

ABSTRACT

As a better understanding of xylanase and cellulase is required for biotechnological applications, we used the central composite design to evaluate the behavior of these *Aspergillus tamarii* enzymes under different screening conditions and with different carbon sources from agro-industrial wastes. The time course profile of enzyme production with three wastes showed that *Aspergillus tamarii* could produce both enzymes at the highest activity levels at 48 h of growth. The induction effect of each waste, tryptone and $CuSO_4$ supplementation was assessed. The induction profile could be correlated to biomass complexity, with increased biomass recalcitrance yielding greater activity. A 2^2 factorial central composite design was used to evaluate the influence of tryptone and $CuSO_4$ concomitantly. $CuSO_4$ supplementation was advantageous for both enzymes, allowing nitrogen to influence the enzymes. Tryptone strongly affected enzyme activity decreasing cellulase but increasing xylanase activity, suggesting close association of cellulase production with a non-organic nitrogen uptake receptor. Our findings suggest that even small changes in the culture medium can greatly affect enzyme activity, so this should be considered when designing fungal enzyme cocktails.

Keywords: Central composite design; Central composite rotatable design; Sugarcane bagasse; Cotton residue; Cellulose pulp.

1. Introduction

The plant cell wall is a complex structure formed by different polysaccharides. Cellulose, hemicellulose and lignin are arranged in an organized and recalcitrant configuration that constitutes one of the limiting factors to enzymatic deconstruction (de Siqueira, E.G. de Siqueira, et al. 2010). In Brazil, sugarcane is the most used biomass for energy generation. However, current research is also interested in sugarcane

bagasse, the fibrous residue remaining after the extraction of sugarcane juice, considering the potential to generate value-added products from its cell wall breakdown (Lima et al. 2014). Other lignocellulosic materials as agro-industrial wastes also present potential to generate energy and value-added products, e.g., cellulosic pulps from eucalyptus (Tonoli et al. 2012) and cotton (de Siqueira, E.G. de Siqueira, et al. 2010). However, the amount of agro-industrial waste produced from agriculture and its disposal is sufficient to influence the environment and human health (Lima et al. 2014). Therefore, studies on the use of a given biomass require innovation and extensive research, as other biomass sources carry potential to produce value-added products.

The fungi of *Aspergillus* species are efficient biomass decomposers and large producers of glycoside hydrolases. In particular, several studies in the literature relate to the production of glycoside hydrolases by *Aspergillus tamarii*, including presenting its potential for biotechnological applications (Boer & Peralta 2000; Gutiérrez-Sánchez et al. 2004; Heinen et al. 2018). The growth of the microorganism constitutes one of the main factors that influence the production of hydrolytic enzymes, with its growth determined by available macronutrients, primarily carbon and nitrogen, as well as micronutrients such as ions and vitamins (Brown et al. 2014). Currently, there is marked interest in studies that investigate the optimization of enzymes for biomass degradation (Sarrouh et al. 2012). Thus, studies focusing on approaches that will lead to a better understanding of enzyme activity profiles against different conditions are of considerable interest for biotechnological applications. The objective of the present study was to explore central composite design as a tool to achieve a better understanding of xylanase and carboxymethyl cellulase (CMCase) production from *A. tamarii*, aiming on the development of more efficient forms of enzymatic saccharification of lignocellulosic biomass.

2. Results and discussion

2.1 Screening in different agro-industrial wastes and different media-composition

From the time course profile of enzyme production with three wastes (Sugar cane bagasse [SB], dirty cotton residue [DC] and dark cellulose pulp [DP]), *A. tamarii* could produce both enzymes at highest activity levels at 48 h of growth (Fig S1). Based on this time of growth, enzyme activities were evaluated using six agro-industrial wastes. Aiming to assess the induction potential of each waste to fungus growth and enzyme production, a comparison of the induction capacity of these residues was performed using One-Way ANOVA and Tukey's test (Fig. 1-A).

According to the statistical analysis performed, the waste that most induced xylanolytic activity was DP, followed by SB, CC (clean cotton residue), DC, FP (filter powder), and WP (white cellulose pulp). All displayed different inductions capacities, even when their content was quite similar, such as DP and WP (cellulosic wastes) and CC, DC, and FP (textile wastes). Moreira et al. (Moreira et al. 2012) showed that dark cellulosic pulp presented recalcitrance for hydrolysis by two xylanases from *Aspergillus terreus*, whereas hydrolysis of the white pulp occurred in a short period. This might explain the higher induction capacity for DP compared to WP, as DP comprises a more recalcitrant and complex carbon source than WP, requiring higher enzyme activities for its degradation. For CMCase, DC was the residue that induced the highest enzyme activity, followed by DP, SB, CC and FP, with WP being the lowest inducer. Similar results were obtained with *Pleorotus ostreatus* (de Siqueira, A.G. de Siqueira, et al. 2010) and *Acrophialophora nainiana* (Silveira et al. 2014), with higher cellulase activity achieved using DC as the carbon source.

To evaluate how nutritional factors may influence the production of hydrolytic enzymes during fungal growth, it was evaluated whether tryptone could affect enzymatic production, as an organic tryptophan-rich source of nitrogen compared to $(NH_4)_2SO_4$ (Medium-1), or whether supplementation with $CuSO_4$ (Medium-2) could affect enzyme production and/or activity. Figure 1-B shows the activities of xylanase and CMCase in the different media. Xylanase activity from DP was increased in Media-2 whereas activity

was strongly inhibited in SB and WP. For DC, CMCase was highly activated in Medium-1 and Medium-2 whereas for xylanase the media did not appear to affect enzyme activity. Conversely, CMCase from FP was inhibited with Medium-1 and Medium-2. Although it is reported in the literature that organic nitrogen sources increase enzyme activity compared to inorganic sources (George et al. 2001), in the present experiment no enzyme was substantially influenced by Medium-1, except for CMCase from DC and FP. Moreover, Medium-2 inhibited two xylanases and one CMCase, which may be due to copper toxicity.

A study conducted by Chen et al. (Chen et al. 2003) demonstrated that values greater than 200 µmol l^{-1} decreased biomass production, with no effect in enzymatic activity. And Vasconcellos et al. (Vasconcellos et al. 2016) demonstrated that addition of 200 µmol l^{-1} $CuSO_4$ during hydrolyses of *A. niger* on sugarcane bagasse at final concentration of 5% increased endoglucanase activity due to decrease of non-productive adsorption of enzymes onto lignin. Lignin can act not only as a barrier to the enzymes but can also support their non-productive adsorption (Siqueira et al. 2017). Considering our results and those from the literature, and assuming that tryptone and copper did increase enzyme activity and the inorganic source did not, we hypothesized that, as the lignocellulose biomass used in this study constitute complex carbon sources with different levels of lignin, and the final concentration used was 1% (w/v), a non-productive enzyme adsorption to lignin may have occurred. We decided to combine the factors to analyze their influence on xylanase and CMCase activities.

2.2 Experimental design to assess combined factor effects

Central Composite Design (CCD) was used to evaluate the influence of these two factors (tryptone and $CuSO_4$) concomitantly on CMCase, using a 2^2 factorial experiment with a central point and two levels for each factor. For xylanase, the CCD model was not adequate to predict the enzyme behavior owing to lack of fit of the model; hence, the

Central Composite Rotatable Design (CCDR) was used with a central point and three levels for each factor.

2.2.1 CCD

Tables S1 and S2 shows that all models were considered significant. Tryptone, $CuSO_4$, and their interaction were also significant, implying that these three variables describe the model. The contour plot of CCD constitutes the graphical representation of this regression equation and is represented in Fig. 2. The highest amount of $CuSO_4$ (24 µmol l^{-1}) and minimum value of tryptone (0.05%) were found to be ideal values to activate CMCase activity in the six different carbon sources. The minimum levels of $CuSO_4$ and tryptone (0.0 µmol l^{-1} and 0.05%, respectively) reveal the lowest values of CMCase activity to all wastes but SB, that the lowest value for CMCase was found with 0.0 µmol l^{-1} and 0.2% of $CuSO_4$ and tryptone, respectively. For tryptone, it could be seen that for DP and WP, the increase of nitrogen level slightly increased the enzyme activity. For SB, FP, and CC the enzyme activity remained minimal regardless of the nitrogen level. For DC, the minimum level of $CuSO_4$ and maximum of tryptone also displayed higher CMCase activity. These results indicate that, for all but DC, the increase of tryptone is not ideal for CMCase activity. The effect of nitrogen in cellulase activity has been previously reported, demonstrating that higher levels of organic and inorganic nitrogen inhibited cellulase production (Pedri et al. 2015). However, for DC the amount of tryptone was also crucial for the CMCase activity. This might have occurred because the content of nitrogen in the biomass was not sufficient for retain high enzyme activities, as it is known that cellulase activity and production are very sensitive to nitrogen levels in the medium (Pedri et al. 2015). And the highest activity with higher levels of Cu^{2+} might be due to decreasing the non-productive enzyme adsorption to lignin, as has been previously observed (Vasconcellos et al. 2016).

2.2.2 CCRD

Tables S3 and S4 shows that the models for all carbon sources were significant and that none presented lack of fit. However, the variables that describe the model were different for each carbon source. Notably, all sources shared significance tryptone^2, implying that small changes in tryptone levels may influence the enzymatic activity. For all but SB, $(CuSO_4)^2$ had the same effect. CCRD is represented in Fig. 3. It can be seen that the average values of $CuSO_4$ (14 µmol l^{-1}) and tryptone (0.11%) were found to be ideal to increase xylanase activity in DP, FP, CC, and DC; with the opposite occurring for WP, in which those average values displayed the lowest xylanase activity. For SB, the average value of tryptone (0.11%) and the highest value of $CuSO_4$ (24 µmol l^{-1}) constituted the ideal. These average values of tryptone reveal that, for all but WP, 0.1% represents ideal for xylanase, as it was described before (Kachlishvili et al. 2006). Notably, the presence of $CuSO_4$ activated xylanase activity, especially for SB, where the highest value of $CuSO_4$ was ideal.

2.2.3 CMCase and xylanase profiles using optimization for factorial planning

Based on the last results obtained, we concluded that not only the carbon source impacted directly on enzyme activity, but also the nitrogen source and the supplementation with copper. We used the numeric prediction of the optimization obtained from each model to justify the behavior of each enzyme in different conditions, as can be seen in Table 1 for CMCase and Table 2 for xylanase. The criterion from the values tested were as follows: for tryptone the interval was 0-0.2%; for $CuSO_4$, the interval was 0-24 µmol l^{-1}. The behavior was assessed based on the increase of each factor. Based on the results it can be assumed that for xylanase the concentration of the tryptone affected its activity because increasing of tryptone was positive for all sources, except DP. The discrepant results for DP and CC may be due to the influence of biomass composition on the enzyme activity, considering that the role of the components of the medium in the enzyme activity depend not only on the nitrogen uptake but also on the lignocellulosic substrate (Kachlishvili et al. 2006). As can be seen in Fig. 3, even without

tryptone (0%), xylanase activity remained higher. For CMCase, the enzyme production was impaired by the presence of tryptone whereas for xylanase the opposite was observed. Studies conducted to optimize both cellulolytic and xylanolytic activities from crude extract showed that when using only inorganic (Jatinder et al. 2006; Pedri et al. 2015) or organic (Gomes et al. 2000) nitrogen sources, the amount of nitrogen to achieve optimized enzyme activities was the same. Conversely, the results found in the present study reflect a contradictory optimization, implying that CMCase production from this fungus may be related to an ability for nitrogen uptake from non-organic sources, as tryptone was the only nitrogen source present.

Finally, the supplementation with $CuSO_4$ was beneficial for both enzymes, with higher values for CMCase (near 24 µmol l^{-1}) than xylanase (near 14 µmol l^{-1}). The effect of increasing enzyme activity may be due to several factors including the effect of Cu^{2+} in decreasing the non-productive enzyme adsorption to lignin; and the synergism of enzymes with copper-containing enzymes, as LPMOs, considering that supplementation of $CuSO_4$ could activate the copper-containing enzymes produced by *A. tamarii*. It should be noted that lignocellulose biomass normally does not present sufficient copper ions (Reza et al. 2013); although presents compounds that can act as electron donors such as biomass-derived soluble compounds and phenols derived from lignin (Hu et al. 2014). In this case, the synergism of the enzymes may be related to such activation with copper.

It may be noted that for each carbon source, xylanase and CMCase underwent different effects depending on the variable levels. As the enzymes can act differently owing to fewer variables and it is known that different components and conditions can affect not only the physiology of the fungi but also the enzyme behavior (Kachlishvili et al. 2006; Brown et al. 2014), additional variables (e.g., pH, temperature, size of inoculum, supplementation of other ions and micronutrients, other sources of nitrogen, agitation, or presence of light) must be studied to evaluate whether the effects generated are more related to characteristics of the enzymes than to the induction of biomass.

The approach of screening enzyme activity using different parameters such as intervals of fungal growth, different residues as the carbon source, and different media composition requires the conducting of specific studies regarding deconstruction of biomass. Our findings further demonstrate that for the design of enzymatic cocktails aiming at biomass degradation, composition and supplementation of the culture medium must be analyzed for each enzyme producer, as the enzyme may act in different ways depending on small variations of the culture medium. A number of issues remain to be considered, including if the rise and fall of xylanase and cellullase activities is reflective of the level of *A. tamarii* in the media, the decrease of these activities correlates with the depletion of available substrate and the incubation with the fungus liberate industrially useful quantities of sugar.

3. Material and methods

3.1. Materials

Cotton residues were donated by Hantex Resíduos Têxteis Ltda. (Gaspar, Brazil). FP, CC and DC were obtained from different stages of cotton processing, thoroughly described previously (de Siqueira, E.G. de Siqueira, et al. 2010). Samples of DP and WP were obtained from different stages of the kraft process. SB was obtained from a local source. Other chemicals were purchased from Sigma Chemical Co. (St. Louis, MO, USA).

3.2. Organism and enzyme production

A. tamarii was deposited under strain code RCFS6 in the fungal culture collection at the Enzymology Laboratory, University of Brasilia, Brazil (genetic heritage number 010237/2015-1). The strain was also deposited in the bank of microorganisms for control of plant pathogens and weeds of the Brazilian Agricultural Research Corporation (Embrapa). The collection is registered at the World Data Centre for Microorganisms (WDCM), under the code MCPPW 1128. Stocks were maintained at -80 °C in 50% glycerol. The strain was molecularly identified by our group as described previously

(Monclaro et al. 2016). An aliquot (2.5 ml) of spore suspension (10^6 spores ml^{-1}) was inoculated into Erlenmeyer flasks containing 250 ml liquid medium supplemented with 1.0% (w/v) of DC, DP, and SB as carbon sources. The standard liquid medium employed was composed of (w/v) 0.7% KH_2PO_4, 0.2% K_2HPO_4, 0.05% $MgSO_4.7H_2O$, 0.1% $(NH_4)_2SO_4$, and 0.06% yeast extract. The cultures were incubated at 28 °C with constant agitation at 120 rpm for 84 h. Aliquots were collected every 24 h during the 84 h and used to estimate enzymatic activity and protein concentration. Six agro-industrial wastes were selected for in-deep analysis of enzymatic activity: FP, CC, DC, DP, WP, and SB. The inoculation procedure was performed the same as described above. For the screening in different culture media, we employed three different liquid media. Control, the standard liquid medium (described previously); Medium-1 and Medium-2 had the same composition as Control, except the first contained tryptone instead of $(NH_4)_2SO_4$ and the second was supplemented with 12 µmol l^{-1} $CuSO_4$. The inoculation procedure was performed the same as described above.

3.3 Enzyme assays

Enzyme activities were measured as described previously (Monclaro et al. 2016). The experiments were carried out in five replicates. Results were expressed as the means ± standard deviations.

3.4 Experimental design

The experimental design employed CCD and CCRD. The experiment used a factorial design of 2^2 with a central point and two independent variables (tryptone and $CuSO_4$). For CMCase, CCD was applied with two levels for each factor and three replicates at the central point. For xylanase, CCRD was applied with three levels for each factor and five replicates at the central point. The selected range for independent variables for CMCase was 0.05-1 % for tryptone and 0.012-0.024 mmol $^{-1}$ for $CuSO_4$; for xylanase was 0.085-1.35 % for tryptone and 0.008-0.022 mmol $^{-1}$ for $CuSO_4$. The response was IU ml^{-1}. The setups for CMCase and xylanase activities were 27 and 39 experimental trials,

respectively. Variables effects over the response, mathematic modeling, plot generation, and statistical significance analyses of the experimental designs were performed using Design-Expert software 11 (State-Ease, Inc., Minneapolis, MN, USA).

3.5 Statistical analysis

Statistical comparisons were carried out using the software R 3.3.2 (R Foundation for Statistical Computing, Vienna, Austria) (Team 2008). Carbon source comparison data were submitted to ANOVA with post hoc Tukey's pairwise comparisons when needed. Inter-media comparison was performed with ANOVA with a post-hoc Dunnett's test for control-group comparison. A Shapiro-Wilk normality test was previously performed for all datasets. Significance level was defined at $p < 0.05$.

Acknowledgments

The authors acknowledge the receipt of financial support from the Brazilian National Council for Scientific and Technological Development (CNPq), Coordination for the Improvement of Higher Education Personnel (CAPES), the Foundation for Research Support of the Federal District (FAPDF), and the National Institute for Science and Technology of Bioethanol.

Conflict of interest

The authors declare that they have no competing interests.

References

Boer CG, Peralta RM. 2000. Production of extracellular protease by Aspergillus tamarii. J Basic Microbiol. 40:75–81.

Brown NA, Ries LNA, Goldman GH. 2014. How nutritional status signalling coordinates metabolism and lignocellulolytic enzyme secretion. Fungal Genet Biol [Internet]. 72:48–63. Available from: http://dx.doi.org/10.1016/j.fgb.2014.06.012

Chen S, Ma D, Ge W, Buswell JA. 2003. Induction of laccase activity in the edible straw mushroom, Volvariella volvacea. FEMS Microbiol Lett. 218:143–148.

George SP, Ahmad A, Rao MB. 2001. A novel thermostable xylanase from Thermomonospora sp.: Influence of additives on thermostability. Bioresour Technol. 78:221–224.

Gomes I, Gomes J, Gomes DJ, Steiner W. 2000. Simultaneous production of high

activities of thermostable endoglucanase and beta-glucosidase by the wild thermophilic fungus Thermoascus aurantiacus. Appl Microbiol Biotechnol [Internet]. 53:461–468. Available from: http://www.ncbi.nlm.nih.gov/pubmed/10803904

Gutiérrez-Sánchez G, Roussos S, Augur C. 2004. Effect of the nitrogen source on caffeine degradation by Aspergillus tamarii. Lett Appl Microbiol. 38:50–55.

Heinen PR, Bauermeister A, Ribeiro LF, Messias JM, Almeida PZ, Moraes LAB, Vargas-Rechia CG, de Oliveira AHC, Ward RJ, Filho EXF, et al. 2018. GH11 xylanase from Aspergillus tamarii Kita: Purification by one-step chromatography and xylooligosaccharides hydrolysis monitored in real-time by mass spectrometry. Int J Biol Macromol [Internet]. 108:291–299. Available from: http://dx.doi.org/10.1016/j.ijbiomac.2017.11.150

Hu J, Arantes V, Pribowo A. 2014. Substrate factors that influence the synergistic interaction of AA9 and cellulases during the enzymatic hydrolysis of biomass. Energy Environ Sci [Internet]. 7:2308–2315. Available from: http://pubs.rsc.org/en/content/articlehtml/2014/ee/c4ee00891j

Jatinder K, Chadha BS, Saini HS. 2006. Optimization of culture conditions for production of cellulases and xylanases by Scytalidium thermophilum using response surface methodology. World J Microbiol Biotechnol. 22:169–176.

Kachlishvili E, Penninckx MJ, Tsiklauri N, Elisashvili V. 2006. Effect of nitrogen source on lignocellulolytic enzyme production by white-rot basidiomycetes under solid-state cultivation. World J Microbiol Biotechnol. 22:391–397.

Lima M a, Gomez LD, Steele-King CG, Simister R, Bernardinelli OD, Carvalho M a, Rezende C a, Labate C a, Deazevedo ER, McQueen-Mason SJ, Polikarpov I. 2014. Evaluating the composition and processing potential of novel sources of Brazilian biomass for sustainable biorenewables production. Biotechnol Biofuels [Internet]. 7:10. Available from: http://www.ncbi.nlm.nih.gov/pubmed/24438499

Monclaro A, Aquino E, Faria R, Ricart C, Freitas S, Midorikawa G, Miller R, Michelin M, Polizeli M. 2016. Characterization of multiple xylanase forms from Aspergillus tamarii resistant to phenolic compounds. Mycosphere. 7:1554–1567.

Moreira LR de S, Ferreira GV, Santos SST, Ribeiro APS, Siqueira FG, Filho EXF. 2012. The hydrolysis of agro-industrial residues by holocellulose-degrading enzymes. Brazilian J Microbiol. 43:498–505.

Pedri ZC, Lozano LMS, Hermann KL, Helm C V, Peralta RM, Tavares LBB. 2015. Influence of nitrogen sources on the enzymatic activity and grown by Lentinula edodes in biomass Eucalyptus benthamii. Braz J Biol [Internet]. 75:940–7. Available from: http://www.scielo.br/scielo.php?script=sci_arttext&pid=S1519-69842015000600940&lng=en&nrm=iso&tlng=en

Reza MT, Lynam JG, Uddin MH, Coronella CJ. 2013. Hydrothermal carbonization: Fate of inorganics. Biomass and Bioenergy [Internet]. 49:86–94. Available from: http://dx.doi.org/10.1016/j.biombioe.2012.12.004

Sarrouh B, Santos TM, Miyoshi A, Dias R, Azevedo V. 2012. Up-To-Date Insight on Industrial Enzymes Applications and Global Market. J Bioprocess Biotech. S4:1–10.

Silveira MHL, de Siqueira FG, Rau M, Silva L da, Moreira LR de S, Ferreira-Filho EX, Andreaus J. 2014. Hydrolysis of sugarcane bagasse with enzyme preparations from *Acrophialophora nainiana* grown on different carbon sources. Biocatal Biotransformation [Internet]. 32:53–63. Available from: http://www.tandfonline.com/doi/full/10.3109/10242422.2013.872634

de Siqueira FG, de Siqueira AG, de Siqueira EG, Carvalho MA, Peretti BMP, Jaramillo PMD, Teixeira RSS, Dias ES, Félix CR, Filho EXF. 2010. Evaluation of holocellulase production by plant-degrading fungi grown on agro-industrial residues. Biodegradation. 21:815–824.

de Siqueira FG, de Siqueira EG, Jaramillo PMD, Silveira MHL, Andreaus J, Couto FA, Batista LR, Filho EXF. 2010. The potential of agro-industrial residues for production of holocellulase from filamentous fungi. Int Biodeterior Biodegrad. 64:20–26.

Siqueira G, Arantes V, Saddler JN, Ferraz A, Milagres AMF. 2017. Limitation of cellulose accessibility and unproductive binding of cellulases by pretreated sugarcane bagasse lignin. Biotechnol Biofuels [Internet]. 10:176. Available from: http://biotechnologyforbiofuels.biomedcentral.com/articles/10.1186/s13068-017-0860-7

Team RDC. 2008. R: A Language and Environment for Statistical Computing. R Found Stat Comput Vienna, Austria [Internet]. Available from: https://www.r-project.org/

Tonoli GHD, Teixeira EM, Corrêa AC, Marconcini JM, Caixeta LA, Pereira-Da-Silva MA, Mattoso LHC. 2012. Cellulose micro/nanofibres from Eucalyptus kraft pulp: Preparation and properties. Carbohydr Polym [Internet]. 89:80–88. Available from: http://dx.doi.org/10.1016/j.carbpol.2012.02.052

Vasconcellos VM, Tardioli PW, Giordano RLC, Farinas CS. 2016. Addition of metal ions to a (hemi)cellulolytic enzymatic cocktail produced in-house improves its activity, thermostability, and efficiency in the saccharification of pretreated sugarcane bagasse. N Biotechnol [Internet]. 33:331–337. Available from: http://dx.doi.org/10.1016/j.nbt.2015.12.002

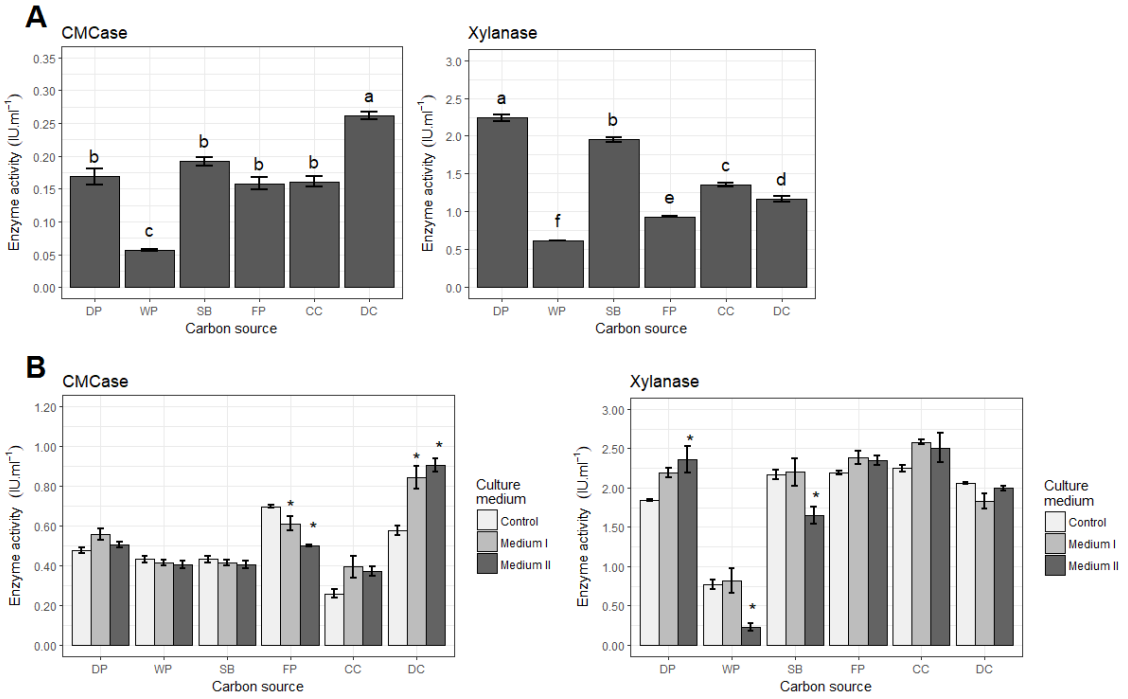

Figure 1. A) Enzymatic profile of *A. tamarii* grown in different agro-industrial wastes. **B)** CMCase activity and xylanolytic activity of Medium-1 and Medium-2 compared to Control. Data presented as mean ± standard error (SE). *Statistically significant difference between the tested medium and control medium within each carbon source group (post-hoc Dunnett's test, α = 0.05).

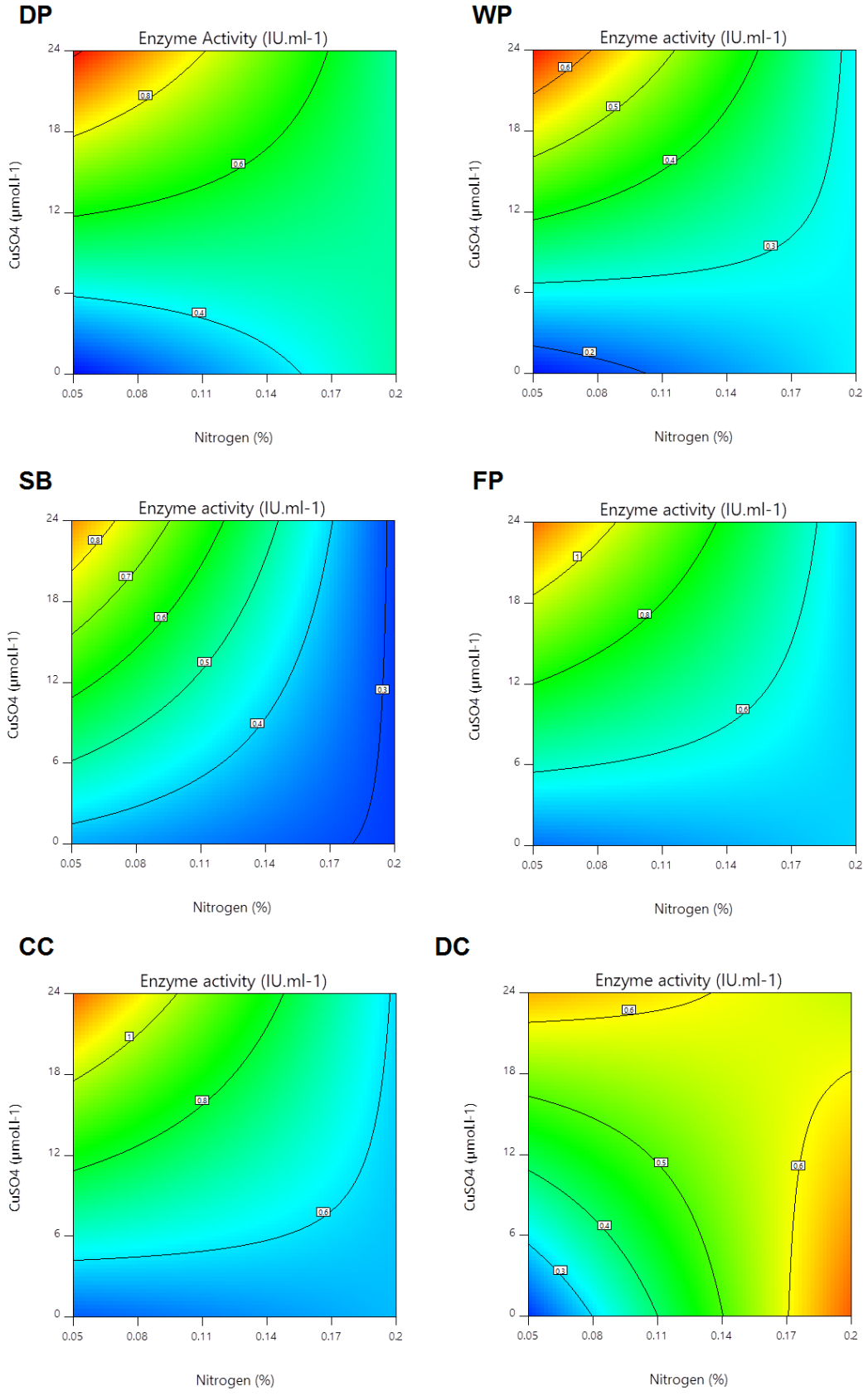

Fig. 2. CCD for cellulolytic activity in different carbon sources**.**

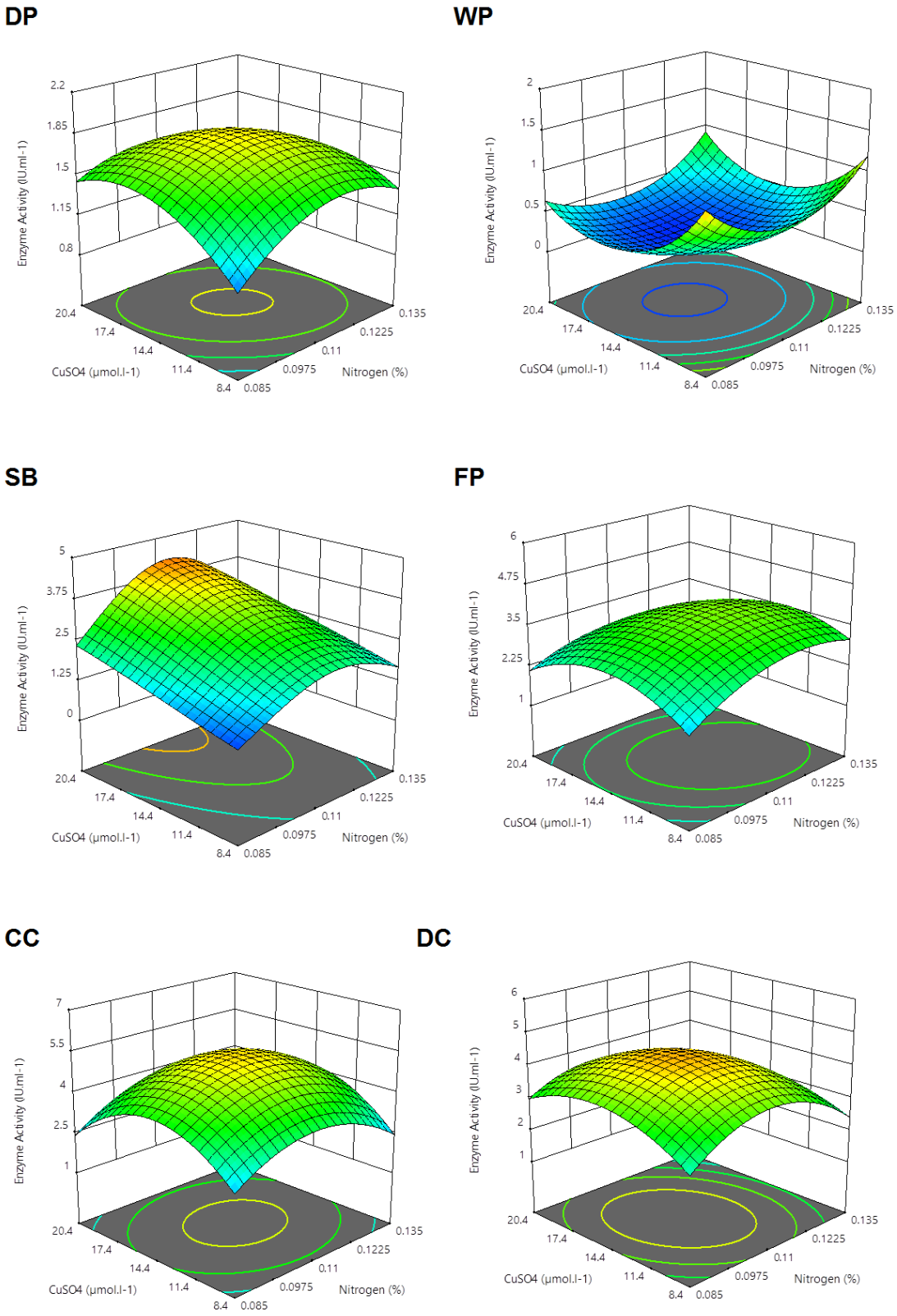

Fig. 3. CCRD of xylanolytic activity in different carbon sources.

Table 1. Effect of the variables over the cellulase activity.

	Effect			Model		Estimated
	↑ Nitrogen	↑ $CuSO_4$	↑ Nitrogen*$CuSO_4$	Nitrogen (0–0.2%)	$CuSO_4$ (0–24 µmol l^{-1})	Enzymatic Activity (IU ml^{-1})
DP	Negative*	Positive*	Negative*	0.002	23.880	1.167
CC	Negative*	Positive*	Negative*	0.004	23.156	0.832
BG	Negative*	Positive*	Negative*	0.002	23.767	1.037
FP	Negative*	Positive*	Negative*	0.001	23.593	1.316
CC	Negative*	Positive*	Negative*	0.000	23.967	1.338
DC	Positive*	Positive*	Negative*	0.012	23.907	0.793

*Statistically significant difference between the tested medium and control medium within each carbon source group (post-hoc Dunnett's test, α = 0.05).

Table 2. Effect of the variables over the xylanase activity.

	Effect					Model		Estimated Enzymatic Activity (IU ml^{-1})
	↑ Nitrogen	↑ $CuSO_4$	↑ Nitrogen*$CuSO_4$	↑ Nitrogen²	↑ $CuSO_4$²	Nitrogen (0–0.2%)	$CuSO_4$ (0–24 µmol l^{-1})	
DP	Positive	Positive	Negative*	Negative*	Negative*	0.111	7.189	1.829
CC	Positive*	Negative*	Positive*	Positive*	Positive*	0.008	0.741	48.216
BG	Positive*	Positive*	Negative	Negative*	Negative	0.111	24.000	0.957
FP	Positive	Negative	Negative	Negative*	Negative*	0.116	13.197	3.948
CC	Positive	Positive	Positive	Negative*	Negative*	0.111	13.904	5.321
DC	Negative*	Negative	Negative	Negative*	Negative*	0.106	13.848	4.396

*Statistically significant difference between the tested medium and control medium within each carbon source group (post-hoc Dunnett's test, α = 0.05).

Supporting Information

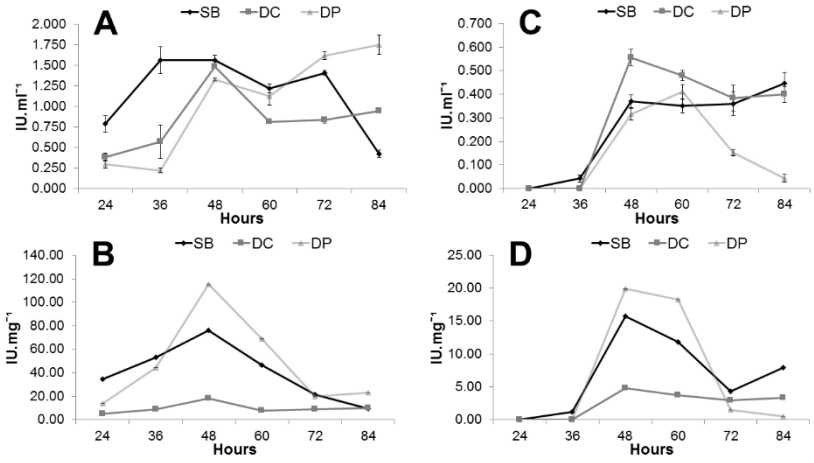

Figure S1. Time course profile of the production of xylanase and CMCase in SB, DC and DP. **A)** Enzymatic activity (IU ml^{-1}) of xylanase; **B)** Specific enzymatic activity (IU mg^{-1}) of xylanase; **C)** Enzymatic activity (IU ml^{-1}) of CMCase; **D)** Specific enzymatic activity (IU mg^{-1}) of CMCase.

Table S1. Analysis of Variance (ANOVA) for the quadratic model generated for CMCase.

Analysis of variance table for DP

Source	SS	DF	MS	F-value	Prob (P) > F
Model	1.028	3	0.343	118.315	<0.0001
Nitrogen	0.047	1	0.047	16.137	0.0006
$CuSO_4$	0.500	1	0.500	172.684	<0.0001
Nitrogen*$CuSO_4$	0.481	1	0.481	166.123	<0.0001
Curvature	0.062	1	0.062	21.418	0.0001
Pure Error	0.064	22	0.003		
Cor Total	1.154	26			
R^2 = 0.8910					
Adj R^2 = 0.8768					
C.V. % = 14.97					

Analysis of variance table for WP

Source	SS	DF	MS	F-value	Prob (P) > F
Model	0.446	3	0.149	44.612	<0.0001
Nitrogen	0.052	1	0.052	15.510	0.0007
$CuSO_4$	0.199	1	0.199	59.586	<0.0001
Nitrogen*$CuSO_4$	0.196	1	0.196	58.740	<0.0001
Curvature	0.035	1	0.035	10.509	0.0037
Pure Error	0.073	22	0.003		
Cor Total	0.555	26			
R^2 = 0.8046					
Adj R^2 = 0.7791					
C.V. % = 17.71					

Analysis of variance table for SB

Source	SS	DF	MS	F-value	Prob (P) > F
Model	0.731	3	0.244	49.795	<0.0001
Nitrogen	0.339	1	0.339	69.300	<0.0001
$CuSO_4$	0.193	1	0.193	39.493	<0.0001
Nitrogen*$CuSO_4$	0.199	1	0.199	40.592	<0.0001
Curvature	0.065	1	0.065	13.196	0.0015
Pure Error	0.108	22	0.005		
Cor Total	0.903	26			
R^2 = 0.8093					
Adj R^2 = 0.7845					
C.V. % = 21.56					

Analysis of variance table for FP

Source	SS	DF	MS	F-value	Prob (P) > F
Model	1.019	3	0.340	55.512	<0.0001
Nitrogen	0.221	1	0.221	36.069	<0.0001
$CuSO_4$	0.387	1	0.387	63.173	<0.0001
Nitrogen*$CuSO_4$	0.412	1	0.412	67.294	<0.0001
Curvature	0.149	1	0.149	24.404	<0.0001

Pure Error	0.135	22	0.006
Cor Total	1.303	26	
R^2 = 0.7821			
Adj R^2 = 0.7537			
C.V. % = 19.14			

Analysis of variance table for CC

Source	SS	DF	MS	F-value	Prob (P) > F
Model	0.979	3	0.326	45.853	<0.0001
Nitrogen	0.200	1	0.200	28.057	<0.0001
$CuSO_4$	0.416	1	0.416	58.389	<0.0001
Nitrogen*$CuSO_4$	0.364	1	0.364	51.111	<0.0001
Curvature	0.203	1	0.203	28.584	<0.0001
Pure Error	0.157	22	0.007		
Cor Total	1.339	26			
R^2 = 0.7311					
Adj R^2 = 0.6961					
C.V. % = 20.56					

Analysis of variance table for DC

Source	SS	DF	MS	F-value	Prob (P) > F
Model	0.451	3	0.150	48.053	<0.0001
Nitrogen	0.119	1	0.119	38.169	<0.0001
$CuSO_4$	0.064	1	0.064	20.579	0.0002
Nitrogen*$CuSO_4$	0.212	1	0.212	67.683	<0.0001
Curvature	0.117	1	0.117	37.478	<0.0001
Pure Error	0.059	19	0.003		
Cor Total	0.628	23			
R^2 = 0.7185					
Adj R^2 = 0.6763					
C.V. % = 15.70					

Table S2. Factorial design matrix of 2^2 with uncoded values for levels of tryptophan and $CuSO_4$ for CMCase.

Factor		Enzymatic Activity (IU ml^{-1})					
Nitrogen (%)	$CuSO_4$ (µmol $^{-1}$)	DP	WP	SB	FP	CC	DC
−1	−1	0.206 ± 0.002	0.157 ± 0.007	0.369 ± 0.021	0.435 ± 0.042	0.474 ± 0.018	0.202 ± 0.043
+1	−1	0.481 ± 0.009	0.281 ± 0.013	0.290 ± 0.022	0.534 ± 0.011	0.565 ± 0.011	0.696 ± 0.043
−1	+1	1.014 ± 0.012	0.669 ± 0.016	0.880 ± 0.094	1.164 ± 0.123	1.195 ± 0.114	0.708 ± 0.119
+1	+1	0.489 ± 0.065	0.283 ± 0.038	0.286 ± 0.016	0.522 ± 0.061	0.589 ± 0.048	0.569 ± 0.059
0	0	0.392 ± 0.022	0.428 ± 0.064	0.440 ± 0.068	0.567 ± 0.05	0.559 ± 0.058	0.647 ± 0.077
0	0	0.431 ± 0.017	0.424 ± 0.073	0.351 ± 0.033	0.530 ± 0.080	0.608 ± 0.072	0.697 ± 0.059
0	0	0.530 ± 0.016	0.402 ± 0.077	0.282 ± 0.021	0.446 ± 0.066	0.425 ± 0.019	0.596 ± 0.083

Table S3. Analysis of variance (ANOVA) for the quadratic model generated for xylanase.

Analysis of variance table for DP

Source	SS	DF	MS	F-value	Prob (P) > F
Model	2.99	5	0.60	12.62	<0.0001
Nitrogen	0.02	1	0.02	0.35	0.5602
$CuSO_4$	0.07	1	0.07	1.44	0.2391
Nitrogen*$CuSO_4$	0.22	1	0.22	4.74	0.0375
Nitrogen²	1.51	1	1.51	31.94	<0.0001
$CuSO_4^2$	1.44	1	1.44	30.40	<0.0001
Residual	1.42	30	0.05		
Lack of Fit	0.30	3	0.10	2.44	0.0861
Pure Error	1.12	27	0.04		
Cor Total	4.41	35			
R^2 = 0.6777					
Adj R^2 = 0.6240					
C.V. % = 14.67					

Analysis of variance table for WP

Source	SS	DF	MS	F-value	Prob (P) > F
Model	4.30	5	0.86	93.64	<0.0001
Nitrogen	0.07	1	0.07	7.35	0.0086
$CuSO_4$	0.64	1	0.64	69.31	<0.0001
Nitrogen*$CuSO_4$	0.04	1	0.04	4.75	0.0330
Nitrogen²	2.00	1	2.00	217.76	<0.0001
$CuSO_4^2$	2.86	1	2.86	311.98	<0.0001
Residual	0.59	64	0.01		
Lack of Fit	0.04	3	0.01	1.52	0.2186
Pure Error	0.55	61	0.01		
Cor Total	4.89	69			
R^2 = 0.8797					
Adj R^2 = 0.8704					
C.V. % = 11.53					

Analysis of variance table for SB

Source	SS	DF	MS	F-value	Prob (P) > F
Model	7.09	5	1.42	36.90	<0.0001
Nitrogen	0.30	1	0.30	7.84	<0.0001
$CuSO_4$	1.70	1	1.70	44.12	<0.0001
Nitrogen*$CuSO_4$	0.03	1	0.03	0.70	0.4114
Nitrogen²	3.48	1	3.48	90.51	<0.0001
$CuSO_4^2$	0.11	1	0.11	2.95	0.0980
Residual	1.00	26	0.04		
Lack of Fit	0.27	3	0.09	2.90	0.0568

Pure Error	0.72	23	0.03		
Cor Total	8.09	31			
R^2 = 0.8765					
Adj R^2 = 0.8527					
C.V. % = 23.47					

Analysis of variance table for FP

Source	SS	DF	MS	F-value	Prob (P) > F
Model	25.55	5	5.11	14.47	<0.0001
Nitrogen	1.32	1	1.32	3.73	0.0629
CuSO4	1.00	1	1.00	2.83	0.1029
Nitrogen*CuSO4	0.46	1	0.46	1.29	0.2652
Nitrogen²	7.53	1	7.53	21.33	0.0001
CuSO4²	15.49	1	15.49	43.89	<0.0001
Residual	10.59	30	0.35		
Lack of Fit	2.54	3	0.85	2.83	0.0569
Pure Error	8.05	27	0.30		
Cor Total	36.14	35			
R^2 = 0.7069					
Adj R^2 = 0.6581					
C.V. % = 20.12					

Analysis of variance table for CC

Source	SS	DF	MS	F-value	Prob (P) > F
Model	71.87	5	14.37	36.15	<0.0001
Nitrogen	0.08	1	0.08	0.20	0.6554
$CuSO_4$	0.04	1	0.04	0.10	0.7550
Nitrogen*$CuSO_4$	0.25	1	0.25	0.62	0.4363
Nitrogen²	28.54	1	28.54	71.77	<0.0001
$CuSO_4$²	51.78	1	51.78	130.22	<0.0001
Residual	13.12	33	0.40		
Lack of Fit	2.36	3	0.79	2.19	0.1098
Pure Error	10.76	30	0.36		
Cor Total	84.99	38			
R^2 = 0.8456					
Adj R^2 = 0.8222					
C.V. % = 17.37					

Analysis of variance table for DC

Source	SS	DF	MS	F-value	Prob (P) > F
Model	36.68	5	7.34	38.59	<0.0001
Nitrogen	2.35	1	2.35	12.36	0.0013
$CuSO_4$	0.02	1	0.02	0.10	0.7542
Nitrogen*$CuSO_4$	0.66	1	0.66	3.49	0.0709
Nitrogen²	25.97	1	25.97	136.61	<0.0001
$CuSO_4$²	13.14	1	13.14	69.11	<0.0001
Residual	6.08	32	0.19		

Lack of Fit	1.25	3	0.42	2.50	0.0795
Pure Error	4.84	29	0.17		
Cor Total	42.77	37			
R^2 = 0.8577					
Adj R^2 = 0.8355					
C.V. % = 13.51					

Table S4. Factorial design matrix of 2^2 with uncoded values for levels of tryptophan and $CuSO_4$ for xylanase.

Factor		Enzymatic Activity (IU ml^{-1})					
Nitrogen	$CuSO_4$	DP	WP	SB	FP	CC	DC
−1	−1	0.904 ± 0.058	1.258 ± 0.258	1.266 ± 0.037	2.072 ± 0.073	2.256 ± 0.053	2.287 ± 0.273
+1	−1	1.248 ± 0.205	1.259 ± 0.147	1.674 ± 0.178	1.850 ± 0.045	2.039 ± 0.094	2.529 ± 0.271
−1	+1	1.512 ± 0.276	0.785 ± 0.325	2.445 ± 0.270	2.362 ± 0.110	2.650 ± 0.458	2.905 ± 0.180
+1	+1	1.155 ± 0.056	1.014 ± 0.269	1.960 ± 0.137	2.087 ± 0.498	3.007 ± 0.487	2.653 ± 0.635
−1.41	0	1.335 ± 0.130	0.751 ± 0.308	0.872 ± 0.051	2.035 ± 0.145	2.954 ± 0.138	2.843 ± 0.138
+1.41	0	1.408 ± 0.041	0.848 ± 0.281	2.085 ± 0.175	3.681 ± 0.399	3.183 ± 0.369	1.384 ± 0.067
0	−1.41	1.509 ± 0.169	1.123 ± 0.256	1.681 ± 0.322	2.728 ± 0.158	2.624 ± 0.057	2.930 ± 0.726
0	+1.41	1.387 ± 0.051	0.535 ± 0.170	4.618 ± 0.113	1.708 ± 0.591	1.890 ± 0.311	2.593 ± 0.122
0	0	1.525 ± 0.429	0.246 ± 0.085	4.184 ± 0.160	4.961 ± 0.657	6.353 ± 0.031	5.020 ± 0.032
0	0	1.719 ± 0.345	0.171 ± 0.049	3.803 ± 0.027	4.090 ± 0.085	5.934 ± 0.058	4.729 ± 0.213
0	0	1.900 ± 0.192	0.171 ± 0.055	3.492 ± 0.090	3.825 ± 0.020	5.340 ± 0.477	4.305 ± 0.023
0	0	2.034 ± 0.094	0.160 ± 0.052	3.001 ± 0.354	3.440 ± 0.196	4.696 ± 0.027	4.071 ± 0.080
0	0	1.777 ± 0.208	0.130 ± 0.012	2.439 ± 0.139	3.181 ± 0.071	4.276 ± 0.222	3.741 ± 0.112

CAPÍTULO 4 – XYLANASE FROM *ASPERGILLUS TAMARII* SHOWS DIFFERENT KINETIC PARAMETERS AND SUBSTRATE SPECIFICITY IN THE PRESENCE OF FERULIC ACID

4. Introdução

A xilana é o segundo principal componente da holocelulose e mais abundante das hemiceluloses. O ácido ferúlico normalmente é encontrado na parede celular com ligações do tipo éster com a hemicelulose (arabinose da xilana) e ligações do tipo éter à lignina. Além disso, pode ser encontrado após pré tratamento de biomassas lignocelulósicas, por ser também um componente fenólico presente na lignina (JÖNSSON; MARTÍN, 2016; KLEPACKA; FORNAL, 2006). Na literatura já foi extensivamente relatado que componentes fenólicos inibem a atividade enzimática, e que eles interagem causando mudanças conformacionais nas enzimas (BOUKARI et al., 2011; MICHELIN et al., 2016; QIN et al., 2016). Porém, há relatos de enzimas ativas e/ou tolerantes ao ácido ferúlico (DE SOUZA MOREIRA et al., 2013; SILVA et al., 2015). Portanto, sabendo-se que componentes fenólicos normalmente estão presentes em biomassas pré tratadas, faz-se necessário um estudo mais aprofundado no mecanismo subjacente a essa interação de um componente fenólico a uma enzima, visando formas de tornar a degradação da biomassa lignocelulósica mais eficiente. Manuscrito em preparação.

Xylanase from *Aspergillus tamarii* shows different kinetic parameters and substrate specificity in the presence of ferulic acid

Antonielle Viera Monclaro[a,*], Guilherme Lima Recalde[a], Francides Gomes da Silva Jr[b], Sonia Maria de Freitas[c], Edivaldo Ximenes Ferreira Filho[a]

[a] *Enzymology Laboratory, University of Brasília, Campus Universitário Darcy Ribeiro, Brasília - DF, 70910-900, Brazil*

[b] *Laboratory of Chemistry, Cellulose and Energy, Department of Forest Sciences, ESALQ, University of São Paulo, Piracicaba, SP, 13418-220, Brazil*

[c] *Molecular Biophysics Laboratory, University of Brasília, Campus Universitário Darcy Ribeiro, Brasília - DF, 70910-900, Brazil*

*Corresponding author at: Enzymology Laboratory, University of Brasília, Campus Universitário Darcy Ribeiro, Brasília - DF, 70910-900, Brazil

E-mail address: antonielle@gmail.com

ABSTRACT

Low-molecular weight xylanases are of great interest for biotechnology industry, mainly because of their characteristics, such as specificity to substrate and catalytic efficiency. Resistance to lignin-derived components is a very interesting feature for an enzyme because it can be used for saccharification of biomass. In this work, a 22 kDa xylanase from *Aspergillus tamarii* was purified by two chromatographic steps, including anionic exchange and gel filtration. The enzyme presented preference for oat spelt, birchwood and beechwood xylans respectively as substrates. AtXyl1 displays the highest activity at pH 5.5 and 55 °C, and showed tolerance over a range of different phenolic compounds. The activity of AtXyl1 was not inhibited when the enzyme was incubated in the presence of oat spelt xylan or birchwood xylan and ferulic acid. On the other hand, the incubation of AtXyl1 with beechwood xylan and ferulic acid resulted in an increase of enzyme activity. The molecular docking of a GH11 xylanase from *Aspergillus niger* with ferulic acid showed the preference for binding inside the catalytic site. The position of ferulic acid was based on the presence or absence of a complexed substrate. When the enzyme from *A. niger* was docked with no substrate in its crystal structure, ferulic acid interacted with Tyr164 and a water molecule. For the enzyme socked with xylo-oligosaccharides, ferulic acid interacted with Ser94, Tyr89 and the xylo-oligosaccharide present in the catalytic site. Thermodynamic parameters from the reaction of AtXyl1 with different substrates and ferulic acid indicate that ferulic acid can cause conformational change in the enzyme, and this can influence the substrate fitting and makes the enzyme tolerant or active toward the substrate. Our findings suggest that enzyme activation or tolerance to phenolic compounds can be correlated to subtle changes in enzyme conformation due to the presence of the phenolic compound.

Key-words: phenolic compounds; GH11; thermodynamic parameters; molecular docking; conformational changes.

1. Introduction

Xylan is the second major component of holocellulose and the most abundant within hemicellulose. It is a heteropolysaccharacaride with varied structure consisting essentially of a β-1,4-xylose backbone with residues such as arabinose and 4-O-methyl glucuronic acid as side chains attached to xylose. The side chains may be extended, wherein the arabinose residues may have additional substitutes, such as ρ-coumaric acid and ferulic acid [1–3]. Ferulic acid (3-methoxy-4-hydroxycinnamic acid) is commonly found in the cell wall linked by ester bonds to hemicellulose and by ether bonds to lignin [4] and can be found after pretreatment of lignocellulose biomass derived from lignin breakdown [5].

Cell wall degrading enzymes are grouped and classified by CAZy (Carbohydrate-Active enZYmes Database – http://www.cazy.org), and their nomenclature is based on both on substrate specificity and molecular mechanism. Classification in families is based on the amino acids sequence. Enzymes within a family usually have unique and very similar tertiary structures, especially in the active site [6]. Xylan-degrading enzymes can be grouped into two categories: those that degrade the polysaccharide backbone (endo-β-1,4-xylanase e β-xylosidases) and those that remove the side chains (accessory enzymes). Endo-β-1,4-xylanases from GH10 and GH11 families can cleave the glyosidic bonds of the xylan backbone but with different specificities, the former being less specific and capable of hydrolyzing substituted forms of xylan and the latter acting strictly on unsubstituted parts of xylan. In addition, they display distinct tertiary structures [7].

The effect of phenolic compounds on carbohydrate-active enzymes has been extensively studied, most of which have inhibitory effects on cellulases and hemicellulases. Ximenes *et al.* [8] showed that lignin-derived components from

pretreated wet cake inhibited cellulases and hemicellulases; similar result was found by Qin *et al.* [9] and Michelin *et al.* [10]. It was suggested that the interaction of the enzyme and lignin-derived components could affect the enzyme structure [11]. Later, it was confirmed that the phenolic compounds could cause conformational change of the enzyme without direct involvement in the active site [12]. Nevertheless, it was reported that some enzymes could tolerate or be active in the presence of some phenolic compounds. XynA, a cellulosomal GH11 xylanase, was slightly inhibited in the presence of lignin [13]. Some studies showed that phenolic compounds did not inhibited the activity of xylanases from *Emericella nidulands* [14]*, Aspergillus terreus* [15] and *A. tamarii* [16]. Moreira *et al*. [17] suggested that the incubation of a xylanase from *A. terreus* with ferulic acid, tryptophan residues might affect binding and/or hydrolysis of substrates and maintain the integrity of the catalytic domain. Thus, since phenolic compounds can interact with enzymes in different ways, the objective of this study was to understand the mechanisms underlying this interaction by using a purified xylanase from *A. tamarii,* aiming an application in rational design of enzymatic cocktails for the degradation of biomass.

2. Material and methods

2.1 Materials

Sephadex S-200 and HiTrap Q FF were purchased from GE Healthcare (São Paulo, Brazil). All the other reagents and substrates were purchased from Sigma Chemical Co. (St. Louis, MO, USA).

2.2 Organism and enzyme production

A. tamarii was deposited under strain code RCFS6 in the fungal culture collection at the Enzymology Laboratory, University of Brasilia, Brazil (genetic heritage number 010237/2015-1). The strain was also deposited in the bank of microorganisms for control of plant pathogens and weeds of the Brazilian Agricultural Research Corporation (Embrapa). The collection is registered at the World Data Centre for Microorganisms

(WDCM), under the code MCPPW 1128. Fungus stocks were maintained at -80 °C in 50% glycerol. This strain was molecularly identified as previously described [16]. An aliquot (2.5 ml) of spore suspension (10^6 spores ml^{-1}) was inoculated into Erlenmeyer flasks containing 250 ml liquid medium supplemented with 1.0% (w/v) of dark cellulose pulp as carbon source. The liquid medium employed was composed of (w/v) 0.7% KH_2PO_4, 0.2% K_2HPO_4, 0.05% $MgSO_4.7H_2O$, 0.1% tryptone and 0.06% yeast extract. The culture was incubated at 28 °C with constant agitation at 120 rpm for 72 h. Crude extract obtained from the culture was filtered through filter paper (Whatman No. 1) and stored at 4 °C.

2.3 Enzyme assay

Enzyme activity was measured by mixing 5 µl of enzyme solution with 5 µl of 2% xylan (oat spelt [OSX], beechwood [BeX] or birchwood [BrX]) and 5 µl of 100 mmol l^{-1} citrate-phosphate buffer (pH 7.0) at 50 °C for 20 min. The amount of reducing sugar released was measured using the DNS method (Miller 1959) at 540 nm in a SpectraMax® Plus 384 (Molecular Devices, Sunnyvale, CA, USA). The enzyme activity was expressed as µmol of reducing sugar released per minute per milliliter (IU ml^{-1}) using xylose as the standard. All experiments were carried out with five replicates. The acceptable standard deviation was less than 20 % of the mean.

2.4 Enzyme purification

A crude extract sample (450 ml) obtained after *A. tamarii* cultivation in liquid medium was concentrated approximately 10-fold by ultrafiltration using an Amicon System (Amicon Inc., USA) with a 50-kDa cut-off point membrane. Based on the specific xylanase activity of ultrafiltrate, this sample was chosen for further purification. Aliquots (5 ml) of the ultrafiltrate were loaded onto HiTrap Q FF ionic column (GE Healthcare) in a ÄKTA purifier (GE Healthcare), previously equilibrated with citrate-phosphate buffer 50 µmol l^{-1} (pH 7.0) and using the same aforementioned buffer with 1 mol l^{-1} of NaCl as the gradient. Fractions (1.0 ml) were eluted at a flow rate of 60 ml h^{-1} and those

corresponding to xylanase activity were pooled and loaded onto Sephacryl S-200 gel filtration column (GE Healthcare). Fractions (1.0 ml) were eluted at a flow rate of 30 ml h^{-1} and those corresponding to xylanase activity were pooled, named AtXyl1 and stored at 4 °C for further characterization. The molecular mass and purity of AtXyl1 were assessed by sodium dodecyl sulfate-polyacrylamide gel electrophoresis (SDS-PAGE) using a 12% gel. The gel was stained for proteins using silver nitrate according to the method of Blum *et al.* [18].

2.5 Enzyme characterization

The effects of temperature and pH on enzyme activity were performed by following the enzyme assay described previously in 1.3 section. For the temperature effect, enzyme and substrate were incubated at the temperature range of 30-80 °C for 30 min; whereas for the pH effect, enzyme and substrate were incubated at pH range of 3.0-8.0 of citrate-phosphate buffer for 30 min at 50 °C. Xylanase activity was expressed as a percentage of the maximum activity observed in the experiment. For assessing the effect of phenolic compounds, these compounds were individually mixed with buffer at a final concentration of 1 mg ml^{-1} and incubated with AtXyl1 at 50 °C for 30 min [15]. Statistical comparison of the effects of phenolic compounds was carried out using PAST 3.11 software [19]. Comparison was performed using ANOVA with a post-hoc Dunnett's test for control-group comparison. A Shapiro-Wilk normality test was performed previously for all data sets. The level of significance was set at $P < 0.05$.

2.6 Molecular docking

Prediction of ligand binding was performed with CASTp [20], using two three-dimensional structures of a GH11 from *Aspergillus niger* available at PDB (Protein Data Bank) [PDB structure code: 1UKR and 2QZ2]. Docking simulations were performed with AutoDock Vina. AutoDock Tools was used to prepare the ligand and 1UKR and 2QZ2 enzymes to determine the space for interaction [21].

2.7 Estimation of thermodynamic parameters

The Binding-Saturation plot of AtXyl1 was assayed over a temperature range of 30-55 °C with ferulic acid (FA) mixed with buffer (50 mM citrate-phosphate pH 5.5) at a final concentration of 1 mg ml^{-1}. The control was distilled water instead of FA. Xylan substrates (OSX, BrX and BeX) were used over a concentration range of 0.006-0.3 µmol l^{-1}. The association and dissociation constants (K_d and K_a) were estimated from the Binding-Saturation plot with a non-linear regression data analysis program (GraphPad Prism® 6). The variations of the standard molar Gibbs free energy (ΔG°), standard molar enthalpy (ΔH°) and standard molar entropy (ΔS°) from the Binding-Saturation plots were estimated by van't Hoff equation, according to Eqs. (1)-(3):

$$\ln K_a = -\frac{\Delta H^\circ}{R} \times \frac{1}{T} + \frac{\Delta S^\circ}{R} \quad (1)$$

$$\Delta G^\circ = \Delta H^\circ - T\Delta S^\circ \quad (2)$$

$$\Delta G^\circ = -RT\ln(K_a) \quad (3)$$

where T is temperature (Kelvin) and R is the ideal gas constant (1.986 cal $mol^{-1}K^{-1}$). When enthalpy is determined by changes in temperature, the heat capacity at constant pressure (ΔC_p) can be estimated according to Eq. (4):

$$\Delta C_p = \frac{\Delta H}{\Delta T} \quad (4)$$

3 Results and discussion

3.1 Purification of AtXyl1

The ultrafiltration step showed that AtXyl1 was only detected in the ultrafiltrate fraction (results not shown). In the first chromatography procedure, the anion exchange chromatography showed a peak with xylanolytic activity corresponding to the non-

retained fraction at pH 7.0. As AtXyl1 did not bind to QFF in pH 7.0, it seems that it could be a basic xylanase. The non-retained peak was subsequently submitted to gel filtration chromatography, resulting in two peaks with xylanolytic activity, as the second one representing AtXyl1 (Fig. 1-A). A SDS-PAGE gel from the fractions with xylanolytic activity was performed to evaluate the purity of the fractions (Fig. 1-B). Based on the high level of purity, the fractions 52-61 were pooled and stored. Yield and purification data are presented in Table 1 with a final 2.29-fold purification and 7.43% yield. Low molecular-weight xylanases from *Aspergillus sp.* have been purified and characterized previously, with different purification steps and yields [16,24–26]. The low value of yield obtained in our study might be due to different reasons: dilute effect caused by gel chromatography, since purified enzymes tend to be unstable when they are not associated [27] or due to proteolysis during the purification steps (especially after the anionic exchange, where the specific activity decreased) or aggregation of the enzymes [28]. Different conditions must be tested during purification to achieve higher values of yield.

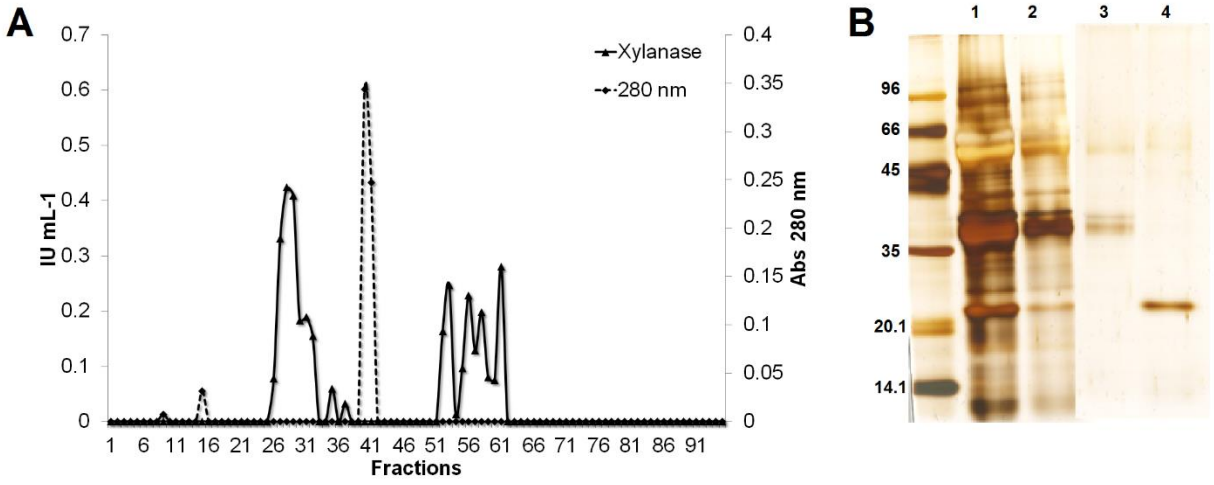

Figure 1. A) Gel filtration profile of AtXyl1 on Sephacryl S-200. Fractions 52-61 were pooled. **B)** SDS-PAGE of purification steps of AtXyl1 from *A. tamarii*. Lane 1: Crude extract of *A. tamarii* when grown in dark cellulose pulp; Lane 2: fractions pooled from HiTrap Q FF anionic exchange; Lane 3: 26-32 fractions pooled from Sephacryl S-200 gel filtration chromatography; Lane 4: 52-61 fractions pooled from Sephadex S-200 gel filtration chromatography.

Table 1. Purification steps of AtXyl1 from *A. tamarii*.

Purification step	Total Volume (ml)	Total Protein (mg)	Total Activity (UI)	Specific Activity (UI mg^{-1})	Purification Factor	Yield (%)
Crude extract	450	42.300	474.300	11.213	1.00	100.00
Ultrafiltration	400	20.000	227.200	11.360	1.01	47.90
HiTrap Q FF	62	0.744	66.526	89.417	7.97	14.03
Sephacryl S-200	156	1.371	35.256	25.711	2.29	7.43

SDS-PAGE revealed a single band after the purification steps. The estimated molecular mass of At Xyl1 was 22 kDa. Low molecular-weights xylanases (around 20 kDa) are classified as belonging to GH11 [22], a family that comprises enzymes with high substrate selectivity, high catalytic efficiency and small size [23].

2.2 *AtXyl1 characterization and molecular docking*

The activity profile of AtXyl1 in different xylan substrates is shown in Figure 2-A. AtXyl1 presented higher activity in OSX, (0.739±0.044 IU.ml $^{-1}$), followed by BrX and BeX, (0.532±0.020 and 0.486±0.031 IU.ml $^{-1}$, respectively). The enzyme presented higher activity at pH 5.5 and 50 °C (Figure 2-B and C, respectively). These values are in agreement with those that are commonly observed for xylanases from *Aspergillus* sp. [16,24–26].

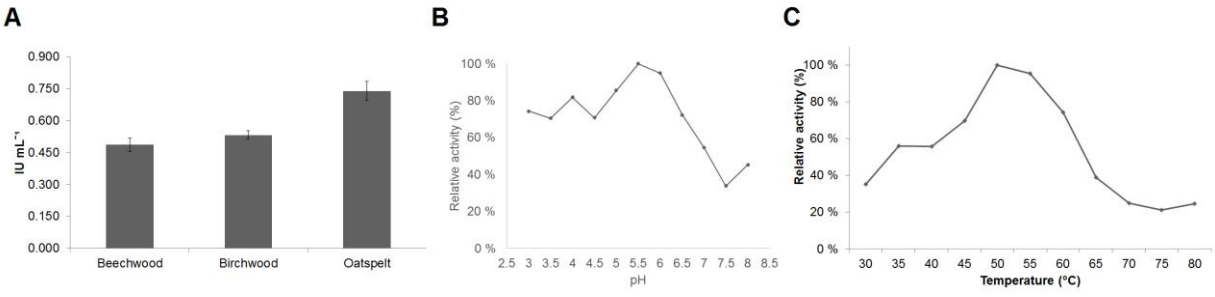

Figure 2. Biochemical characterization of AtXyl1. **A)** AtXyl1.activity in different xylan substrates. **B)** The effect of pH on AtXyl1 activity. **C)**The effect **of** temperature on AtXyl1 activity.

Phenolic compounds, generated during pretreatment of biomass, are known to be inhibitors of a variety of holocellulose-degrading enzymes [8,10,12,29,30]. In the present work, we evaluated the effect of a range of phenolic compounds (representing those normally found in pretreated biomass) on xylanase activity (Table 2). Vanillin inhibited and increased AtXyl1 activity when OSX and BrX were used as substrates, respectively. The incubation of AtXyl1 with tannic acid and BrX as substrate resulted in an increase in enzyme activity. The effect of FA on AtXyl1 showed that the highest activity was obtained with BeX as substrate. A previous study [16] showed that FA, at 1 mmol l^{-1} concentration, increased activity of multiple forms of xylanase from *A. tamarii* when OSX was the substrate. Similar results were found previously, where xylanases from *Emericela nidulans* and *A. terreus* could tolerate FA at a concentration of 1 mmol l^{-1} [14,15]. The main phenolic compounds derived from lignin do not inhibit AtXyl1, which is of great interest for the saccharification of lignocellulose biomass, since the enzyme can tolerate the presence of these compounds during the hydrolysis. However, the mechanism behind this phenomenon is not fully elucidated.

Table 2. The effect of phenolic compounds on AtXyl1 activity.

Phenolic compound (1 mg ml^{-1})	Relative Activity (%)		
	OSX	BrX	BeX
Vanilin	73*	110*	110
Tannic Acid	83	112*	112
p-Cumaric Acid	93	100	109
Cinnamic Acid	80	104	116
Ferulic Acid	100	103	120*
4-HydroxyBenzoic Acid	81	102	112

* Indicates statistical difference in Dunnett's test.

In order to obtain a better understanding of how FA binds to GH11 xylanase, and considering that third-dimensional structure is conserved between GH11 members [23], two different three-dimensional structures of the same *A. niger* GH11 xylanase available

in PDB were used: one without xylo-oligosaccharides [30] (structure code PDB: 1UKR) and one with xylo-oligosaccharides [31] (PDB structure code: 2QZ2). Molecular docking simulations were performed with FA within the catalytic domain of the enzyme. For the structure without xylo-oligossacharides, the most energetic position was for FA interacting with a tyrosine (Tyr164) and a water molecule close to the C-terminus of the enzyme (Figure 3-A). Moreira *et al.* [17] showed that, for two xylanases from *A. terreus* incubated with FA, different tryptophan environments in the vicinity of the active sites could explain the affinity for phenolic compounds, since tryptophan residues were shifted when they were analyzed by fluorescence spectroscopy and the kinetic parameters of the tested xylanases changed. Boukari *et al.* [12] also found that 1 mmol l^{-1} of FA induced conformational changes at GH11 xylanase from *Thermobacillus xylanilyticus*. By mapping the binding region of the anchoring experiment, one can see that there is a tryptophan (Trp172) near Tyr164 (Figure 3-B). Although the anchor simulations do not predict any binding to Trp172, we may assume that the Tyr164 neighborhood structure is altered by binding to FA and this may cause the Trp172 to change. For the GH11 xylanase structure with xylo-oligossacharides, the most energetic position was not interacting with Tyr164, but with two other residues (Ser94 and Tyr89) closer to the N-terminus of the enzyme. FA was also interacting with the xylo-oligosaccharide within the catalytic domain (Figure 4). One might ask why this interaction with these amino acid residues was not proposed for the first docking simulation (for the enzyme without xylo-oligosaccharides), since both positions showed the same affinity (around -6 kcal mol -1)? Then, the two structures were overlapped in order to evaluate differences between structures (Figure 5) regarding those amino acids residues (Tyr 164, Ser94 and Tyr 89). It was detected a subtle change for Ser94: its –OH orientation in the presence of xylo-oligosaccharides. This orientation was fundamental for the interaction of FA with Ser94 and Tyr89, explaining why Ser94 did not show affinity for the docking simulation when the enzyme was resolved without xylo-oligosaccharides. Ser94 and Tyr89 are located in

the so-called "thumb" loop, a very important flexible region for catalytic events, which can perform close open movement based on temperature and substrate binding [23]. A study conducted by Cervera Tison *et al.* [31] showed that amino acids residues presents in the thumb region of a GH11 xylanase from *Penicillium griseofulvum* were important to give resistance to XIP-I, a xylanase-inhibitor protein derived from wheat, especially by causing strong steric clashes. Therefore, Ser94 may play a key role in the tolerance and / or activation of this enzyme in the presence of FA, and its location is crucial for this behavior. More studies are needed to better understand this phenomenon, as Ser94 is not conserved in different microorganisms but the structures domains are [23].

It seems that the thumb region of the enzyme plays a role in the tolerance and/or activation with FA - especially when the substrate is complexed with the enzyme. Considering that protein folding is driven by hydrophobic interactions and that there is temperature dependence of the thermodynamic parameters that control folding stability [32], the thermodynamic parameters of AtXyl1 in the presence of FA were estimated with different naturally occurring xylans (OSX, BeX and BrX). The use of different xylans in kinetic studies is of great importance, since it has already been reported that different activities toward xylans with distinct features (e.g. solubility, chain length, degree of substitutes, substitution patterns) can be explained by structural conformation of the enzyme [33]. BrX, OSX and BeX have a higher content of *O*-acetyl groups [34], arabino substituent [35] and 4-*O*-methylglucurono substituent [36], respectively. These xylans can present different characteristics, such as arabino groups increasing viscosity of the solution, while the presence of glucuronic acid side chains makes the xylan more soluble [37]. Acetylation of xylan can also change its solubility, as well as interchain interactions with cellulose [38].

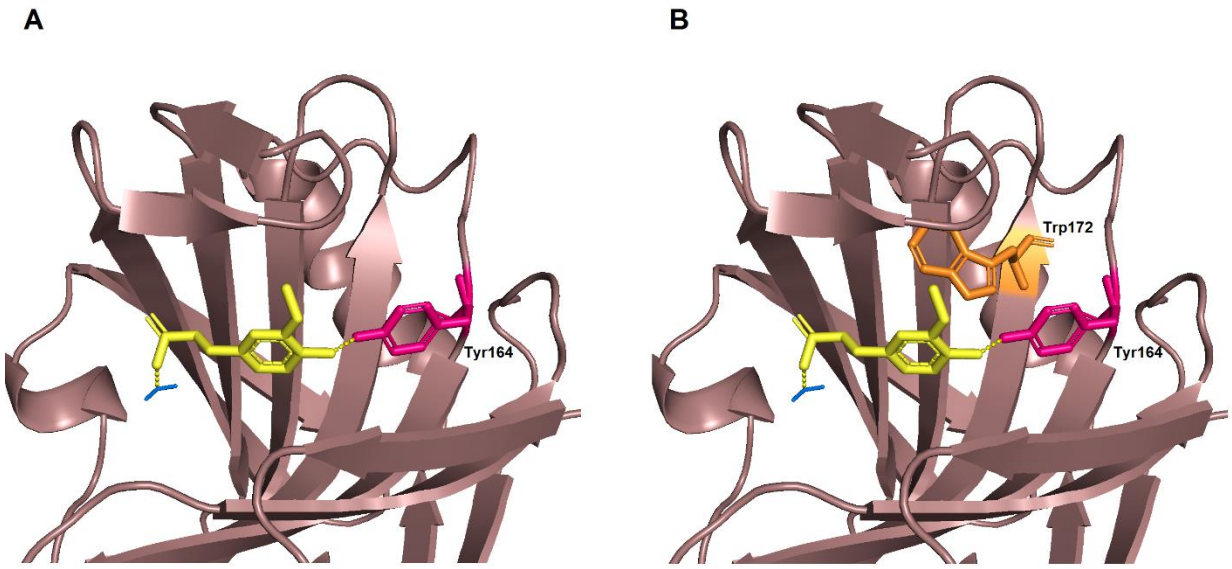

Figure 3. Molecular docking of a GH11 xylanase from *A. niger* (PDB structure code: 1UKR) with FA. **A)** Interaction between FA (yellow), Tyr164 (pink) and a water molecule (blue). **B)** The presence of a tryptophan (orange) near the interaction between FA, Tyr164 and the water molecule.

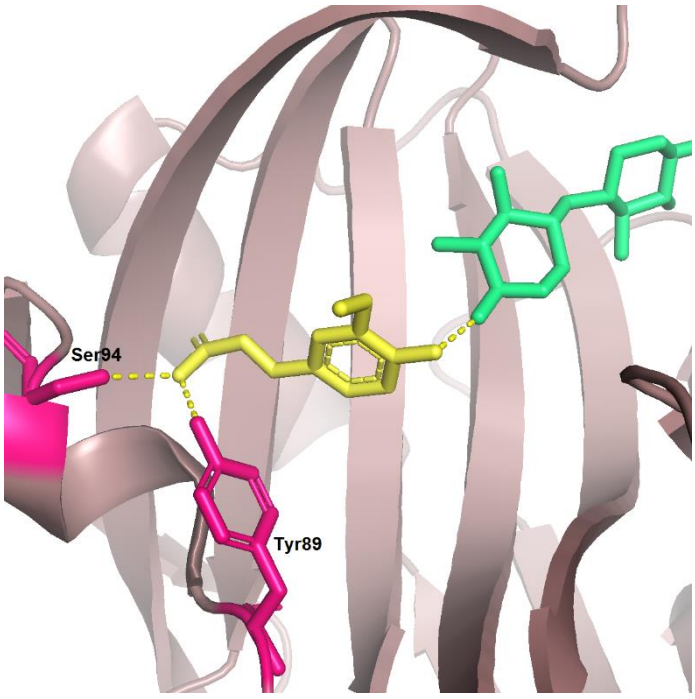

Figure 4. Molecular docking of a GH11 xylanase from *A. niger* (PDB structure code: 2QZ2) with FA. Interaction between two amino acids residues (pink) with FA (yellow) and xylo-oligosaccharide (green).

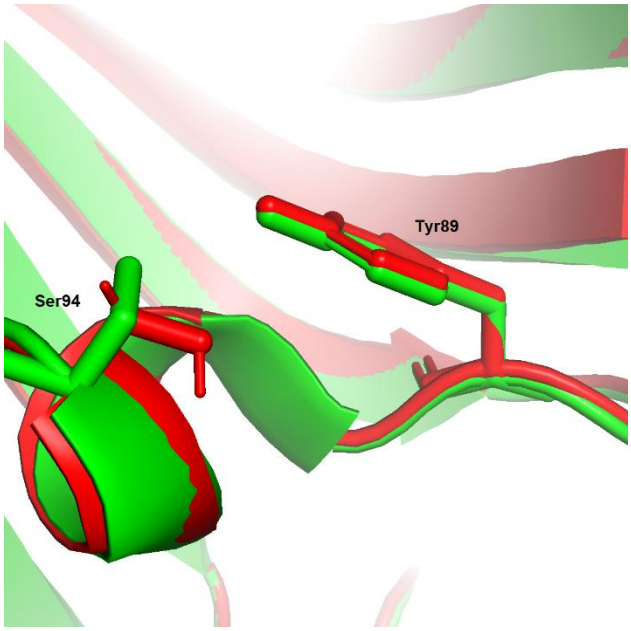

Figure 5. Overlapping both GH11 xylanase three-dimensional structures from *A. niger* (PDB code: 1UKR in red and 2QZ2 in green).

3.2 Estimation of thermodynamic parameters of AtXyl1

Table 3 summarizes the thermodynamic parameters of AtXyl1 from the binding saturation assay. These parameters were estimated at a temperature range of 30-50°C, in which was the increasing slope of enzymatic activity according to the optimum temperature of the enzyme (Figure 2-C). All the interactions were exothermic (ΔH < 0.0) and the enthalpy values ranged from 2.569 to 17.938 cal mol^{-1}. For the pure enzyme without FA, the most entropic reaction was achieved with BrX as substrate, followed by OSX and BeX. The values of these different parameters reflect a large affinity for BrX (-13.451 kcal mol^{-1}) compared to BeX (-2.664 kcal mol^{-1}). Similar results were found for other xylanases from *Aspergillus* sp., where higher activity was detected in BrX, followed by OSX and BeX [39,40]. The -ΔH, ΔS and -ΔCp values increased when the enzyme was incubated without FA and using OSX and BrX as substrates. When incubated with FA, BeX showed to be the most favorable substrate, with higher levels of -ΔG, -ΔH, ΔS and -ΔCp compared to control, where the increase of these values agrees with Table 2. This experiment showed that, for BrX or OSX as substrates, the enzyme had more

affinity in the absence of FA; for BeX, the enzyme had more affinity in the presence of FA. Changes in entropy can be a result from hampering side-chains conformers in the native structure due to flexibility that occur upon ligand binding [41,42]. It is interesting to note that this occurred with xylan that has a higher content of glucuronic acid; since these side chain residues can behave as a polyelectrolyte complex [38], the charge of these side chains during the enzymatic complex-FA could have induced the formation of salt bridges between amino acids with opposite charges [43]. Furthermore, the changes in heat capacity after ligand binding show that there is a dependence of the enthalpy change, which can be linked to the conformational rearrangement and the hydrogen bonding of the solvent [44,45].

These notorious differences in the thermodynamic parameters might be correlated to a modification in the three dimensional structure of the enzymes when the complex xylanase-FA was formed and was acting toward different xylans.

Based on the last statement and considering that: 1) Enzyme activity was not impaired by the presence of FA for all xylans (Table 2); 2) FA did influence the affinity of the enzyme for the substrate (Table 3) and with different values regarding the type of the xylan; 3) Molecular docking shows that FA interact with amino acid residues in the thumb region of the enzyme; we can propose that modifications in the three-dimensional structure of the thumb region in the presence of FA, are responsible for those changes in the kinetic parameters, also influenced by different features from the substrate. Although these aspects are relevant for application in biotechnology industry, many different questions still have to be addressed, for example the role of Ser94 in GH11 xylanase structure from *A. niger* and if this phenomenon is observed in GH11 xylanases from other microorganisms; and the impact of xylan side chains in stability and catalytic efficiency of xylanases. Concentration of the phenolic compound is also another interesting issue, since all the studies have reported tolerance of the enzyme toward phenolic compounds at 1 mmol $^{-1}$ concentration. A better understanding of the

conformational changes that underlies the tolerance/activation will also be useful for rational designing of enzymatic cocktails aiming different applications.

Table 3. Thermodynamic parameters of AtXyl1 when incubated with different types of xylan and with/without the presence of ferulic acid**.**

AtXyl1	ΔG (kcal mol^{-1})	ΔH (kcal mol^{-1})	ΔS (cal $mol^{-1}K^{-1}$)	ΔCp (cal $mol^{-1}K^{-1}$)
OSX + FA	-7.584±1.000	-5.030±0.724	8.571±2.316	-201.190±28.971
OSX + H_2O	-11.006±1.293	-6.817±0.939	14.055±2.981	-272.686±37.577
BrX + FA	-6.743±0.764	-4.638±0.555	7.066±1.762	-185.508±22.216
BrX + H_2O	-13.451±1.653	-8.105±1.198	17.938±3.820	-324.203±47.921
BeX + FA	-8.653±0.820	-5.589±0.819	10.283±0.132	-223.560±32.768
BeX + H_2O	-2.664±0.245	-1.898±0.177	2.569±0.570	-75.925±7.080

4. *Conclusion*

AtXyl1 was purified from *A. tamarii* by two-purification steps. It presented a tolerance over a range of different phenolic compounds. AtXyl1 was activated by vanillin and tannic acid when birchwood xylan was the substrate; while ferulic acid activated AtXyl1 when beechwood xylan was the substrate. The molecular docking of the enzyme predicted a possible interaction of ferulic acid in the catalytic site of a GH11 xylanase from *A. niger*; where the interaction occurred with different amino acid residues based on the presence or absence substrate. Thermodynamic parameters indicate that, when the enzyme is incubated with ferulic acid, the phenolic compound is responsible for conformational change in the enzyme, and this change can influence the substrate fitting, hence modifying enzyme activity toward different substrates. Our findings suggest that the activation or tolerance of xylanase to phenolic compounds can be correlated to subtle changes in enzyme conformation.

Acknowledgments

The authors acknowledge the receipt of financial support from the Brazilian National Council for Scientific and Technological Development (CNPq), the Coordination for the Improvement of Higher Education Personnel (CAPES), the Foundation for Research

Support of the Federal District (FAPDF) and the National Institute for Science and Technology of Bioethanol.

Conflict of interest

The authors declare that they have no competing interests.

References

[1] Dodd D, Cann IK. Enzymatic deconstruction of xylan for biofuel production. Glob Chang Biol Bioenergy 2009;1:2–17. doi:10.1111/j.1757-1707.2009.01004.x.
[2] Minic Z, Jouanin L. Plant glycoside hydrolases involved in cell wall polysaccharide degradation. Plant Physiol Biochem 2006;44:435–49. doi:10.1016/j.plaphy.2006.08.001.
[3] Polizeli MLTM, Rizzatti ACS, Monti R, Terenzi HF, Jorge JA, Amorim DS. Xylanases from fungi: Properties and industrial applications. Appl Microbiol Biotechnol 2005;67:577–91. doi:10.1007/s00253-005-1904-7.
[4] Klepacka J, Fornal Ł. Ferulic acid and its position among the phenolic compounds of wheat. Crit Rev Food Sci Nutr 2006;46:639–47. doi:10.1080/10408390500511821.
[5] Jönsson LJ, Martín C. Pretreatment of lignocellulose: Formation of inhibitory by-products and strategies for minimizing their effects. Bioresour Technol 2016;199:103–12. doi:10.1016/j.biortech.2015.10.009.
[6] Henrissat B, Callebaut I, Lehn P, Mornon J, Davies G. Conserved catalytic machinery and the prediction of a common fold for several families of glycosyl hydrolases. Proc Natl Acad Sci U S A 1995;92:7090–4.
[7] Moreira LRS, Filho EXF. Insights into the mechanism of enzymatic hydrolysis of xylan. Appl Microbiol Biotechnol 2016;100:5205–14. doi:10.1007/s00253-016-7555-z.
[8] Ximenes E, Kim Y, Mosier N, Dien B, Ladisch M. Deactivation of cellulases by phenols. Enzyme Microb Technol 2011;48:54–60. doi:10.1016/j.enzmictec.2010.09.006.
[9] Qin L, Li WC, Liu L, Zhu JQ, Li X, Li BZ, et al. Inhibition of lignin-derived phenolic compounds to cellulase. Biotechnol Biofuels 2016;9:1–10. doi:10.1186/s13068-016-0485-2.
[10] Michelin M, Ximenes E, de Lourdes Teixeira de Moraes Polizeli M, Ladisch MR. Effect of phenolic compounds from pretreated sugarcane bagasse on cellulolytic and hemicellulolytic activities. Bioresour Technol 2016;199:275–8. doi:10.1016/j.biortech.2015.08.120.
[11] Kaya F. Influence of lignin and its degradation products on\nenzymatic hydrolysis of xylan. J Biot 2000;80:241–7.
[12] Boukari I, O'Donohue M, Rémond C, Chabbert B. Probing a family GH11 endo-β-1,4-xylanase inhibition mechanism by phenolic compounds: Role of functional phenolic groups. J Mol Catal B Enzym 2011;72:130–8. doi:10.1016/j.molcatb.2011.05.010.
[13] Morrison D, van Dyk JS, Pletschke BI. The effect of alcohols, lignin and phenolic compounds on the enzyme activity of Clostridium cellulovorans XynA. BioResources 2011;6:3132–41.
[14] Silva C de OG, Aquino EN, Ricart CAO, Midorikawa GEO, Miller RNG, Filho EXF. GH11 xylanase from Emericella nidulans with low sensitivity to inhibition by ethanol and lignocellulose-derived phenolic compounds. FEMS Microbiol Lett 2015;362:1–9. doi:10.1093/femsle/fnv094.

[15] De Souza Moreira LR, De Carvalho Campos M, De Siqueira PHVM, Silva LP, Ricart CAO, Martins PA, et al. Two β-xylanases from Aspergillus terreus: Characterization and influence of phenolic compounds on xylanase activity. Fungal Genet Biol 2013;60:46–52. doi:10.1016/j.fgb.2013.07.006.
[16] Monclaro A, Aquino E, Faria R, Ricart C, Freitas S, Midorikawa G, et al. Characterization of multiple xylanase forms from Aspergillus tamarii resistant to phenolic compounds. Mycosphere 2016;7:1554–67. doi:10.5943/mycosphere/si/3b/7.
[17] De Souza Moreira LR, Da Cunha Morales Álvares A, Da Silva FG, De Freitas SM, Filho EXF. Xylan-degrading enzymes from Aspergillus terreus: Physicochemical features and functional studies on hydrolysis of cellulose pulp. Carbohydr Polym 2015;134:700–8. doi:10.1016/j.carbpol.2015.08.040.
[18] Blum H, Beier H, Gross HJ. Improved silver staining of plant proteins, RNA and DNA in polyacrylamide gels. Electrophoresis 1987;8:93–9. doi:10.1002/elps.1150080203.
[19] Hammer Ø, Harper DAT a. T, Ryan PD. PAST: Paleontological Statistics Software Package for Education and Data Analysis. Palaeontol Electron 2001;4(1):1–9. doi:10.1016/j.bcp.2008.05.025.
[20] Dundas J, Ouyang Z, Tseng J, Binkowski A, Turpaz Y, Liang J. CASTp: Computed atlas of surface topography of proteins with structural and topographical mapping of functionally annotated residues. Nucleic Acids Res 2006;34:116–8. doi:10.1093/nar/gkl282.
[21] Trott O, Olson A. NIH Public Access. J Comput Chem 2010;31:455–61. doi:10.1002/jcc.21334.AutoDock.
[22] Biely P, Vršanská M, Tenkanen M, Kluepfel D. Endo-β-1,4-xylanase families: Differences in catalytic properties. J Biotechnol 1997;57:151–66. doi:10.1016/S0168-1656(97)00096-5.
[23] Paës G, Berrin JG, Beaugrand J. GH11 xylanases: Structure/function/properties relationships and applications. Biotechnol Adv 2012;30:564–92. doi:10.1016/j.biotechadv.2011.10.003.
[24] Heinen PR, Bauermeister A, Ribeiro LF, Messias JM, Almeida PZ, Moraes LAB, et al. GH11 xylanase from Aspergillus tamarii Kita: Purification by one-step chromatography and xylooligosaccharides hydrolysis monitored in real-time by mass spectrometry. Int J Biol Macromol 2018;108:291–9. doi:10.1016/j.ijbiomac.2017.11.150.
[25] Duarte G, Moreira L, Gómez-Mendoza D, Siqueira FG De, Batista L, Amaral L, et al. Use of Residual Biomass from the Textile Industry as Carbon Source for Production of a Low-Molecular-Weight Xylanase from Aspergillus oryzae. Appl Sci 2012;2:754–72. doi:10.3390/app2040754.
[26] Camacho NA, Aguilar O G. Production, purification, and characterization of a low-molecular-mass xylanase from Aspergillus sp. and Its application in baking. Appl Biochem Biotechnol - Part A Enzym Eng Biotechnol 2003;104:159–71. doi:10.1385/ABAB:104:3:159.
[27] Andrews P. The gel-filtration behaviour of proteins related to their molecular weights over a wide range. Biochem J 1965;96:595–606. doi:10.1042/bj0960595.
[28] Gräslund S, Nordlund P, Weigelt J, Hallberg BM, Bray J, Gileadi O, et al. Protein production and purification. Nat Methods 2008;5:135–46. doi:10.1038/nmeth.f.202.Protein.
[29] Tejirian A, Xu F. Inhibition of enzymatic cellulolysis by phenolic compounds. Enzyme Microb Technol 2011;48:239–47. doi:10.1016/j.enzmictec.2010.11.004.
[30] Kim Y, Ximenes E, Mosier NS, Ladisch MR. Soluble inhibitors/deactivators of cellulase enzymes from lignocellulosic biomass. Enzyme Microb Technol

2011;48:408–15. doi:10.1016/j.enzmictec.2011.01.007.
[31] Cervera Tison M, André-Leroux G, Lafond M, Georis J, Juge N, Berrin JG. Molecular determinants of substrate and inhibitor specificities of the Penicillium griseofulvum family 11 xylanases. Biochim Biophys Acta - Proteins Proteomics 2009;1794:438–45. doi:10.1016/j.bbapap.2008.11.024.
[32] Cooper A. Heat capacity effects in protein folding and ligand binding: A re-evaluation of the role of water in biomolecular thermodynamics. Biophys Chem 2005;115:89–97. doi:10.1016/j.bpc.2004.12.011.
[33] van Gool MP, van Muiswinkel GCJ, Hinz SWA, Schols HA, Sinitsyn AP, Gruppen H. Two novel GH11 endo-xylanases from Myceliophthora thermophila C1 act differently toward soluble and insoluble xylans. Enzyme Microb Technol 2013;53:25–32. doi:10.1016/j.enzmictec.2013.03.019.
[34] Biely P, Puls J, Schneider H. Acetyl xylan esterases in fungal cellulolytic systems. FEBS Lett 1985;186:80–4. doi:10.1016/0014-5793(85)81343-0.
[35] Saake B, Erasmy N, Schmekal E, Puls J. Isolation and characterization of arabinoxylan from oat spelts. Hemicellul Sci Technol 2003;80:52–65. doi:10.1021/bk-2004-0864.ch004.
[36] Puls J, Tenkanen M, Korte HE, Poutanen K. Products of hydrolysis of beechwood acetyl-4-O-methylglucuronoxylan by a xylanase and an acetyl xylan esterase. Enzyme Microb Technol 1991;13:483–6. doi:10.1016/0141-0229(91)90006-V.
[37] Ebringerová A, Heinze T. Xylan and xylan derivatives - Biopolymers with valuable properties, 1: Naturally occurring xylans structures, isolation procedures and properties. Macromol Rapid Commun 2000;21:542–56. doi:10.1002/1521-3927(20000601)21:9<542::AID-MARC542>3.0.CO;2-7.
[38] Pawar PM-A, Koutaniemi S, Tenkanen M, Mellerowicz EJ. Acetylation of woody lignocellulose: significance and regulation. Front Plant Sci 2013;4:1–8. doi:10.3389/fpls.2013.00118.
[39] Damásio ARDL, Silva TM, Almeida FBDR, Squina FM, Ribeiro DA, Leme AFP, et al. Heterologous expression of an Aspergillus niveus xylanase GH11 in Aspergillus nidulans and its characterization and application. Process Biochem 2011;46:1236–42. doi:10.1016/j.procbio.2011.01.027.
[40] He H, Qin Y, Li N, Chen G, Liang Z. Purification and Characterization of a Thermostable Hypothetical Xylanase from Aspergillus oryzae HML366. Appl Biochem Biotechnol 2015;175:3148–61. doi:10.1007/s12010-014-1352-x.
[41] Doig AJ, Sternberg MJE. Side-chain conformational entropy in protein folding. Protein Sci 1995;4:2247–51. doi:10.1002/pro.5560041101.
[42] Stone MJ. NMR relaxation studies of the role of conformational entropy in protein stability and ligand binding. Acc Chem Res 2001;34:379–88. doi:10.1021/ar000079c.
[43] Horn D, Heuck CC. Charge determination of proteins with polyelectrolyte titration. J Biol Chem 1983;258:1665–70.
[44] Olsson TSG, Williams MA, Pitt WR, Ladbury JE. The Thermodynamics of Protein-Ligand Interaction and Solvation: Insights for Ligand Design. J Mol Biol 2008;384:1002–17. doi:10.1016/j.jmb.2008.09.073.
[45] Vega S, Abian O, Velazquez-Campoy A. On the link between conformational changes, ligand binding and heat capacity. Biochim Biophys Acta - Gen Subj 2016;1860:868–78. doi:10.1016/j.bbagen.2015.10.010.

CAPÍTULO 5 - FUNGAL LYTIC POLYSACCHARIDE MONOOXYGENASES FROM FAMILY AA9: RECENT DEVELOPMENTS AND APPLICATION IN LIGNOCELULLOSE BREAKDOWN

5. Introdução

Esta revisão focou nas LPMOs da família AA9 no contexto de hidrólise de biomassa lignocelulósica e biorefinaria. Sabendo-se da importância atual dessas enzimas para degradação e conversão da biomassa para produtos de valor agregado, a revisão foi elaborada baseada nos últimos achados sobre sua estrutura e modo de ação e foi discutido seu papel em relação ao sinergismo com outras enzimas e perspectivas futuras para aplicação industrial em biorefinarias.

International Journal of Biological Macromolecules 102 (2017) 771–778

Contents lists available at ScienceDirect

International Journal of Biological Macromolecules

journal homepage: www.elsevier.com/locate/ijbiomac

Review

Fungal lytic polysaccharide monooxygenases from family AA9: Recent developments and application in lignocelullose breakdown

Antonielle Vieira Monclaro*, Edivaldo Ximenes Ferreira Filho

Enzymology Laboratory, University of Brasília, Campus Universitário Darcy Ribeiro, Brasília, DF, 70910-900, Brazil

ARTICLE INFO

Article history:
Received 20 December 2016
Received in revised form 20 April 2017
Accepted 21 April 2017
Available online 24 April 2017

Keywords:
Fungi
Cellulose
Biorefinery

ABSTRACT

Fungal lytic polysaccharide monooxygenases (LPMOs) from family AA9 are oxidative enzymes that, in the past few years, have changed the paradigm of cellulose conversion. They are key factor in the lignocellulose breakdown and are widely distributed among fungi. This review focuses on LPMOs from family AA9 and gives an overview of recent discoveries relative to their structure, mode of action, and synergism with other enzymes. Finally, several aspects regarding their potential applications toward deconstruction of biomass and biorefinery processes are discussed.

Contents

1. Introduction

Overcoming the recalcitrance of lignocellulosic biomass to enzymatic deconstruction and generating value-added products, as 2nd-generation biofuels, is one of the major challenges for the biotechnology industry. In this context, the circular economy – a model of regenerative industrial economy, aiming to reduce wastes and higher productivity based on biorefinery platforms – presents great relevance in boosting technological advances [1].

Microbial systems able to perform hydrolytic attack have been extensively studied, especially glycoside hydrolases from fungi [2,3]. Over the last 6 years, LPMOs have changed the concept of enzymatic polysaccharide conversion, demonstrating that plant biomass degradation by microorganisms occurs not only through hydrolytic attack but also through an oxidative attack [4,5].

The "Auxiliary Activity" (AA) families represent a widespread group of redox enzymes that act together with glycosyl hydrolases (GH), polysaccharide lyases, and carbohydrate esterases (http://www.cazy.org/) toward decreasing the recalcitrance of plant cell walls through different mechanisms of action and using various substrates. There are thirteen classes of AA, of which four are LPMOs – AA9, AA10, AA11, and AA13. AA9, originally classified as GH61, are copper-dependent enzymes from fungi [6]. They act in the oxidative depolymerization of polysaccharide along with molecular oxygen and an external electron donor [7,8]. Some enzymes

* Corresponding author.
E-mail address: antonielle@gmail.com (A.V. Monclaro).

http://dx.doi.org/10.1016/j.ijbiomac.2017.04.077
0141-8130/

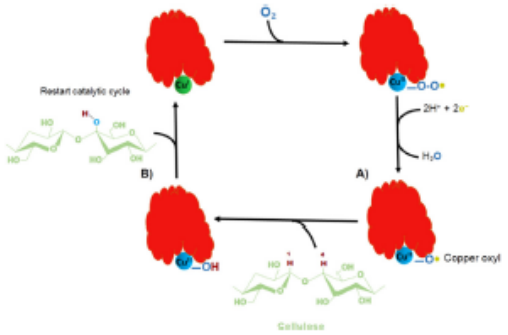

Fig. 1. Oxyl mechanism for cellulose hydroxylation by AA9. A) copper oxyl abstraction of a hydrogen atom from the substrate carbon; B) substrate hydroxylation.

specifically oxidize C1 carbon, while others only oxidize C4, or oxidize both C1 and C4 carbons [9].

The first AA9 described was presumably the Cell protein from *Agaricus bisporus* [10]. It is a cellulase-encoding gene and its sequence displays not only a core of 233 amino acids, but also a domain rich in proline-serine-threonine and a cellulose-binding domain. Later, in 1997, the amino acid similarity between EG1V, an endoglucanase from *Trichoderma reeset*, and Cell from *A. bisporus*, led to the clustering of both enzymes in the new glycosyl hydrolase family 61 [11,12]. This family was thought to display a weak endoglucanase activity, but little was known about their mechanism or function [13], only that GH61 proteins could greatly enhance cellulase activity and require divalent metal ions to enable their activity [4]. However, in a landmark study, Vaaje-Kostald et al. [5] discovered that CBP21 (chitin-binding protein) from *Serratia marcescens* could catalyze chain breaks through oxidation, and that GH61 could potentially display the same activity. The copper-oxidative nature of enzymes belonging to the GH61 family was later confirmed [14–16].

The AA9 family is largely distributed among fungi. Harris et al. [4] reported one of the first phylogenetic analyzes of AA9. They used 300 known or predicted proteins with homology to GH61 family and demonstrated that the two major phyla, ascomycetes and basidiomycetes, present multiple genes encoding GH61 in their genomes. Kracher et al. [17] analyzed 97 fungal genomes, 92% of which presented genes encoding LPMOs. Some ectomycorrhizal fungi lacking typical cellulases possess LPMO genes, but their importance remains unclear [18]. Considering the presence of GHs active in lignocellulose degradation processes, the prevalence of AA9 LPMO genes in fungi genomes is low compared to β-glucosidase genes (GH1 and GH3), but very similar to that of endoglucanases (GH5, GH8, and GH45) and cellobiohydrolases (GH6 and GH7) genes [17,19]. This indicates that there is a need for different enzymes, playing various roles, to degrade different substrates [20]. The presence of a range of cellulolytic and LPMO AA9 genes probably contributes to establishing a synergistic effect during fungal biomass degradation [18,21], enabling the degradation of the least accessible regions of plant cell walls [16].

2. Oxidative reaction

The currently model suggested to explain the oxidative reaction was proposed by Kjaergaard et al. [22] and Kim et al. [23] (Fig. 1). It involved a molecular oxygen binding and the reduction of LPMO-Cu(II) to LPMO-Cu(I) to form the copper-oxyl intermediate [Cu^{II}]-O-O•. This intermediate abstracts a hydrogen atom from the substrate carbon (Fig. 1-A), subsequently hydroxylating the substrate *via* an oxygen-rebound mechanism (Fig. 1-B) and leading to destabilization and breakage of the adjacent glycosidic bond through an elimination reaction. Even so, more data and detailed calculations are required, in order to precisely explain the electronic transitions that are ongoing at the active site.

It is well-known that LPMO active sites are flexible and can accommodate both states of cooper [24]. Kjaeegard et al. [22] observed that, based on the coordination geometries for Cu(I) and Cu(II)-AA9 in solution, the active site structure reacts rapidly for inner-sphere reductive activation of O_2 by Cu(II)-superoxide formation. Additionally, the rapid superoxide release from the reaction product is consistent with the appearance of hydrogen peroxide because of the disproportionation of two superoxide ions. However, the release of this superoxide is limited when the substrate is bound to the enzyme. A recent review by Walton and Davies [25] focused on the description of catalytic mechanisms of LPMOs and described the four main existing catalytic cycles that involve LPMOs binding O_2 before the substrate. They also considered the situation in which O_2 binds to LPMOs in the presence of substrate and described three main catalytic cycles, two of which are involved in the production of peroxylated species (R-OOH species), and the third one included hydrogen atom abstraction through Cu(II)-oxyl species. The data presented by Courtade et al. [26] suggested that electron transfer (ET) event occurs before substrate binding. Because CDH could not bind to LPMOs in the presence of substrate to supply the two electrons needed, and the reduction of Cu(II) to Cu(I) only involves the transfer of one electron, this would imply that LPMOs could be able to store a second electron, or that the first transferred electron could lead to the subsequent oxidation of a tyrosine or tryptophan residue present in the vicinity of the active site.

3. Electron donors

As mentioned before, LPMOs require substances acting as electron donors to reduce LPMO-Cu(II) to LPMO-Cu(I). For this reaction, four electrons are required per O_2 molecule utilized, two being provided by the substrate and the other two delivered by different electron donors [6,27]. The main electron donors, either derived from natural or exogenous sources, are small molecule reductants such as gallic and ascorbic acids, biomass-derived soluble compounds, phenols derived from lignin or fungi, the CDH enzyme and members of the AA3 family, and light-harvesting pigments [17,18,28,29]. Langston et al. [30] and Phillips et al. [15] revealed the first evidence of the LPMO-CDH synergy system, nowadays three main systems are known to efficiently reduce LPMOs. The first system involves the heme b domain of CDH, which interacts directly with the copper site, enabling an ET event between this domain and the copper ion of LPMOs, with CDHs being able to transfer 2 electrons [26,31]. The second system involves phenols acquired from plant biomass or fungi, which can act as electron donors. There are some indications suggesting that lignin could also act as an electron donor, depending on its redox state. Westereng et al. [32] demonstrated the existence of a long-range ET from lignin toward the active site of LPMOs, as well as a collection of different small molecules originated from biomass (as fragments of lignin or secondary metabolites) and microbial metabolites (in this case, probably in the absence of other electron donors). Hu et al. [28] also demonstrated that LPMOs could use non-cellulosic biomass components, even at low concentrations, such as soluble compounds, lignin, and potentially hemicellulose. Kracher et al. [17] showed that members of glucose-methanol-choline (GMC) oxidoreductases use diphenols derived from lignin or fungi as redox mediators. Thirdly, some members of the AA3 family proved to be catalytically efficient as electron donors for LPMOs. Garajova et al.

[33] showed that glucose dehydrogenase and aryl-alcohol quinone oxidoreductase could also act as electron donors. Tangthirasunu et al. [34] showed that, in the presence of a mutant CDH, LPMO from *P. ansertna* is still active, suggesting that AA3_2 flavo-oxidase would be a potential candidate to provide electrons, since it increases in the secretome in the presence of the mutant CDH. Interestingly, Coutarde et al. [26] proposed that all the electrons required for the reaction are already present in LPMOs prior to their previous substrate binding, as they have the ability to store one electron, probably under the oxidized form of tyrosine or tryptophan.

Recently, new tools have been developed to improve our knowledge about the mode of action of LPMOs. An experimental system consisting of a photocalyst of vanadium-doped TiO_2 can promote light-driven water oxidation and supply LPMOs with electrons through a linear kinetic mechanism, avoiding side reactions as H_2O_2 production and providing valuable information about the catalytic mechanism. As the kinetic of oxidative cleavage is hard to obtain due to the fact that monitoring this parameter tend to yield non-linear curves, in a light-controlled electron flow this system can be used to study the redox state of LPMOs as well as their catalytic cycle [35].

4. Structural studies

According to the Carbohydrate-Active enZYmes (CAZy) database, nine LPMO structures from six different fungal AA9 are available: *Hypocrea jecorina* [13]; *Thielavia terrestris* [4]; *Thermoascus aurantiacus* [14]; *Neurospora crassa* [31,36,37]; *Phanerochaete chrysosporium* [38]; and *Lentinus similis* [39]. The AA9 enzymes display a common tertiary structural motif that resembles the immunoglobulin (Ig) domain and fibronectin type III (FnIII) (β-sandwich modules, forming seven to nine anti-parallel β-strands with Greek Key topology, which might be raised by α-helical loops) [8,40]. The overall structural stability is provided by hydrophobic cores, inter-strand backbone hydrogen bonds, and the presence of disulfide bridges [40]. The catalytic center is located on a flat surface on one side of the β-sandwich fold (Fig. 2) [38]. The LPMO domains show three extended and variable loops that are implicated in shaping the substrate-binding surface and could regulate substrate specificity (L2, LC, and LS). The first one, the L2 loop region, closer to the N-terminal, presents a disulfide bond, connecting L2 to strand β8. The second one, a C-terminal loop, contains no secondary structure elements, but is a very flexible region. The third one, LS, forms hydrophobic interactions with LC and is very flexible (Fig. 2A) [38].

Pichia pastoris is the most commonly used expression system to produce AA9 enzymes, due to its capacity to provide the glycosylation that might occur in AA9, additionally is readily available in academic laboratories. Considering the importance of the N-terminal His, Tanghe et al. [41] reported that the native secretion signal is more accurate to increase the yield of secreted recombinant enzymes, and several factors need to be taken into account when expressing AA9. Kim et al. [42] were able to express a functional CgAA9 in *E. coli*, an expression system that lacks post-translational modifications. Nevertheless, post-translational modifications on CgAA9 could confer higher synergism.

5. Catalytic site and regioselectivity of LPMOs

The catalytic site is formed by metal-binding amino acid residues: an N-terminal histidine and an additional histidine, which are involved in the coordination of cooper ions (Fig. 2). This structure is called the "histidine brace," and the first histidine may be methylated (Fig. 2C) [14], although this methylation is not necessary to enable the enzymatic activity [38]. Tyrosine is also a conserved amino acid residue within the catalytic site of AA9 [37] (Fig. 2).

The active site is embedded on the surface of the LPMO and forms a type II copper center. When AA9 are in the oxidized state, Cu(II) coordination involves extra ligands and forms an distorted octahedral geometry, whereas in the reduced state, Cu(I) is typically in a three-coordinate T-shaped configuration within the histidine brace [4,31,36,37]. The surface surrounding the active site on the surface of LPMOs can vary between them (Fig. 2), influencing the regioselectivity of the oxidation process [27]. The surface of AA9 might be flat or contoured, and this topography appears to be dependent on the shape of the substrate. Moreover, the size of the substrate might indicate the interaction of AA9–enzyme's binding to cello-oligosaccharides or to extended polysaccharides will depend on residues that mediate hydrogen bond interactions in catalytic site. Likewise, the metal ion can influence the structural plasticity of the site [26,39]. The catalytic site is oriented toward the surface of cellulose during catalysis and usually presents an equitable balanced number of positive and negative surface charges [43]. A study carried out by Eibinger et al. [44] showed that a LPMO from *N. crassa* introduces carboxyl groups to initiate the depolymerization of surface-exposed crystalline areas of cellulosic substrates, and subsequently degrades them into shorter and thinner insoluble fragments. This initial process shows that substrate morphology could be a key factor toward enabling the synergy between LPMOs and GHs.

LPMOs AA9 can be divided into three regioselective hydroxylation groups: type-1 LPMO named LPMO1 and type-2 LPMO named LPMO2, that hydroxylate glycosidic positions in C1 and C4, respectively, and type-3 LPMO named LPMO3, that hydroxylates both C1 and C4. In addition, a subgroup of LPMO3, named LPMO3*, that hydroxylates C1, has also been described [27]. This division does not necessarily predict all AA9 LPMOs' regioselectivities, as PaLPMO9H from *Podospora anserina* is predicted as type 2 but behaves as type 3 [45]. One of the main conserved amino acid near the catalytic site, tyrosine, is present in the protein-facing axial position. Borisova et al. [37] compared seven AA9 structures and reported differences that could be associated to regioselectivity: whilst LPMO1 have a tyrosine in the substrate-binding surface, hindering the access to this region, LPMO2 have an alanine or an aspartate, pointing away from the copper ion and contributing to higher permissiveness. LPMO3 have a proline instead of tyrosine, being an intermediate between LPMO1 and LPMO2. These differences in amino acid residues directly affect the accessibility of the solvent-facing axial position.

In the presence of water, aldonic acid and 4-ketoaldoses have been reported as the corresponding products of the oxidation of the pyranose ring situated at the C1 and C4 positions, respectively [27]. As a released product, 4-ketoaldose has a less stable structure than aldonic acid [46]. C1 oxidations of cellulose are more subjected to decrystallization than C4, which favors aldonic acid formation. If only C1 oxidation occurs, it may increase product inhibition and reduce processive substrate turnover; whereas C4 oxidation might reduce product inhibition. Therefore, the equilibrium between the two reducing end-products promotes processive cellulose turnover, accelerating degradation and promoting decrystallization [9]. Li et al. [47] identified the aldonic acid utilization pathway in *N. crassa*. It involves an extracellular hydrolase, a cellobionic acid transporter, and cellobionic acid phosphorylase. The same pathway is probably used by other fungi, whereas LPMOs are widespread among saprophytic fungi. However, to the best of our knowledge, no 4-ketoaldose specific pathway has been detected in fungi to date.

Using peptide pattern recognition (PPR) for sequence analysis, the AA9 family from LPMO was divided into 47 subfamilies for annotation. This division is not clearly correlated with the

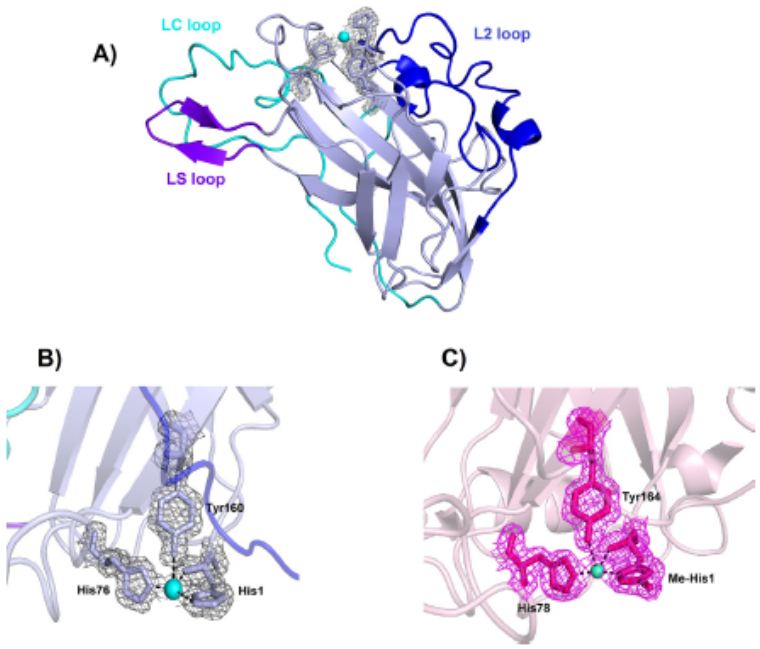

Fig. 2. Structural views of AA9 LPMOs. A) PcHGH61D crystal structure (*P. chrysosporium* – PDB: 4B5Q) [38] with the bound copper atom represented as a sphere in cyan. The L2, LS and LC loops are colored with different shades of blue. B) Electron density of active site of PcHGH61D with copper shown in cyan; C) Electron density of active site of LsAA9 (*L. similis* – PDB: 5ACJ) with copper shown in cyan and with a N-terminal methylated histidine [39].

regioselectivity of AA9 enzymes because there is not enough knowledge about their substrate specificities, and many members present different substrate preferences and specificities [18,20]. So far, LPMO activity has been detected against cellulose [14], xyloglucan [48], starch [49,50], and xylan [46,51]. Jagadeeswaran et al. [21] showed that different carbon sources, other than cellulose, such as xylan, xyloglucan, and pectin, can upregulate AA9 LPMOs in various ways, in terms of induction levels and timing. Moreover, no AA9 acting on pectin has been detected to date.

6. Assays

The first AA9 LPMO activity assay was measured indirectly, along with their synergism with cellulases (cellobiohydrolases and endoglucanases), using a *p*-hydroxybenzoic acid hydrazide (PAHBAH) reaction [4]. Nowadays, the current assay used to determine LPMO activity is based on a side-reaction. In the presence of reductants, such as ascorbic acid or CDH, the Cu(II) is reduced and the molecular oxygen is activated. The horseradish peroxidase processes the hydrogen peroxide released and Amplex Red is reduced to Resorufin. The formation of hydrogen peroxide is directly proportional to the LPMO concentration [52]. Nevertheless, this method is not accurate enough for complex samples such as crude extracts from fungi, since the side-reaction can detect hydrogen peroxide released from other enzymes such as glucose oxidase, lignin peroxidase, aryl-alcohol oxidase, among others. Furthermore, reducing end-products generated by glycosyl hydrolases are easily detected and quantified, whereas non-reducing end-products are not. Therefore, sensitive analytical and chromatographic methods were designed and adapted to obtain a good separation resolution between oxidized and native cello-oligosaccharides [53]. The high-performance anion-exchange chromatography (HPAEC), combined with pulsed amperometric detection (PAD) is well established to analyze C1-oxidized products and can also be used to detect C4-oxidized ones, but due to the instability of C4-oxidized products in alkaline conditions, this method is not precise enough to enable quantification. This method is fast and sensitive, but incompatible with mass spectrometry (MS) [53]. Recently, two methods were improved to enable the identifications of C1 and C4 oxidized products in non-destructive conditions. Porous graphitized carbon liquid chromatography (PGC–LC) and hydrophilic interaction chromatography (HILIC) are not as sensitive as HPAEC, but are compatible with MS, and are able to detect both oxidized products simultaneously in complex samples. Moreover, the PGC method has an additional advantage as it enables the purification of C4 oxidized products and therefore, their use as standards [54]. Regarding kinetic studies of AA9 LPMO, there is a lack of information about these data, especially because the complexity of monitoring oxidative cleavage. A study conducted by Frandsen et al. [39] used Förster resonance energy transfer (FRET) to monitor kinetic of an AA9 from *L. similis* with fluorescence-labeled cellotetraose. In this case, this enzyme showed a classic Michaelis-Menten model of action, acting on soluble oligosaccharides.

7. Carbohydrate-binding module

In AA families, various ancillary modules are observed. In AA9, this ancillary modes would be located at the C-terminus, as an N-terminal location would hamper the catalysis [6]. CBMs are independent domains presenting a flat face structure with hydrophobic amino acids. They are connected to the catalytic domain through

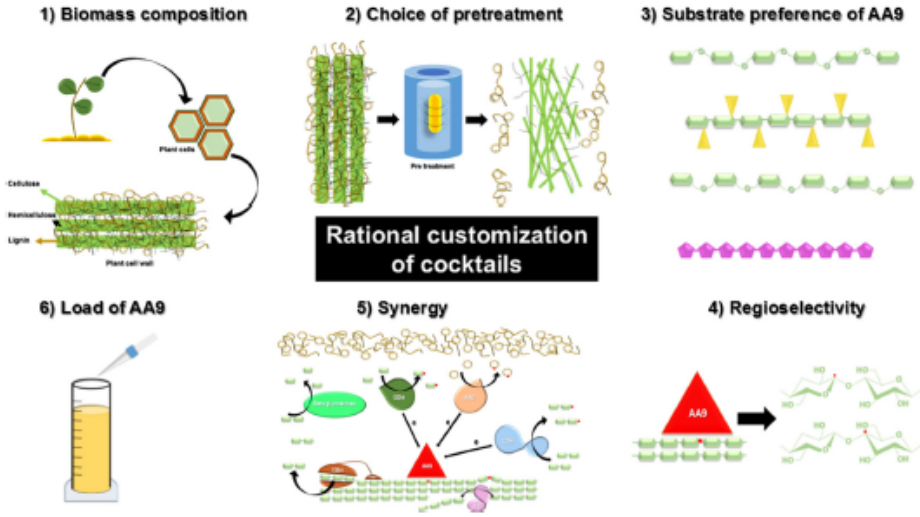

Fig. 3. Essential aspects to consider for the rational customization of AA9 cocktails toward applications in biorefinery. 1) Biomass composition, in relation with the main polysaccharide composition and lignin content; 2) Choice of pretreatment, depicted in the figure as a reactor for autohydrolysis; 3) Substrate preference of AA9, considering the substrates toward which AA9 has already demonstrated activity; 4) Regioselectivity of AA9, since it can be LPMO1, LPMO2, or LPMO3; 5) Synergy with other enzymes, to achieve an efficient degradation of biomass; 6) Load of AA9 in the cocktail.

linkers that present a variable composition of amino acids, but mostly proline-serine-threonine residues. It is known that CBMs play different roles in biomass degradation, as recognizing polysaccharides, determining substrate specificity, increasing enzymatic efficiency, and potentially causing substrate cleavage [55,56].

In fungi, AA9 are widely distributed, with organisms exhibiting multiple AA9 genes; some of them presenting CBM modules. This confirms the broad functional diversity of these enzymes, probably contributing to the synergic effect observed during biomass degradation, and promoting cellulose degradation [7,21]. In fact, several studies indicated that CBMs could improve LPMO activity and increase cellulose degradation [28,37,45]. However, Crouch et al. [57] showed that CBMs could also inhibit LPMO activity, since this effect is enzyme- and substrate-specific and regulates the mode of action of the oxygenases.

8. Proteomic studies

Analysis of the secretome of *H. jecorina* in different insoluble biomasses, as sugarcane bagasse, birch wood, spruce wood, and pure cellulose, demonstrated that all biomasses were able to induce LPMO production, but at different levels [58]. One study using *Mycellophthora thermophile M77* growing in pure cellulose, different pretreated sugarcane bagasses, wheat bran, milled soybeans, and fructooligosaccharides, revealed that this fungus secreted different sets of enzymes depending on the cell wall composition of the biomass used, focusing on the hydrolysis and oxidation of cellulose and other biomass components [59]. The secretome of *Pleurotus ostreatus*, a basidiomycete model fungus for delignification, growing on poplar wood or wheat straw, revealed that even if this organism possesses 18 LPMOs annotated in its genome, no LPMO was detected [60]. Curiously, Delmas et al. [61] used RNA sequencing of *Aspergillus niger* grown on wheat straw to study the gene expression of plant cell wall-degrading enzymes, and showed that no AA9 LPMO could be detected. However, this could be due to the insufficient amount of time left for transcript accumulation (24 h). Nevertheless, this indicates that LPMO might play alternative roles in these organisms, other than the hydrolysis of biomass.

A comparative study of different basidiomycete fungi secretomes (*Schizophyllum commune*, *P. chrysosporium*, *Ceriporiopsis subvermispora*, and *Gloephyllum trabeum*) during solid-state fermentation, using Jerusalem artichoke stalk as the carbon source, revealed that eight, three, and one AA9 LPMO members were identified in *S. commune*, *P. chrysosporium*, and *G. trabeum*, respectively, while no AA9 LPMO could be detected in *C. subvermispora* [62]. When *Aspergillus nidulans* was grown on different starches, nine AA9 LPMOs were identified, but with different expression patterns, indicating that they have a biological significance when it comes to starch degradation and interaction with amylolytic hydrolases [63]. Jagadeeswaran et al. [21] identified nine AA9 LPMO sequences in *A. nidulans*. The analysis of these sequences revealed that this fungus contains a complete set of all three subtypes of LPMOs, most of them being single domain proteins.

The nutritional source can control the content of proteins secreted, based on its nature and chemical composition. Complex carbon sources, such as lignocellulose biomass, can up-regulate the diversity of different enzymes and other intra- and extracellular components [3,64]. This may be a strategy aimed at enabling the adaptation of saprophytic fungi to different lignocellulose biomasses [64]. And these studies revealed that, beside ascomycetes and basidiomycetes have multiple AA9 LPMOs, their induction profiles and diversity are associate with polysaccharide constituents of plant biomass. These proteomic studies have provided insights into the diversity of these proteins and have revealed that not only biomass composition is directly related to the induction of AA9 diversity, but also the absence of expressed genes in proteomes indicates that these enzymes may have different roles besides the hydrolysis of biomass.

9. Synergy in biomass degradation

Nowadays, the use of LPMOs in cocktails to achieve an efficient saccharification of lignocellulosic biomass is a key factor. Different aspects need to be considered when designing new cocktails, as shown in Fig. 3.

Formerly, it was accepted that the presence of lignin in biomass saccharification was disadvantageous to enzymes. Currently, as LPMOs have been supplemented to the new generation of enzyme cocktails, lignin can play a role in activating this process. Hu et al. [28] demonstrated that the pretreatment of biomass could influence the oxidative activity of LPMOs with no need to add external electron donors, probably because of the presence of soluble biomass compounds and lignin, mainly when the substrate was not washed after pretreatment [65]. In terms of choosing the best pretreatment method for lignocellulosic biomass conversion in biorefinery, a study by Rodrigues-Zuniga et al. [66] showed that hydrothermal pretreatment was better for the preservation of lignin's reactivity toward influencing the oxidative activity of LPMOs. Hu et al. [67] argued that protein loading in biomass degradation, to achieve effective hydrolysis, needs to be optimized, and that just a small amount of AA9 was sufficient, irrelative of the nature of the substrate used or the concentration. However, another factor that needs to be considered is the synergistic effects between LPMOs and hydrolytic enzymes. Kim et al. [51] reported that AA9 from *Chaetomium globosum* can act synergistically with xylanase in pure xylan hydrolysis using xylan-containing pretreated biomass. Hu et al. [67] concluded that xylanase is highly biomass-dependent when it comes to performing the hydrolysis of pretreated biomasses. Considering the observations made in the studies mentioned above, more attention should be given to rationalizing the customization of cellulose cocktails in the lignocellulosic biorefinery industry. Taking into account specificities and regioselectivities of LPMOs; the pretreatment strategy along with the potential benefit of lignin, as well as the biomass composition and LPMO loading levels, paramount consideration should be given to this parameters toward optimizing processes [65,68,69]. Moreover, one of the main factor involved is the interplay between oxidative enzymes, classical GHs, and their CBMs in cellulose hydrolysis [51]. Understanding this interplay will have major implications for the development of enzymatic cocktails used in biomass conversion.

Finally, another aspect that needs to be taken into consideration is the supplementation with enzymes that have no direct role in biomass degradation. In the redox cycle of AA9, in the absence of substrate and in the presence of O_2 and an electron donor, superoxide will be released and spontaneously transformed into hydrogen peroxide [22]. Subsequently, hydrogen peroxide can react with copper and iron, forming ROS and hydroxyl radicals, being directly or indirectly prejudicial to enzymes. A study conducted by Scott et al. [70] concluded that the addition of catalase is successful in protecting cellulases from oxidative inactivation by hydrogen peroxide, leading to a longer saccharification process by improving the half-life of enzymes.

10. Concluding remarks

LPMOs from family AA9 represent a revolution in the biotechnology industry, which turned to biomass conversion for 2nd-generation biofuels. And their use is a promising approach toward waste biorefinery platforms development, and play a very important role in the efficient implementation of the circular economy [1]. Therefore, in-depth characterization of LPMOs is a crucial step towards understanding the biological impact and industrial potential of these enzymatic systems. Nevertheless, many issues still need to be addressed.

Information about the catalytic mechanism of LPMOs and the interaction of these enzymes with substrates is difficult to obtain owing to the fact that there are several types of polymeric substrates and that they are usually insoluble, large, and possess C—H bonds displaying different features. There is a large and diverse range of AA9 enzymes with different specificities and regioselectivities, acting on different substrates. The mechanisms leading to the acquisition of each of these specific traits have not yet been fully elucidated. In addition, there are still many interrogations regarding CBMs of AA9 that need to be answered, such as what is guiding and determining the binding specificity and how exactly do these modules affect enzyme efficiency. It is likely that natural processes have led to a specialization of these enzymes toward achieving the degradation of specific biomasses.

In conclusion, along with the comprehensive characterization of different sets of LPMOs and their potential uses, it is also paramount to have a holistic approach regarding these enzymes and their roles in nature, considering fungi evolution and functional biology within the context of their ecological niches. Such understanding will guide studies towards their most efficient use in biomass conversion.

Acknowledgments

The authors acknowledge the receipt of financial support from the Brazilian National Council for Scientific and Technological Development (CNPq), Coordination for the Improvement of Higher Education Personnel (CAPES) (http://www.capes.gov.br/), Foundation for Research Support of the Federal District (FAPDF), and the National Institute for Science and Technology of Bioethanol.

References

[1] R. Liguori, V. Faraco, Biological processes for advancing lignocellulosic waste biorefinery by advocating circular economy, Bioresour. Technol. 215 (2016) 13–20, http://dx.doi.org/10.1016/j.biortech.2016.04.054.
[2] F.G. de Siqueira, E.G. de Siqueira, P.M.D. Jaramillo, M.H.L. Silveira, J. Andreaus, F.A. Couto, L.R. Batista, E.X.F. Filho, The potential of agro-industrial residues for production of holocellulase from filamentous fungi, Int. Biodeterior. Biodegrad. 64 (2010) 20–26, http://dx.doi.org/10.1016/j.ibiod.2009.10.002.
[3] Z. Zhang, A.A. Donaldson, X. Ma, Advancements and future directions in enzyme technology for biomass conversion, Biotechnol. Adv. 30 (2012) 913–919, http://dx.doi.org/10.1016/j.biotechadv.2012.01.020.
[4] P.V. Harris, D. Welner, K.C. McFarland, E. Re, J.C. Navarro Poulsen, K. Brown, R. Salbo, H. Ding, E. Vlasenko, S. Merino, F. Xu, J. Cherry, S. Larsen, L. Lo Leggio, Stimulation of lignocellulosic biomass hydrolysis by proteins of glycoside hydrolase family 61: Structure and function of a large, enigmatic family, Biochemistry 49 (2010) 3305–3316, http://dx.doi.org/10.1021/bi100009p.
[5] G. Vaaje-Kolstad, B. Westereng, S.J. Horn, Z. Liu, H. Zhai, M. Sorlie, V.G.H. Eijsink, An oxidative enzyme boosting the enzymatic conversion of recalcitrant polysaccharides, Science (80-.) 330 (2010) 219–222, http://dx.doi.org/10.1126/science.1192231.
[6] A. Levasseur, E. Drula, V. Lombard, P.M. Coutinho, B. Henrissat, Expansion of the enzymatic repertoire of the CAZy database to integrate auxiliary redox enzymes, Biotechnol. Biofuels 6 (2013) 41, http://dx.doi.org/10.1186/1754-6834-6-41.
[7] S.J. Horn, G. Vaaje-Kolstad, B. Westereng, V.G. Eijsink, Novel enzymes for the degradation of cellulose, Biotechnol. Biofuels 5 (2012) 45, http://dx.doi.org/10.1186/1754-6834-5-45.
[8] G.R. Hemsworth, B. Henrissat, G.J. Davies, P.H. Walton, Discovery and characterization of a new family of lytic polysaccharide monooxygenases, Nat. Chem. Biol. 10 (2013) 122–126, http://dx.doi.org/10.1038/nchembio.1417.
[9] J.V. Vermaas, M.F. Crowley, G.T. Beckham, C.M. Payne, Effects of lytic polysaccharide monooxygenase oxidation on cellulose structure and binding of oxidized cellulose oligomers to cellulases, J. Phys. Chem. B 119 (2015) 6129–6143, http://dx.doi.org/10.1021/acs.jpcb.5b00778.
[10] C.F. Raguz, S. Yagüe, E. Wood, D.A. Thurston, Isolation and characterization of a cellulose-growth-specific gene from Agaricus bisporus, Gene 119 (1992) 183–190.
[11] M. Saloheimo, T. Nakari-Setala, M. Tenkanen, M. Penttila, cDNA cloning of a Trichoderma reesei cellulase and demonstration of endoglucanase activity by expression in yeast, Eur. J. Biochem. 249 (1997) 584–591, http://dx.doi.org/10.1111/j.1432-1033.1997.00584.x.
[12] B. Henrissat, G. Daviest, Structural and sequece-based classification of glycoside hydrolases, Curr. Opin. Chem. Biol. 7 (1997) 637–644.
[13] S. Karkehabadi, H. Hansson, S. Kim, K. Piens, C. Mitchinson, M. Sandgren, The first structure of a glycoside hydrolase family 61 member, Cel61B from hypocrea jecorina, at 1.6 Å resolution, J. Mol. Biol. 383 (2008) 144–154, http://dx.doi.org/10.1016/j.jmb.2008.08.016.
[14] R.J. Quinlan, M.D. Sweeney, L. Lo Leggio, H. Otten, J.-C.N. Poulsen, K.S. Johansen, K.B.R.M. Krogh, C.I. Jorgensen, M. Tovborg, A. Anthonsen, T. Tryfona, C.P. Walter, P. Dupree, F. Xu, G.J. Davies, P.H. Walton, Insights into the

oxidative degradation of cellulose by a copper metalloenzyme that exploits biomass components, Proc. Natl. Acad. Sci. 108 (2011) 15079–15084, http://dx.doi.org/10.1073/pnas.1105776108.
[15] C.M. Phillips, W.T. Beeson, J.H. Cate, M.A. Marletta, Cellobiose dehydrogenase and a copper-dependent polysaccharide monooxygenase potentiate cellulose degradation by neurospora crassa, ACS Chem. Biol. 6 (2011) 1399–1406, http://dx.doi.org/10.1021/cb200351y.
[16] B. Westereng, T. Ishida, G. Vaaje-Kolstad, M. Wu, V.G.H. Eijsink, K. Igarashi, M. Samejima, J. Ståhlberg, S.J. Horn, M. Sandgren, The putative endoglucanase pcGH61D from phanerochaete chrysosporium is a metal-dependent oxidative enzyme that cleaves cellulose, PLoS One 6 (2011), http://dx.doi.org/10.1371/journal.pone.0027807.
[17] D. Kracher, S. Scheiblbrandner, A.K.G. Felice, E. Breslmayr, M. Preims, K. Ludwicka, D. Haltrich, V.G.H. Eijsink, R. Ludwig, Extracellular electron transfer systems fuel cellulose oxidative degradation, Science 352 (2016), http://dx.doi.org/10.1126/science.aaf3165.
[18] M. Dimarogona, E. Topakas, P. Christakopoulos, Cellulose degradation by oxidative enzymes, Comput. Struct. Biotechnol. J. 2 (2012) 1–8, http://dx.doi.org/10.5936/csbj.201209015.
[19] L. Žifčáková, P. Baldrian, Fungal polysaccharide monooxygenases: new players in the decomposition of cellulose, Fungal Ecol. 5 (2012) 481–489, http://dx.doi.org/10.1016/j.funeco.2012.05.001.
[20] P.K. Busk, L. Lange, Classification of fungal and bacterial lytic polysaccharide monooxygenases, BMC Genomics 16 (2015) 368, http://dx.doi.org/10.1186/s12864-015-1601-6.
[21] G. Jagadeeswaran, L. Gainey, R. Prade, A.J. Mort, A family of AA9 lytic polysaccharide monooxygenases in Aspergillus nidulans is differentially regulated by multiple substrates and at least one is active on cellulose and xyloglucan, Appl. Microbiol. Biotechnol. (2016) 1–13, http://dx.doi.org/10.1007/s00253-016-7505-9.
[22] C.H. Kjaergaard, M.F. Qayyum, S.D. Wong, F. Xu, G.R. Hemsworth, D.J. Walton, N.A. Young, G.J. Davies, P.H. Walton, K.S. Johansen, K.O. Hodgson, B. Hedman, E.I. Solomon, Spectroscopic and computational insight into the activation of O_2 by the mononuclear Cu center in polysaccharide monooxygenases, Proc. Natl. Acad. Sci. U. S. A. 111 (2014) 8797–8802, http://dx.doi.org/10.1073/pnas.1408115111.
[23] S. Kim, J. Ståhlberg, M. Sandgren, R.S. Paton, G.T. Beckham, Quantum mechanical calculations suggest that lytic polysaccharide monooxygenases use a copper-oxyl, oxygen-rebound mechanism, Proc Natl. Acad. Sci. U. S. A. 111 (2014) 149–154, http://dx.doi.org/10.1073/pnas.1316609111.
[24] M. Gudmundsson, S. Kim, M. Wu, T. Ishida, M.H. Momeni, G. Vaaje-Kolstad, D. Lundberg, A. Royant, J. Ståhlberg, V.G.H. Eijsink, G.T. Beckham, M. Sandgren, Structural and electronic snapshots during the transition from a Cu(II) to Cu(I) metal center of a lytic polysaccharide onooxygenase by x-ray photoreduction, J. Biol. Chem. 289 (2014) 18782–18792, http://dx.doi.org/10.1074/jbc.M114.563494.
[25] P.H. Walton, G.J. Davies, On the catalytic mechanisms of lytic polysaccharide monooxygenases, Curr. Opin. Chem. Biol. (2016) 1–13, http://dx.doi.org/10.1016/j.cbpa.2016.04.001.
[26] G. Courtade, R. Wimmer, Å.K. Røhr, M. Preims, A.K.G. Felice, M. Dimarogona, G. Vaaje-Kolstad, M. Sørlie, M. Sandgren, R. Ludwig, V.G.H. Eijsink, F.L. Aachmann, Interactions of a fungal lytic polysaccharide monooxygenase with β-glucan substrates and cellobiose dehydrogenase, Proc. Natl. Acad. Sci. U. S. A. 113 (2016) 5922–5997, http://dx.doi.org/10.1073/pnas.1602566113.
[27] V.V. Vu, W.T. Beeson, C.M. Phillips, J.H.D. Cate, M.A. Marletta, Determinants of regioselective hydroxylation in the fungal polysaccharide monooxygenases, J. Am. Chem. Soc. 136 (2014) 562–565, http://dx.doi.org/10.1021/ja409384b.
[28] J. Hu, V. Arantes, A. Pribowo, Substrate factors that influence the synergistic interaction of AA9 and cellulases during the enzymatic hydrolysis of biomass, Energy Environ. Sci. 7 (2014) 2308–2315, http://dx.doi.org/10.1039/C4EE00891J.
[29] D. Cannella, K.B. Möllers, N.-U. Frigaard, P.E. Jensen, M.J. Bjerrum, K.S. Johansen, C. Felby, Light-driven oxidation of polysaccharides by photosynthetic pigments and a metalloenzyme, Nat. Commun. 7 (2016) 1–8, http://dx.doi.org/10.1038/ncomms11134.
[30] J.A. Langston, T. Shaghasi, E. Abbate, F. Xu, E. Vlasenko, M.D. Sweeney, Oxidoreductive cellulose depolymerization by the enzymes cellobiose dehydrogenase and glycoside hydrolase 61, Appl. Environ. Microbiol. 77 (2011) 7007–7015, http://dx.doi.org/10.1128/AEM.05815-11.
[31] T.-C. Tan, D. Kracher, R. Gandini, C. Sygmund, R. Kittl, D. Haltrich, B.M. Hällberg, R. Ludwig, C. Divne, Structural basis for cellobiose dehydrogenase action during oxidative cellulose degradation, Nat. Commun. 6 (2015) 7542, http://dx.doi.org/10.1038/ncomms8542.
[32] B. Westereng, D. Cannella, J. Wittrup Agger, H. Jørgensen, M. Larsen Andersen, V.G.H. Eijsink, C. Felby, Enzymatic cellulose oxidation is linked to lignin by long-range electron transfer, Sci. Rep. 5 (2015) 18561, http://dx.doi.org/10.1038/srep18561.
[33] S. Garajova, Y. Mathieu, M.R. Beccia, C. Bennati-Granier, F. Biaso, M. Fanuel, D. Ropartz, B. Guigliarelli, E. Record, H. Rogniaux, B. Henrissat, J.-G. Berrin, Single-domain flavoenzymes trigger lytic polysaccharide monooxygenases for oxidative degradation of cellulose, Sci. Rep. 6 (2016) 28276, http://dx.doi.org/10.1038/srep28276.
[34] N. Tangthirasunun, D. Navarro, S. Garajova, D. Chevret, L. Chan Ho Tong, V. Gautier, K.D. Hyde, P. Silar, J.-G. Berrin, Investigation of the role played by cellobiose dehydrogenases from *Podospora anserina* during lignocellulose degradation, Appl. Environ. Microbiol. (2016), http://dx.doi.org/10.1128/AEM.02716-16 (AEM. 02716-16).
[35] B. Bissaro, Z. Forsberg, Y. Ni, F. Hollmann, G. Vaaje-Kolstad, V.G.H. Eijsink, Fueling biomass-degrading oxidative enzymes by light-driven water oxidation, Green Chem. 18 (2016) 5357–5366, http://dx.doi.org/10.1039/C6GC01666A.
[36] X. Li, W.T. Beeson IV, C.M. Phillips, M.A. Marletta, J.H.D. Cate, Structural basis for substrate targeting and catalysis by fungal polysaccharide monooxygenases, Structure 20 (2012) 1051–1061, http://dx.doi.org/10.1016/j.str.2012.04.002.
[37] A.S. Borisova, T. Isaksen, M. Dimarogona, A.A. Kognole, G. Mathiesen, A. Várnai, Å.K. Røhr, C.M. Payne, M. Sørlie, M. Sandgren, V.G.H. Eijsink, Structural and functional characterization of a lytic polysaccharide monooxygenase with broad substrate specificity, J. Biol. Chem. 290 (2015) 22955–22969, http://dx.doi.org/10.1074/jbc.M115.660183.
[38] M. Wu, G.T. Beckham, A.M. Larsson, T. Ishida, S. Kim, C.M. Payne, M.E. Himmel, M.F. Crowley, S.J. Horn, B. Westereng, K. Igarashi, M. Samejima, J. Ståhlberg, V.G.H. Eijsink, M. Sandgren, Crystal structure and computational characterization of the lytic polysaccharide monooxygenase GH61D from the basidiomycota fungus Phanerochaete chrysosporium, J. Biol. Chem. 288 (2013) 12828–12839, http://dx.doi.org/10.1074/jbc.M113.459396.
[39] K.E.H. Frandsen, T.J. Simmons, P. Dupree, J.N. Poulsen, G.R. Hemsworth, L. Ciano, E.M. Johnston, M. Tovborg, K.S. Johansen, P. von Freiesleben, L. Marmuse, S. Fort, S. Cottaz, H. Driguez, B. Henrissat, N. Lenfant, F. Tuna, A. Baldansuren, G.J. Davies, L. Lo Leggio, P.H. Walton, The molecular basis of polysaccharide cleavage by lytic polysaccharide monooxygenases, Nat. Chem. Biol. 12 (2016) 298–303, http://dx.doi.org/10.1038/nchembio.2029.
[40] E.A. Span, M.A. Marletta, The framework of polysaccharide monooxygenase structure and chemistry, Curr. Opin. Struct. Biol. 35 (2015) 93–99, http://dx.doi.org/10.1016/j.sbi.2015.10.002.
[41] M. Tanghe, B. Danneels, A. Camattari, A. Glieder, I. Vandenberghe, B. Devreese, I. Stals, T. Desmet, Recombinant expression of trichoderma reesei Cel61A in pichia pastoris: optimizing yield and N-terminal processing, Mol. Biotechnol. 57 (2015) 1010–1017, http://dx.doi.org/10.1007/s12033-015-9887-9.
[42] I.J. Kim, K.H. Nam, E.J. Yun, S. Kim, H.J. Youn, H.J. Lee, I.G. Choi, K.H. Kim, Optimization of synergism of a recombinant auxiliary activity 9 from Chaetomium globosum with cellulase in cellulose hydrolysis, Appl. Microbiol. Biotechnol. 99 (2015) 8537–8547, http://dx.doi.org/10.1007/s00253-015-6592-3.
[43] I. Patel, D. Kracher, S. Ma, S. Garajova, M. Haon, C.B. Faulds, J.-G. Berrin, R. Ludwig, E. Record, Salt-responsive lytic polysaccharide monooxygenases from the mangrove fungus Pestalotiopsis sp. NCi6, Biotechnol. Biofuels 9 (108) (2016), http://dx.doi.org/10.1186/s13068-016-0520-3.
[44] M. Eibinger, T. Ganner, P. Bubner, S. Rošker, D. Kracher, D. Haltrich, R. Ludwig, H. Plank, B. Nidetzky, Cellulose surface degradation by a lytic polysaccharide monooxygenase and its effect on cellulase hydrolytic efficiency, J. Biol. Chem. 289 (2014) 35929–35938, http://dx.doi.org/10.1074/jbc.M114.602227.
[45] C. Bennati-Granier, S. Garajova, C. Champion, S. Grisel, M. Haon, S. Zhou, M. Fanuel, D. Ropartz, H. Rogniaux, I. Gimbert, E. Record, J.-G. Berrin, Substrate specificity and regioselectivity of fungal AA9 lytic polysaccharide monooxygenases secreted by Podospora anserina, Biotechnol. Biofuels 8 (2015) 90, http://dx.doi.org/10.1186/s13068-015-0274-3.
[46] M. Frommhagen, S. Sforza, A.H. Westphal, J. Visser, S.W.A. Hinz, M.J. Koetsier, W.J.H. van Berkel, H. Gruppen, M.A. Kabel, Discovery of the combined oxidative cleavage of plant xylan and cellulose by a new fungal polysaccharide monooxygenase, Biotechnol. Biofuels 8 (2015) 101, http://dx.doi.org/10.1186/s13068-015-0284-1.
[47] X. Li, K. Chomvong, V.Y. Yu, J.M. Liang, Y. Lin, J.H.D. Cate, Cellobionic acid utilization: from Neurospora crassa to Saccharomyces cerevisiae, Biotechnol. Biofuels 8 (2015) 120, http://dx.doi.org/10.1186/s13068-015-0303-2.
[48] J.W. Agger, T. Isaksen, A. Várnai, S. Vidal-Melgosa, W.G.T. Willats, R. Ludwig, S.J. Horn, V.G.H. Eijsink, B. Westereng, Discovery of LPMO activity on hemicelluloses shows the importance of oxidative processes in plant cell wall degradation, Proc. Natl. Acad. Sci. U. S. A. 111 (2014) 6287–6292, http://dx.doi.org/10.1073/pnas.1323629111.
[49] V.V. Vu, W.T. Beeson, E.A. Span, E.R. Farquhar, M.A. Marletta, A family of starch-active polysaccharide monooxygenases, Proc. Natl. Acad. Sci. U. S. A. 111 (2014) 13822–13827, http://dx.doi.org/10.1073/pnas.1408090111.
[50] L. Lo Leggio, T.J. Simmons, J.-C.N. Poulsen, K.E.H. Frandsen, G.R. Hemsworth, M.A. Stringer, P. von Freiesleben, M. Tovborg, K.S. Johansen, L. De Maria, P.V. Harris, C.-L. Soong, P. Dupree, T. Tryfona, N. Lenfant, B. Henrissat, G.J. Davies, P.H. Walton, Structure and boosting activity of a starch-degrading lytic polysaccharide monooxygenase, Nat. Commun. 6 (2015) 5961, http://dx.doi.org/10.1038/ncomms6961.
[51] I.J. Kim, H.J. Youn, K.H. Kim, Synergism of an auxiliary activity 9 (AA9) from Chaetomium globosum with xylanase on the hydrolysis of xylan and lignocellulose, Process Biochem. 51 (2016) 1445–1451, http://dx.doi.org/10.1016/j.procbio.2016.06.017.
[52] R. Kittl, D. Kracher, D. Burgstaller, D. Haltrich, R. Ludwig, Production of four Neurospora crassa lytic polysaccharide monooxygenases in Pichia pastoris monitored by a fluorimetric assay, Biotechnol. Biofuels. 5 (2012) 79, http://dx.doi.org/10.1186/1754-6834-5-79.
[53] B. Westereng, J.W. Agger, S.J. Horn, G. Vaaje-Kolstad, F.L. Aachmann, Y.H. Stenstrøm, V.G.H. Eijsink, Efficient separation of oxidized cello-oligosaccharides generated by cellulose degrading lytic polysaccharide

monooxygenases, J. Chromatogr. A. 1271 (2013) 144–152, http://dx.doi.org/10.1016/j.chroma.2012.11.048.
[54] B. Westereng, M.T. Arntzen, F.L. Aachmann, A. Várnai, V.G.H. Eijsink, J.W. Agger, Simultaneous analysis of C1 and C4 oxidized oligosaccharides, the products of lytic polysaccharide monooxygenases acting on cellulose, J. Chromatogr. A. 1445 (2016) 46–54, http://dx.doi.org/10.1016/j.chroma.2016.03.064.
[55] H.J. Gilbert, J.P. Knox, A.B. Boraston, Advances in understanding the molecular basis of plant cell wall polysaccharide recognition by carbohydrate-binding modules, Curr. Opin. Struct. Biol. 23 (2013) 669–677, http://dx.doi.org/10.1016/j.sbi.2013.05.005.
[56] D.W. Abbott, A.L. van Bueren, Using structure to inform carbohydrate binding module function, Curr. Opin. Struct. Biol. 28 (2014) 32–40, http://dx.doi.org/10.1016/j.sbi.2014.07.004.
[57] L.I. Crouch, A. Labourel, P.H. Walton, G.J. Davies, H.J. Gilbert, The contribution of non-catalytic carbohydrate binding modules to the activity of lytic polysaccharide monooxygenases, J. Biol. Chem. 291 (2016) 7439–7449, http://dx.doi.org/10.1074/jbc.M115.702365.
[58] O. Bengtsson, M. Arntzen, G. Mathiesen, M. Skaugen, V.G.H. Eijsink, A novel proteomics sample preparation method for secretome analysis of Hypocrea jecorina growing on insoluble substrates, J. Proteomics 131 (2016) 104–112, http://dx.doi.org/10.1016/j.jprot.2015.10.017.
[59] H.B. dos Santos, T.M.S. Bezerra, J.G.C. Pradella, P. Delabona, D. Lima, E. Gomes, S.D. Hartson, J. Rogers, B. Couger, R. Prade, Myceliophthora thermophila M77 utilizes hydrolytic and oxidative mechanisms to deconstruct biomass, AMB Express 6 (2016) 103, http://dx.doi.org/10.1186/s13568-016-0276-y.
[60] E. Fernández-Fueyo, F.J. Ruiz-Dueñas, M.F. López-Lucendo, M. Pérez-Boada, J. Rencoret, A. Gutiérrez, A.G. Pisabarro, L. Ramírez, A.T. Martínez, A secretomic view of woody and nonwoody lignocellulose degradation by *Pleurotus ostreatus*, Biotechnol. Biofuels 9 (2016) 49, http://dx.doi.org/10.1186/s13068-016-0462-9.
[61] S. Delmas, S.T. Pullan, S. Gaddipati, M. Kokolski, S. Malla, M.J. Blythe, R. Ibbett, M. Campbell, S. Liddell, A. Aboobaker, G.A. Tucker, D.B. Archer, Uncovering the genome-wide transcriptional responses of the filamentous fungus aspergillus niger to lignocellulose using RNA sequencing, PLoS Genet. 8 (2012), http://dx.doi.org/10.1371/journal.pgen.1002875.
[62] N. Zhu, J. Liu, J. Yang, Y. Lin, Y. Yang, L. Ji, M. Li, H. Yuan, Comparative analysis of the secretomes of Schizophyllum commune and other wood-decay basidiomycetes during solid-state fermentation reveals its unique lignocellulose-degrading enzyme system, Biotechnol. Biofuels 9 (2016) 42, http://dx.doi.org/10.1186/s13068-016-0461-x.
[63] L. Nekiunaite, M.Ø. Arntzen, B. Svensson, G. Vaaje-Kolstad, M. Abou Hachem, Lytic polysaccharide monooxygenases and other oxidative enzymes are abundantly secreted by Aspergillus nidulans grown on different starches, Biotechnol. Biofuels 9 (2016) 187, http://dx.doi.org/10.1186/s13068-016-0604-0.
[64] N.A. Brown, L.N.A. Ries, G.H. Goldman, How nutritional status signalling coordinates metabolism and lignocellulolytic enzyme secretion, Fungal Genet. Biol. 72 (2014) 48–63, http://dx.doi.org/10.1016/j.fgb.2014.06.012.
[65] G. Müller, A. Várnai, K.S. Johansen, V.G.H. Eijsink, S.J. Horn, Harnessing the potential of LPMO-containing cellulase cocktails poses new demands on processing conditions, Biotechnol. Biofuels 8 (2015) 187, http://dx.doi.org/10.1186/s13068-015-0376-y.
[66] U.F. Rodríguez-Zúñiga, D. Cannella, R. de, C. Giordano, R. de, L.C. Giordano, H. Jørgensen, C. Felby, Lignocellulose pretreatment technologies affect the level of enzymatic cellulose oxidation by LPMO, Green Chem. 17 (2015) 2896–2903, http://dx.doi.org/10.1039/C4GC02179G.
[67] J. Hu, R. Chandra, V. Arantes, K. Gourlay, J. Susan van Dyk, J.N. Saddler, The addition of accessory enzymes enhances the hydrolytic performance of cellulase enzymes at high solid loadings, Bioresour. Technol. 186 (2015) 149–153, http://dx.doi.org/10.1016/j.biortech.2015.03.055.
[68] M.G. Resch, B.S. Donohoe, P.N. Ciesielski, J.E. Nill, L. Magnusson, M.E. Himmel, A. Mittal, R. Katahira, M.J. Biddy, G.T. Beckham, Clean fractionation pretreatment reduces enzyme loadings for biomass saccharification and reveals the mechanism of free and cellulosomal enzyme synergy, ACS Sustain. Chem. Eng. 2 (2014) 1377–1387, http://dx.doi.org/10.1021/sc500210w.
[69] F.F. Sun, J. Hong, J. Hu, J.N. Saddler, X. Fang, Z. Zhang, S. Shen, Accessory enzymes influence cellulase hydrolysis of the model substrate and the realistic lignocellulosic biomass, Enzyme Microb. Technol. 79–80 (2015) 42–48, http://dx.doi.org/10.1016/j.enzmictec.2015.06.020.
[70] B.R. Scott, H.Z. Huang, J. Frickman, R. Halvorsen, K.S. Johansen, Catalase improves saccharification of lignocellulose by reducing lytic polysaccharide monooxygenase-associated enzyme inactivation, Biotechnol. Lett. 38 (2016) 425–434, http://dx.doi.org/10.1007/s10529-015-1989-8.

CAPÍTULO 6 - ESTUDOS DO MECANISMO DE DEGRADAÇÃO OXIDATIVA DE BIOMASSA LIGNOCELULÓSICA POR MONOOXIGENASES LÍTICAS DE POLISSACARÍDEOS (LPMOs) DE *ASPERGILLUS TAMARII*

6.1 Introdução

Estudos sobre a caracterização funcional de todas as enzimas de um único microrganismo é uma etapa crucial para o entendimento do impacto biológico e do potencial industrial desses sistemas enzimáticos. Sabe-se que as LPMOs atuam diretamente na sacarificação enzimática da biomassa lignocelulolósica e aumentam a eficiência de outras enzimas através de sinergismo, tanto que atualmente essas enzimas já estão inclusas em coquetéis enzimáticos (HU et al., 2015). Dentre os fungos extensamente estudados, o *A. oryzae* é um fungo saprófito filogeneticamente próximo ao *A. tamarii* e amplamente utilizando industrialmente. Seu genoma apresenta 8 genes codificando AA9 LPMOs, enquanto que o transcriptoma de *A. tamarii* apresenta 7 genes codificando AA9 LPMOs. Ambos os fungos possuem um número considerável de genes para essa enzima, principalmente com outros microrganismos do gênero *Aspergillus*. Os fungos representam um modelo de sistema enzimático apropriado para se estudar a desconstrução oxidativa da biomassa, pois além de demonstrarem potencial na decomposição da biomassa, nenhuma de suas AA9 foram caracterizadas. Além disso, por serem microrganismos filogeneticamente próximos, a comparação entre suas enzimas pode ser importante para compreender relações filogenéticas entre eles e elucidar o porquê que há uma grande quantidade da mesma enzima presente no mesmo microrganismo.

6.2 Objetivos do Capítulo

Análises *in silico* das AA9 de *A. oryzae* e *A. tamarii*. Clonagem e expressão heteróloga de 9 LPMOs em *Pichia pastoris.*. Purificação de três AA9 de *A. tamarii* e uma AA9 de *A. oryzae*. Análise de seus produtos de reação e caracterização bioquímica, focando em sinergismos e bioprocessos.

6.3 Materiais e Métodos

6.3.1 Escolha das LPMOs candidatas

6.3.1.1 Obtenção das sequências das LPMOs de *A. tamarii*

As sequências foram provenientes do RNA-seq realizado por Midorikawa (GLAUCIA EMY OKIDA MIDORIKAWA, 2014), onde *A. tamarii* foi cultivado

utilizando bagaço de cana-de-açúcar e glicose como fonte de carbono, por 36 e 48 hoas, em meio líquido e meio sólido. Os sete genes preditos para AA9 foram identificados. Para confirmar os domínios conservados de AA9, as sequências foram submetidas ao banco de dados dbCAN (disponível em http://csbl.bmb.uga.edu/dbCAN/), que compila informações sobre sequências e anotações dos genes das CAZymes (HUANG et al., 2017), e Uniprot (disponível em: http://www.uniprot.org/).

6.3.1.2 Obtenção das sequências das LPMOs de *A. oryzae*

O genoma do fungo *A. oryzae* foi sequenciado em 2005 (MACHIDA et al., 2005) e as sequências completas dos genes estão depositadas no banco de dados *GenBank*, do *National Center for Biotechnology Information* (NCBI).

6.3.1.3 Comparação entre as LPMOs de *A. tamarii* e *A. oryzae*

Após a confirmação dos domínios presentes, as sequências dos transcritos foram submetidas à ferramenta Translate tool (disponível em http://web.expasy.org/translate/) para avaliação de ORFs (*open reading frame),* considerando ATG como códon iniciador e TAA ou TGA como códon de parada. Sabendo-se que todas AA9 possuem histidina como o primeiro aminoácido após o peptídeo sinal (TANGHE et al., 2015), as ORFs foram submetidas então à ferramenta SignalP 4.1 (disponível em http://www.cbs.dtu.dk/services/SignalP/) para predição dos peptídeos sinais e confirmação do primeiro aminoácido ser uma histidina (códons: CAT e CAC). Após a confirmação, as análises *in silico* realizadas foram: i) ferramenta ProtParam (disponível em: http://web.expasy.org/protparam/) para computar parâmetros físicos e químicos da sequência de aminoácidos; ii) ferramenta NetNGlyc 1.0 (disponível em: http://www.cbs.dtu.dk/services/NetNGlyc/) para predição de N-glicosilações; iii) ferramenta NetOGlyc 4.0 (disponível em: http://www.cbs.dtu.dk/services/NetOGlyc/) para predições de O-glicosilações; e v) ferramenta MUSCLE (disponível em: https://www.ebi.ac.uk/Tools/msa/muscle/) para alinhamentos múltiplos das sequências. Para comparação de aminoácidos conservados entre genes ortólogos de diferentes espécies de *Aspergillus*, as sequência foram obtidas no banco de dados *GenBank*, do *National Center for Biotechnology Information* (NCBI).

6.3.2 Estratégia de clonagem em PichiaPink™

As sequências selecionadas não continham o peptídeo sinal e foram harmonizadas (ANGOV et al., 2008) para clonagem em *P. pastoris*. A harmonização combina, através de um algoritmo, a frequência de uso dos códons inerentes ao hospedeiro nativo (*A.*

tamarii e *A. oryzae)* com os códons mais próximos possíveis no hospedeiro heterólogo (*P. pastoris).* Os genes foram sintetizadas pela empresa GenScript® e o vetor pUC57 foi utilizado para clonagem.

6.3.2.1 Preparação do plasmídio pUC57

Para a transformação por choque térmico, as células quimicamente compententes One Shot® TOP10 de *Escherichia coli* da Invitrogen™ foram utilizadas. A transformação por choque térmico foi realizada da seguinte forma: 10 µl da One Shot® TOP10 termo competente com 0.5 µl do plasmídio. A mistura foi incubada em gelo por 30 minutos, logo após esse período a mistura foi rapidamente incubada a 42 ºC por 30 segundos e em seguida novamente incubada no gelo. Para a recuperação das células transformadas, foram adicionados 1 ml de meio S.O.C. (*Super Optimal broth with Catabolite repression*), seguido por incubação a 37 ºC e 225 rpm por 1 hora. Após esse período, 20-200 µl células foram plaqueadas em meio LB (*Luria-Bertani*) sólido, contendo 10 µg/ml do antibiótico ampicilina. As placas foram então incubadas a 37ºC por aproximadamente 16 horas. Após as 16 horas de incubação, duas colônias foram selecionadas e cultivadas (separadamente) durante a noite em 7 ml de meio líquido BHI (*Brain Heart Infusion*) contendo 10 µg/ml de ampicilina. Da cultura *overnight*, 1 ml foi utilizado para fazer estoque em glicerol 50%, o restante para extração do plasmídio, utilizando o kit de purificação *Nucleaspin® plasmid* da MACHEREY-NAGEL GmbH & Co. KG. A concentração de DNA foi determinada com o kit Qubit dsDNA BR, da Invitrogen™.

6.3.2.2 Ensaio de restrição no plasmídio pUC57

A liberação dos genes de interesse com eas enzimas de restrição a partir dos plasmídios isolados ocorreu da seguinte forma: 1 µg do plasmídio isolado (podendo chegar no total de 16 µl), 2 µL de tampão 10x FD (*Fast Digest*), 1 µL de *EcoRI* e 1 µL de *Acc65I* (Thermo Scientific™), enzimas de restrição. A reação foi incubada por 30 minutos a 37 ºC. Após, as amostras foram aplicadas em gel de agarose 1%, 80 Volts, por 40 minutos. As bandas correspondentes aos genes de interesse foram excisadas do gel e purificadas com o kit *NucleoSpin® Gel and PCR Clean-up* da MACHEREY-NAGEL GmbH & Co. KG. A concentração de DNA foi medida com o kit Qubit dsDNA BR, da Invitrogen™.

6.3.2.3 Inserção no plasmídio pGAP em *E. coli* TOP10

Os genes provenientes da digestão foram ligados ao plasmídio previamente linerarizado pPINK-GAP (VÁRNAI et al., 2014), através do kit Quick Ligation™ da *New England BioLabs*®. A reação de ligação ocorreu baseado na seguinte equação:

$$[\text{inserto}] = \frac{[\,vetor]x\ tamanho\ do\ inserto}{tamanho\ do\ vetor} \qquad \text{Eq.(1)}$$

Foram combinadas 50 ng de pPINK-GAP com os insertos, na proporção 3 (inserto):1 (vetor). A reação ocorreu a temperatura ambiente por 5 minutos, em seguida resfriada em gelo. A transformação foi feita com as células quimicamente compententes One Shot® TOP10 de *E. coli*, conforme descrito na seção 5.3.2.1. A partir da cultura *overnight*, quatro a oito colônias foram selecionadas para confirmação da transformação correta. A PCR foi realizada com o kit *Q5® High-Fidelity DNA Polymerase*, da *New England BioLabs*. Os *primers* GAPseq e CYCr foram utilizados. A confirmação da amplificação dos genes de interesse foi realizada por eletroforese em gel de agarose 1%, 80 V por 40 minutos.

6.3.2.4 Linearização do plasmídio pPINK-GAP

O plasmídio pPINK-GAP foi linearizado com apenas uma enzima de restrição da seguinte forma: 10 µg do plasmídio isolado (podendo chegar no total de 40 µl), 5 µL de tampão 10x FD (*Fast Digest*) e 1 µL da enzima de restrição *BspTI* (Thermo Scientific™). A reação foi incubada por 30 minutos a 37ºC. A precipitação do plasmídio foi realizada da seguinte forma: 125 µl de etanol 100% e 5 µl de acetato de sódio 3 mM foram adicionados à reação e os tubos foram centrifugados a 20.000 x g por 15 minutos; o sobrenadante foi descartado, o *pellet* foi lavado com 80 µl de etanol 100% e os tubos foram novamente centrifugados a 20.000 x g por 15 minutos; o sobrenadante foi decartado. Após evaporção completa do etanol, o *pellet* foi ressuspendido em 15-30 µl de água esterilizada.

6.3.2.5 Preparo de células eletrocompetentes

As células de PichiaPink™ utilizadas nas etapas de transformação foram preparadas da seguinte forma: uma colônia da linhagem de PichiaPink™ foi inoculada em tubo tipo Falcon (50 mL) contendo 5 mL de meio YPD e incubada a 30ºC *overnight*. No dia seguinte, a densidade óptica de 600 nm (OD-600) foi medida e os inóculos foram diluídos em YPD (*Yeast extract-Peptone-Dextrose*) para que a OD-600 começasse em

torno de 0,002. Após 20 horas de incubação, a OD-600 começou a ser medido de hora em hora, até que a cultura alcançasse a OD-600 entre 1,0-1,5 abs. Assim que a concentração foi alcançada, a cultura foi centrifugada a 1500 x g por 5 minutos a 4 °C. O sobrenadante foi descartado e as células foram ressuspendidas em 100 ml de meio YPD suplementado com 20 ml de HEPES 1M pH 8,0 e 2,5 ml de DTT 1 M. As células foram incubadas a 30 °C por 15 minutos, centrifugadas novamente a 1500 x g por 5 minutos a 4 °C e o sobrenadante foi descartado. As células foram ressuspensas em 250 ml de água estéril gelada, centrifugada a 1500 x g por 5 minutos a a 4 °C e o sobrenadante foi descartado. As células foram ressuspensas em 50 ml de água estéril gelada, centrifugada a 1500 x g por 5 minutos a a 4 °C e o sobrenadante foi descartado. As células foram ressuspensas em 10 ml de sorbitol 1 M, centrifugada a 1500 x g por 5 minutos a a 4 °C e o sobrenadante foi descartado. Após essa última etapa, as células foram ressuspensas em 500 µL de sorbitol 1 M, aliquotadas em frações de 80 µL e imediatamente armazenadas a -80º C.

6.3.2.6 Eletroporação

As células eletrocompetentes de PichiaPink™ foram utilizadas para eletroporação. As alíquotas foram descongeladas em gelo e 15 µl de plasmídio linearizado (ou concentração de 5-10 µg) foi adicionado à aliquota. A reação foi transferida para uma cubeta de eletroporação de 0,2 mm de largura e incubada no gelo por 5 minutos. A cubeta foi pulsada no eletroporador com as seguintes constantes: 1,5 kV, 25 µFm e 200 Ω. Essas constantes resultaram em 4,5-5 ms de pulso constante. Imediatamente após o pulso, 1 ml de meio YPDS (meio próprio de PichiaPink™) foi adicionado às células e misturado por pipetagem. A mistura foi transferida para um tubo Eppendorf de 1,5 ml e incubada por 30 °C por pelo menos 2 horas e no máximo 12 horas, sem rotação. Após a incubação, 50 µl da mistura foi adicionada em placa PAD (*Pichia Drop Out Adenine*) para seleção das colônias de PichiaPink™ recombinantes. As placas foram incubadas por 30 °C de 3-10 dias. De três a oito colônias foram escolhidas para serem novamente plaqueadas, e a partir dessas foram feitos testes de expressão.

A levedura PichiaPink™ é uma linhagem autoxotrófica de adenina, por ter deleção do gene ade2. O gene ade2 é responsável por codificar a proteína fosforibosilaminoimidazol carboxilase, envolvida na biosíntese de nucleotídeos purínicos. Na ausência de transcrição de ade2, os precursores purínicos se acumulam nos vacúolos, e se tornam vermelhos. A pigmentação das colônias é tido então como marcador

de seleção e triagem. O vetor pPINK-HC, ao ser corretamente transformado, insere novamente o gene ade2 deletado no cromossoma da linhagem, reestabelecendo a via de biosíntese de adenina. Dessa forma, as colônias transformadas não possuem acúmulo de precursor, sendo brancas e de fácil seleção (VÁRNAI et al., 2014).

6.3.2.7 Clonagem e ligação de genes truncados

Os genes truncados foram obtidos das sequências clonadas em pPINK-GAP. O sistema de ligação *In-Fusion*®, da Clontech Laboratories, Inc., foi utilizado. Para obtenção dos genes truncados amplificados, *primers* foram desenhados para utilização nesse sistema. Por isso, alguns fatores precisaram ser considerados: 1) Os *primers reverses* precisaram ter 15 bases homólogas às bases do fragmento de DNA que seriam inseridos (no caso, o vetor pPINK-GAP); 2) Os *primers forwards* precisaram ser gene-específicos, possuir 18-25 bases de tamanho, teor de G-C entre 40-60% e T_M (*melting temperature)* entre 58-65 °C (a diferença com o *primer reverse* não podia ultrapassar de 4 °C). A ferramenta online pDRAW32 (disponível em: http://www.acaclone.com/) auxiliou no desenho. Os genes truncados foram amplificados do vetor pPINK-GAP com o inserto original. A PCR foi realizada com o kit *Q5® High-Fidelity DNA Polymerase*, da *New England BioLabs*. Os insertos amplificadas foram aplicadas em gel de agarose 1%, 80 Volts, por 40 minutos. As bandas correspondentes aos genes de interesse foram excisadas e purificadas com o kit *NucleoSpin® Gel and PCR Clean-up* da MACHEREY-NAGEL GmbH & Co. KG. A ligação do inserto ao plasmídio pPINK-GAP linearizado e sem vetor se deu da seguinte forma: num total de 10 µl de reação, foram misturados 100 ng de fragmento de PCR purificado com 100 ng de vetor linearizado, e 2 µl da ligase HD do kit *In-Fusion*®. A reação foi incubada a 50 °C por 15 minutos e colocada no gelo logo depois. A reação foi diluída 5x e utilizada para transformação nas células quimicamente compententes One Shot® TOP10 de *E. coli*. As etapas seguintes de clonagem e eletroporação já foram descritas nos tópicos anteriores.

6.3.3 Expressão e purificação das LPMOs candidatas

6.3.3.1 Testes de expressão

A partir das colônias de PichiaPink™ transformadas, testes de expressão foram conduzidos, para checar a expressão gênica de cada transformante. Para cada transformante, duas a oito colônias foram escolhidas. O teste de expressão se deu em três dias da seguinte forma: no primeiro dia, foram utilizados 25 ml de meio BGMY estéril (1% [m/v] de extrato de levedura, 2% [m/v] de peptona, 100 mM de fosfato de potássio

pH 6,0, 1,34% [m/v] de YNB e 1% [v/v] de glicerol) em Erlenmeyers de 250 ml. Após o inóculo de cada colônia, os frascos foram incubados a 30 °C a 200 rpm *overnigth*. No segundo dia, foi adicionado 1% (v/v) de glicerol à cultura. No terceiro dia, os frascos foram centrifugados a 8000 g por 15 minutos e o sobrenadante foi armazenado a 4 °C. Para checar a expressão enzimática, para cada 1350 µl de amostra foi adicionado 150 µl de ácido tricloroacético 100% (v/v). As amostras foram incubadas a 4 °C por 1 hora. Em seguida, as amostras foram centrifugadas a 18.600 g por 15 minutos a 4,0º C, e então lavadas com 1000 µl de etanol 100% e centrifugadas novamente. Este processo foi feito duas vezes. Após a última etapa de centrifugação, as amostras foram ressuspensas em 15 µl de água destilada e 5 µl de tampão de amostra ([tris-HCl 125 mmol/l, pH 6,8; SDS 2,0% (v/v); azul de bromofenol 0,05% (m/v); glicerol 20% (v/v) e β-mercaptoetanol 5,0% (v/v)] e fervidas por 5 minutos. As amostras foram então aplicadas em um gel de poliacrilamida pré-fabricado (Mini-PROTEAN® TGX Stain-Free™ Precast Gels da Bio-Rad Laboratories) e a corrida se deu à temperatura ambiente, com voltagem fixa em 200 V, por 30 minutos. As proteínas foram detectadas por fluorescência, pois a formulação do gel continha componentes que modificavam os triptofanos e podiam ser detectados por luz UV. Para determinação das massas moleculares aparentes fori utilizado o marcador de massa molecular BenchMark™ (Thermo Fisher Scientific), com 15 proteínas recombinantes que variam a massa entre 10 a 200 kDa.

6.3.3.2 Produção e purificação de *AtAA9.1_SD* e *AtAA9.1_SD*

A partir do resultado do teste de expressão, a colônia que demonstrou melhor nível de expressão foi selecionada. Uma nova expressão foi realizada, que se deu em quatro dias: no primeiro dia, foram utilizados 25 ml de meio BGMY para o pré-inóculo em Erlenmeyers de 250 ml. Após o inóculo de cada colônia, os frascos foram incubados a 30 °C a 200 rpm *overnigth*. No segundo dia, os 25 ml do inóculo *overnight* foram adicionados à 450 ml de meio BMGY estéril, e os frascos foram novamente incubados a 30 °C a 200 rpm *overnigth*. No terceiro dia, foi adicionado 1% (v/v) de glicerol à cultura. No quarto dia, os frascos foram centrifugados a 8000 g por 15 minutos. O sobrenadante obtido foi concentrado 10x no concentrador de fluxo tangencial VivaFlow® 200 com corte de 10 kDA (Sartorius Stedim Biotech GmbH, Alemanha), e depois foi feita diálise com o tampão Tris-HCl 20 mM pH 8,0 até que a amostra chegasse à condutância de 2-4 mS/cm. A amostra foi submetida então a uma cromatografia de troca iônica em uma resina do tipo HiTrap Q FF 5 ml, em um sistema cromatográfico automatizado

ÄKTAprime plus (GE HealthCare Bio-Sciences AB, Suécia). A resina foi previamente equilibrada com tampão Tris-HCl 20 mM pH 8,0 até a condutância 2-4 mS/cm. O volume de amostra aplicado foi de 100 ml e o fluxo de corrida foi de 5 ml/min. O pico da fração correspondente às proteínas que não se ligaram foi coletada, para posterior análise. Um gradiente de NaCl (0-0,5 M) foi aplicado à coluna, e as frações referentes ao pico de absorbância em 280 nm foram reunidas As frações dos picos não retidos e retidos foram submetidas à eletroforese de gel de poliacrilamida, para detecção das proteínas de interesse através de sua massa molecular. As frações correspondentes à massa da proteína foram reunidas, dialisadas contra o tampão Bis-Tris 20 mM pH 6,0 através do concentrador de centrífuga Vivaspin® 20, e concentradas até alcançar 2 ml. A cromatografia de exclusão molecular foi a etapa de purificação seguinte realizada, em uma resina HiLoad Superdex 75 16/600 de 120 ml (GE HealthCare Bio-Sciences AB, Suécia), em um sistema cromatográfico automatizado ÄKTA purifier (GE HealthCare Bio-Sciences AB, Suécia). A resina foi previamente equilibrada com tampão Bis-Tris 20 mM pH 6,0 suplementada com 150 mM de NaCl. O volume de amostra aplicado foi de 2 ml e o fluxo de corrida foi de 0,75 ml/min. As frações referentes aos picos de absorbância em 280 nm foram coletadas e submetidas à eletroforese de gel de poliacrilamida, para detecção da proteína pura através de sua massa molecular. As frações puras correspondentes à massa da proteína foram coletadas e concentradas através do concentrador de centrífuga Vivaspin® 20 até alcançar 1 ml. As quantificações protéicas foram realizadas através da lei de *Lambert-Beer:*

$$A = e.b.c \qquad \text{Eq.(2)}$$

Onde **A** se refere à absorbância a 280 nm; **e** equivale à absortividade molar em L/mol/cm (usando valores teóricos calculados pela ferramenta ProtParam do servidor ExPASy); **b** é o comprimento do caminho que a luz tem que atravessar na solução (em centímetros); **c** é a concentração do elemento que absorve na solução, em mol/L.

As enzimas foram submetidas à saturação de cobre, para que elas saíssem do seu estado apo- para o estado holo-. Baseado na concentração obtida anteriormente, a apo-enzima foi saturada numa proporção 5 (cobre):1 (enzima) utilizando uma solução de 33 mM de $CuSO_4$. Para obtenção da holo-enzima, foi utilizada uma resina de dessanilização

de bancada G-25 de 5 ml (PD MidiTrap, GE HealthCare Bio-Sciences AB, Suécia). O volume final de holoenzima foi de 1 ml.

6.3.4 Caracterização das LPMOs purificadas

A reação enzimática foi realizada da seguinte forma: 0,5-1 µM de LPMO purificada incubada com 0,2% (m/v) de celulose Avicel inchada com ácido fosfórico (PASC) preparada de acordo com Wood (WOOD, 1988), 50 mM de tampão Bis-Tris pH 6,0 e 1 mM de ácido ascórbico como o doador de elétrons. A mistura foi incubada *overnigth* a 37 °C e 1000 rpm em um Eppendorf ThermoMixer®. No dia seguinte, o produto de reação foi filtrado em filtros de 0,45 µM, para retirada do substrato insolúvel, e analisado por Cromatografia Iônica de Alta Performance (HPAEC) com detecção amperiométrica pulsada (PAD) utilizando um Dionex™ ICS-5000 acoplado a uma coluna CarboPac PA1 (Thermo Fisher Scientific). A metodologia utilizada foi descrita previamente (WESTERENG et al., 2013). Outros substratos foram testados para avalição enzimática, nas mesmas condições descritas anteriormente: celopentose (C5), celohexose (C6), xiloglucana (TXG), xilana (BWX), e liquenana (Lich), na concentração de 1% (m/v). Para controle negativo, a cada reação não foi adicionado ácido ascórbico. Para avaliação do padrão de oxidação, foi utilizada a enzima NcLPMO9C de *Neurospora crassa* (BORISOVA et al., 2015); o ensaio foi realizado nas mesmas condições de reação das AA9. Celo-oligossacarídeos com com DP de 1-6 foram utilizados como padrões para o ensaio com os celo-oligômeros.

6.4 Resultados e discussão

6.4.1 Escolha das LPMOs candidatas

Através dos múltiplos alinhamentos das sequências e identificação dos domínios conservados, realizados pelo Uniprot e dbCAN tanto com as enzimas de *A. oryzae* quanto as de *A. tamarii*, a estrutura dos domínios foi representada na Figura 3. Baseado em sua semelhança de domínios conservados, as AA9 foram subdivididas em 8 espécies. Além das sequências preditas apresentarem um domínio conservado para AA9, algumas apresentaram domínios conservados de módulo de ligação ao carboidrato (CBM) da família 1. De acordo com o CAZy, o CBM1 é um módulo exclusivo dos fungos, que se liga preferencialmente à celulose, mas tem atividade em quitina também. Esse módulo possui a característica de apresentar resíduos de cisteínas conservados em sua composição, responsáveis pelo dobramento correto do módulo (LARROQUE et al.,

2012). Os *linkers* de CBM costumam ser altamente O-glicosilados, para evitar proteólise. Normalmente são estruturas finas e flexíveis, que servem para que o CBM consiga ancorar e dar mais mobilidade ao domínio conservado. Tipicamente, essas regiões se apresentam com alto teor de aminoácidos serina, treonina (que sofrem as O-glicosilações) e alanina.

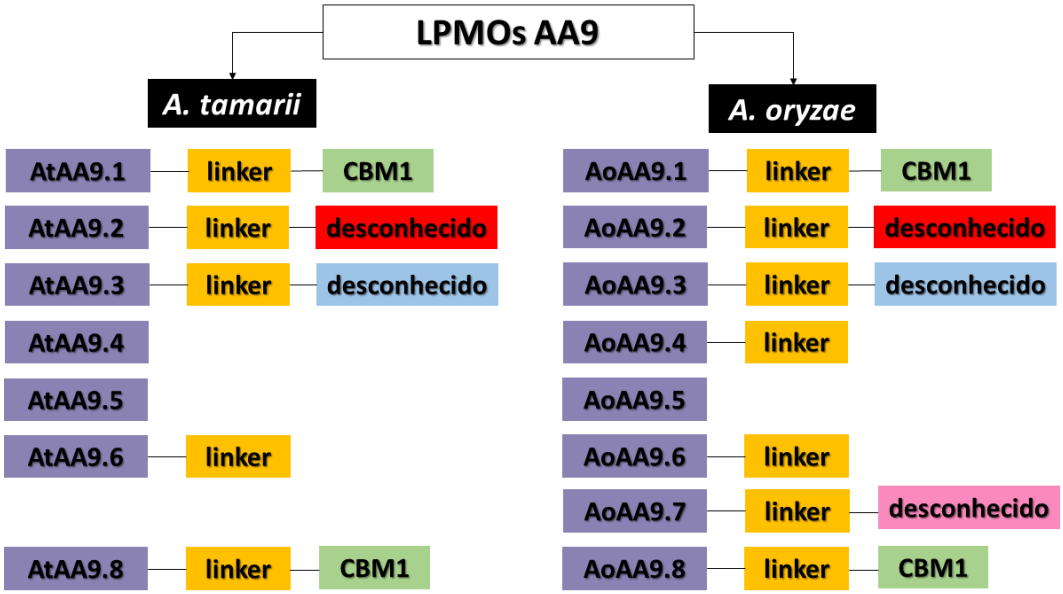

Figura 3. Representação esquemática dos domínios conservados encontrados nas LPMOs da família AA9 presente em *A. tamarii* e *A. oryzae.*

Além dos CBM, prováveis domínios desconhecidos foram identificados nas porções C-terminas das enzimas AtAA9.2 e AtAA9.3 de *A. tamarii* e AoAA9.2, AoAA9.3 e AoAA9.7 de *A. oryzae*. Múltiplos alinhamentos desses módulos foram realizados pelo Uniprot, a fim de encontrar estruturas parecidas (resultados não mostrados). Em relação ao módulo da AA9.2, a busca por sequências similares encontrou 57 estruturas semelhantes, sendo 41 pertencentes à LPMOs de *Aspergillus* sp. e *Penicillium* sp., o que demonstra ser uma estrutura única a essas espécies. As outras 11 estruturas encontradas não possuiram homologia com as LPMOs e não se encontravam no C-terminal. O módulo de AA9.3 de *A. tamarii* é menor, comparado ao de *A. oryzae.* Além disso, nos resultados do alinhamento, houve muita variação na porção C-terminal, indicando variações de *splicing* alternativo entre espécies. O módulo de AA9.7 aparentemente demonstra ter uma estrutura mais rígida por ter duas cisteínas presentes,

indicando possíveis pontes dissulfetos, além de possuir vários aminoácidos positivamente carregados. As enzimas AA9.6 apresentaram apenas um *linker* em sua composição, sem um domínio identificado. As enzimas AA9.4 demonstraram diferenças entre suas estruturas, onde AoAA9.4 apresenta um *linker*, enquanto a sequência de AtAA9.4 foi identificada como um fragmento.

Baseado nos dados de RNA-seq obtidos por Midorikawa et al. (2014), onde *A. tamarii* foi cultivado em meio líquido e meio sólido contendo bagaço de cana-de-açúcar como fonte de carbono por 36 e 48 horas (Tabela 1), nos homólogos de cada enzima previamente caracterizados (Tabela 2), e nas informações provenientes da análise de estrutura das enzimas (Figura 3), pode-se analisar quais AA9 seriam mais adequadas para caracterização enzimática, visando aplicação dessas à degradação da biomassa.

Tabela 1. Regulação de transcritos de AA9 em bagaço de cana de açúcar comparado com glicose como fonte de carbono.

Proteína	**36h**	**48h**	**Proteína**	**36h**	**48h**
Meio líquido			**Meio sólido**		
AtAA9.1	4.7	5.3	AtAA9.1	3.5	2.6
AtAA9.2	0.78	2.1	AtAA9.2	2.3	2.4
AtAA9.3	1.4	1.1	AtAA9.3	-1.9	-3.8
AtAA9.4	7.0	6.7	AtAA9.4	6.6	4.1
AtAA9.5	10.5	11.0	AtAA9.5	8	7.3
AtAA9.6	-	-	AtAA9.6	1.9	-1.0
AtAA9.8	5.5	6.1	AtAA9.8	5.6	3.7

Tabela 2. Homólogos de cada AA9 previamente caracterizados

Proteína	**LPMO homólogo**	**Característica**	**Referência**
AtAA9.1	LsLPMO9A	Oxidação em C4	(FRANDSEN et al., 2016)
AtAA9.2	TaLPMO9A	Oxidação em C1/C4, ativa em xiloglucana	(QUINLAN et al., 2011)
AtAA9.3	-	Nenhum grupo caracterizado	-
AtAA9.4	AN3046	Oxidação em C1, ativa em xiloglucana	(JAGADEESWARAN et al., 2016)
AtAA9.5	TaLPMO9A	Oxidação em C1/C4, ativa em xiloglucana	(QUINLAN et al., 2011)
AtAA9.6	TaLPMO9A	Oxidação em C1/C4	(QUINLAN et al., 2011)
AtAA9.8	AN3046	Oxidação em C1, ativa em xiloglucana	(JAGADEESWARAN et al., 2016)

Pode-se observar que as enzimas AtAA9.1, AtAA9.2, AtAA9.5 e AtAA9.8 tiveram aumento no acúmulo de transcritos ao longo do tempo. Isso indica alto potencial

dessas enzimas na degradação da biomassa, ao terem aumento de expressão gênica ao longo do tempo. Além disso, pelos homólogos próximos caracterizados, elas possuem modos de ações diferentes, indicando que o aumento da expressão gênica de quatro enzimas da mesma família pode estar correlacionado com sinergismo para degradação da biomassa. As enzimas AtAA9.1 e AtAA9.8 carregam um CBM1, domínio conservado em enzimas homólogas de *Aspergillus* sp. e *Penicillium* sp. Além disso, dentre seus homólogos caracterizados, uma apresenta oxidação em C1 e a outra em C4, o que as torna boas candidatas para comparação. As enzimas AtAA9.2 e AtAA9.5 tiveram homologia com a mesma enzima, TaLPMO9A. Ao analisar suas sequências, percebe-se que o domínio LPMO de AtAA9.2 tem 68% de homologia com o de AtAA9.5, o que os torna interessantes para comparação pelo alto grau de homologia, diferindo pela presença do domínio desconhecido. Comparando AtAA9.5 com AoAA9.5, elas possuem 23 aminoácidos de diferença, sendo que para AtAA9.5 aparentemente houve uma deleção de alguns pares de base. Considerando que AtAA9.5, enzima que apresenta um único domínio, foi a que apresentou maior expressão gênica na degradação do bagaço, porém a sequência obtida não aparentava estar correta, a enzima AoAA9.5 demonstrou ser uma candidata interessante para caracterização e efeito sinérgico com as outras enzimas. Dessa forma, os candidatos escolhidos para clonagem foram: AtAA9.1, AtAA9.2, AtAA9.8 e AoAA9.5. Além disso, as versões truncadas de seus domínios catalíticos (sem a presença do CBM) também foram utilizados para clonagem.

6.4.2 Clonagem em PichiaPink™

Os genes de interesse inseridos no plasmídio pPINK-GAP estão representados na Figura 4. Os genes estão inseridos entre o promotor GAP e CYC1. O promotor GAP (gliceraldeído-3-fosfato desidrogenase) é constitutivo e, comparado com o promotor AOX1, simplifica o cultivo evitando o consumo do metanol como fonte de carbono, além de alcançar concentrações de proteínas produzidas pela levedura equiparáveis com leveduras que utilizam o promotor AOX1 (VÁRNAI et al., 2014).

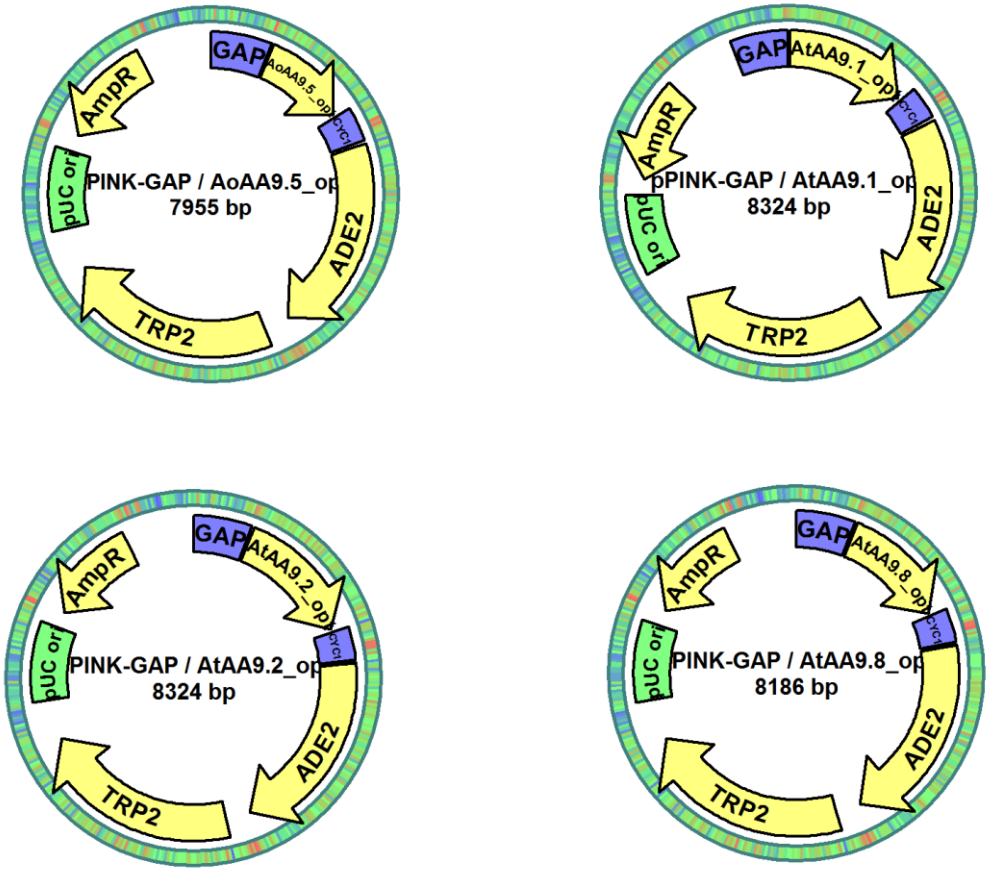

Figura 4. Representação dos plasmídios pPINK/GAP com as quatro enzimas candidatas.

Os genes foram inseridos de tal forma no plasmídio pPINK/GAP que se iniciassem (códon ATG) logo após o sítio de restrição da enzima *EcoRI* e fossem terminados (códon TAG) antes do sítio de restrição da enzima *Acc65I*. A partir dos genes inseridos no plasmídio, foram feitas as amplificações dos genes truncados, sem os domínios não catalíticos. Para que os genes truncados amplificados pudessem ser inseridos em novos plasmídios, o *primer forward* possuía um sítio de ancoragem equivalente ao sítio de restrição da enzima *EcoRI*, e o *primer reverse* possuía um sítio de ancoragem equivalente ao sítio de restrição da enzima *Acc65I*, conforme demonstrado na figura 5. Em azul, os sítios de ancoragem inseridos em cada *primer*. Em rosa o códon inicando ATG. Os nucleotídeos em vermelho indicam onde há formação da extremidade coesiva (“sticky end”).

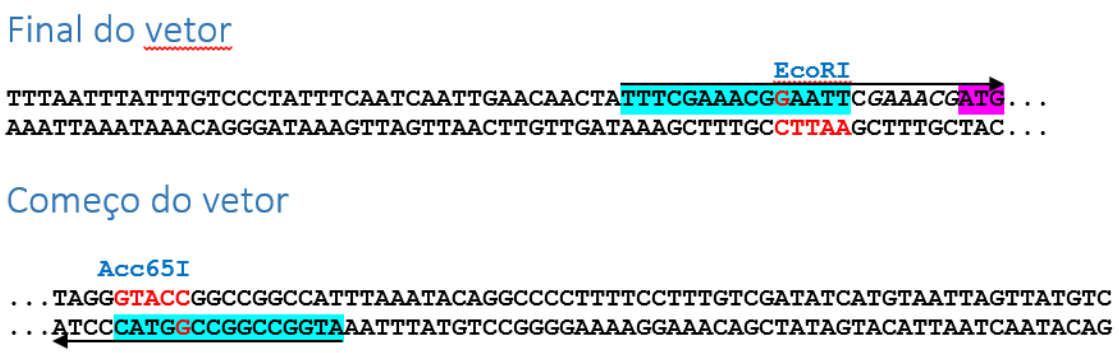

Figura 5. Sítios de restrição de *EcoRI* e *Acc65I* no vetor.

Os primers utilizados estão descritos na Tabela 3, sendo que em azul estão destacados os sítios de ancoragem e em rosa o códon iniciador das LPMOs (histidina), já que elas foram clonadas sem peptídeo sinal.

Tabela 3. Primers desenhados para proteínas truncadas.

	Primer forward	*Primer reverse*
AtAA9.1	5'-TTT CGA AAA GGA ATT CGA AAG CAT GAA GTC -3 '	5' – ATG GCC CGG TAC CCT AAC CAT CCC AAA – 3'
AtAA9.2	5'-TTT CGA AAA GGA ATT CGA AAG CAT GTC TAT -3 '	5' – ATG GCC CGG TAC CCT AAC CAG AAT ACA – 3'
AtAA9.8	5'-TTT CGA AAA GGA ATT CGA AAG CAT GAA GTC -3 '	5' – ATG GCC CGG TAC CCT AAC CAG ACC AAA – 3'

Para confirmar que os genes de interesse estavam inseridos no plasmídio pPINK-GAP, uma PCR de colônia foi realizada, utilizando *primers* para GAP e CYC1 (Figura 6). O tamanho dos genes são: AtAA9.1: 1130 pb (par de base); *AtAA9.1_SD* ("single domain"): 702 pb; AtAA9.2: 1146 pb; *AtAA9.2_SD*: 732 pb; AtAA9.8: 1000 pb; AtAA9.8_SD: 711 pb; AoAA9.5: 760 pb.

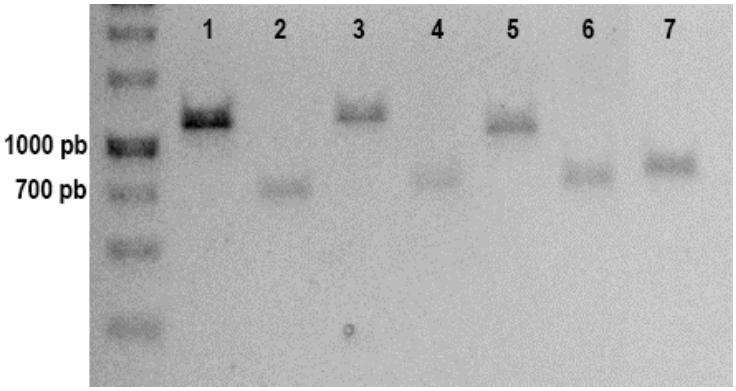

Figura 6. Gel de agarose com PCR de colônia de transformantes. **1** – AtAA9.1; **2** – AtAA91_SD; **3** – AtAA9.2; **4** – *AtAA9.2_SD*, **5** – AtAA9.8, **6** – AtAA9.8_SD, **7** – AoAA9.5.

Após a confirmação dos genes inseridos nos plasmídios apresentarem massas similares às calculadas, os plasmídios recombinates foram linearizados com a enzima *BspTI*. É um sítio de restrição raro e se encontra no domínio TRP2 do plasmídio pPINK-GAP.

6.4.3 Teste de expressão das LPMOs candidatas

Os plasmídios recombinantes foram eletroporados e plaqueados. Após 3 dias, colônias positivas para os transformantes apareceram, como é demonstrado na Figura 7.

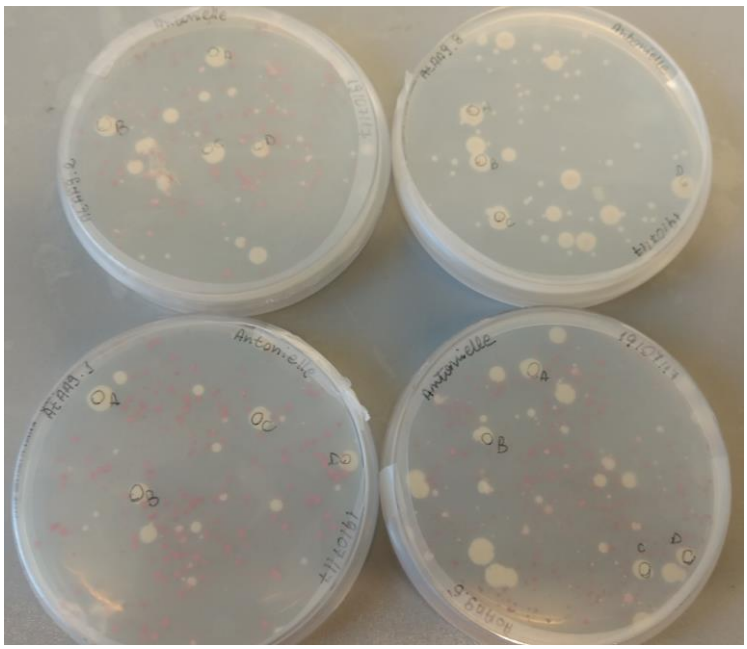

Figura 7. Colônias de PichiaPink™ após eletroporação. Em branco, tranformantes positivos. Em vermelho, transformantes negativos.

Duas a oito colônias foram selecionadas para um teste de expressão, baseado na quantidade de transformantes positivos que cresceram nas placas. As figuras 8-14 mostram o resultado dos testes.

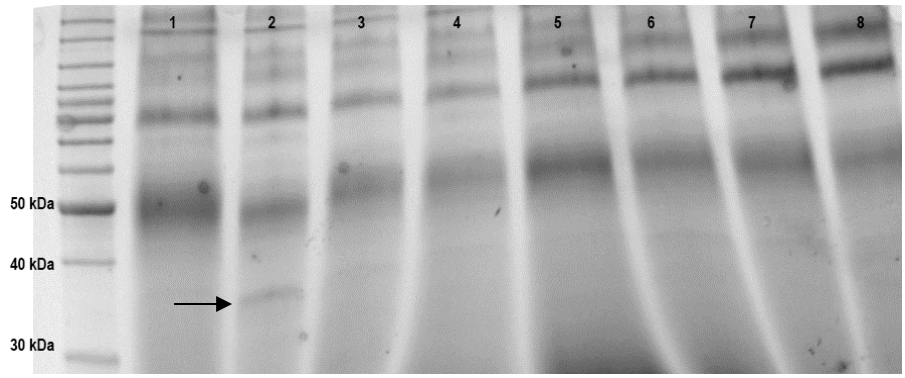

Figura 8. Teste de expressão de AtAA9.1. Massa molecular teórica calculada: 38,63 kDa. Seta preta indica provável expressão da enzima. Colunas 1-8: colônias selecionadas para o teste.

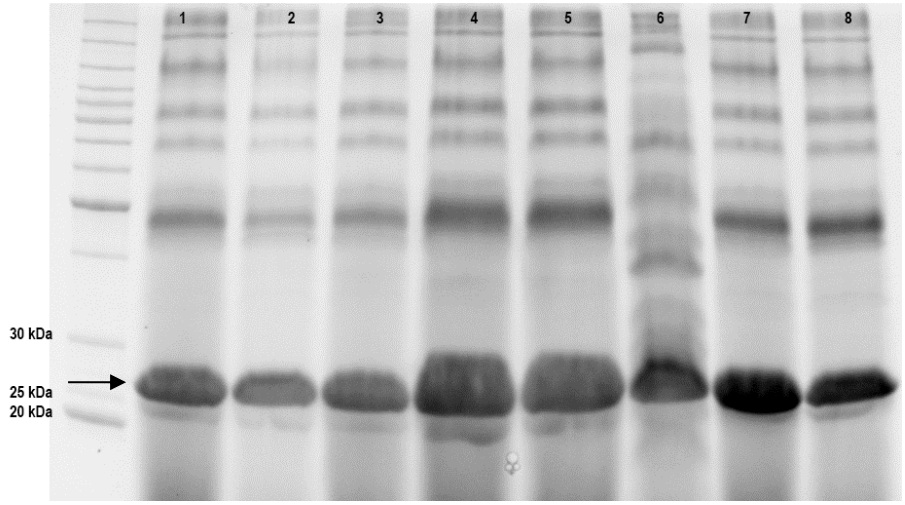

Figura 9. Teste de expressão de *AtAA9.1_SD*. Massa molecular teórica calculada: 27 kDa. Seta preta indica alta expressão da enzima. Colunas 1-8: colônias selecionadas para o teste.

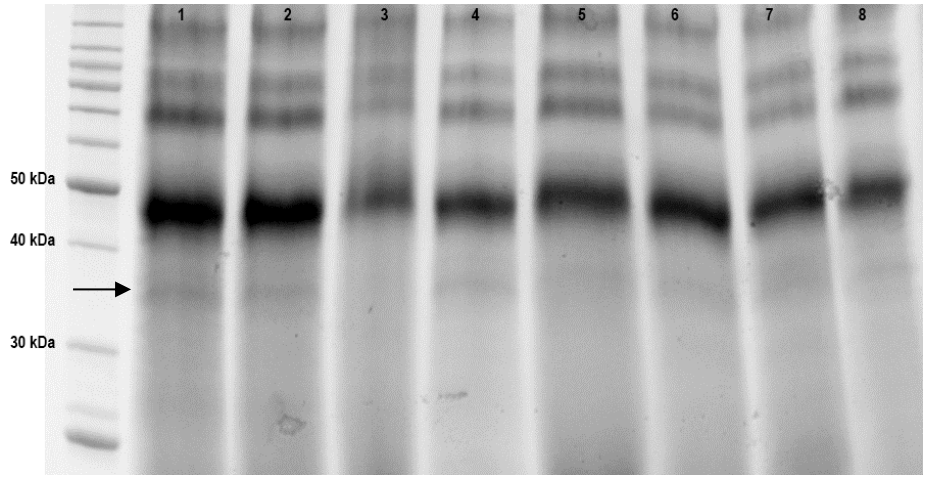

Figura 10. Teste de expressão de AtAA9.2. Massa molecular teórica calculada: 38,03 kDa. Seta preta indica provável expressão da enzima. Colunas 1-8: colônias selecionadas para o teste.

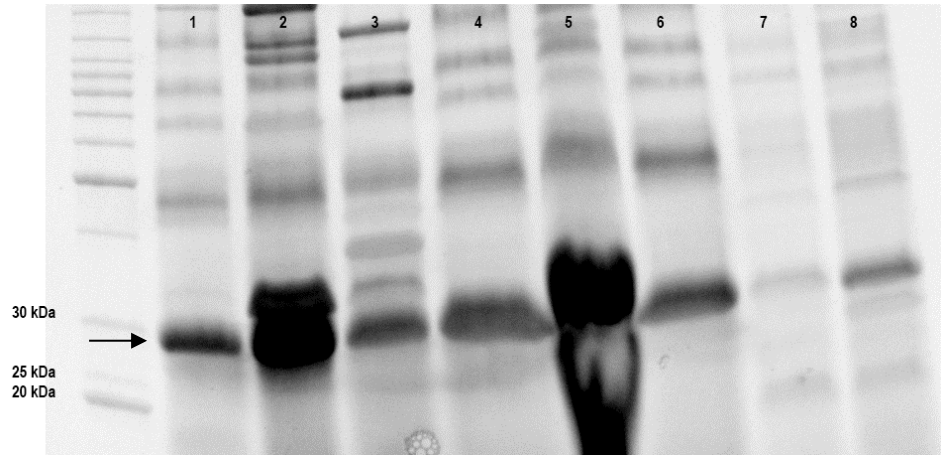

Figura 11. Teste de expressão de *AtAA9.2_SD*. Massa molecular teórica calculada: 29 kDa. Seta preta indica alta expressão da enzima. Colunas 1-8: colônias selecionadas para o teste.

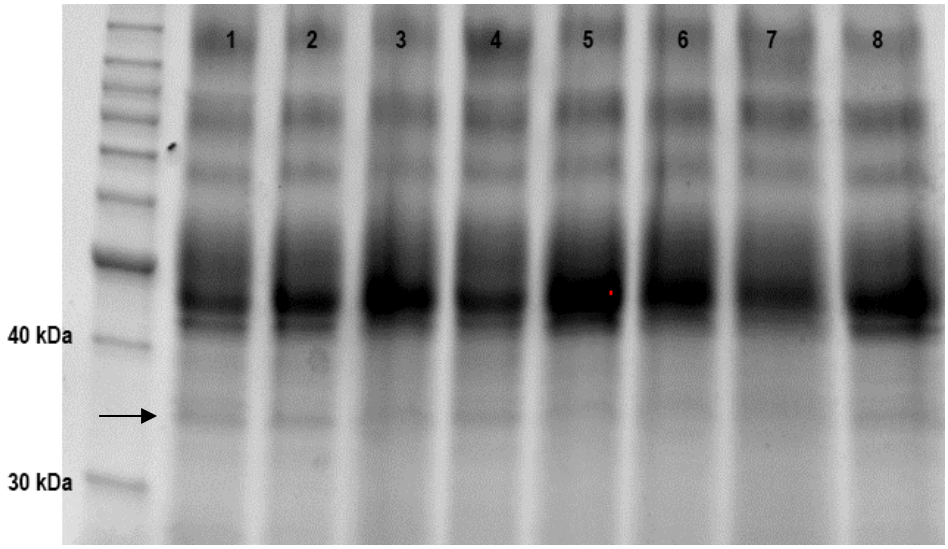

Figura 12. Teste de expressão de AtAA9.8. Massa molecular teórica calculada: 34,86 kDa. Seta preta indica provável expressão da enzima. Colunas 1-8: colônias selecionadas para o teste.

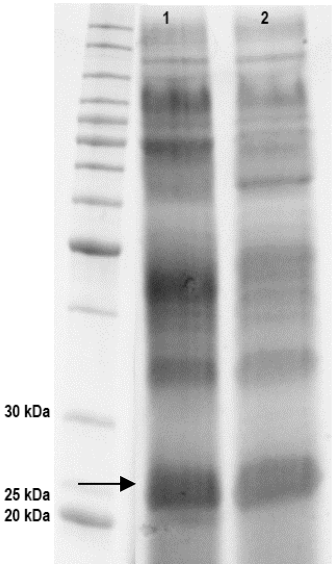

Figura 13. Teste de expressão de AtAA9.8_SD. Massa molecular teórica calculada: 26 kDa. Seta preta indica alta expressão da enzima. Colunas 1-2: colônias selecionadas para o teste.

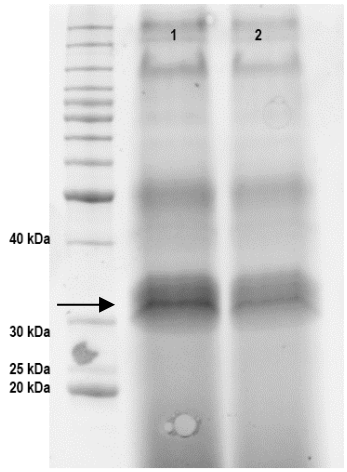

Figura 14. Teste de expressão de AoAA9.5. Massa molecular teórica calculada: 26,11 kDa. Seta preta indica alta expressão da enzima. Colunas 1-2: colônias selecionadas para o teste.

Como pode-se perceber, as enzimas que possuíam um domínio extra (AtAA9.1, AtAA9.2 e AtAA9.8) não tiveram níveis altos de expressão comparados às versões que somente possuíam o módulo catalítico. Vários fatores podem afetar a expressão de genes de proteínas heterólogas em *P. pastoris*, como preferência do códon, transcrição modulada pelo promotor, translocação determinada pelo peptídeo sinal, processamento e dobramento no retículo endoplasmático e Golgi, secreção da célula e proteólise (DALY; HEARN, 2005; HOHENBLUM et al., 2004). Considerando que a linhagem PichiaPink™ possui quatro genes de protease deletados, e que algumas proteínas heterólogas tiveram alto nivel de expressão, pode-se pressupor que os problemas na expressão não estão relacionados com a transcrição e sim com a secreção. A proteína pode ter tido um dobramento incorreto devido tanto à glicosilação alterada ou pela falta de outra modificação pós-traducional que não ocorreu (DALY; HEARN, 2005).

6.4.4 Purificação de *AtAA9.1_SD* e *AtAA9.2_SD*

Baseado no resultado do teste de expressão, as enzimas *AtAA9.1_SD* e *AtAA9.2_SD* foram selecionadas primeiramente para expressão devido ao alto nível de expressão (Figs. 9 e 11) obtido por todas as colônias.

Na primeira etapa de purificação foi utilizada uma resina de troca aniônica. As amostras foram dialisadas até que alcançassem o pH 8.0 Tris-HCl, na forca iônica correspondente à 20 mM, que ficou em torno de 2-4 mS/cm. Como o pI teórico calculado das proteínas foi 5,20 e 4,75 para *AtAA9.1_SD* e *AtAA9.2_SD*, respectivamente, ao entrar em contato com um pH maior que seu pI, as amostras ficaram na forma desprotonada,

com carga negativa. Dessa forma, elas se ligaram à coluna Q FF, que possui uma amina quaternária de carga positiva. As figuras 15-21 mostram o gel das frações obtidas na purificação das enzimas.

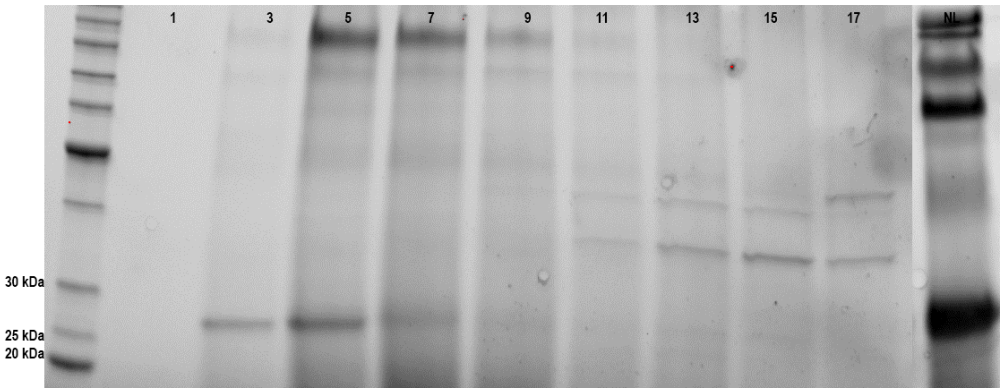

Figura 15. Frações de cromatografia de troca iônica em Q FF de *AtAA9.1_SD*. 1-17: frações ímpares coletadas com a abertura do gradiente. NL: frações não ligadas à coluna.

A colônia 4 (Figura 9) foi escolhida para expressar a enzima em grande quantidade. Baseado na massa molecular predita da *AtAA9.1_SD*, pode-se perceber que a proteína não se ligou à resina. Isso signfica que no pH 8,0, não necessariamente a enzima estava com carga líquida total negativa. O volume da fração não ligada correspondeu à 100 ml. Essa fração foi extensivamente dialisada com tampão Bis-Tris pH 6,0 20 mM e concentrada para um volume final de 2 ml. Essa fração foi então aplicada numa coluna Superdex 75. As frações puras provenientes da cromatografia estão representadas nas figura 16.

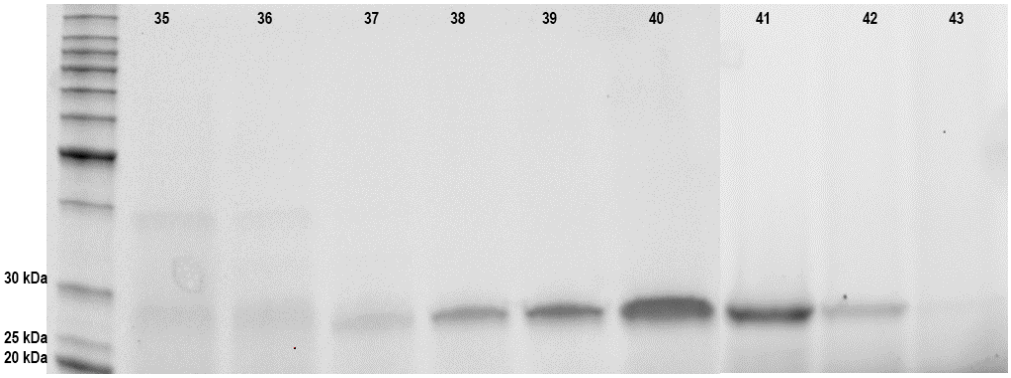

Figura 16. Frações de cromatografia de exclusão molecular em Superdex 75 de *AtAA9.1_SD*. 35-43: frações correspondentes ao pico de absorbância de UV.

As frações 38-42 foram reunidas, concentradas para 1 ml e quantificadas através da lei de *Lambert-Beer*. Considerando seu coeficiente de extinção molar predito (e = 39545/M.cm) e a absorbância de 0,564 em 280 nm, a concentração estimada da enzima foi de 14,4 µM. Para a saturação da enzima, foram utilizados 71,5 µM de $CuSO_4$.

Para a enzima *AtAA9.2_SD*, a colônia 4 (Figura 11) foi escolhida para expressar a enzima em grande quantidade. A figura 17 representa o fracionamento por troca iônica da enzima *AtAA9.2_SD*.

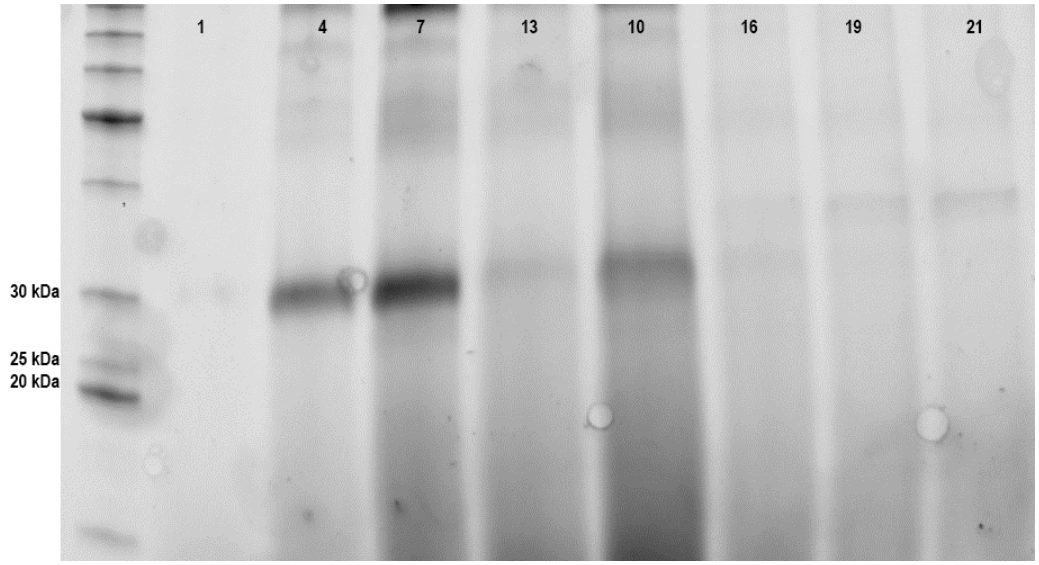

Figura 17. Frações de cromatografia de troca iônica em Q FF de *AtAA9.2_SD*. 1-21: frações coletadas com a abertura do gradiente.

Baseado na massa molecular predita da *AtAA9.2_SD*, pode-se perceber que a proteína saiu entre as frações 4-13. Isso signfica que no pH 8,0 a enzima estava com carga líquida total negativa. As frações 3-13 foram coletadas, totalizando um volume de 16,5 ml.. Essa fração foi extensivamente dialisada com tampão Bis-Tris pH 6,0 20 mM e concentrada para um volume final de 2 ml. Essa fração foi então aplicada numa coluna Superdex 75. As frações puras provenientes da cromatografia estão representadas nas figura 18.

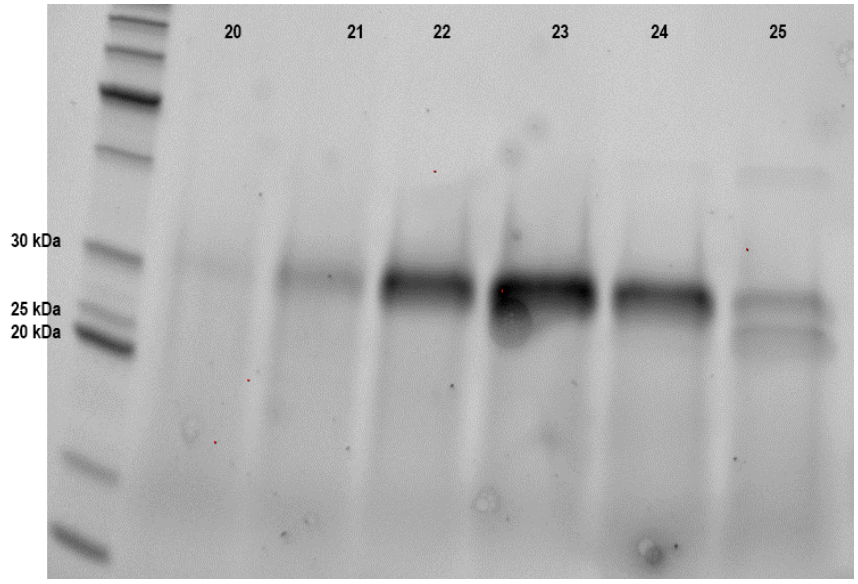

Figura 18. Frações de cromatografia de exclusão molecular em Superdex 75 de *AtAA9.2_SD*. 20-25: frações correspondentes ao pico de absorbância de UV.

As frações 38-42 foram reunidas, concentradas para 1 ml e quantificadas através da lei de *Lambert-Beer*. Considerando seu coeficiente de extinção molar predito (e = 41620/M.cm) e a absorbância de 0,248 em 280 nm, a concentração estimada da enzima foi de 6 µM. Para a saturação da enzima, foram utilizados 30 µM de $CuSO_4$.

As etapas de purificação usadas para as duas enzimas – troca aniônica em pH básico seguida de gel filtração - foram as mesmas utilizadas para NcLPMO9C (BORISOVA et al., 2015), demonstrando que é um procedimento eficiente e rápido para obtenção dessas enzimas.

Obtidas as enzimas purificadas e em sua forma apo, a próxima etapa foram as caracterizações bioquímicas.

6.4.5 Caracterização bioquímica de *AtAA9.1_SD* e *AtAA9.2_SD*

As enzimas foram testadas com vários substratos para avaliar o padrão de oxidação e se há atividade em outros substratos, não somente celulose. Além disso, o doador de elétrons utilizado foi o ácido ascórbico (AscA). O primeiro substrato utilizado foi PASC (figura 19 e 20).

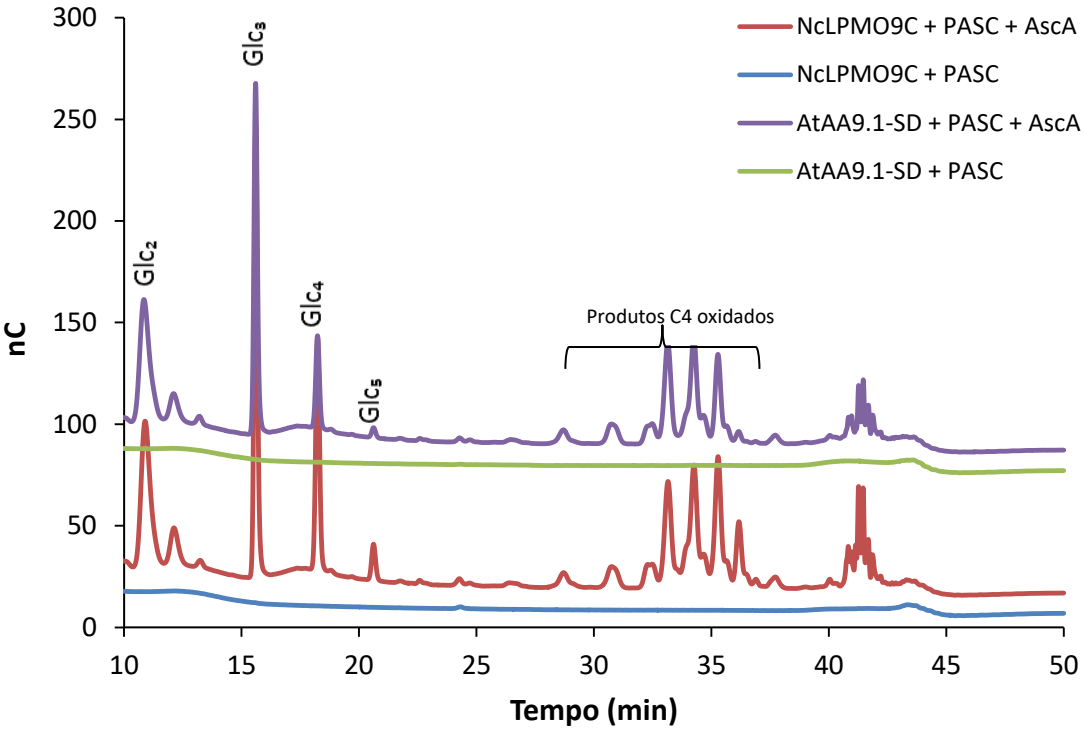

Figura 19. Perfil de produtos gerados analisados por HPAEC-PAD, de *AtAA9.1_SD* e NcLPMO9C em PASC.

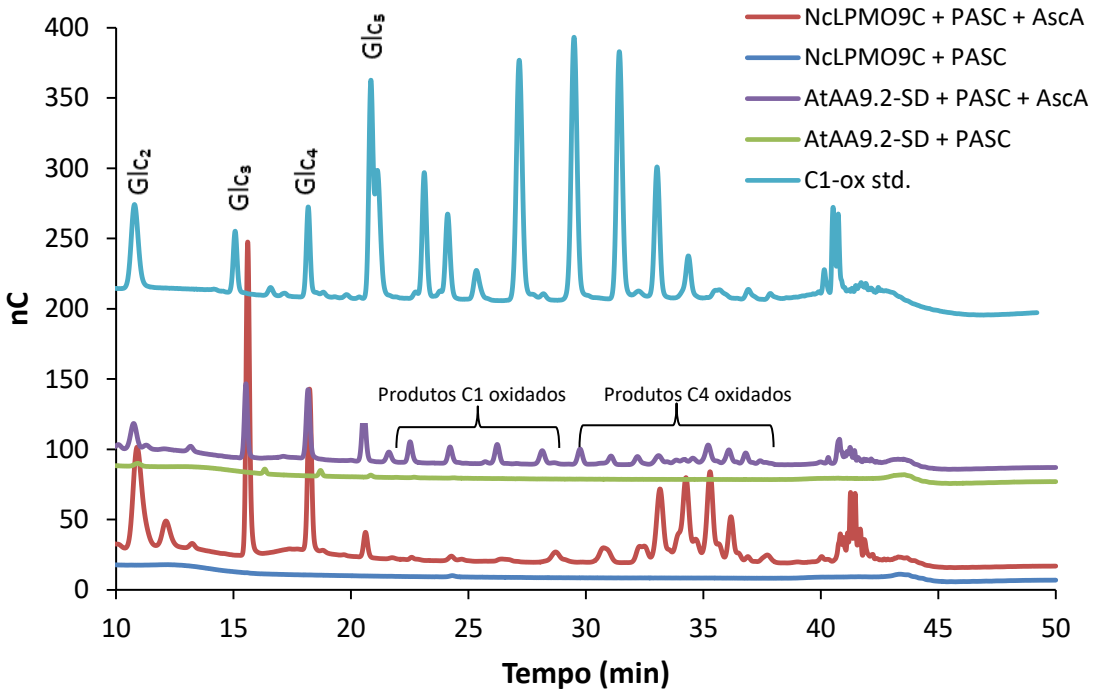

Figura 20. Perfil de produtos gerados analisados por HPAEC-PAD, de *AtAA9.2_SD* e NcLPMO9C em PASC.

A enzima NcLPMO9C é notoriamente conhecida por oxidar a posição C4 (ISAKSEN et al., 2014), sendo utilizada como padrão para essa clivagem. Como pode-se observar, a enzima *AtAA9.1_SD* possui exatamente o mesmo padrão de clivagem que NcLPMO9C, sendo considerada oxidativa de C4 (ou LPMO2). Já a enzima *AtAA9.2_SD* possui ação nas posições C1 e C4, sendo considerada oxidativa em C1/C4 (LPMO3). Interessante notar que o padrão de clivagem delas se assemelha com os homólogos mais próximos já caracterizados. Isso provavelmente se dá pela posição dos aminoácidos conservados que especificam o padrão de clivagem. Para as enzimas que clivam na posição C1, há um resíduo de tirosina na área de superfície de contato ao substrato, que esconde o acesso dessa área ao substrato; para enzimas que clivam na posição C4, há a presença de resíduo de alanina ou aspartato no lugar da tirosina, permitindo maior permissividade da enzima ao substrato para alcançar a posição C4; enquanto que para as enzimas que clivam tanto na posição C1 quanto C4, há um resíduo de prolina, sendo um intermediário em permissividade (BORISOVA et al., 2015). Porém essa classificação não sempre determina o padrão de clivagem, pois a enzima PaLPMO9H, de *Podospora anserina*, foi predita como tipo 2 porém atuou como tipo 3 (BENNATI-GRANIER et al., 2015). As enzimas foram testadas também contra celopentose (Glc5) e celohexose (Glc6) (Figura 21 e 22).

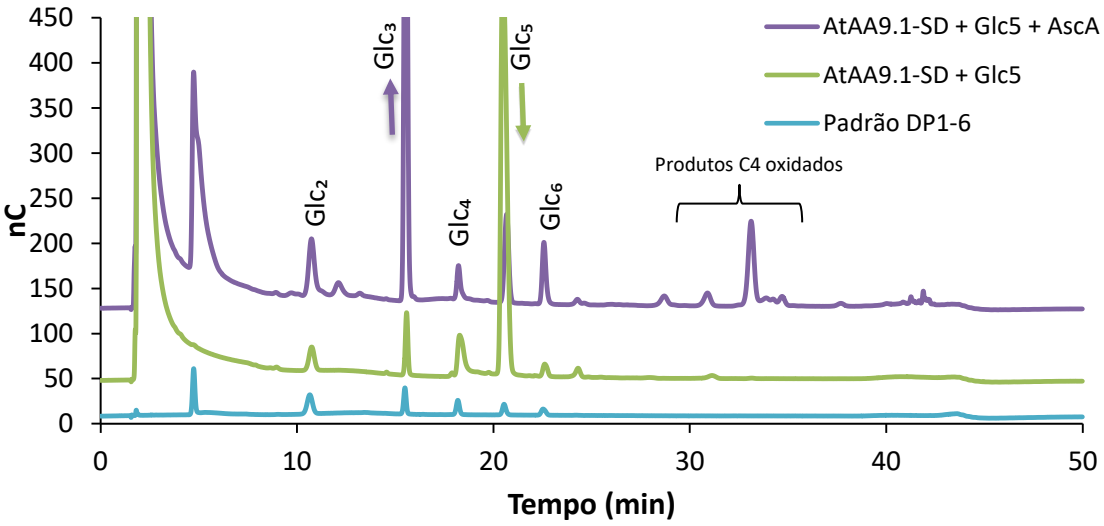

Figura 21. Perfil de produtos gerados analisados por HPAEC-PAD, de *AtAA9.1_SD* em celopentose.

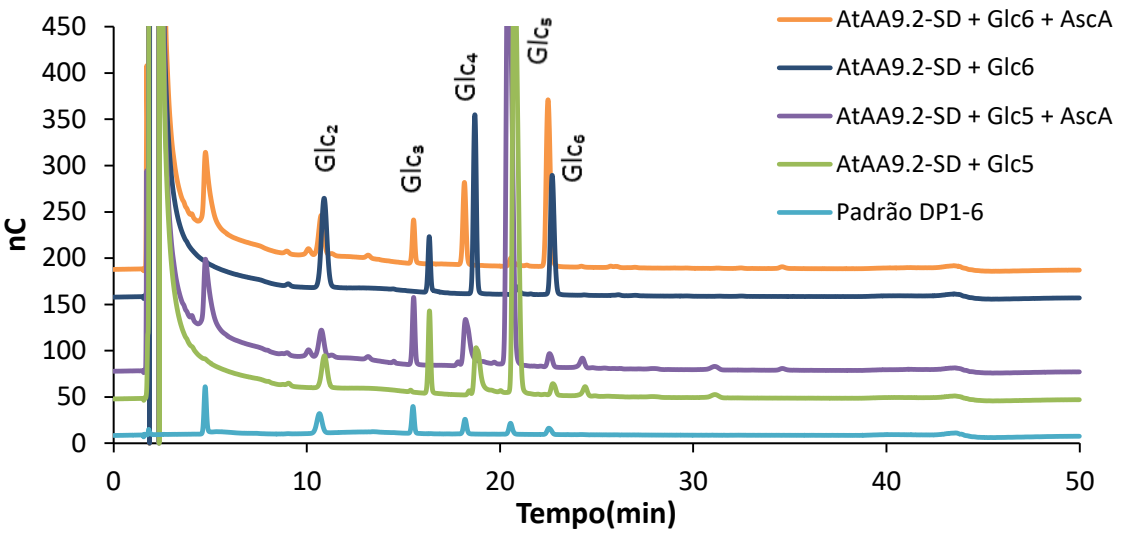

Figura 22. Perfil de produtos gerados analisados por HPAEC-PAD, de *AtAA9.2_SD* em celopentose e celohexose.

Enquanto a enzima *AtAA9.2_SD* não apresentou atividade nos celo-oligossacarídeos, *AtAA9.1_SD* apresentou atividade em celopentose. Pode-se perceber na figura 20 que o pico de Glc5 diminuiu enquanto o de Glc3 aumentou, com produção de picos oxidados em C4, conforme mostra a figura. LPMOs ativas em celo-oligossacarídeos já foram descritas antes (BENNATI-GRANIER et al., 2015; ISAKSEN et al., 2014), sendo considerado que ação em oligossacarídeos podem indicar atividade em hemicelulose que contenha glicoses em suas cadeias laterais. As figuras 23 e 24 mostram a atividade das enzimas em xiloglucana (TGX).

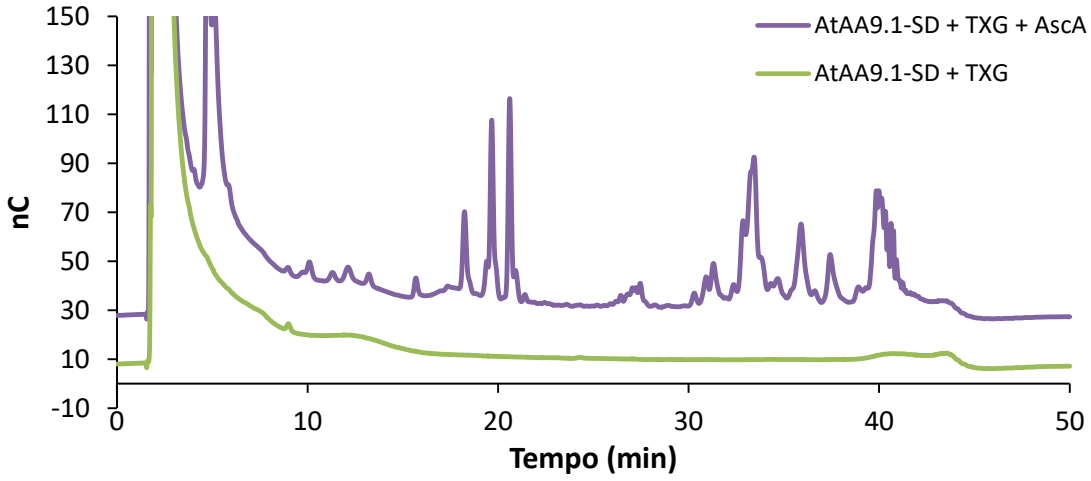

Figura 23. Perfil de produtos gerados analisados por HPAEC-PAD, de *AtAA9.1_SD* em xiloglucana.

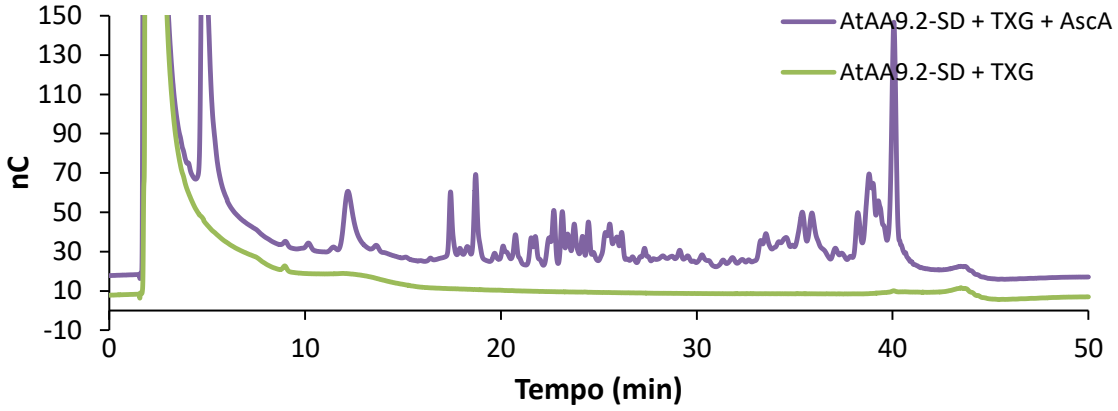

Figura 24. Perfil de produtos gerados analisados por HPAEC-PAD, de *AtAA9.2_SD* em xiloglucana.

Ambas as enzimas demonstraram ter uma suposta atividade em xiloglucana. Interessante notar que o padrão de clivagem foi diferente para cada enzima. Para *AtAA9.1_SD*, que possui oxidação em C4, percebe-se que o gráfico foi menos complexo (menos presença de picos) que o de *AtAA9.2_SD*, que é oxidativa em C1/C4. Um estudo realizado por Kojima *et al*. (KOJIMA et al., 2016) demonstrou que a enzima NcLPMO9C, uma LPMO de *N. crassa* com oxidação em C4, possui um padrão de clivagem muito parecido com a de *AtAA9.1_SD*; enquanto a enzima GtLPMO9A-2, uma LPMO de *Gleophyllum trabeum* com oxidação em C1/C4, demonstrou um padrão de clivagem muito parecido com a de *AtAA9.2_SD*, assim como a FgLPMO9A, LPMO de *Fusarium graminearum*, com atividade em C1/C4 (NEKIUNAITE et al., 2016). A xiloglucana é um substrato solúvel que possui uma cadeia principal de glicose com abundantes substituições de α-1,6 xilose, sendo estes podendo conter galactose ou arabinose como substituinte (MISHRA; MALHOTRA, 2009). A xiloglucana de tamarindo, substrato utilizado, possui uma cadeia principal de glicose, com 3 unidades de glicose substituidas com xilose, e uma glicose sem substituinte. Os resultados encontrados por Kojima *et al.* (KOJIMA et al., 2016) e Nekiunaite *et al.* (NEKIUNAITE et al., 2016) demonstraram que NcLPMO9C liberou apenas produtos oxidados em C4 enquanto que GtLPMO9A-2 e FgLPMO9A liberaram uma mistura de produtos oxidados em C1 e C4, onde esses produtos de clivagem foram analisados por MALDI-TOF. Dentre os produtos analisados, identificou-se que ambas enzimas que atuam como C1/C4 conseguiram acessar os grupos substituídos e não substituídos da xiloglucana, gerando maior espectro de produtos oxidados, enquanto que a enzima que oxida C1 conseguiu acessar apenas os grupos de glicose não substituídos, provavelmente devido a um impedimento estérico do substrato.

Para afirmar que o padrão de clivagem de *AtAA9.1_SD* e *AtAA9.2_SD* foi similar ao dessas LPMOs, é necessário identificar os produtos de reação por MALDI-TOF, análise que está em progresso no momento.

O próximo substrato testado foi xilana de birchwood (BrX) (Figura 25 e 26).

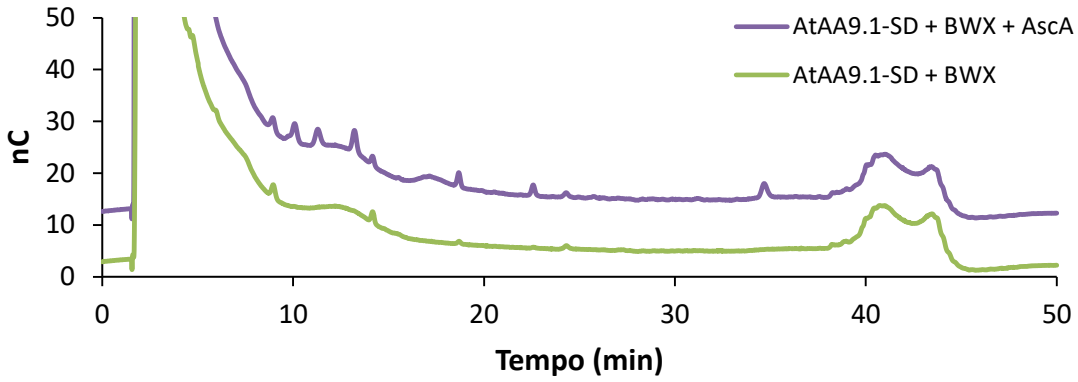

Figura 25. Perfil de produtos gerados analisados por HPAEC-PAD, de *AtAA9.1_SD* em xilana.

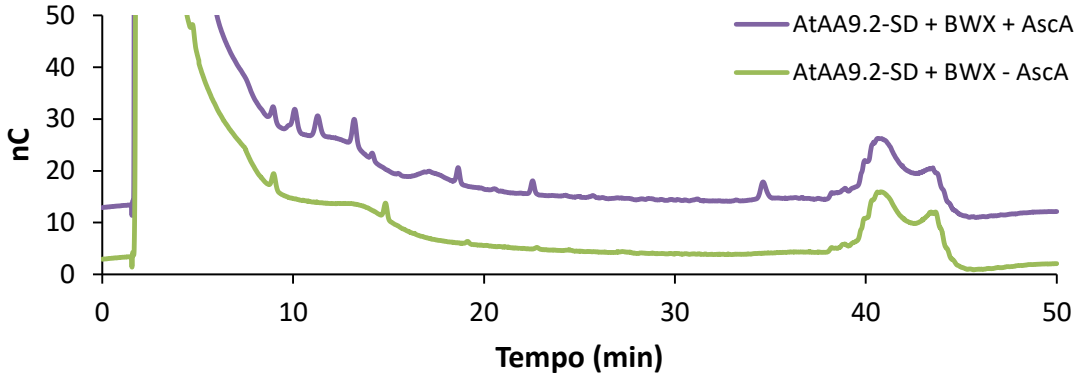

Figura 26. Perfil de produtos gerados analisados por HPAEC-PAD, de *AtAA9.2_SD* em xilana.

Ambas as enzimas demonstraram ter uma suposta atividade em xilana, com um padrão semelhante entre elas, porém não houve complexidade nos cromatogramas. A primeira LPMO identificada com atividade em xilana, MtLPMO9A, foi descrita por Frommhagen *et al.* (FROMMHAGEN et al., 2015), obtida de *Myceliophtora thermophila C1*. Porém, a enzima demonstrou atividade somente quando celulose foi adicionada. Recentemente, uma família nova de LPMOs, AA14, foi identificada, tendo atividade em xilana quando esta está adsorvida na celulose cristalina e não em solução, e sem atividade em celulose. Até o presente momento, não foi descrita uma LPMO da família AA9 ativa

diretamente na xilana. Porém, não se pode afirmar que houve atividade de fato de *AtAA9.1_SD* e *AtAA9.2_SD* pois os produtos de reação não foram identificados. A análise por MALDI-TOF está em progresso, assim como uma nova reação das enzimas com xilana e celulose, para avaliar se o padrão de clivagem foi similar ao de MtLPMO9A.

O último substrato analisado foi liquenina, que consiste de unidades de glicose ligadas por ligações do tipo β-1,3 e β-1,4 (Figura 27 e 28).

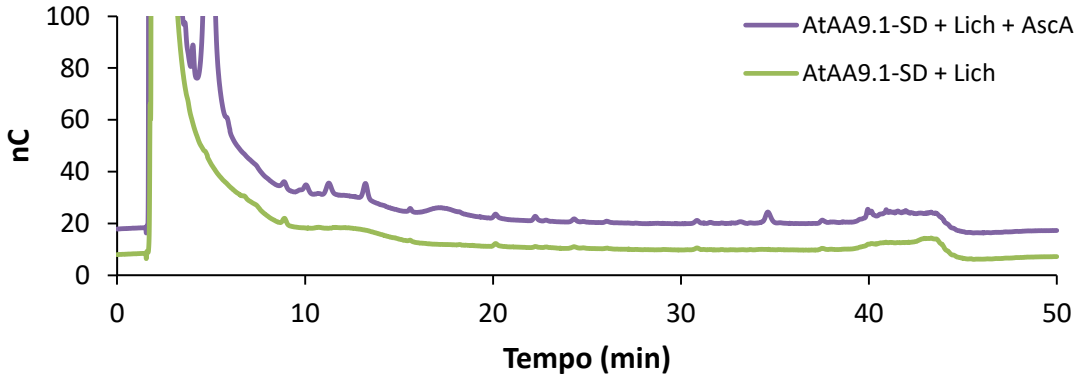

Figura 27. Perfil de produtos gerados analisados por HPAEC-PAD, de *AtAA9.1_SD* em liquenana.

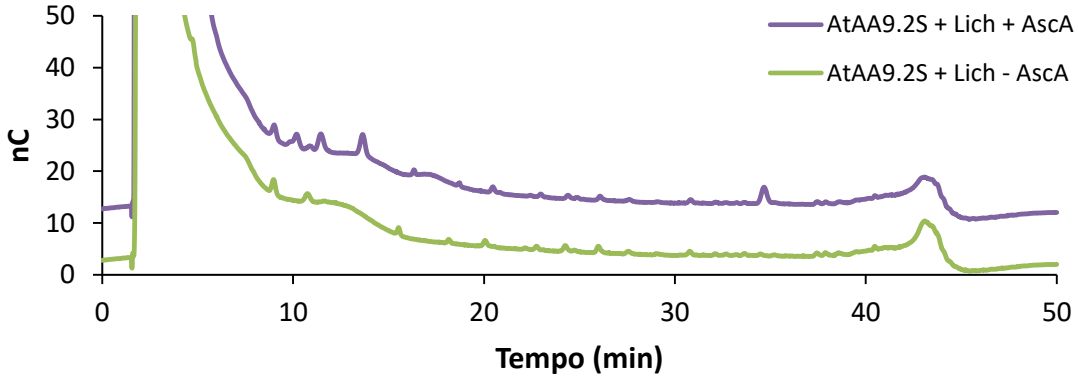

Figura 28. Perfil de produtos gerados analisados por HPAEC-PAD, de *AtAA9.1_SD* em liquenana.

Pode-se perceber que as enzimas tiveram um padrão diferente, onde *AtAA9.1_SD* demonstrou ter uma possível atividade, enquanto *AtAA9.2_SD* não. NcLPMO9C (AGGER et al., 2014), enzima com ação em C4, assim como *AtAA9.2_SD*, também foi identificada com ação em liquenana. PaLPMO9H também demonstrou atividade em liquenana, porém, diferentemente de NcLPMO9C, ela demonstrou ampla afinidade a vários substratos, com o requerimento mínimo para ação, de ligações do tipo β-1,4 entre

unidades de glicose (BENNATI-GRANIER et al., 2015). A análise por MALDI-TOF está em progresso para analisar os produtos de reação e confirmar a atividade em liquenana.

6.5 Conclusões

Os dados obtidos pelo RNA-seq demonstraram ser uma estratégia interessante para aquisição de sequências viáveis de proteínas, pois o perfil de expressão dos genes de *A. tamarii* no bagaço de cana-de- açúcar já foi um indicativo pertinente de escolha de proteínas candidatas para serem analisadas. Provavelmente a quantidade de transcrito acumulados durante a degradação do bagaço de cana-de-açúcar está relacionado com a estrutura da parede celular que o fungo encontra para degradar, induzindo que diferentes enzimas sejam produzidas baseado na recalcitrância encontrada. A partir das enzimas candidatas, a utilização de um sistema de expressão heterólogo demonstrou ser crucial, pois, especialmente para enzimas com atividade oxidativa, a purificação das enzimas fazendo *screening* por atividade enzimática é oneroso e com muita variabilidade. O sistema de expressão PichiaPink™ mostrou ser excelente para produção de enzimas com domínios únicos. Não foi um sistema interessante para expressar os genes das enzimas que possuem um domínio extra, dessa forma, faz-se necessário testar diferentes tipos de sistema de expressão para esse tipo de enzima. Foram caracterizadas duas AA9 com regioseletividade diferente para oxidação, uma em C4 e outra em C1/C4. As enzimas *AtAA9.1_SD* e *AtAA9.2_SD* de *A. tamarii* demonstraram potencial para degradação de biomassa por possuírem ampla especificidade ao substrato, sendo ativas em celulose (PASC), xiloglucana e possivelmente xilana. Além disso, *AtAA9.1_SD* demonstrou atividade em celopentose e possivelmente em liquenana. A ação num amplo espectro de substratos indica que a degradação da biomassa pelo fungo saprófito é orquestrado não só por diferentes enzimas, mas por enzimas da mesma família mas com características distintas, como a regioseletividade. Por suas diferentes características, as enzimas apresentam um potencial de aplicação em coquetéis enzimáticos focados em degradar diferentes biomassas.

6.6 Perspectivas futuras

Para uma melhor compreensão das principais AA9 do fungo e o seu papel na degradação da biomassa, outras candidatas estão sendo analisadas. Além disso, análises por espectrometria de massa para identificação de produtos oxidados de reação também estão sendo efetuados, para que as potenciais atividades em diferentes substratos sejam confirmadas. As enzimas serão cristalizadas, na presença e ausência do substrato, para

melhor elucidação de sua estrutura, especificidade ao substrato e regioseletividade. Por fim, estudos na hidrólise do bagaço de cana-de-açúcar *in natura* e pré-tratado serão realizados para estudos envolvendo sinergismo das diferentes enzimas na degradação da biomasas.

CONCLUSÃO GERAL

O objeto de estudo principal dessa tese foi o fungo *A. tamarii* e seu potencial na degradação de biomassa lignocelulósica. Esse potencial na degradação foi estudado de forma mais aprofundada visando três diferentes abordagens: a primeira, que avaliou a influência de componentes do cultivo nas atividades enzimáticas e concluiu que além de ferramentas estatísticas serem extremamente úteis para analisar comportamento enzimático em diferentes circustâncias, pequenas variações em meios de cultivo afetam a atividade enzimática, e que isso deve ser levado em conta ao planejar coquetéis enzimáticos para degradação de biomassa. A segunda abordagem procurou elucidar o mecanismo adjacente à ativação enzimática na presença de um derivado fenólico, implicando em possíveis aplicações na tolerância de enzimas à componentes fenólicos de biomassas pré tratadas, focando em otimizações na degradação da biomassa. A última abordagem caracterizou duas AA9 que demonstraram aplicação na degradação da biomassa, por apresentarem regioseletividade distinta e ampla especificidade a diferentes substratos. Demonstrou-se então que, além do potencial latente do fungo *A. tamarii* para degradação da biomassa lignocelulósica, suas enzimas possuem habilidades intrínsecas que podem ser aproveitadas no contexto de conversão enzimática em uma biorefinaria.

Fungos são microrganismos singulares, extremamente adaptados ao planeta em diferentes condições, e com imensa implicação e aplicação à humanidade, em contextos de saúde humana à aplicações biotecnológica para o bem estar social. Logo, conhecimentos adquiridos sobre eles são de notória importância para manutenção da vida no planeta.

REFERÊNCIA BIBLIOGRÁFICA

ABBOTT, D. W.; VAN BUEREN, A. L. Using structure to inform carbohydrate binding module function. **Current Opinion in Structural Biology**, v. 28, n. 1, p. 32–40, 2014.

ACHYUTHAN, K. E. et al. Supramolecular self-assembled chaos: Polyphenolic lignin's barrier to cost-effective lignocellulosic biofuels. **Molecules**, v. 15, n. 12, p. 8641–8688, 2010.

ADRIO, J. L.; DEMAIN, A. L. Fungal biotechnology. **International Microbiology**, v. 6, n. 3, p. 191–199, 2003.

AGBLEVOR, F. A. et al. Storage and characterization of cotton gin waste for ethanol production. **Resources, Conservation and Recycling**, v. 46, n. 2, p. 198–216, 2006.

AGGER, J. W. et al. Discovery of LPMO activity on hemicelluloses shows the importance of oxidative processes in plant cell wall degradation. **Proceedings of the National Academy of Sciences of the United States of America**, v. 111, n. 17, p. 6287–6292, 2014.

ANANDAN, D.; MARMER, W. N.; DUDLEY, R. L. Isolation, characterization and optimization of culture parameters for production of an alkaline protease isolated from Aspergillus tamarii. **Journal of Industrial Microbiology and Biotechnology**, v. 34, n. 5, p. 339–347, 2007.

ANGOV, E. et al. Heterologous protein expression is enhanced by harmonizing the codon usage frequencies of the target gene with those of the expression host. **PLoS ONE**, v. 3, n. 5, p. 1–10, 2008.

ARO, N.; PAKULA, T.; PENTTILÄ, M. Transcriptional regulation of plant cell wall degradation by filamentous fungi. **FEMS Microbiology Reviews**, v. 29, n. 4, p. 719–739, 2005.

BENKO, Z. et al. Evaluation of the role of xyloglucanase in the enzymatic hydrolysis of lignocellulosic substrates. **Enzyme and Microbial Technology**, v. 43, n. 2, p. 109–114, 2008.

BENNATI-GRANIER, C. et al. Substrate specificity and regioselectivity of fungal AA9 lytic polysaccharide monooxygenases secreted by Podospora anserina. **Biotechnology for biofuels**, v. 8, p. 90, 2015.

BISSARO, B. et al. Oxidative cleavage of polysaccharides by monocopper enzymes depends on H2O2. **Nature Chemical Biology**, v. 13, n. 10, p. 1123–1128, 2017.

BOER, C. G.; PERALTA, R. M. Production of extracellular protease by Aspergillus tamarii. **Journal of Basic Microbiology**, v. 40, n. 2, p. 75–81, 2000.

BOERJAN, W.; RALPH, J.; BAUCHER, M. L <scp>IGNIN</scp> B <scp>IOSYNTHESIS</scp>. **Annual Review of Plant Biology**, v. 54, n. 1, p. 519–546, 2003.

BORISOVA, A. S. et al. Structural and functional characterization of a lytic polysaccharide monooxygenase with broad substrate specificity. **Journal of Biological Chemistry**, v. 290, n. 38, p. 22955–22969, 2015.

BOUKARI, I. et al. Probing a family GH11 endo-β-1,4-xylanase inhibition mechanism by phenolic compounds: Role of functional phenolic groups. **Journal of Molecular Catalysis B:**

Enzymatic, v. 72, n. 3-4, p. 130–138, 2011.

BOUWS, H.; WATTENBERG, A.; ZORN, H. Fungal secretomes - Nature's toolbox for white biotechnology. **Applied Microbiology and Biotechnology**, v. 80, n. 3, p. 381–388, 2008.

BROWN, N. A.; RIES, L. N. A.; GOLDMAN, G. H. How nutritional status signalling coordinates metabolism and lignocellulolytic enzyme secretion. **Fungal Genetics and Biology**, v. 72, n. July, p. 48–63, 2014.

CHAN, L. G. et al. Conversion of Agricultural Streams and Food-Processing By-Products to Value-Added Compounds using Filamentous Fungi. **Annual Review of Food Science and Technology**, v. 9, n. January, p. 1–21, 2018.

CLAASSEN, P. A. M. et al. Utilisation of biomass for the supply of energy carriers. **Applied Microbiology and Biotechnology**, v. 52, n. 6, p. 741–755, 1999.

CONAB. Acompanhamento da safra brasileira de Cana-de-açúcar: terceiro levantamento - safra 2016/2017. **Companhia Nacional de Abastecimento - CONAB**, v. 3, n. 3, p. 174, 2016.

CONESA, A. et al. The secretion pathway in filamentous fungi: a biotechnological view. **Fungal genetics and biology : FG & B**, v. 33, n. 3, p. 155–71, 2001.

COTTY, P. J. Aflatoxin-producing potential of communities of Aspergillus section Flavi from cotton producing areas in the United States. **Mycological Research**, v. 101, n. 6, p. 698–704, 1997.

COUTURIER, M. et al. Lytic xylan oxidases from wood-decay fungi unlock biomass degradation. **Nature Chemical Biology**, n. january, 2018.

DALY, R.; HEARN, M. T. W. Expression of heterologous proteins in Pichia pastoris: A useful experimental tool in protein engineenring and production. **Journal of Molecular Recognition**, v. 18, n. 2, p. 119–138, 2005.

DE SIQUEIRA, F. G. et al. The potential of agro-industrial residues for production of holocellulase from filamentous fungi. **International Biodeterioration and Biodegradation**, v. 64, n. 1, p. 20–26, 2010.

DE SOUZA MOREIRA, L. R. et al. Two β-xylanases from Aspergillus terreus: Characterization and influence of phenolic compounds on xylanase activity. **Fungal Genetics and Biology**, v. 60, p. 46–52, 2013.

DE VRIES, R. P. et al. Aspergillus Enzymes Involved in Degradation of Plant Cell Wall Polysaccharides. **Microbiology and Molecular Biology Reviews**, v. 65, n. 4, p. 497–522, 2001.

DIMAROGONA, M.; TOPAKAS, E.; CHRISTAKOPOULOS, P. CELLULOSE DEGRADATION BY OXIDATIVE ENZYMES. **Computational and Structural Biotechnology Journal**, v. 2, n. 3, p. 1–8, 2012.

DODD, D.; CANN, I. K. Enzymatic deconstruction of xylan for biofuel production. **Glob Change Biol Bioenergy**, v. 1, n. 1, p. 2–17, 2009.

DUARTE, G. et al. Use of Residual Biomass from the Textile Industry as Carbon Source for Production of a Low-Molecular-Weight Xylanase from Aspergillus oryzae. **Applied Sciences**,

v. 2, n. 4, p. 754–772, 2012.

DUQUE JARAMILLO, P. M. et al. Liquid-liquid extraction of pectinase produced by Aspergillus oryzae using aqueous two-phase micellar system. **Separation and Purification Technology**, v. 120, p. 452–457, 2013.

EL-GINDY, A. A.; SAAD, R. R.; FAWZI, E. M. **Purification of β-xylosidase from Aspergillus tamarii using ground oats and a possible application on the fermented hydrolysate by Pichia stipitisAnnals of Microbiology**, 2015.

FARANI DE SOUZA, D.; GIATTI MARQUES DE SOUZA, C.; PERALTA, R. M. Effect of easily metabolizable sugars in the production of xylanase by Aspergillus tamarii in solid-state fermentation. **Process Biochemistry**, v. 36, n. 8-9, p. 835–838, 2001.

FRANDSEN, K. E. H. et al. The molecular basis of polysaccharide cleavage by lytic polysaccharide monooxygenases. **Nature Chemical Biology**, v. 12, n. 4, p. 298–303, 2016.

FRISVAD, J. C. Taxonomy, chemodiversity and chemoconsistency of aspergillus, penicillium and talaromyces species. **Frontiers in Microbiology**, v. 5, n. DEC, p. 1–7, 2014.

FROMMHAGEN, M. et al. Discovery of the combined oxidative cleavage of plant xylan and cellulose by a new fungal polysaccharide monooxygenase. **Biotechnology for biofuels**, v. 8, n. 1, p. 101, 2015.

GHORAI, S. et al. Fungal Biotechnology in Food and Feed Processing. **Comprehensive Biotechnology, Second Edition**, v. 3, n. 5-6, p. 603–615, 2011.

GILBERT, H. J.; KNOX, J. P.; BORASTON, A. B. Advances in understanding the molecular basis of plant cell wall polysaccharide recognition by carbohydrate-binding modules. **Current Opinion in Structural Biology**, v. 23, n. 5, p. 669–677, 2013.

GLAUCIA EMY OKIDA MIDORIKAWA. **Aspergillus seção Flavi: Caracterização molecular de espécies aflatoxigênicas da castanha do Brasil e análise do transcritoma de Aspergillus oryzae em relação a degradação enzimática do bagaço da cana-de-açúcar**. [s.l.] University of Brasília, 2014.

GODET, M.; MUNAUT, F. Molecular strategy for identification in Aspergillus section Flavi: RESEARCH LETTER. **FEMS Microbiology Letters**, v. 304, n. 2, p. 157–168, 2010.

GOUDA, M. K.; ABDEL-NABY, M. A. Catalytic properties of the immobilized Aspergillus tamarii xylanase. **Microbiol Res**, v. 157, n. 4, p. 275–281, 2002.

GRIMM, L. H. et al. Morphology and productivity of filamentous fungi. **Applied Microbiology and Biotechnology**, v. 69, n. 4, p. 375–384, 2005.

GUIMARÃES, L. H. S. et al. Screening of filamentous fungi for production of enzymes of biotechnological interest. **Brazilian Journal of Microbiology**, v. 37, n. 4, p. 474–480, 2006.

GUTIÉRREZ-SÁNCHEZ, G.; ROUSSOS, S.; AUGUR, C. Effect of the nitrogen source on caffeine degradation by Aspergillus tamarii. **Letters in Applied Microbiology**, v. 38, n. 1, p. 50–55, 2004.

HARRIS, P. V. et al. Stimulation of lignocellulosic biomass hydrolysis by proteins of glycoside

hydrolase family 61: Structure and function of a large, enigmatic family. **Biochemistry**, v. 49, n. 15, p. 3305–3316, 2010.

HEMSWORTH, G. R. et al. Discovery and characterization of a new family of lytic polysaccharide monooxygenases. **Nature Chemical Biology**, v. 10, n. 2, p. 122–126, 2013.

HEMSWORTH, G. R. et al. Lytic Polysaccharide Monooxygenases in Biomass Conversion. **Trends in Biotechnology**, v. 33, n. 12, p. 747–761, 2015.

HENRISSAT, B. et al. Conserved catalytic machinery and the prediction of a common fold for several families of glycosyl hydrolases. **Proceedings of the National Academy of Sciences of the United States of America**, v. 92, p. 7090–7094, 1995.

HOHENBLUM, H. et al. Effects of Gene Dosage, Promoters, and Substrates on Unfolded Protein Stress of Recombinant Pichia pastoris. **Biotechnology and Bioengineering**, v. 85, n. 4, p. 367–375, 2004.

HORN, S. J. et al. Novel enzymes for the degradation of cellulose. **Biotechnology for Biofuels**, v. 5, n. 1, p. 45, 2012.

HU, H. L. et al. Improved enzyme production by co-cultivation of Aspergillus niger and Aspergillus oryzae and with other fungi. **International Biodeterioration and Biodegradation**, v. 65, n. 1, p. 248–252, 2011.

HU, J. et al. The addition of accessory enzymes enhances the hydrolytic performance of cellulase enzymes at high solid loadings. **Bioresource Technology**, v. 186, p. 149–53, 2015.

HU, J.; ARANTES, V.; PRIBOWO, A. Substrate factors that influence the synergistic interaction of AA9 and cellulases during the enzymatic hydrolysis of biomass. **Energy & Environmental Science**, v. 7, p. 2308–2315, 2014.

HUANG, L. et al. dbCAN-seq: a database of carbohydrate-active enzyme (CAZyme) sequence and annotation. **Nucleic Acids Research**, v. 46, n. October 2017, p. 516–521, 2017.

IBÁ. Anuário Estatístico da Indústria Brasileira de Árvore - 2017. p. 100, 2017.

ISAKSEN, T. et al. A C4-oxidizing lytic polysaccharide monooxygenase cleaving both cellulose and cello-oligosaccharides. **Journal of Biological Chemistry**, v. 289, n. 5, p. 2632–2642, 2014.

ITO, Y. et al. Aspergillus pseudotamarii, a new aflatoxin producing species in Aspergillus section Flavi. **Mycological Research**, v. 105, n. 2, p. 233–239, 2001.

JAGADEESWARAN, G. et al. A family of AA9 lytic polysaccharide monooxygenases in Aspergillus nidulans is differentially regulated by multiple substrates and at least one is active on cellulose and xyloglucan. **Applied Microbiology and Biotechnology**, p. 1–13, 2016.

JAYANI, R. S.; SAXENA, S.; GUPTA, R. Microbial pectinolytic enzymes: A review. **Process Biochemistry**, v. 40, n. 9, p. 2931–2944, 2005.

JEGANNATHAN, K. R.; NIELSEN, P. H. Environmental assessment of enzyme use in industrial production-a literature review. **Journal of Cleaner Production**, v. 42, p. 228–240, 2013.

JÖNSSON, L. J.; MARTÍN, C. Pretreatment of lignocellulose: Formation of inhibitory by-products and strategies for minimizing their effects. **Bioresource Technology**, v. 199, p. 103–112, 2016.

KIM, S. et al. Quantum mechanical calculations suggest that lytic polysaccharide monooxygenases use a copper-oxyl, oxygen-rebound mechanism. **Proceedings of the National Academy of Sciences of the United States of America**, v. 111, n. 1, p. 149–154, 2014.

KJAERGAARD, C. H. et al. Spectroscopic and computational insight into the activation of O2 by the mononuclear Cu center in polysaccharide monooxygenases. **Proceedings of the National Academy of Sciences of the United States of America**, v. 111, n. 24, p. 8797–802, 2014.

KLEPACKA, J.; FORNAL, Ł. Ferulic acid and its position among the phenolic compounds of wheat. **Critical Reviews in Food Science and Nutrition**, v. 46, n. 8, p. 639–647, 2006.

KOJIMA, Y. et al. Characterization of an LPMO from the brown-rot fungus Gloephyllum trabeum with broad xyloglucan specificity, and its action on cellulose-xyloglucan complexes. **Applied and Environmental Microbiology**, v. 82, n. 22, p. 6557–6572, 2016.

KRACHER, D. et al. **Extracellular electron transfer systems fuel cellulose oxidative degradation.** [s.l: s.n.].

KULKARNI, N.; SHENDYE, A.; RAO, M. Molecular and biotechnological aspects of xylanases. **FEMS Microbiology Reviews**, v. 23, n. 4, p. 411–456, 1999.

LARROQUE, M. et al. The unique architecture and function of cellulose-interacting proteins in oomycetes revealed by genomic and structural analyses. **BMC Genomics**, v. 13, n. 1, 2012.

LEE R. LYND, PAUL J. WEIMER, WILLEM H. VAN ZYL, I. S. P. Microbial Cellulose Utilization: Fundamentals and Biotechnology. **Microbiology and Molecular Biology Reviews**, v. 66, n. 3, p. 506–577, 2002.

LEVASSEUR, A. et al. Expansion of the enzymatic repertoire of the CAZy database to integrate auxiliary redox enzymes. **Biotechnology for biofuels**, v. 6, n. 1, p. 41, 2013.

LIMA, M. A et al. Evaluating the composition and processing potential of novel sources of Brazilian biomass for sustainable biorenewables production. **Biotechnology for biofuels**, v. 7, n. 1, p. 10, 2014.

LO LEGGIO, L. et al. Structure and boosting activity of a starch-degrading lytic polysaccharide monooxygenase. **Nature Communications**, v. 6, p. 5961, 2015.

MACHIDA, M. et al. Genome sequencing and analysis of Aspergillus oryzae. **Nature**, v. 438, n. 7071, p. 1157–1161, 2005.

MALVESSI, E.; DA SILVEIRA, M. M. Influence of medium composition and pH on the production of polygalacturonases by Aspergillus oryzae. **Brazilian Archives of Biology and Technology**, v. 47, n. 5, p. 693–702, 2004.

MCCARTER, J. D.; STEPHEN WITHERS, G. Mechanisms of enzymatic glycoside hydrolysis. **Current Opinion in Structural Biology**, v. 4, n. 6, p. 885–892, 1994.

MCKELVEY, S. M.; MURPHY, R. A. Analysis of wide-domain transcriptional regulation in solid-state cultures of Aspergillus oryzae. **Journal of Industrial Microbiology and Biotechnology**, v. 37, n. 5, p. 455–469, 2010.

MCKENDRY, P.; MCKENDRY, P. Energy production from biomass (part 3): gasi cation technologies. **Bioresource Technology**, v. 83, n. July 2001, p. 55–63, 2002.

MEYER, V. Genetic engineering of filamentous fungi - Progress, obstacles and future trends. **Biotechnology Advances**, v. 26, n. 2, p. 177–185, 2008.

MICHELIN, M. et al. Effect of phenolic compounds from pretreated sugarcane bagasse on cellulolytic and hemicellulolytic activities. **Bioresource Technology**, v. 199, p. 275–278, 2016.

MINIC, Z.; JOUANIN, L. Plant glycoside hydrolases involved in cell wall polysaccharide degradation. **Plant Physiology and Biochemistry**, v. 44, n. 7-9, p. 435–449, 2006.

MISHRA, A.; MALHOTRA, A. V. Tamarind xyloglucan: a polysaccharide with versatile application potential. **Journal of Materials Chemistry**, v. 19, n. 45, p. 8528, 2009.

MME (MINISTÉRIO DE MINAS E ENERGIA). Resenha Energética Brasileira. p. 26, 2017.

MONCLARO, A. et al. Characterization of multiple xylanase forms from Aspergillus tamarii resistant to phenolic compounds. **Mycosphere**, v. 7, n. September, p. 1554–1567, 2016.

MONCLARO, A. V.; FILHO, E. X. F. Fungal lytic polysaccharide monooxygenases from family AA9: Recent developments and application in lignocelullose breakdown. **International Journal of Biological Macromolecules**, v. 102, p. 771–778, 2017.

MONTEBELLO, A. E. S.; BACHA, C. J. C. Impactos da reestruturação do setor de celulose e papel no Brasil sobre o desempenho de suas indústrias. **Estudos Econômicos**, v. 43, n. 1, p. 109–137, 2013.

MOREIRA, L. R. S.; FILHO, E. X. F. An overview of mannan structure and mannan-degrading enzyme systems. **Applied Microbiology and Biotechnology**, v. 79, n. 2, p. 165–178, 2008.

NEKIUNAITE, L. et al. FgLPMO9A from Fusarium graminearum cleaves xyloglucan independently of the backbone substitution pattern. **FEBS Letters**, v. 590, p. 3346–3356, 2016.

NEVALAINEN, K. M. H.; TE'O, V. S. J.; BERGQUIST, P. L. Heterologous protein expression in filamentous fungi. **Trends in Biotechnology**, v. 23, n. 9, p. 468–474, 2005.

PAPAGIANNI, M. Fungal morphology and metabolite production in submerged mycelial processes. **Biotechnology Advances**, v. 22, n. 3, p. 189–259, 2004.

PAULY, M. et al. Molecular domains of the cellulose/xyloglucan network in the cell walls of higher plants. **Plant Journal**, v. 20, n. 6, p. 629–639, 1999.

PERCIVAL ZHANG, Y. H.; HIMMEL, M. E.; MIELENZ, J. R. Outlook for cellulase improvement: Screening and selection strategies. **Biotechnology Advances**, v. 24, n. 5, p. 452–481, 2006.

PIROTA, R. D. P. B.; DELABONA, P. S.; FARINAS, C. S. Enzymatic hydrolysis of sugarcane bagasse using enzyme extract and whole solid-state fermentation medium of two newly isolated

strains of aspergillus oryzae. **Chemical Engineering Transactions**, v. 38, p. 259–264, 2014.

POLIZELI, M. L. T. M. et al. Xylanases from fungi: Properties and industrial applications. **Applied Microbiology and Biotechnology**, v. 67, n. 5, p. 577–591, 2005.

QIN, L. et al. Inhibition of lignin-derived phenolic compounds to cellulase. **Biotechnology for Biofuels**, v. 9, n. 1, p. 1–10, 2016.

QUINLAN, R. J. et al. Insights into the oxidative degradation of cellulose by a copper metalloenzyme that exploits biomass components. **Proceedings of the National Academy of Sciences**, v. 108, n. 37, p. 15079–15084, 2011.

RAFAELA, V.; EURICH, P.; FRANCO, J. D. M. Gerenciamento de resíduos sólidos de indústria de fios em cooperativa agroindustrial. n. 1, p. 1–6, 2002.

SARROUH, B. et al. Up-To-Date Insight on Industrial Enzymes Applications and Global Market. **Journal of bioprocessing & biotechniques**, v. S4, n. 002, p. 1–10, 2012.

SILVA, C. DE O. G. et al. GH11 xylanase from Emericella nidulans with low sensitivity to inhibition by ethanol and lignocellulose-derived phenolic compounds. **FEMS Microbiology Letters**, v. 362, n. 13, p. 1–9, 2015.

SILVA, C. O. G.; VAZ, R. P.; FILHO, E. X. F. Bringing plant cell wall-degrading enzymes into the lignocellulosic biorefinery concept. **Biofuels, Bioproducts and Biorefining**, p. 1–13, 2017.

SPAN, E. A.; MARLETTA, M. A. The framework of polysaccharide monooxygenase structure and chemistry. **Current Opinion in Structural Biology**, v. 35, p. 93–99, 2015.

SUKUMARAN, R. K.; SINGHANIA, R. R.; PANDEY, A. Microbial cellulases - Production, applications and challenges. **Journal of Scientific and Industrial Research**, v. 64, n. 11, p. 832–844, 2005.

SZENDEFY, J.; SZAKACS, G.; CHRISTOPHER, L. Potential of solid-state fermentation enzymes of Aspergillus oryzae in biobleaching of paper pulp. **Enzyme and Microbial Technology**, v. 39, n. 6, p. 1354–1360, 2006.

T GOTO, D. T. W. AND Y. I. Aflatoxin and cyclopiazonic acid production by a sclerotium-producing Aspergillus tamarii strain. **Applied and Environmental Microbiology**, v. 62, n. 11, p. 4036–4038, 1996.

TANGHE, M. et al. Recombinant Expression of Trichoderma reesei Cel61A in Pichia pastoris: Optimizing Yield and N-terminal Processing. **Molecular Biotechnology**, v. 57, n. 11-12, p. 1010–1017, 2015.

TE BIESEBEKE, R. et al. Identification of secreted proteins of Aspergillus oryzae associated with growth on solid cereal substrates. **Journal of Biotechnology**, v. 121, n. 4, p. 482–485, 2006.

VAAJE-KOLSTAD, G. et al. An Oxidative Enzyme Boosting the Enzymatic Conversion of Recalcitrant Polysaccharides. **Science**, v. 330, n. 6001, p. 219–222, 2010.

VÁRNAI, A. et al. Expression of endoglucanases in Pichia pastoris under control of the GAP promoter. **Microbial Cell Factories**, v. 13, n. 1, p. 57, 2014.

VERMANI, M. et al. Physico-chemical and clinico-immunologic studies on the allergenic significance of Aspergillus tamarii, a common airborne fungus. **Immunobiology**, v. 216, n. 3, p. 393–401, 2011.

VIIKARI, L. et al. Xylanases in bleaching: From an idea to the industry. **FEMS Microbiology Reviews**, v. 13, n. 2-3, p. 335–350, mar. 1994.

VLASENKO, E. et al. Substrate specificity of family 5, 6, 7, 9, 12, and 45 endoglucanases. **Bioresource Technology**, v. 101, n. 7, p. 2405–2411, 2010.

VU, V. V et al. A family of starch-active polysaccharide monooxygenases. **Proceedings of the National Academy of Sciences of the United States of America**, v. 111, n. 38, p. 13822–7, 2014a.

VU, V. V. et al. Determinants of regioselective hydroxylation in the fungal polysaccharide monooxygenases. **Journal of the American Chemical Society**, v. 136, n. 2, p. 562–565, 2014b.

WEERACHAVANGKUL, C. et al. Alkaliphilic endoxylanase from lignocellulolytic microbial consortium metagenome for biobleaching of eucalyptus pulp. **Journal of Microbiology and Biotechnology**, v. 22, n. 12, p. 1636–1643, 2012.

WESTERENG, B. et al. Efficient separation of oxidized cello-oligosaccharides generated by cellulose degrading lytic polysaccharide monooxygenases. **Journal of Chromatography A**, v. 1271, n. 1, p. 144–152, 2013.

WONG, K. K.; TAN, L. U.; SADDLER, J. N. Multiplicity of beta-1,4-xylanase in microorganisms: functions and applications. **Microbiological reviews**, v. 52, n. 3, p. 305–317, 1988.

WOOD, T. M. Preparation of crystalline, amorphous, and dyed cellulase substrates. In: **Methods in Enzymology**. [s.l: s.n.]. v. 160p. 19–25.

WU, M. et al. Crystal structure and computational characterization of the lytic polysaccharide monooxygenase GH61D from the basidiomycota fungus Phanerochaete chrysosporium. **Journal of Biological Chemistry**, v. 288, n. 18, p. 12828–12839, 2013.

ZHANG, Z.; DONALDSON, A. A.; MA, X. Advancements and future directions in enzyme technology for biomass conversion. **Biotechnology Advances**, v. 30, n. 4, p. 913–919, 2012.

ANEXO 1 – ARTIGO PUBLICADO NA MYCOSPHERE EM 2016: CHARACTERIZATION OF MULTIPLE XYLANASE FORMS FROM ASPERGILLUS TAMARII RESISTANT TO PHENOLIC COMPOUNDS.

Mycosphere 7(10) 1554-1567 (2016)www.mycosphere.org ISSN 2077 7019

Article – special issue
Doi 10.5943/mycosphere/si/3b/7

Characterization of multiple xylanase forms from *Aspergillus tamarii* resistant to phenolic compounds

Monclaro AV[1], Aquino EN[1,2], Faria RF[1], Ricart CAO[2], Freitas SM[3], Midorikawa GEO[4], Miller RNG[4], Michelin M[5], Polizeli MLTM[5] and Filho EXF[1]

[1]Enzymology Laboratory, University of Brasília, Campus Universitário Darcy Ribeiro, Brasília - DF, 70910-900. e-mail: eximenes@unb.br
[2]Biochemistry and Protein Chemistry Laboratory, University of Brasília, Campus Universitário Darcy Ribeiro, Brasília - DF, 70910-900
[3]Molecular Biophysics Laboratory, University of Brasília, Campus Universitário Darcy Ribeiro, Brasília - DF, 70910-900
[4]Microbiology Laboratory, University of Brasília, Campus Universitário Darcy Ribeiro, Brasília - DF, 70910-900
[5]Microbiology and Cellular Biology Laboratory, University of São Paulo, Ribeirão Preto – SP, 14040-901

Monclaro AV, Aquino EN, Faria RF, Ricart CAO, Freitas SM, Midorikawa GEO, Miller RNG, Michelin M, Polizeli MLTM, Filho EXF 2016 – Characterization of multiple xylanase forms from *Aspergillus tamarii* resistant to phenolic compounds. Mycosphere 7(10), 1554–1567, Doi 10.5943/mycosphere/si/3b/7

Abstract

Aspergillus tamarii was cultivated in different textile wastes. Xylanases with high levels of enzymatic activity were produced after two days cultivation, with constant production for up to seven days. Two xylanases, namely Xyl-1 and Xyl-2, with molecular masses of 35.5 and 22 kDa, respectively, were isolated from the crude extract and purified by ultrafiltration and gel filtration chromatography. Xyl-1 and Xyl-2 were more active at pH 6.0, and 60° C and 40° C, respectively. The respective K_M and V_{max} values on soluble oat spelt xylan were 4.30 $mg.mL^{-1}$ and 0.249 $IU.mL^{-1}$ (Xyl-1) and 18.92 $mg.mL^{-1}$ and 1.103 $IU.mL^{-1}.s^{-1}$ (Xyl-2). Dynamic light scattering (DLS) was used to evaluate purification steps, effective in assessing the degree of purity of the samples, the presence of aggregations and the size of the enzymes. Tween-80 at 0.1% was an efficient dispersing agent for avoiding aggregation of proteins and did not influence enzyme activity. Purified and partially purified xylanases were activated with auto-hydrolysis liquor from corncob and with ferulic acid, a phenolic compound derived from lignocellulosic biomass. These findings of this study indicate that *A. tamarii* produces multiple forms of xylanases with considerable potential in different biotechnological applications.

Keywords – Corncob autohydrolysis liquor – dynamic light scattering – ferulic acid – textile wastes

Introduction

The plant cell wall of lignocellulosic biomass, which is an important component of agro-industrial residues, is a complex structure composed of three principal components: cellulose, hemicellulose and lignin (Siqueira et al. 2009). Within the context of biotechnological

Submitted 21 March 2016, Accepted 20 September 2016, Published 11 October 2016
Corresponding Author: Filho EXF – e-mail – eximenes.1@gmail.com

applications, second generation bioethanol conversion from agro-industrial wastes represents a promising renewable energy source and an alternative to the use of fossil resources. The polysaccharides within plant cell walls are arranged in an organized manner, forming structures that are highly recalcitrant to enzymatic degradation (Siqueira et al. 2009). As such, efficient hydrolysis of plant cell wall material is one of the main challenges for the biofuel industry.

Xylan is the most abundant component of hemicellulose. It is a heteropolysaccharide with a varied structure, which essentially consists of β-1,4-xylose units in the backbone and L-arabinofuranosyl and methyl glucuronic acid as side groups. The xylose units can be acetylated and L-arabinofuranosyl may have additional side groups such as ferulic acid and ρ-coumaric acid. These residues can be cross-linked with lignin, thus maintaining the integrity of plant cell walls (Polizeli et al. 2005).

Brazil is today one of the major global cotton producers, with cultivation of this cash crop contributing significantly to the national economy (Siqueira et al. 2009). One of the environmental problems related to the cultivation of cotton is the amount of cotton residue generated, which can be five times higher than the total amount of fiber produced (Agblevor et al. 2006). The conversion of this residue into valuable by-products is currently under extensive study, with potential application identified in the biorefinary industry for fuel production (Caldeira-Pires et al. 2013).

Most industrial enzymes are produced by bacteria, yeasts and fungi that are able to ferment specific substrates. A number of fungi from the genus *Aspergillus* are effective decomposers of lignocellulosic biomass and efficient producers of xylanases (Moreira et al. 2013). *Aspergillus tamarii* and *Aspergillus flavus* are closely related species, with *A. tamarii* a non-aflatoxin producer (Ito et al. 2001) and known to be a xylanase producer (Ferreira et al. 1999, Souza et al. 2001).

This study describes the characterization of xylanases in *A. tamarii* BLU37, a strain isolated from natural composting of textile residues in Brazil with potential for application in the biorefinary and biofuel industries. We evaluated both the fungal strain's ability to produce xylanases using different textile residues as a carbon source, as well as the influence of different phenolic compounds on enzyme activities.

Materials & Methods

Residue and chemicals

All reagents and substrates were purchased from Sigma Chemical Co. (St. Louis, USA). Sephacryl S-100, Sephadex G-50 and HiTrap Q FF were purchased from GE Healthcare (São Paulo, Brazil). Cotton residues were donated by Hantex Resíduos Têxteis Ltda (Gaspar, Brazil). All experiments were carried out in quintuplicate. The standard deviation was less than 20% of the mean.

Residue pretreatment

Filter powder (FP) and clean cotton residue (CC) were pretreated as previously described by Duarte et al. (2012). The pretreated filter powder and pretreated clean cotton residue are hereafter referred to as tFP and tCC, respectively.

Organism and enzyme production

A. tamarii BLU37 was originally isolated from natural composting of textile industry residues and deposited in the fungal collection at The Enzymology Laboratory, University of Brasília, Brazil (gene pool access authorization number 010237/2015-1). Ribosomal DNA Internal Transcribed Spacer (rDNA ITS) regions, together with β-tubulin and calmodulin genes, were used as conserved molecular markers to identify the fungus to species level (Midorikawa et al. 2008). The isolate was maintained in PDA medium (2% potato broth, 2% dextrose and 2%

agar). An aliquot (5 mL) of spore suspension (10^8 spores.mL^{-1}) was inoculated into Erlenmeyer flasks containing 500 mL of liquid medium adjusted to pH 7.0 and containing 1.0% (w/v) of FP, tFP, CC and tCC as carbon sources. Two liquid media were employed: a standard liquid medium composed of (w/v) 0.7% KH_2PO_4, 0.2% K_2HPO_4, 0.05% $MgSO_4.7H_2O$, 0.1% $(NH_4)_2SO$ and 0.06% yeast extract; and an alternative liquid medium composed of (w/v) 0.7% KH_2PO_4, 0.2% K_2HPO_4, 0.05% $MgSO_4.7H_2O$ and 0.16% $(NH_4)_2SO$. The cultures were incubated at 28°C with constant agitation at 120 rpm for 7 days. The crude extracts obtained from these cultures were filtered through filter paper (Whatman No. 1). For xylanase induction, aliquots were collected every 24 h during 7 days and used to estimate enzyme activity and protein concentration.

Enzyme assay

The xylanase activity was measured by mixing 5 µL of enzyme solution with 10 µL of oat spelt xylan (10 mg.mL^{-1}) in 50 mM sodium acetate buffer (pH 5.0) at 50°C for 30 minutes. The reaction was interrupted by the addition of 30 µL of 3,5-dinitrosalicylic acid and immediate boiling for 10 min at 97°C (Miller 1959). The release of reducing sugar was measured at 540 nm in a SpectraMax® Plus 384 (Molecular Devices, US) and xylanase activity was expressed as µmol of reducing sugar released per minute per milliliter (IU.mL^{-1}) using xylose as standard. Endoglucanase (CMCase), pectinase and mannanase activities were evaluated according to Duarte et al. (2012). Protein concentration was measured by the Bradford method (Bradford 1976), using bovine serum albumin as standard.

Enzyme purification

A crude extract sample (350 mL) obtained after *A. tamarii* cultivation in standard liquid medium was concentrated approximately 10-fold by ultrafiltration using an Amicon System (Amicon Inc., USA) with a 10-kDa cut-off point membrane. Based on the specific xylanase activity of ultrafiltrate, this sample was chosen for further purification. Aliquots (300 mL) of the ultrafiltrate were subjected to lyophilization (Freeze Dryer Liobrás, Brazil) for 48 h. The lyophilized material was re-suspended in 50 mM sodium phosphate buffer (pH 7.0) containing 150 mM NaCl and 0.02% NaN_3. Aliquots (5 mL) of re-suspended material were loaded onto Sephadex G-50 and/or Sephacryl S-100 (GE Healthcare) gel filtration systems, previously equilibrated using the same aforementioned buffer conditions. Fractions (1.5 mL) were eluted at a flow rate of 15 mL.h^{-1} and those corresponding to xylanase activity were pooled and stored at 4° for further characterization.

Enzyme characterization

For kinetic experiments, soluble oat spelt xylan was prepared as described by Filho et al. (1993). The substrate was used over a concentration range of 1-40 mg.mL^{-1}. K_M and V_{max} were estimated from the Michaelis-Menten equation with a non-linear regression data analysis program (GraphPad Prism® 6). The effects of temperature and pH were evaluated according to Duarte et al. (2012).

Dynamic Light Scattering and Tween-80 effect

Dynamic light scattering (DLS) measurements were conducted in triplicate with a Zetasizer Nanoseries (Malvern, London, UK). Conducetd at room temperature, an average of 15 acquisition scans were conducted, with total acquisition time set to 60 s. The purified and partially purified xylanases were dissolved in 50 mM sodium phosphate buffer (pH 7.0) solution. The DLS measurements were also made in the presence of 0.1% (v/v) Tween-80 under the same aforementioned conditions.

Effect of corncob autohydrolysis liquor

The autohydrolysis process was conducted 30-minute intervals, as previously described by Michelin et al. (2012). Corncob particles were decomposed to soluble compounds. The resulting liquor samples were separated from the solid by vacuum filtration and used as a liquid substrate. Two distinct assays were performed for assessment of xylanolytic activity of enzymes after incubation with corncob liquor. The first assay was carried out by incubating 5 µL of enzyme sample with 5 µL of xylan (20 $mg.mL^{-1}$) in 50 mM sodium acetate buffer (pH 5.0) and 5 µL of 10-fold diluted liquor solution. The second was performed by incubating 5 µL of enzyme sample with 5 µL of 50 mM sodium acetate buffer (pH 5.0) and 5 µL of 10-fold diluted liquor solution. The enzyme assay conditions were as described previously. The control reaction was performed by incubating 5 µL of enzyme sample with 5 µL of 50 mM sodium acetate buffer (pH 5.0) and 5 µL of xylan (20 $mg.mL^{-1}$).

Effect of phenolic compounds

Phenolic compounds at a concentration of 2 mM were individually mixed with xylanases and incubated at 50°C for 30 min, as described by Moreira et al. (2013). Enzymatic assays of xylanases in the presence of phenolic compounds were perfomed as described previously.

Statistical analysis

Analysis of experimental data for enzyme activities was analyzed with the software PAST 3.11. Data were submitted to factorial ANOVA and post hoc Tukey's Pairwise Comparisons with significance $P < 0.05$.

Electrophoresis

Sodium dodecyl sulfate-polyacrylamide gel electrophoresis (SDS-PAGE) was performed using a 12% gels according to Laemmli (1970). Protein bands were silver stained according to Blum et al. (1987). A zymogram technique was adapted from Bischoff et al. (2006) for detection of xylanase activities. Replicate denaturing electrophoretic gels were co-polymerized with 1% of oat spelt xylan solution and stained with 0.1% Congo red solution for 1h at room temperature for xylanase activity. Gels were washed with a 1.0 M NaCl solution to remove excess dye and fixed with 0.5% acetic acid.

Mass Spectrometry

Proteins of interest were separated by SDS-PAGE and excised from gels. After spot picking, excised gels were washed with potassium ferricyanide and sodium thiosulphate to remove silver staining. The proteins were reduced with DTT, alkylated with iodoacetamide, and digested in-gel with trypsin, as described by Zhang et al. (2007). The resulting peptides were extracted with 1.0% (v/v) TFA, loaded onto a 600-nm AnchorChip™ (Bruker Daltonics, Germany) and air-dried at room temperature. α-cyiano-4-hydroxycinnamic acid (CHCA - 5$µg.µL^{-1}$) matrix solution was mixed with the samples on the surface of an AnchorChip™ plate and subjected to MS analysis using a MALDI-TOF/TOF mass spectrometer (Autoflex II, BrukerDaltonics). The peptide mass spectrum was processed and database searches conducted against sequences of fungal proteins in UniProtKB/Swiss-Prot, taxonomy other fungi, using the software FlexControl 2.2 (Bruker Daltonics). Search parameters comprised: error tolerance for peptide mass lower than 50 ppm, one or zero missed cleavage sites for trypsin, carbamidomethylation as fixed modification, methionine oxidation and acetylation of N-terminal as variable modifications.

Results

Molecular identification

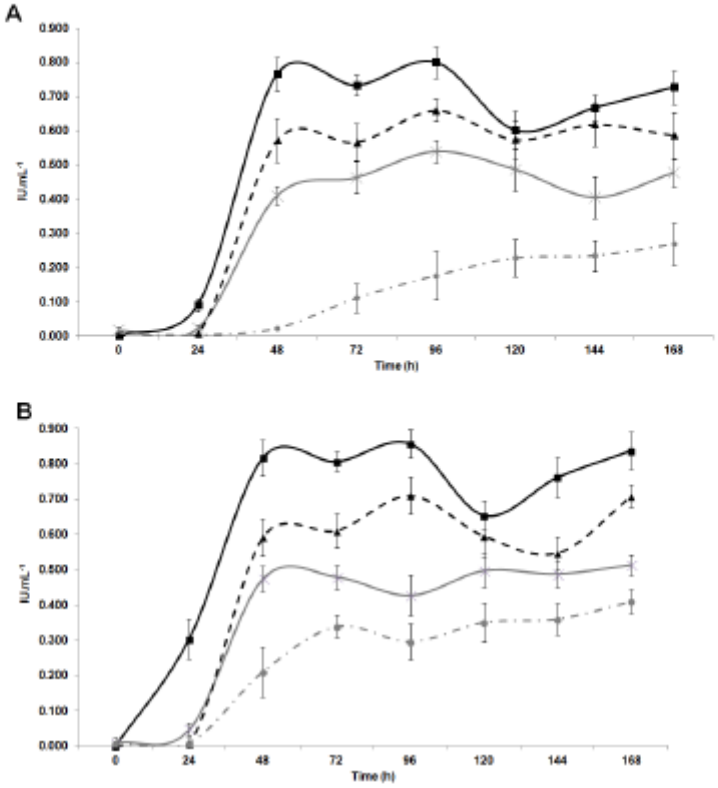

Fig. 1 – Induction profiles of xylanase activity ($IU.mL^{-1}$) from *A. tamarii* grown on filter powder (A) and clean cotton residue (B). Dotted lines - pretreated wastes. Continuous line - untreated wastes. Black lines - standard medium. Grey lines - alternative medium.

The rDNA ITS region was adequate for robust identification of the fungal isolate to genus level, based on significant sequence similarities with Aspergillus species. Analysis of the β-tubulin and calmodulin gene regions, which are appropriate markers for resolving closely related Aspergillus species (Pildain et al. 2008), confirmed identity with *A. tamarii*.

Growth curve profile

Fungal enzyme production profiles during growth periods can vary with the complexity of biomass and major organic sources, such as nitrogen and carbon. As expected, xylanolytic activity ($IU.ml^{-1}$) analysis revealed specific enzyme profiles following growth on each textile residue (Fig. 1). There were evidential differences between the curves, wherein growth on the standard medium (black lines) resulted in higher xylanolytic activity compared to activities after growth on the alternative medium (grey lines). Untreated residues (continuous line) induced more xylanolytic activity compared to pretreated residues (dotted lines).

Based on the induction profile of xylanases and protein production we established 3 days for fungal growth in pretreated residues and 4 days in untreated residues using the standard liquid medium. The xylanase activity values of tFP and tCC were 0.527 ± 0.038 $IU.mL^{-1}$ and 0.585 ± 0.025 $IU.mL^{-1}$, respectively, after 3 days of growth. The xylanase activity values of FP and CC were 0.620 ± 0.045 $IU.mL^{-1}$ and 0.705 ± 0.036 $IU.mL^{-1}$, respectively, after 4 days of

growth. Xylanase was most active in all cultures, followed by pectinase, CM-cellulase and mannanase activities (data not shown). The highest values for xylanase specific activities were 12.4 $IU.mg^{-1}$ for tCC; 7.821 $IU.mg^{-1}$ for FP; 4.757 $IU.mg^{-1}$ for tFP and 3.296 $IU.mg^{-1}$ for CC.

Enzyme production and purification

After ultrafiltration, the highest values of specific xylanase activities were obtained for the ultrafiltrate samples of tFP (217.17 $IU.mg^{-1}$), FP (74.5 $IU.mg^{-1}$), tCC (52.42 $IU.mg^{-1}$) and CC (42.5 $IU.mg^{-1}$). SDS-PAGE of the four ultrafiltrates revealed protein bands with molecular weights ranging from 20 to 96 kDa, while zymogram analysis showed single protein bands of 22 and 35 kDa which were confirmed with a positive stain for xylanase activity (Fig. 2).

Ultrafiltrate samples from pretreated residues were loaded onto Sephadex G-50 and from untreated residues were loaded onto Sephacryl S-100 gel filtration systems. The elution profile for both gel filtration chromatography procedures revealed two major peaks, displaying xylanase activity. Xylanases from ultrafiltrate tFP eluted from G-50 (Fig. 3) were purified with a one single-step procedure (Fig. 4) and were named Xyl-1 (35 kDa) and Xyl-2 (22 kDa). Xylanases from ultrafiltrate FP eluted from S-100 were partially purified (data not shown) and were named Xyl-3 (35 kDa) and Xyl-4 (22 kDa). Xylanases from ultrafiltrate CC eluted from S-100 were partially purified (data not shown) and were named Xyl-5 (35 kDa) and Xyl-6 (22 kDa). Finally, xylanases from ultrafiltrate tCC eluted from G-50 were partially purified (data not shown) and were named Xyl-7 (35 kDa) and Xyl-8 (22 kDa). It can be seen that Xyl-1, Xyl-3, Xyl-5 and Xyl-7 display the same molecular weight (35 kDa), as do Xyl-2, Xyl-4, Xyl-6 and Xyl-8 (22 kDa).

Peptide mass fingerprint analysis by mass spectrometry of Xyl-1 identified five peptides with a 19% sequence coverage and a matching score of 55, confirmed by the homology of Xyl-1 as an endo-β-1,4-xylanase F1 from *A. oryzae* RIB40 (reference genome strain) (Fig. 5). The predicted nominal molecular mass of 35,552 kDa for this protein was identified and confirmed by the apparent molecular weight of the purified protein on SDS-PAGE gels and zymograms.

Enzyme characterization

The purified enzymes Xyl-1 and Xyl-2 were submitted to optimal pH characterization; they presented higher activity at pH 6.0 and retained at least 40% of activity over a pH range of 3.5-9.0. Optimum temperature, K_M ($mg.mL^{-1}$) and V_{max} ($IU.mL^{-1}.s^{-1}$) values are summarized in Table 1. All xylanases retained at least 50% of their activity over the range of 30-60°C.

To evaluate the purity and self-association tendency of the xylanases, DLS measurements were performed. The DLS-derived intensity and mass distributions for Xyl-1 without Tween-80 (Fig. 6-A) showed one peak with a molecular weight of $1.58.10^6 \pm 2.35.10^5$ kDa and size of 531.2 ± 72.93 nm. The peak was monodisperse, meaning one population of large particles, and demonstrating the self-association tendency of xylanase at pH 7.0 and concentration of 0.3 $\mu g.mL^{-1}$. When the non-ionic surfactant Tween-80 was added (Fig. 6-B), two monodispersed peaks with different mass distribution appeared. One peak appeared with the same molecular weight and size of the aggregate and another peak appeared with low intensity but higher mass distribution, with a molecular weight of 105.6 ± 23.3 kDa and 8.721 ± 1.258 nm in size, corresponding to xylanases self-assembled as a trimer. The monodisperse feature of this peak clearly demonstrates that the sample remained homogeneous, with a polidispersivity of 13.5%, indicating that just one population size is present in this condition. Similar results were found with other xylanases (data not shown), where peaks corresponding to a larger size than the average were observed, indicating the self-association tendency of these enzymes. To assess whether Tween-80 affected xylanolytic activity, an assay with the samples containing 0.1% Tween-80 was performed after DLS measurement. The results showed a slight increase of xylanase activity for all enzymes (data not shown).

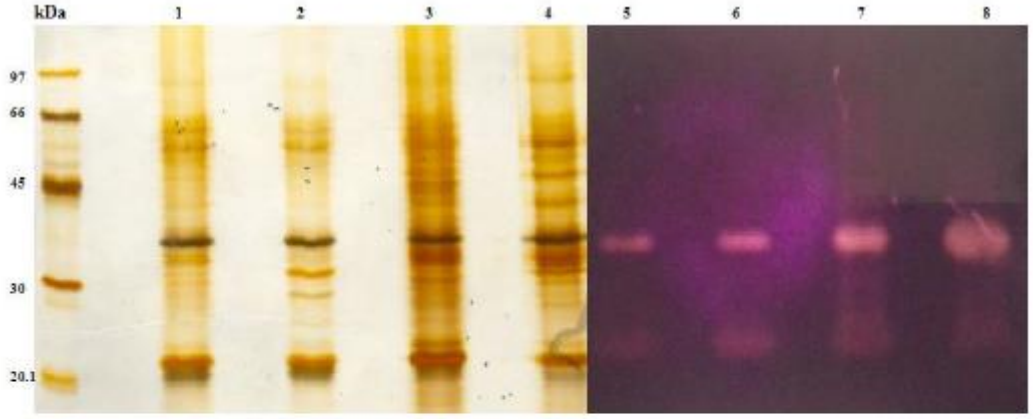

Fig. 2 – SDS-PAGE (lines 1–4) and zymogram (lines 5–8) analysis of ultrafiltrates. Lanes: 1 and 5 – ultrafiltrate FP. Lane 2 and 6 – ultrafiltrate tFP. Lane 3 and 7 – ultrafiltrate CC. Lane 4 and 8 – ultrafiltrate tCC.

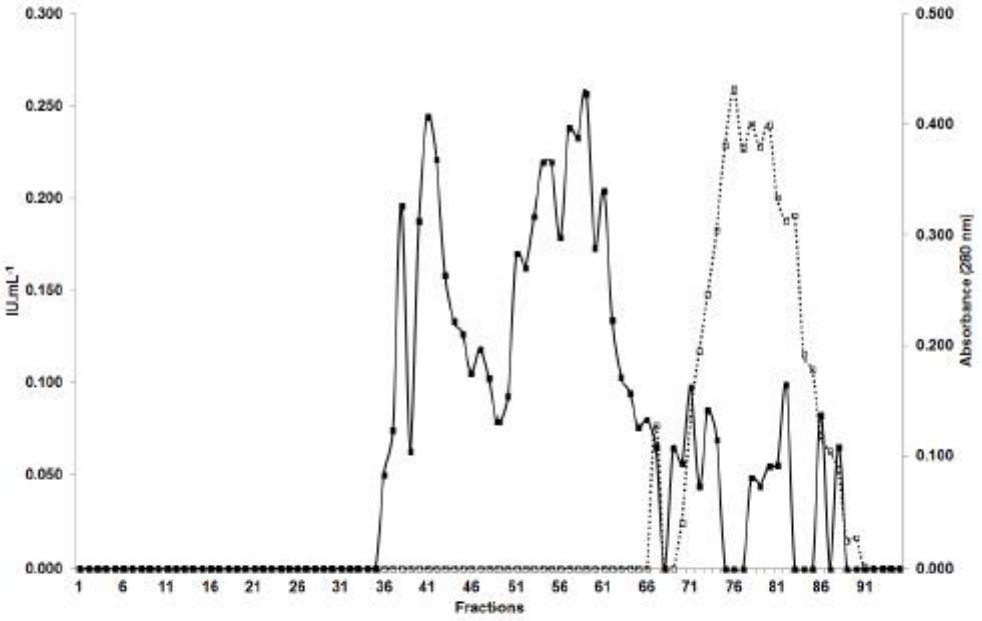

Fig. 3 – Chromatography profile of ultrafiltrate tFP in Sephadex G-50. Continuous line – xylanolytic activity ($IU.mL^{-1}$). Dotted line – UV absorbance at 280 nm.

Effect of corncob autohydrolysis liquor

Two distinct assays were performed to assess the xylanolytic activity after incubation with corncob liquor. The first assay was conducted by incubating xylanases with liquor and substrate, whilst the second was conducted by incubating xylanases with liquor and buffer replacing the substrate (Table 2). Table 2 shows that the incubation of corncob liquor with substrate increased all xylanase activities, with the exception of Xyl-5. In the absence of substrate, corncob liquor had no effect in Xyl-1 and inhibited the others xylanases.

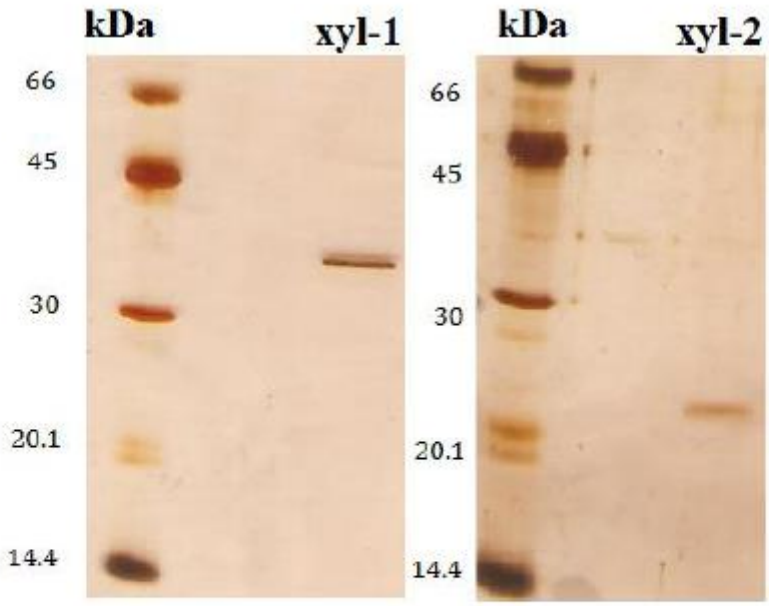

Fig. 4 – SDS-PAGE of purified fractions of tFP on Sephadex G-50 – xyl-1 and xyl-2.

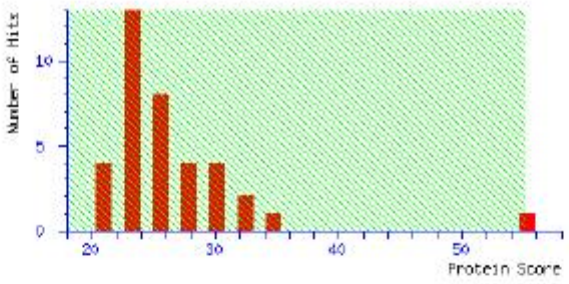

Protein sequence coverage: 19%

Matched peptides shown in ***bold red***.

```
  1 MVHLKALASG TLPASLASSA VISRQAAASI NDAFVAHGKK YFGTCSDQAL
 51 LQNSQNEAIV RADFGQLTPE NSMKWDALEP SQGSFSFAGA DFLADYAKTN
101 NKLVRGHILV WHSQLPSWVQ GITDKDTLTE VIKNHITTIM QRYKGQIYAW
151 DVVNEIFDED GTLRDSVFSQ VLGEDFVRIA FETAREADPN AKLYINDYNL
201 DSADYAKTKG MVSYVKKWLD AGVPIDGIGS QSHYSANGPP VSGAKGALTA
251 LASTGVSEVA VTELDIEGAS SESYLEVVNA CLDVSSCVGI TVWGVSDKDS
301 WRSSTSPLLF DSNYQAKDAY NAIIDAL
```

Start – End	Observed	Mr(expt)	Mr(calc)	ppm	M	Peptide
62 – 74	1437.6216	1436.6143	1436.6606	-32.2	0	R.ADFGQLTPENSMK.W
165 – 178	1597.6455	1596.6382	1596.7784	-87.8	0	R.DSVFSQVLGEDFVR.I
179 – 185	807.4190	806.4117	806.4286	-21.0	0	R.IAFETAR.E
193 – 207	1777.7061	1776.6989	1776.8206	-68.5	0	K.LYINDYNLDSADYAK.T
303 – 317	1657.6202	1656.6129	1656.7995	-113	0	R.SSTSPLLFDSNYQAK.D

Fig. 5 – Matching score and sequence coverage of Xyl-1 in mass spectrometry

1561

Table 1 Biochemical characterization of xylanases.

	Molecular mass (kDa)	K_M (mg.mL^{-1})	V_{max} (IU.mL^{-1}.s^{-1})	Optimum temperature (°C)
Xyl-1	35	04.30	0.249	60
Xyl-2	22	18.92	1.103	40
Xyl-3	35	32.25	1.071	50
Xyl-4	22	10.35	0.637	50
Xyl-5	35	18.80	1.264	60
Xyl-6	22	11.12	0.202	50
Xyl-7	35	25.32	0.571	50
Xyl-8	22	37.27	1.495	50

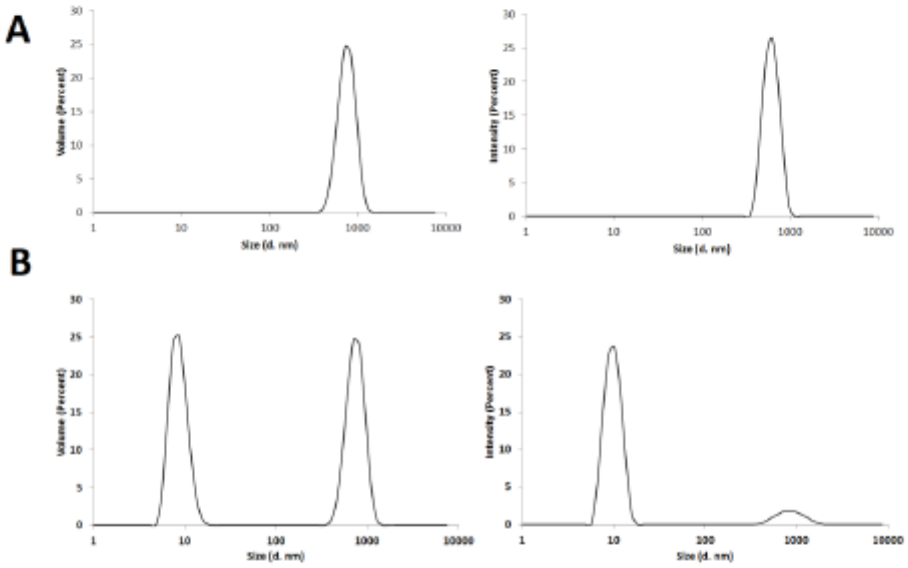

Fig. 6 – DLS measurement of Xyl-1, volume per size at left and intensity per size at right. A – Xyl-1 without 0.1% Tween-80. B – Xyl-1 with 0.1% Tween-80.

Table 2 Effect of corncob liquor and substrate on xylanase activity

	Control activity (IU.mL^{-1})	With substrate	Without substrate
		Relative activity (%)	Relative activity (%)
Xyl-1	0.100 ± 0.005	139.43 ± 0.13*	115.04 ± 0.14
Xyl-2	0.232 ± 0.016	150.70 ± 0.14*	31.16 ± 0.10*
Xyl-3	0.350 ± 0.020	124.07 ± 0.08	43.09 ± 0.10*
Xyl-4	0.300 ± 0.028	133.80 ± 0.17*	36.76 ± 0.10*
Xyl-5	0.262 ± 0.021	82.03 ± 0.17*	20.46 ± 0.15*
Xyl-6	0.087 ± 0.012	187.47 ± 0.16*	65.20 ± 0.07*
Xyl-7	0.290 ± 0.033	129.02 ± 0.30*	61.57 ± 0.46*
Xyl-8	0.127 ± 0.015	216.13 ± 0.45*	75.99 ± 0.23*

* Indicates statistical differences in Tukey's pairwise test.

Effect of phenolic compounds

The inhibitory effect of phenols was evaluated by incubating xylanases with phenolic compounds derived from the breakdown of lignocellulosic biomass and known as inhibitors of enzymatic activity. The residual xylanase activity after incubation was measured (Table 3).

Table 3 Effect of phenolic compounds on xylanase activity.

	Relative activity (%)			
	Xyl-1	Xyl-3	Xyl-5	Xyl-7
Control	100.00 ± 0.11	100.00 ± 0.01	100.00 ± 0.13	100.00 ± 0.06
Ferulic acid	151.49 ± 0.77*	171.86 ± 2.67*	135.91 ± 1.02*	137.66 ± 0.37*
ρ-Coumaric acid	70.9 ± 1.04*	112.19 ± 1.55	87.7 ± 0.92	96.55 ± 0.48
Cinnamic acid	84.68 ± 0.90	100.56 ± 0.69	95.75 ± 0.48	91.24 ± 0.32
Vanillin	92.33 ± 0.83	131.23 ± 0.38	93.41 ± 0.39	106.36 ± 0.90
4-Hydroxy-benzoic acid	93.13 ± 0.20	118.07 ± 0.07	88.81 ± 0.09	98.93 ± 0.87
Tannic acid	99.31 ± 0.76	119.19 ± 0.93	100.32 ± 0.34	96.55 ± 0.56
	Relative activity (%)			
	Xyl-2	Xyl-4	Xyl-6	Xyl-8
Control	100.00 ± 0.08	100.00 ± 0.05	100.00 ± 0.14	100.00 ± 0.12
Ferulic acid	121.74 ± 0.64*	120.52 ± 1.35*	204.56 ± 1.22*	167.85 ± 1.43*
ρ-Coumaric acid	106.7 ± 0.81	112.3 ± 0.17	127.4 ± 0.67	104.16 ± 1.49
Cinnamic acid	102.45 ± 0.60	98.51 ± 0.40	128.48 ± 1.33	102.97 ± 0.89
Vanillin	50.65 ± 0.94*	120.33 ± 3.04*	119.59 ± 1.33	85.11 ± 2.08
4-Hydroxy-benzoic acid	122.70 ± 0.64*	120.93 ± 0.54*	126.22 ± 0.55	98.21 ± 1.43
Tannic acid	92.75 ± 0.34	113.06 ± 0.57	161.08 ± 1.33*	85.71 ± 1.19

* Indicates statistical differences in Tukey's pairwise test.

It can be seen that ferulic acid significantly increased all xylanase activities. Xyl-1 was inhibited by ρ-Coumaric acid, Xyl-2 was activated by 4-Hydroxy-benzoic acid and strongly inhibited by vanillin, Xyl-4 was activated by 4-Hydroxy-benzoic acid and vanillin, and Xyl-6 was activated by tannic acid. The strongest activation effect was observed when ferulic acid was incubated with Xyl-6 (204.56 ± 1.22 % of relative activity compared with the control). The strongest inhibition effect was observed when vanillin was incubated with Xyl-2 (50.65 ± 0.94 % of relative activity compared with the control).

Discussion

Based on the induction profiles observed on both residues following 48 h of fungal growth, the enzymatic activities observed revealed that the xylanases were secreted at a constant rate, indicating continued access to the hemicellulose fibers over the cultivation timecourse. This demonstrates that these secreted enzymes in *A. tamarii* BLU37 are capable of hydrolysing biomass with high efficiency. The xylanolytic activity values observed were lower in pretreated residues when compared to untreated residues. This indicates that pretreatment was effective in reducing hemicellulose content, as with less substrate present in the biomass, there is an expected reduction in enzyme production, or a reduced induction effect. Induction effects on enzymatic activity and on saccharification have been reported in previous studies (Saykhedkar et al. 2012, Brown et al. 2014, Martins et al. 2014) and all correlate the amount of substrate with enzymatic activity. Xylanase activity profiles differed between residues in alternative and standard medium. The alternative medium, which contained only ammonium sulfate as nitrogen

source, resulted in lower enzymatic activity values than observed following growth on the standard medium, which was supplemented with yeast extract. This indicates that xylanase production may have been negatively affected by the absence of yeast extract, revealing the importance of its inclusion in a minimal medium for *A. tamarii* growth, contributing not only as a nitrogen source, but also as a source of essential vitamins and amino acids.

Biomass substrates are known to induce certain microorganisms to secrete enzyme systems and multi-enzymes with different molecular weights and with specialized functions and features in order to hydrolyze efficiently the cellulose and hemicellulose contents of the plant cell wall (Wong et al. 1988). In this study, xylanases with molecular weight greater than 10 kDa were detected in the ultrafiltrate, revealing the ability of endo-β-1,4-xylanases to change their conformation and pass through membranes with a cutoff of 10 kDa. The characterization of the purified and partially purified xylanases showed that *A. tamarii* can produce multiple forms of xylanases with similar molecular weights but with different features, explicit by different K_M and V_{max} values, and probably induced by different carbon sources and biomass composition. Although xylanase Xyl-1 was produced by *A. tamarii*, peptide mass fingerprint analysis showed a similarity with endo-β-1,4-xylanase F1 (XynF1) from *A. oryzae* RIB40, with five matched peptides, resulting in 19% coverage. Multiplicity forms of xylanase might be controlled by complex carbon sources where the fungus grows, indicating that not only a diversity of xylanase, but other intra and extra-cellular components are up-regulated by biomass composition and nutrient factors (Raman et al. 2009, Gladden et al. 2012). This diversity likely occurs so that saprophytic fungi can adapt to different lignocellulosic biomass substrates, through recognition of substrate and activation of pathway-specific transcription factors (Brown et al, 2014). Certain factors can explain this differential expression, such as growth conditions, epigenetic regulation, differential RNA processing and post-translational modification such as glycosylation, although the kind of modification that is triggered by the type of substrate and the pathways involved remain unclear (Raman et al. 2009, Gladden et al. 2012, Brown et al. 2014).

Two low molecular-weight xylanases were purified with one single chromatographic step. Optimum pH and temperature were the same as reported in previous studies that characterized similar xylanases from *A. oryzae* (Kitamoto et al. 1999, Duarte et al. 2012). Xyl-1 retained at least 40% of its activity in the pH range of 3.5-9.0, indicating its potential application in the animal feed industry, where xylanase is normally used as an additive and where high activity is required in different pH environments (Krengel et al. 1996). Another potential application is in enzymatic pulp pre-bleaching, where alkaline conditions are required throughout the process (Weerachavangkul et al. 2012).

DLS measurements with Tween-80 revealed enzymatic protein disaggregation and an increase in enzymatic activity. These results might be related to the exposure of catalytic sites after protein disaggregation, in agreement with increased enzymatic activity in the presence of Tween-80, as reported by Do et al. (2013). Tween-80 is normally used as a surfactant in the lignocellulosic biomass conversion during pretreatment and to recycle enzymes that are nonspecifically adsorbed to lignin (Van Dyk and Pletschke, 2012). An interesting application of Tween-80 would be in liquid-liquid extraction procedures in enzymatic processes, as an alternative to Triton X-114 in the micellar two-phase system, given that Tween-80 was shown to be an efficient disaggregation and non-denaturing agent.

In order to evaluate the potential industrial application of the enzymes in biomass hydrolysis, the xylanases were incubated with corncob autohydrolysis liquor. According to Michelin et al. (2012), the composition of this liquor is mainly composed of xylooligosaccharides (25.39 $g.L^{-1}$), together with other oligosaccharides (glycosaccharides and arabinosaccharides), monosaccharides (xylose, glucose, arabinose), and furfural and hydroxymethylfurfural at concentrations of 0.19 $g\text{-}L^{-1}$ and 0.77 $g.L^{-1}$, respectively. Considering that xylanases can be inhibited by the presence of xylooligosaccharides, furfural and hydroxymethylfurfural (Polizeli et al. 2005), the results showed that, despite the inhibition of

Xyl-5, the xylanases proved to be very active on xylooligosaccharides. This activation indicates that the substrate present (oat spelt xylan 2%) was probably not sufficient to saturate the catalytic sites of the enzymes, such that they were still capable of hydrolyzing more soluble substrate, demonstrating a great catalytic efficiency. Without the presence of the oat spelt xylan, the liquor proved to be an alternative substrate for Xyl-1, which showed activity when incubated in the presence of liquor. An interesting perspective for this liquor would be its use as a specific enzymatic substrate, targeting the preference of the xylanase to more deconstructed substrates, as this liquor contains hemicellulose soluble fractions of corncob. Another perspective would be as carbon source for xylanase production in liquid cultures (Michelin et al. 2012).

Although phenols from lignocellulosic biomass have been reported to inhibit enzyme activity (Kim et al. 2011) our study revealed an increase in xylanase activity in all enzymes incubated with ferulic acid, with some xylanases showing activity in the presence of one or more phenolic compounds. A similar result was found by Moreira et al. (2013) in which one purified xylanase from *A. terreus* had its activity increased when incubated with different phenolic compounds, with no loss of activity after 7 days incubation at room temperature. According to Kaya et al. (2000), the addition of phenolic compounds at low concentrations (up to 0.05%) inhibited xylanase activity of a commercial xylanase preparation (Irgazyme-40S, Ciba-Geigy Corporation, Greensboro NC). Studies have shown that inhibitory effects of phenolic compounds can occur by protein conformational changes, inducing steric inactivation (Boukari et al. 2011). The activation effect found is probably related to conformational changes associated with amino acid residues involved in maintaining the integrity of the active sites or in binding and/or hydrolysis of the substrate in the vicinity of the active site (Moreira et al. 2015).

The xylanases studied here demonstrate that their productivity and activity is related to nutrient uptake by the saprophytic fungus. Additionally, the different biochemical features of the multiple forms of xylanases could indicate a direct correlation with the biomass that induces production. Typically, xylan present in plant cell wall limits access to cellulose more directly than lignin; thereby xylan is considered as the major recalcitrant polysaccharide of the plant cell wall (Selig et al. 2009). Based on this, these multiple forms of xylanases with resistance to phenolic compounds show potential for application in second generation bioethanol industries, given that following biomass pretreatment the enzymes could support the presence of soluble lignin and hydrolyze xylan, exposing the cellulose surface to further attack. These enzymes also tolerate higher levels of soluble xylose during hydrolysis. In conclusion, *A. tamarii* BLU37 demonstrated considerable potential as a fungal strain for application in the second generation bioethanol industry.

Acknowledgments

The authors acknowledge the receipt of financial support from the Brazilian National Council for Scientific and Technological Development (CNPq), the Coordination for the Improvement of Higher Education Personnel (CAPES), the Foundation for Research Support of the Federal District (FAPDF) and the Bioethanol National Institute for Science and Technology.

References

Agblevor FA, Cundiff JS, Li MW. 2006 – Storage and characterization of cotton gin waste for ethanol production. Resources, Conservation and Recycling 46, 198–216.

Bischoff K, Rooney A, Li XL, et al. 2006 – Purification and characterization of a family 5 endoglucanase from a moderately thermophilic strain of *Bacillus licheniformis*. Biotechnology Letters 28, 1761–1765.

Blum H, Beier H, Gross HJ. 1987 – Improved silver staining of plant proteins, RNA and DNA in polyacrylamide gels. Electrophoresis 8, 93–99.

Boukari I, O'Donohue M, Rémond C, Chabbert B. 2011 – Probing a family GH11 endo–β–1,4–xylanase inhibition mechanism by phenolic compounds: Role of functional phenolic groups. Journal of Molecular Catalysis B: Enzymatic 72, 130–138

Bradford MM. 1976 – A rapid and sensitive method for the quantitation of microgram quantities of protein utilizing the principle of protein–dye binding. Analytical Biochemistry 72, 248–254.

Brown NA, Ries LNA, Goldman GH. 2014 – How nutritional status signalling coordinates metabolism and lignocellulolytic enzyme secretion. Fungal Genetics and Biology 72, 48–63.

Caldeira–Pires A, da Luz SM, Palma–Rojas S, et al. 2013 – Sustainability of the biorefinery industry for fuel production. Energies 6, 329–350.

Do TT, Quyen DT, Nguyen TN, Nguyen VT. 2013 – Molecular characterization of a glycosyl hydrolase family 10 xylanase from *Aspergillus niger*. Protein Expression and Purification 92, 196–202.

Duarte GC, Moreira LRS, Gómes–Mendoza DP, et al. 2012 – Use of residual biomass from the textile industry as carbon source for production of a low–molecular–weight xylanase from *Aspergillus oryzae*. Applied Sciences 2, 754–772.

Ferreira G, Boer CG, Peralta RM. 1999 – Production of xylanolytic enzymes by *Aspergillus tamarii* in solid state fermentation. FEMS Microbiology Letters 173, 335–339.

Filho EXF, Puls J, Coughlan MP. 1993 – Biochemical characteristics of two endo–β–1,4–xylanases produced by *Penicillium capsulatum*. Journal of Industrial Microbiology 11, 171–180.

Gladden JM, Eichorst SA, Hazen TC, et al. 2012 – Substrate Pertubation Alter the Glycoside Hydrolase Activities and Community Composition of Switchgrass–Adapted Bacterial Consortia. Biotechnology and Bioengineering 109, 1140–1145.

Ito Y, Peterson SW, Wicklow DT, Goto T. 2001. *Aspergillus pseudotamarii*, a new aflatoxin producing species in *Aspergillus* section *Flavi*. Mycology Research 2, 223–239.

Kaya F, Heitmann JA, Joyce TW. 2000 – Influence of lignin and its degradation products on enzymatic hydrolysis of xylan. Journal of Biotechnology 80, 241–247.

Kim Y, Ximenes E, Mosier NS, Ladisch MR. 2011 – Soluble inhibitors/deactivators of cellulase enzymes from lignocellulosic biomass. Enzyme and Microbial Technology 48, 408–415.

Kitamoto N, Yoshino S, Ohmya K, Tsukagoshi N. 1999 – Purification and characterization of the Overexpressed *Aspergillus oryzae* Xylanase, XynF1. Bioscience, Biotechnology and Biochemistry 63, 1791-1794.

Krengel U, Dijkstra BW. 1996 – Three–dimensional Structure of Endo–1,4–β–xylanase I from *Aspergillus niger*: molecular basis for its low pH optimum. Journal of Molecular Biology 263, 70–78.

Laemmli UK. 1970 – Cleavage of structural proteins during the assembly of the head of bacteriophage T4. Nature 227, 680–685.

Martins I, Garcia H, Varela A, et al. 2014 – Investigating *Aspergillus nidulans* secretome during colonization of cork cell walls. Journal of Proteomics 98, 175–188.

Michelin M, Polizeli MLTM, Ruzene DS, et al. 2012 – Production of xylanase and β–xylosidase from autohydrolysis liquor of corncob using two fungal strains. Bioprocess and Byosystems Engineering 35, 1185–1192.

Midorikawa GEO, Pinheiro MRR, Vidigal BS, et al. 2008 – Characterization of *Aspergillus flavus* strains from Brazilian Brazil nuts and cashew by RAPD and ribosomal DNA analysis. Letters in Applied Microbiology 47, 12–18.

Miller GL. 1959 – Use of dinitrosalicylic acid reagent for determination of reducing sugar. Analytical Chemistry, 426–428.

Moreira LRS, Álvares ACM, Silva Jr FG, et al. 2015 – Xylan–degrading enzymes from *Aspergillus terreus*: Physicochemical features and functional studies on hydrolysis of cellulose pulp. Carbohydrate Polymers 10, 700–708.

Moreira LRS, Campos MC, Siqueira PHVM, et al. 2013 – Two β–xylanases from *Aspergillus terreus*: Characterization and influence of phenolic compounds on xylanase activity. Fungal Genetics and Biology 60, 46–52.

Pildain MB, Frisvad JC, Vaamonde G, et al. 2008 – Two novel aflatoxin producing Aspergillus species from Argentinean peanuts. International Journal of Systematic and Evolutionary Microbiology 58, 725–735.

Polizeli MLTM, Rizzati ACS, Monti R, et al. 2005 – Xylanases from fungi: properties and industrial applications. Applied Microbiology and Biotechnology 67, 577–591.

Raman B, Pan C, Hurst GB, et al. 2009 – Impact of Pretreated Switchgrass and Biomass Carbohydrates on Clostridium thermocellum ATCC 27405 Cellulosome Composition: A Quantitative Proteomic Analysis. Plos One 4, 4:1–13.

Saykhedkar S, Ray A, Ayoubi–Canaan P, et al. 2012 – A time course analysis of the extracellular proteome of *Aspergillus nidulans* growing on sorghum stover. Biotechnology for Biofuels 5, 1–17.

Selig MJ, Adney WS, Himmel ME, Decker SR. 2009 – The impact of cell wall acetylation on corn stover hydrolysis by cellulolytic and xylanolytic enzymes. Cellulose 16, 711–722.

Siqueira FG, Siqueira EG, Jaramillo PMD, et al. 2009 – The potential of agro–industrial residues for production of holocellulase from filamentous fungi. *International* Biodeterioration & Biodegradation 64, 20–26.

Souza DF, Souza CGM, Peralta RM. 2001 – Effect of easily metabolizable sugars in the production of xylanase by *Aspergillus tamarii* in solid–state fermentation. Process Biochemistry 36, 835–838.

Van Dyk JS, Pletschke BI. 2012 – A review of lignocellulose bioconversion using enzymatic hydrolysis and synergistic cooperation between enzymes – Factors affecting enzymes, conversion and synergy. Biotechnology Advances 30, 1458–1480.

Weerachavangkul C, Laothanachareon T, Boonyapakron K, et al. 2012 – Alkaphilic endoxylanase from lignocellulolytic microbial consortium metagenome for biobleaching of eukalyptus pulp. Journal of Microbiology and Biotechonology 22, 1636–1643.

Wong KKY, Tan LUL, Saddler JN. 1988 – Multiplicity of β–1,4–xylanases in microorganisms: functions and applications. Microbiological Reviews 52, 305–317.

Zhang X, Shi L, Shu S, et al. 2007 – An improved method of sample preparation on AnchorChip™ targets for MALDI–MS and MS/MS and its application in the liver proteome project. Proteomics 7, 2340–2349.

ANEXO 2 – CAPÍTULO DE LIVRO PUBLICADO NO FUNGAL BIOMOLECULES: SOURCES, APPLICATIONS AND RECENT DEVELOPMENTS EM 2015: LIGNOCELLULOSE-DEGRADING ENZYMES: AN OVERVIEW OF THE GLOBAL MARKET.

Chapter 6

Lignocellulose-degrading enzymes: An overview of the global market

Paula M. D. Jaramillo, Helder A. R. Gomes, Antonielle V. Monclaro, Caio O. G. Silva and Edivaldo X. F. Filho

Laboratory of Enzymology, Department of Cellular Biology, University of Brasília, Brasília, Brazil

6.1 Introduction

Recalcitrance to saccharification is a major limitation for the enzymatic conversion of lignocellulosic biomass to valuable end products. An intricate arrangement between polysaccharides (hemicellulose and cellulose) of the cell wall matrix and lignin makes the cell wall structure a challenge for carbohydrase and ligninase enzyme systems from different sources (Siqueira and Filho 2010). The combination of hemicellulose and lignin provides a protective sheath around the cellulose, which must be modified or removed before hydrolysis of cellulose can occur, and the crystalline structure of cellulose makes it highly insoluble and resistant to attack. The amorphous lignin structure is covalently linked to hemicelluloses and fills the spaces in the cell wall between cellulose and hemicelluloses, with cellulose structure in a tightly packed bundles encased within a complex sheath of hemicelluloses and lignin (Gourlay et al. 2012; Hu and Ragauskas 2012). Cellulose, hemicellulose and lignin comprise 40–60, 20–40 and 10–25% of the dry biomass, respectively (Hamelinck et al. 2005). Although a chemical pathway to lignocellulose utilization, including for biofuels (Sanderson 2011), may turn out to be simpler than an enzyme route and apart from the expensive process of enzyme technology, it is important to consider the role of enzyme systems in overcoming the recalcitrance of lignocellulose deconstruction. Thus, the removal of lignin is a key challenge to increase enzyme access to the hemicellulose and cellulose structures.

The growing demand for various industrial purposes has catalysed efforts to convert lignocellulosic biomass to valuable products such as biofuels, chemicals and animal feed. Large efforts have been carried out over the past 50 years to determining the roles of enzyme systems within the lignocellulosic structure breakdown (Gourlay et al. 2012). Lignocellulose is a complex substrate, which requires a consortium of enzymes acting in synergism for its complete deconstruction (van Dyk and Pletschke 2012). Although the native lignocellulose is recalcitrant to breakdown from enzymes, the enzymatic hydrolysis of lignocellulose is viewed as the most viable strategy to produce sugars and other end products. According to Horn et al. (2012), the bulk terrestrial biomass resource in a future bio-economy will be lignocellulosic biomass, and its enzymatic conversion will be a key technology in

Fungal Biomolecules: Sources, Applications and Recent Developments, First Edition. Edited by Vijai Kumar Gupta, Robert L. Mach and S. Sreenivasaprasad.

future biorefineries. Conventional resources mainly fossil fuels are becoming limited because of the rapid increase in energy demand. This imbalance in energy demand and supply has placed immense pressure not only on consumer prices but also on the environment, prompting mankind to look for sustainable energy resources (Fernando et al. 2006). Lignocellulosic biomass is one such renewable resource from which various useful chemicals and fuels can be produced. By exploiting new chemical, biological and mechanical technologies, the biorefineries offer the promise of greatly expanding the use of renewable lignocellulosic biomass, as well as a means of transitioning to a more energy efficient and environmentally sustainable chemical and energy economy (Bohlmann and César 2006; Fernando et al. 2006). Each year, more than 40 million tonnes of inedible plant material are produced (Sanderson 2011). However, much of this material is thrown away. Lignocellulosic materials, such as agricultural and forest residues, are the most abundant renewable feedstocks on the planet, with approximately 200 billion tonnes produced annually in the world (Hu and Ragauskas 2012). According to Chandel et al. (2012), geopolitical, economic and employment concerns have been prompting researchers, entrepreneurs and policymakers to focus on harnessing the potential of lignocellulosic feedstock commercialization, especially in bioethanol industry. This chapter addresses recent developments related to global market for lignocellulose-degrading enzymes.

6.2 The global market for industrial enzymes

The production of enzymes is a pursuit central to the biotechnology industry (Headon and Walsh 1994; Kirk et al. 2002). Enzyme technology can be defined as the application of free enzymes and whole-cell biocatalysts in the production of goods and services (van Beilen and Li 2002). In 1998, the Organisation for Economic Co-operation and Development (OECD) reported that the value created by enzyme technology is much larger and is a significant portion of the so-called biotechnology-related sales, which were estimated to be between US$80 and US$130 billion/year. The world market for industrial enzymes was estimated at US$625–700 million for 1989–1990 with a projection of US$1 billion in 1995 (Neidleman 1991). Since then, the estimated scenario of industrial enzymes applications has grown from $1 billion in 1995 to US$1.5 billion in 2000 (Kirk et al. 2002). Business Communications Company Inc. (BCC) reported that the global sales of industrial enzymes were valued at $2 billion in 2004 in tune with an average annual growth rate of 3.3%. Comnys (Focus on Catalysts, January 2013) predicted 2013 as an enzymic year for a number of reasons, including the production in large scale and the development of genetically engineered enzymes. Within the context to transform biomass into biofuel and other chemicals, another report of Focus on Catalysts (February 2013) indicated that the world market for industrial enzymes was estimated by Novozymes to be worth €2.6 billion (US$3.4 billion), about 10% of the total catalyst market of US$30–35 billion. Furthermore, it was stressed that the market for industrial enzymes could expand to €5–10 billion or even higher taking into account that cellulosic fuel production shifts from the research and development (R&D) phase to full commercial-scale phase of fuels and chemicals, with enzymes occupying a significantly bigger share of the global catalyst sales. Bhat (2000) reported that approximately 20% of the greater than US$1 billion of the world's sale of industrial enzymes consists of cellulases, hemicellulases and pectinases and that the world market for industrial enzymes would increase in the range of US$1.7–2.0 billion by the year 2005. The estimated value of the world enzyme market was about US$4.3 billion in 2008, and it was forecasted to grow to almost US$5.1 billion by 2009 (Fazary and Ju 2008). However, more recently, the global market for industrial enzymes was estimated at US$3.3 billion in 2010 and expected to reach US$4.4 billion by 2015 (Binod et al. 2013). The Global Industry Analysts Inc. (GIA) made a less optimistic announcement in 2011. In this case, the global market for industrial enzymes was forecasted to reach US$3.74 billion by the year 2015. In addition, global enzyme market was also estimated to rise 7% at a healthy pace to $8.0 billion in 2015 (Li et al. 2012), and in 2016, the enzyme market was expected to reach US$6 billion (www.bccresearch.com, 2013).

It is relevant to consider that key factors such as driving market growth include new enzyme technologies endeavouring to enhance cost efficiencies and productivity and growing interest among consumers in substituting petrochemical products with other

organic compounds such as enzymes. The global fuel ethanol enzymes industry constituted about 11% of the global industrial enzymes market in 2009, and this market has increased at an annual growth rate of 15–20% in the past few years. A report from the Freedonia Group Inc. predicted the global market for enzymes to expand by 7.6%/year to US$6 billion in 2011, and this growth would be sustained by strong demand for different sectors of enzyme technology applications, including bioethanol manufacture. However, GIA reported in 2011 that the demand of lignocellulose-degrading enzymes in the process of ethanol production is likely to slowdown in the near future as several countries are increasingly re-evaluating the usage of food-derived raw materials in the manufacture of ethanol. According to a market report published by the Transparency Market Research, global biofuel enzymes demand was worth $1.02 billion in 2011 and is expected to reach US$1.65 billion in 2018, growing at a compound annual growth rate (CAGR) of 7.6% from 2013 to 2018 (http://www.prnewswire.com/).

The perspectives for the industrial enzymes on a commercial scale, including lignocellulose-degrading enzymes, show developing economies of Asia-Pacific, Eastern Europe and Africa and Middle East regions emerged as the fastest growing markets for industrial enzymes (Sarrouh et al. 2012). The highest growth rate will be achieved by the Asia-Pacific and other developing regions as increasing *per capita* incomes result in more intensive use of enzymes, with North America and Western Europe falling behind. The United States and Europe collectively command a major share (40 and 25%, respectively) of the world industrial enzymes market (Sarrouh et al. 2012; Binod et al. 2013), with the production of enzymes mainly concentrated in few developed nations, including Denmark, Switzerland, Germany, the Netherlands and the United States (Li et al. 2012). However, several multinational companies have invested in the enzyme industry in China with a global share of 20%. Approximately 100 companies produced enzymes in China with a total capacity of 700 thousand metric tons in 2010. The rest of Asia has a global share of 15%. India has a marginal share in the global market for industrial enzymes (Binod et al. 2013). But it is gaining global visibility because of the investment opportunities. The enzyme segment in India is forecasted to grow at CAGR of 15% until 2015 (Chandel et al. 2007a). According to Li et al. (2012), almost 4000 enzymes are known, and of these, approximately 200 microbial original types are used commercially. Although the truly industrial scale is restricted to the production of enzymes, markets for industrial enzymes continue to grow, while the continued emphasis on biotechnological endeavours has generated demand for an ever-increasing number of additional biocatalysts. In 1998, worldwide enzyme sales amounted to over US$1.5 billion, with a predicted annual growth rate ranging from 2% in the leather industry to 15% in paper production to 25% in feed enzymes (van Beilen and Li 2002). The world enzyme demand scenario shows 12 major producers and 400 minor suppliers. Three top enzyme companies (Denmark-based Novozymes, US-based DuPont and Switzerland-based Roche) produce nearly 75% of the total enzymes. Xylanase and cellulase are the major lignocellulose-degrading enzymes used in the industrial enzyme market (Sarrouh et al. 2012). GIA analysis on global enzyme market for bioethanol sector proposes that the development of novel and superior performing products and rapid advances in the technology would enable industrial enzyme manufacturers to cash on the vast untapped potential in the market. Thus, sectors such as bioethanol have succeeded in drawing significant attention of the investors and are self-sufficient in undertaking new product development activities and in launching novel and unique products in the market, thus offering new opportunities to the industrial enzyme manufacturers. In order to enhance their prospects in other segments also, industrial enzyme manufacturers are increasingly using the bioethanol enzyme developing technologies for developing other application-specific enzymes.

6.3 Lignocellulose-degrading enzymes

Lignocellulose represents a valuable resource of unexplored sustainable carbon and is predominantly composed of cellulose, hemicellulose and lignin (Chandel et al. 2007b; Siqueira and Filho 2010; Zhang et al. 2012). Figure 6.1 shows an overview of lignocellulosic biomass degradation by a variety of enzyme systems and some alternatives to industrial utilization of lignocellulosic biomass. An enzymatic synergism is required for the complete hydrolysis of lignocellulose, and basically, some enzymes hydrolyses terminal

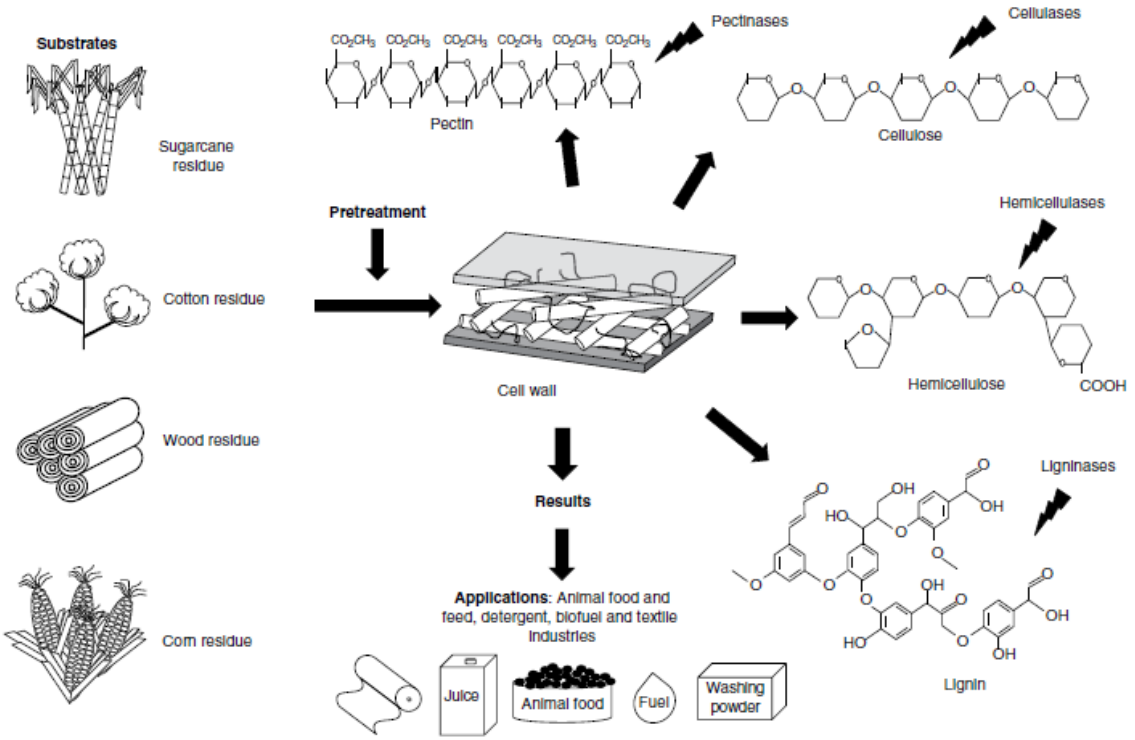

Figure 6.1 The enzymatic degradation of lignocellulosic biomass

glycosidic linkages and liberate oligomer units from non-reducing and reducing ends (exo-acting mechanism), while others cleave internal glycosidic bonds at random or at specific positions, usually internally (endo-acting mechanism). Holocellulases, including cellulase, hemicellulase and pectinase, show two conserved mechanisms of acid/base hydrolysis of the glycosidic bonds with retention or inversion of the anomeric configuration at the cleavage point (Davies and Henrissat 1995; Siqueira and Filho 2010; van Zyl et al. 2010). Retention occurs by way of double displacement and inversion via a single displacement reaction (Rye and Withers 2000). Both mechanisms involve stabilization of an oxacarbonium ion by electrostatic interaction and a pair of carboxylic acids at the active site. The three major lignin-degrading enzymes are heme-containing and H_2O_2-dependent lignin peroxidase (LiP), manganese peroxidase (MnP) and Cu-containing laccase (Minussi et al. 2002; Sena-Martins et al. 2008; Hamid and Ur-Rehman 2009). Laccase catalyses the oxidation of various substrates with the simultaneous reduction of molecular oxygen to water, while LiP is capable of oxidizing a variety of reducing substrates including polymeric substrates and MnP oxides Mn^{2+} to Mn^{3}, which oxides phenolic structures to phenoxyl radicals (Maciel et al. 2010).

Elucidation of the mechanism of action of lignocellulose-degrading enzymes with natural polymeric substrates is complicated because the latter undergoes repetitive attack by the enzymes. Moreover, the crystalline structure of cellulose and its association with hemicelluloses and lignin severely impair its susceptibility to enzymatic hydrolysis, increasing processing costs (Ekwe et al. 2013). Other key factors that contribute to inefficient hydrolysis include non-productive adsorption of enzymes by lignin and other structural components and the presence of naturally occurring enzyme inhibitors. However, considerable information relevant to the mechanism of action can be obtained by determining the products of hydrolysis and kinetic parameters using appropriate substrates.

Lignocellulose-degrading enzymes are produced by a variety of fungal genera, including *Trichoderma* and *Aspergillus*. *Trichoderma* strains were early identified as producers of lignocellulose-degrading enzymes, especially cellulases (Ryu and Mandels 1980). Many enzymes are commercially available, and numerous industrial applications have been described. The majority of lignocellulose-degrading enzymes are applied in various fields, including technical use, food manufacturing, paper bleaching, biofuel, textile industry and as tools for R&D (Howard et al. 2003). Successful utilization of lignocellulose as a renewable carbon source depends on the development of economically feasible process technologies for the production of enzymes. Several commercial lignocellulose-degrading enzymes have been developed from a few fungal species. With the improved understanding of the enzyme production biochemistry, fermentation processes and recovery methods, an increasing number of industrial enzymes can be foreseeable. According to the World Economic Forum report (King 2010), the market for pretreatment chemicals, enzymes and new organisms is estimated to yield US$10 billion in revenues by 2020. This market is highly competitive, has small profit margins and is technologically intensive. Sharp (1987) reported years ago eight policies towards biotechnology development, including substantial support for basic research, increasing emphasis on applied research, expansion of traditional policies for supporting R&D, a new emphasis on linkage between academic and industrial research, gradual convergence towards corporatist or quasi-corporatist policies, the popularity of the collaborative approach, the promotion of small firms and the venture capital market and concern with the regulatory environment. The policies described earlier can also be considered strategic tools for a balanced development of the global market for lignocellulose-degrading enzyme. As described by Neidleman (1991), the biocatalysts research development will increase as more enzymes are demonstrated to carry out commercially significant reactions under non-traditional conditions and with competitive economics compared with existing chemical and enzymatic processes. A major challenge of enzyme technology is to focus on new concepts such as biorefinery, which can produce, for example, food, energy (liquid, gas, heat and electricity), high value-added chemicals, feed and fibre. The use of tools such as recombinant gene technology, protein engineering and directed evolution has revolutionized the development of industrial enzymes (Kirk et al. 2002). As consequence, these advances have made it possible to provide tailor-made lignocellulose-degrading enzymes displaying new activities and adapted to new process conditions, enabling a further expansion of their industrial use (Carrez and Soetart 2005).

6.4 The biorefinery concept for lignocellulose-degrading enzymes

According to Bohlmann and César (2006), the term 'biorefinery' is described as future processing complexes that will use renewable agricultural residues, plant-based starch and other lignocellulosic materials as feedstocks to produce a wide range of chemicals, fuels and bio-based materials. Biorefinery can also be defined as a facility that integrates biomass conversion processes and equipment to produce fuels, power and chemicals from biomass (http://www.nrel.gov/biomass/biorefinery.html). Thus, the goal of a biorefinery is to transform biomass into useful products using a combination of technologies and processes (Fernando et al. 2006; Smith 2007; Carvalheiro et al. 2008; Demirbas 2009).

The World Economic forum of 2010 pointed out biorefinery as one potential solution that may help mitigate the threat of climate change and the seemingly boundless demand for energy, fuels, chemicals and materials (King 2010). Among the potential large-scale industrial biorefineries, the lignocellulose feedstock (LCF) biorefinery will most probably be pushed through with highest success (Kamm and Kamm 2004; Fernando et al. 2006). As reported by Rosillo-Calle and Walter (2006), an attractive advantage of large-scale ethanol production from lignocellulose is that the latter is very abundant and spread over most countries around the world. Furthermore, for temperate countries, where crop productivity is much lower, lignocellulose is particularly attractive for large-scale ethanol production (Tyson et al. 2005). In the LCF biorefinery, the hard fibrous plant materials is initially cleaned and broken down into three fractions (hemicellulose, cellulose and lignin) via chemical digestion or enzymatic hydrolysis (Fernando et al. 2006; Huang et al. 2008). The sugar polymers (hemicellulose and cellulose) can be converted to their component sugars through enzymatic hydrolysis. The hydrolysis of cellulose to glucose produces useful products, such as ethanol, acetic acid, acetone, butanol, succinic acid and other fermentation products. Lignin fractions have potential to produce monoaromatic hydrocarbons, adhesive or binder and fuel for direct combustion (Couto and Herrera 2006). However, Fernando et al. (2006) pointed out that there are no obvious, natural enzymes to split the naturally occurring lignin into its basic monomers as easily as is possible for naturally formed polymeric carbohydrates or proteins.

The lignocellulose-degrading enzymes are part of the context of technological routes able to fractionate, extract, separate and convert the raw material into different intermediates or final, including food, chemicals, biomaterials and energy (Zhang 2008; Sukumaran et al. 2009). Consequently, this would have effects in maximizing economic gains, minimizing the negative environmental aspects and improving the effectiveness and sustainability of agro-industrial chains. Among the variety of possible products from the biorefinery, liquid transportation fuels in the form of ethanol, hereafter called bioethanol, is a prominent product for LCF biorefinery (Huang et al. 2008; Luque et al. 2008; Limayem and Ricke 2012). Agricultural residues (e.g. corn stover, crop straws, sugarcane bagasse), herbaceous crops (e.g. alfalfa, switchgrass), forestry wastes, wood (hardwoods, softwoods), wastepaper and municipal waste are examples of lignocellulosic biomass described as the potential feedstock for second-generation bioethanol (Mielenz 2001; Demirbas 2009; Bhatia et al. 2012; Näyhä and Pesonen 2012). The bioethanol market is expected to reach 100×10^9 l in 2015 (Bhatia et al. 2012). The United States and Brazil are the main bioethanol producers in the world, respectively. In 2009, the United States was responsible for the production of 39.5×10^9 l of ethanol using corn as a feedstock, while Brazil produced about 30×10^9 l of ethanol using sugarcane.

The conversion of lignocellulosic materials to bioethanol requires a number of basic unit operations including pretreatment, enzyme production, hydrolysis, fermentation and ethanol recovery (Lynd 1996; Fang et al. 2010; Naik et al. 2010). Many factors have to be considered for realizing commercialization of bioethanol, including agricultural resources, concerted efforts to ensure the industry's sustainability, domestic markets for biofuels, investment capital and active R&D (Huang et al. 2008; Demirbas 2009; Klein-Marcuschamer et al. 2010). The production of bioethanol from lignocellulosic feedstocks can be achieved through two very different processing routes: biochemical and thermochemical (Demirbas 2009; Naik et al. 2010). However, the biochemical route faces technical barriers, especially for enzymatic hydrolysis. Those barriers comprise low specific activity of current commercial enzymes, high cost of enzyme production and lack of understanding of

enzyme biochemistry and mechanistic fundamentals. The contribution of enzyme costs to the economics of lignocellulosic biofuel production is a topic of intense discussion (Aden and Foust 2009). Despite the cost of enzymes for saccharifying lignocellulosic biomass that has been dramatically decreased over the past decade, biomass saccharification remains a key cost barrier, and further reduction in enzyme cost is needed (Sukumaran et al. 2009). However, other authors implicitly assume that it is not, either because they estimate the cost to be relatively low or because they assume that it will decrease with technological innovation or other advances (Aden and Foust 2009). Although the cost of enzymes is a matter of intense discussion, enzymatic and related technologies are gaining popularity and a greater chance of gaining a share of large sums that may be invested in the manufacture of advanced biofuels. According to Bloomberg New Energy Finance (Focus on Catalysts, May 2013), a total of up to US$510 billion was estimated for investments in biofuels between 2011 and 2030. The same report emphasized that the reduction in production costs as a reason for the growing interest in enzyme technologies among investors.

It is worth to mention that technical enzymes are valued at just over US$1 billion in 2010 and the second highest sales of technical enzymes occurred in the bioethanol market (Sarrouh et al. 2012). An estimative cost made by the state of technology in 2010 showed that enzymes remain the second largest contributor to operating cost in the process, after feedstock, representing an estimated cost of approximately US$0.30–0.50/gal of ethanol (McMillan et al. 2011). Other reports show an estimated cost of US$0.10–0.40/gal (Klein-Marcuschamer et al. 2012). The contribution of enzyme costs to bioethanol production can be lowered by shifting to lower-cost feedstocks, reducing the fermentation times and reducing the complexity of the process to drive down capital costs (Klein-Marcuschamer et al. 2012). Within this context, it is important to emphasize the use of enzymes that are more stable, better pretreatment technologies that enable high saccharification yields at lower enzyme loadings and methods that reduce the presence of phenolic compounds, which are responsible for enzyme inhibition and deactivation (Duarte et al. 2012). An estimative cost made by Klein-Marcuschamer et al. (2012) shows that enzyme loading of 5 FPU/g cellulose would be achieved at 20% solid loading achieving 70% conversion in 5 days. Solid-state fermentation was described by Sukumaran et al. (2009) as an attractive technology that can bring down the production cost of cellulases, providing several advantages like the lower cost of operation, lesser infrastructure requirements, ability to operate with less skilled manpower and above all ability to use cheap agro-industrial residues and biomass as raw materials.

A process model for a lignocellulosic ethanol biorefinery was proposed and based in six targeted biorefinery scenario mapping (Klein-Marcuschamer et al. 2010). For our convenience, we will only give the focus on scenarios that deal with the use of enzymes. The scenario number two deals with increasing cellulase activity with protein engineering as a tool to reduce the cellulase costs and increasing the kinetic activity of the enzymes or using a lower enzyme loading in the process or the residence time of enzymatic saccharification. The scenario number 3 proposes the use of biomass modified to have 20% lower lignin content, whereas the effects of lignin have been described as a barrier for an effective enzymatic hydrolysis of lignocellulose, interfering with sugar solubilization by limiting the accessibility of enzymes to the cellulose fibres during saccharification and by adsorbing active enzyme. However, lignin represents a potentially valuable resource for aromatic chemicals, such as phenols, but limitations in its enzymatic conversion technology suggest its utilization as a fuel to provide heat and power for the LCF biorefinery (Smith 2007).

Based in the model devised by the National Renewable Energy Laboratory (http://www.nrel.gov/biomass/biorefinery.html), a simple biorefinery concept has been proposed that is built on three different platforms, including biochemical, thermochemical and microorganism platforms (King 2010). The biochemical platform is based on biochemical conversion processes and focuses on the fermentation of sugars extracted from biomass feedstocks. However, an additional enzymatic step is required to extract the sugars from lignocellulosic biomass. Despite of the strategic relevance of lignocellulose-degrading enzymes for biorefinery concept, numerous technological and strategic challenges still hamper commercial industrialization. A related technical challenge is the need to develop more efficient and robust enzymes, particularly for the conversion of lignocellulosic material from a variety of feedstock like corn cobs, stover, wheat straw, bagasse, rice and woody biomass. The use of development of energy crops that are less resistant to enzymatic

hydrolysis is also required. Biomass pretreatment can help improve the biomass accessibility to downstream enzymatic process with a development of a broad spectrum of lignocellulosic biomass pretreatment methods that enhance enzymatic accessibility to cellulose. In addition, the use of more efficient enzymes will bring down biomass conversion costs. Downstream processing is a major cost factor (up to 50%) in bioprocesses, mainly because of rather dilute product streams (van Beilen and Li 2002). A further yield-related challenge is the need to develop microbial cell factories, that is, production hosts that produce a desired enzyme in high yields and with high specific activity. Besides, engineering enzymes with improved catalytic efficiency, searching nature for more efficient enzymes and accessory proteins and designing synthetic enzyme cocktails may contribute to improve lignocellulose breakdown. It is important to remember that several factors are responsible to an inefficient lignocelluloses breakdown, including the recalcitrant structure of lignocellulose, non-productive adsorption of enzymes by structural components of plant cell wall and the presence of naturally occurring enzyme inhibitors, leading to an increase in processing costs (Ekwe et al. 2013). To overcome these factors, it is also important to take into account the role of non-hydrolytic proteins such as swollenin, loosenin, expansins, GH61 and CBM33 in disrupting the lignocelluloses structure (amorphogenesis) and enhancing the effectiveness of enzymatic hydrolysis (Arantes and Saddler 2010). Swollenin, loosenin and expansins are described to act through disruption of the hydrogen-bonding network. On the other hand, copper-dependent lytic polysaccharide monooxygenases (LPMOs), previously known as GH61 and CBM33, are involved in the oxidative cleavage of crystalline cellulose into a variety of native and oxidized cellodextrins with varying degrees of polymerization (Gourlay et al. 2012; Horn et al. 2012; Ekwe et al. 2013).

It is also clear that a better understanding of the role of these non-hydrolytic proteins will contribute to the development and design of more efficient commercial enzyme preparations and enzyme/sugar-based biorefinery (Arantes and Saddler 2011; Gourlay et al. 2012). In addition, significant improvements in lignocellulose hydrolysis may be obtained by the synergistic action of these non-hydrolytic proteins with hydrolytic enzymes. High-level synergism, including hetero- and homo-synergisms, may be possible in the presence of auxiliary proteins that can access insoluble biomass and disrupt highly ordered polymer packaging, thereby facilitating attack by lignocellulose-degrading enzymes (Ekwe et al. 2013). The search for novel enzymes and microorganisms from specific or extreme environments by using tools such as isolation and metagenome is also relevant. According to Bohlmann and César (2006), the biorefinery of the future is likely to integrate both bioconversion and chemical 'cracking' technologies. It is important to emphasize that improved lignocellulose fractionation and pretreatment methods, reactor designs optimized for conversion of renewable feedstocks and improved catalysts and catalytic processes, both synthetic and biological, are key technologies to speed up the process of transition to next-generation biorefineries (Ragauskas et al. 2006; Carvalheiro et al. 2008; Naik et al. 2010). Therefore, the development of the second-generation biofuels derived from lignocelluloses will be in favour of demand growth over a long time. The rapid increase in world energy prices made enzyme-related processes and products more cost-effective and facilitated the legislation of a rapid expansion of the bioethanol market (Li et al. 2012). Within the development of low-cost enzyme-based processes, results obtained by Genencor International and Novozymes Biotech showed a reduction of up to 30-fold drop in the cost of enzymes for hydrolysis process of lignocellulosic materials for biofuel production (Mussatto et al. 2010).

6.5 Final remarks

Enzyme producers are facing new challenges with the rapid growth in the global market for the material, which is used to process biomass (carbohydrates) into sugars and sugars to fuels and other chemicals. In addition, efficient and cost-effective methods of isolating, replicating and purifying accessory enzymes and minor proteins from natural enzymatic mixtures need to be established, capable of consistently meeting some critical purity standards. Advancements and future directions in enzyme technology for biomass conversion include the shift to systematic characterizations of *de novo* mixtures of purified proteins (Zhang et al. 2012). This would have effect in facilitating progression towards feedstock assay-based rapid enzyme mixture optimization. The great diversity of lignocellulosic feedstock available for conversion processes and efforts to improve the

economic viability of enzymatic hydrolysis would require the construction of a database of enzymatic activities and kinetics (Zhang et al. 2012). Current efforts to optimize *de novo* enzyme mixtures will eventually need to incorporate feedstock variations and pretreatment methods prior to the genetic elimination of superfluous enzymes from fungal and bacterial sources, lest synergistic activities be overlooked for more realistic biomass. Enzymatic technology currently has a greater chance of gaining a share of large sums that may be invested in advanced technologies, including biofuel production (Mussatto et al. 2010). Significant reduction in production costs is among the reasons for the growing interest in enzyme technologies among investors. However, according to Jegannathan and Nielsen (2013), some steps should also be taken to overcome barriers such as lack of knowledge of enzymatic processes, traditional thinking among manufacturers and suppliers and governmental bureaucracy during approval of new solutions. The same authors suggest a series of complementary efforts with sustainability concerns to improve the economic viability of enzymatic hydrolysis, including the following: increase sustainability stakeholder collaboration in product, increase sustainability target setting on corporate social responsibility and report progress in sustainability index chains, continue documenting environmental impacts of new and existing biological solutions, streamline public approval of new biotechnological solutions and increase openness on production, use of enzymes in industry and phasing out subsidies to fossil fuels and implementing green tax schemes. It is also possible to conclude from the previous text that the effects of enzyme technology on the changing patterns of international production trade and investment would have important implications for the environment.

In conclusion, the biorefinery concept is connected to regions with a potential of producing lignocellulosic biomass. In this case, Brazil emerges as a promising alternative for the development of biomass biorefineries, which can produce energy, chemicals, materials and biofuels (Mussatto et al. 2010). Several factors support these claims with emphasis on agricultural resources, concerted efforts to ensure the industry's sustainability, domestic market for biofuels, investment capital and active R&D (Bohlmann and César 2006; Soccol et al. 2010; Castro and Castro 2012).

References

Aden, A. and T. Foust. 2009. Technoeconomic analysis of the dilute sulfuric acid and enzymatic hydrolysis process for the conversion of corn stover to ethanol. Cellulose 16: 535–545.

Arantes, V. and J. N. Saddler. 2010. Access to cellulose limits the efficiency of enzymatic hydrolysis: the role of amorphogenesis. Biotechnol. Biofuels 3: 1–11.

Arantes, V. and J. N. Saddler. 2011. Cellulose accessibility limits the effectiveness of minimum cellulase loading on the efficient hydrolysis of pretreated lignocellulosic substrates. Biotechnol. Biofuels 4: 3.

Bhat, M. K. 2000. Cellulases and related enzymes in biotechnology. Biotechnol. Adv. 18: 355–383.

Bhatia, L., S. Johri and R. Ahmad. 2012. An economic and ecological perspective of ethanol production from renewable agro waste: a review. AMB Express 2: 65.

Binod, P., P. Palkhiwala, R. Gaikaiwari, K. M. Nampoothiri, A. Duggal, K. Dey and A. Pandey. 2013. Industrial enzymes – present status and future perspective for India. J. Sci. Ind. Res. 72: 271–286.

Bohlmann, G. M. and M. A. César. 2006. The Brazilian opportunities for biorefineries. Ind. Biotechnol. 2: 127–132.

Carrez, D. and W. Soetart. 2005. Looking ahead in Europe: white biotech by 2025. Ind. Biotechnol. 1: 95–101.

Carvalheiro, F., L. C. Duarte and F. M. Gírio. 2008. Hemicellulose biorefineries: a review on biomass pretreatments. J. Sci. Ind. Res. 67: 849–864.

Castro, S. M. and A. M. Castro. 2012. Assessment of the Brazilian potential for the production of enzymes for biofuels from agroindustrial materials. Biomass Conv. Bioref. 2: 87–107.

Chandel, A. K., R. Rudravaram, L. V. Rao, P. Ravindra and M. L. Narasu. 2007a. Industrial enzymes in bioindustrial sector development: an Indian perspective. J. Commerce. Biotechnol. 13: 283–291.

Chandel, A. K., E. S. Chan, R. Rudravaram1, M. L. Narasu, L.V. Rao and P. Ravindra. 2007b. Economics and environmental impact of bioethanol production technologies: an appraisal. Biotechnol. Mol. Biol. Rev. 2: 14–32.

Chandel, A. K., G. Chandrasekhar, M. B. Silva and S. S. Silva. 2012. The realm of cellulases in biorefinery development. Crit. Rev. Biotechnol. 32: 187–202.

Couto, S. R. and J. L. T. Herrera. 2006. Industrial and biotechnological applications of laccases: a review. Biotechnol. Adv. 24: 500–513.

Davies, G. and B. Henrissat. 1995. Structures and mechanisms of glycosyl hydrolases. Structure 3: 853–859.

Demirbas, M. F. 2009. Biorefineries for biofuel upgrading: a critical review. Appl. Energy 86: S151–S161.

Duarte, G. C., L. R. S. Moreira, P. M. D. S. Jaramillo and E. X. F. Filho. 2012. Biomass-derived inhibitors of holocellulases. Bioenergy Res. 5: 768–777.

Ekwe, E., I. Morgenstern, A. Tsang, R. Storms and J. Powlowski. 2013. Non-hydrolytic cellulose active proteins: research progress and potential application in biorefineries. Ind. Biotechnol. 9: 123–131.

Fang, X., Y. Shen, J. Zhao, X. Bao and Y. Qu. 2010. Status and prospect of lignocellulosic bioethanol production in China. Biores. Technol. 101: 4814–4819.

Fazary, A. E. and Y.-H. Ju. 2008. The large-scale use of feruloyl esterases in industry. Biotechnol. Mol. Biol. Rev. 3: 95–110.

Fernando, S., S. Adhikari, C. Chandrapal and N. Murali. 2006. Biorefineries: current status, challenges, and future direction. Energy Fuels. 20: 1727–1737.

Gourlay, K., V. A. Arantes and J. N. Saddler. 2012. Use of substructure-specific carbohydrate binding modules to track changes in cellulose accessibility and surface morphology during the amorphogenesis step of enzymatic hydrolysis. Biotechnol. Biofuels 5: 51.

Hamelinck, C. H., G. van Hooijdonk and A. P. C. Faaij. 2005. Ethanol from lignocellulosic biomass: techno-economic performance in short-, middle- and long-term. Biomass Bioenergy. 28: 384–410.

Hamid, M. and K. Ur-Rehman. 2009. Potential applications of peroxidases. Food Chem. 115: 1177–1186.

Headon, D. R. and G. Walsh. 1994. The industrial production of enzymes. Biotechnol. Adv. 12: 635–646.

Horn, S. J., G. Vaaje-Kolstad, B. Westereng and V. G. H. Eijsink. 2012. Novel enzymes for the degradation of cellulose. Biotechnol. Biofuels 5: 45.

Howard, R. L., E. Abtosi, E. L. J. van Rensburg and S. Howard. 2003. Lignocellulose biotechnology: issues of bioconversion and enzyme production. Afr. J. Biotechnol. 2: 602–619.

Hu, F. and A. Ragauskas. 2012. Pretreatment and lignocellulosic chemistry. Bioenergy Res. 5: 1043–1066.

Huang, H.-J., S. Ramaswamy, U. W. Tschirner and B. V. Ramarao. 2008. A review of separation technologies in current and future biorefineries. Sep. Purif. Technol. 62: 1–21.

Jegannathan, K. R. and P. H. Nielsen. 2013. Environmental assessment of enzyme use in industrial production – a literature review. J. Clean. Prod. 42: 228–240.

Kamm, B. and M. Kamm. 2004. Biorefinery – systems. Chem. Biochem. Eng. Q. 18: 1–6.

King, D. 2010. The future of industrial biorefineries. Geneva: World Economic Forum.

Kirk, O., T. V. Borchert and C. C. Fuglsang. 2002. Industrial enzyme applications. Curr. Opin. Biotechnol. 13: 345–351.

Klein-Marcuschamer, D., P. Oleskowicz-Popiel, B. A. Simmons and H. W. Blanch. 2010. Technoeconomic analysis of biofuels: a wiki-based platform for lignocellulosic biorefineries. Biomass Bioenergy. 34: 1914–1921.

Klein-Marcuschamer, D., P. Oleskowicz-Popiel, B. A. Simmons and H. W. Blanch. 2012. The challenge of enzyme cost in the production of lignocellulosic biofuels. Biotechnol. Bioeng. 109: 1083–1087.

Li, S., X. Yang, S. Yang, M. Zhu and X. Wang. 2012. Technology prospecting on enzymes: application, marketing and engineering. Comput. Struct. Biotechnol. J. 2: e201209017.

Limayem, A. and S. C. Ricke. 2012. Lignocellulosic biomass for bioethanol production: current perspectives, potential issues and future prospects. Progr. Energy Combust. Sci. 38: 449–467.

Luque, R., L. Herrero-Davila, J. M. Campelo, J. H. Clark, J. M. Hidalgo, D. Luna, J. M. Marinas and A. A. Romero. 2008. Biofuels: a technological perspective. Energy Environ. Sci. 1: 542–564.

Lynd, L. R. 1996. Overview and evaluation of fuel ethanol from cellulosic biomass: technology, economics, the environment and policy. Annu. Rev. Energy Environ. 21: 403–465.

Maciel, M. J. M., A. C. Silva and H. C. T. Ribeiro. 2010. Industrial and biotechnological applications of ligninolytic enzymes of basidiomycota: a review. Electron. J. Biotechnol. 13: 1–12.

McMillan, J. D., E. W. Jennings, A. Mohagheghi and M. Zuccarello. 2011. Comparative performance of precommercial cellulases hydrolyzing pretreated corn stover. Biotechnol. Biofuels. 4: 29.

Mielenz, J. R. 2001. Ethanol production from biomass: technology and commercialization status. Curr. Opin. Microbiol. 4: 324–329.

Minussi, R. C., G. M. Pastore and N. Durán. 2002. Potential applications of laccase in the food industry. Trends Food Sci. Technol. 13: 205–216.

Mussatto, S. I., G. Dragone, P. M. R. Guimarães, J. P. A. Silva, L. M. Carneiro, I. C. Roberto, A. Vicente, L. Domingues and J. A. Teixeira. 2010. Technological trends, global market, and challenges of bio-ethanol production. Biotechnol. Adv. 28: 817–830.

Naik, S. N., V. V. Goud, P. K. Rout and A. K. Dalai. 2010. Production of first and second generation biofuels: a comprehensive review. Renew. Sustain. Energy Rev. 14: 578–597.

Näyhä, A. and H.-L. Pesonen. 2012. Diffusion of forest biorefineries in Scandinavia and North America. Technol. Forecast. Soc. Change 79: 1111–1120.

Neidleman, S. L. 1991. New applications of biocatalysts. Curr. Opin. Biotechnol. 2: 390–394.

Ragauskas, A. J., C. K. Williams, B. H. Davison, G. Britovsek, J. Cairney, C. A. Eckert, W. J. Frederick Jr., J. P. Hallett, D. J. Leak, C. L. Liotta, J. R. Mielenz, R. Murphy, R. Templer and T. Tschaplinski. 2006. The path forward for biofuels and biomaterials. Nature 27: 484–489.

Rosillo-Calle, F. and A. Walter. 2006. Global market for bioethanol: historical trends and future prospects. Energy Sustain. Dev. 10: 20–32.

Rye, C. S. and S. G. Withers. 2000. Glycosidase mechanisms. Curr. Opin. Biol. 4: 573–580.

Ryu, D. D. Y. and M. Mandels. 1980. Cellulases: biosynthesis and applications. Enzyme Microb. Technol. 2: 91–102.

Sanderson, K. 2011. Lignocellulose: a chewy problem. Nature 474: S12–S14.

Sarrouh, B., T. M. Santos, A. Miyoshi, R. Dias and V. Azevedo. 2012. Up-to-date insight on industrial enzymes applications and global market. J. Bioprocess Biotech. S4: 002.

Sena-Martins, G., E. Almeida-Vara and J. C. Duarte. 2008. Eco-friendly new products from enzymatically modified industrial lignins. Ind. Crop. Prod. 27: 189–195.

Sharp, M. 1987. National policies towards biotechnology. Technovation 5: 281–304.

Siqueira, F. G. and E. X. F. Filho. 2010. Plant cell wall as a substrate for the production of enzymes with industrial applications. Mini-Rev. Org. Chem. 7: 54–60.

Smith, W. 2007. Literature review: state of the art in biorefinery development (NFC 07/008). Tamutech Consultancy.

Soccol, C. R., L. P. S. Vandenberghe, A. B. P. Medeiros, S. G. Karp, M. Buckeridge, L. P. Ramos, A. P. Pitarelo, V. Ferreira-Leitão, L. M. F. Gottschalk, M. A. Ferrara, E. P. S. Bon, L. M. P. Moraes, J. A. Araújo and F. A. G. Torres. 2010. Bioethanol from lignocelluloses: status and perspectives in Brazil. Biores. Technol. 101: 4820–4825.

Sukumaran, R. K., R. R. Singhania, G. M. Mathew and A. Pandey. 2009. Cellulase production using biomass feed stock and its application in lignocellulose saccharification for bio-ethanol production. Renew. Energy 34: 421–424.

Tyson, K. S., J. Bozell, R. Wallace, E. Petersen and L. Moens. 2005. Biomass oil analysis: research needs and recommendations. NREL Technical Report. Available from http://www.eere.energy.gov/biomass/pdfs/34796.pdf (accessed 1 August 2005).

van Beilen, J. B. and Z. Li. 2002. Enzyme technology: an overview. Curr. Opin. Biotechnol. 13: 338–344.

van Dyk, J. S. and B. I. Pletschke. 2012. A review of lignocellulose bioconversion using enzymatic hydrolysis and synergistic cooperation between enzymes-Factors affecting conversation and synergy. Biotechnol. Adv. 30: 1458–1480.

van Zyl, W. H., S. H. Rose, K. Trollope and J. F. Gorgens. 2010. Fungal β-mannanases: mannan hydrolysis, heterologous production and biotechnological applications. Process Biochem. 45: 1203–1213.

Zhang, Y.-H. P. 2008. Reviving the carbohydrate economy via multi-product lignocellulose biorefineries. J. Ind. Microbiol. Biotechnol. 35: 367–375.

Zhang, Z., A. A. Donaldson and X. Ma. 2012. Advancements and future directions in enzyme technology for biomass conversion. Biotechnol. Adv. 30: 913–919.